

Diplomarbeit

Evaluation of the Electromagnetic Field Distribution Near Mobile Communication Base Stations

ausgeführt durch

ARC Seibersdorf research GmbH

und mit dem

Institut für Nachrichtentechnik und Hochfrequenztechnik

zum Zwecke der Erlangung des akademischen Grades eines Diplom Ingenieurs
unter der Leitung von

O.Univ.Prof. Dipl.-Ing. Dr.techn. Ernst BONEK
E389

Institut für Nachrichtentechnik und Hochfrequenztechnik

und

DI Dr.techn. Georg Neubauer
Geschäftsfeld ITM - Mobile Communications Safety
ARC Seibersdorf research GmbH

eingereicht an der technischen Universität Wien
Fakultät Elektrotechnik und Informationstechnik

von

Patrick Preiner
Matr. Nr. 96 25 109

Inzersdorferstrasse 113a/40
1100 Wien

Wien, im November 2004

Acknowledgement

I would like to thank my examiner Ernst Bonek and my supervisor Georg Neubauer, who has given me the opportunity to work at this interesting, inspiring and instructive project.

I would like to show my gratitude to Richard Überbacher, Wolfram Giczi, Harald Haider, Gernot Schmid, Agnes Kaczmarczyk, Stefan Cecil and Kurt Lamedschwandner at the departments for Mobile Communication Safety and High Frequency Engineering at the *ARC Seibersdorf Research GmbH* for sharing their knowledge, creative ideas and for valuable opinions on the contents of this thesis.

Further I would like to mention Mobilkom Austria, especially Manfred Ruttner, who made it possible to perform several measurements in their office building.


And last but not least my parents who always supported me on my way through my study time and made it possible for me to go this way.

This Diploma Thesis was Performed in Cooperation with:

ARC Seibersdorf research GmbH
(Mobile Communication Safety)

and

Technical University Vienna
(Institute of Communication and Radio-Frequency Engineering)


AUSTRIAN RESEARCH CENTERS
SEIBERSDORF

 Institute of
Communications and
Radio-Frequency Engineering

 TECHNISCHE
UNIVERSITÄT
WIEN
VIENNA
UNIVERSITY OF
TECHNOLOGY

Contents

Summary	1
Zusammenfassung	2
Introduction	3
Entirety and Purpose	3
List Of Symbols	5
Acronyms	6
1 Problem Definition	8
2 Methods and Measurements	12
2.1 Measurement Set-Up	12
2.1.1 Frequencies	18
2.1.2 Volumes	18
2.1.3 Areas	20
2.1.4 Axis	20
2.2 Frequency Selective Measurement Methods - Add3D	21
2.3 Evaluation of the Measurement Data	24
2.4 Uncertainty Considerations	26
2.5 Fading Effects	26
3 Measurement Campaign - Mobilkom Austria Room A07A011	28
3.1 Overview	28
3.2 GSM 900 - Cube Measurements	30
3.2.1 Mean, Standard Deviation and Amplitude Distribution	30
3.2.2 Cumulative Distribution Function and Probability Density Function	31
3.2.3 Identification of the Probability Density Function	37
3.2.4 Local Distribution of the Measurement Data	37
3.3 DCS 1800 - Cube Measurements	42
3.3.1 Mean, Standard Deviation and Amplitude Distribution	43
3.3.2 Cumulative Distribution Function and Probability Density Function	43
3.3.3 Identification of the Probability Density Function	47
3.3.4 Local Distribution of the Measurement Data	47
3.4 UMTS - Cube Measurements	51
3.4.1 Mean, Standard Deviation and Amplitude Distribution	51
3.4.2 Cumulative Distribution Function and Probability Density Function	53

3.4.3	Identification of the Probability Density Function	53
3.4.4	Local Distribution of the Measurement Data	55
3.5	Ultra High Frequency (UHF) - FS ORF2 - Cube Measurements . . .	58
3.5.1	Mean, Standard Deviation and Amplitude Distribution . . .	59
3.5.2	Cumulative Distribution Function and Probability Density Function	59
3.5.3	Identification of the Probability Density Function	63
3.5.4	Local Distribution of the Measurement Data	63
3.6	Very High Frequency (VHF) - Cube Measurements	65
3.6.1	Mean, Standard Deviation and Amplitude Distribution . . .	67
3.6.2	Cumulative Distribution Function and Probability Density Function	67
3.6.3	Identification of the Probability Density Function	67
3.6.4	Local Distribution of the Measurement Data	71
3.7	GSM 900 - Small Cube Measurements	74
3.7.1	Mean, Standard Deviation and Amplitude Distribution . . .	75
3.7.2	Cumulative Distribution Function and Probability Density Function	77
3.7.3	Identification of the Probability Density Function	77
3.7.4	Local Distribution of the Measurement Data	80
3.8	DCS 1800 - Small Cube Measurements	83
3.8.1	Mean, Standard Deviation and Amplitude Distribution . . .	83
3.8.2	Cumulative Distribution Function and Probability Density Function	83
3.8.3	Identification of the Probability Density Function	87
3.8.4	Local Distribution of the Measurement Data	87
3.9	Ultra High Frequency - Small Cube Measurements	90
3.9.1	Mean, Standard Deviation and Amplitude Distribution . . .	90
3.9.2	Cumulative Distribution Function and Probability Density Function	91
3.9.3	Identification of the Probability Density Function	95
3.9.4	Local Distribution of the Measurement Data	95
3.10	GSM 900 - Axis Measurements	98
3.10.1	Mean, Standard Deviation and Amplitude Distribution . . .	99
3.10.2	Cumulative Distribution Function and Probability Density Function	99
3.10.3	Identification of the Probability Density Function	99
3.11	DCS 1800 - Axis Measurements	103
3.11.1	Mean, Standard Deviation and Amplitude Distribution . . .	103
3.11.2	Cumulative Distribution Function and Probability Density Function	105
3.11.3	Identification of the Probability Density Function	109

4	Measurement Campaign - <i>ARC Seibersdorf research GmbH</i> office building	112
4.1	GSM 900 - Room TOX 7 - Cube Measurements	112
4.1.1	Mean, Standard Deviation and Amplitude Distribution	113
4.1.2	Cumulative Distribution Function and Probability Density Function	113
4.1.3	Identification of the Probability Density Function	113
4.1.4	Local Distribution of the Measurement Data	118
4.2	GSM 900 - Room CC2-17 - Area Measurements	121
4.2.1	Mean, Standard Deviation and Amplitude Distribution	125
4.2.2	Cumulative Distribution Function and Probability Density Function	126
4.2.3	Identification of the Probability Density Function	126
4.2.4	Local Distribution of the Measurement Data	131
5	Variation in Time	134
5.1	Continuous Measurements at the Mobilkom Austria Office Building	134
5.1.1	GSM 900	134
5.1.2	DCS 1800	141
5.1.3	UMTS	147
5.1.4	UHF - FS ORF2	147
5.1.5	VHF - UKW	150
5.2	Continuous Measurements at the <i>ARC Seibersdorf research GmbH</i> office building	153
5.2.1	GSM 900 - Room CC2-17	154
5.2.2	GSM 900 - Room TOX 7	158
6	Simulation	162
6.1	Simulation of the "Mobilkom Austria - Scenario"	162
6.1.1	Mean, Standard Deviation and Amplitude Distribution	165
6.1.2	Cumulative Distribution Function and Probability Density Function	165
6.1.3	Identification of the Probability Density Function	173
6.1.4	Local Distribution of the Measurement Data	177
6.2	Comparison of Simulations and Measurements	189
6.3	Additional Evaluations of Cubes within the Simulated Area	193
7	Averaging Methods	210
7.1	Different Templates	210
7.2	Deviations of the Mean Value: Templates - Measured Cubes	212
7.3	Statements Regarding the Deviations of the Mean Value: Templates - Measured Cubes	226
8	Discussion and Conclusion	230

Appendix	i
A Far Field Calculation	i
B Antenna Factor and Cable Attenuation Factor	ii
C COST 259	iii
Literature	v

Summary

The goal of this project was to evaluate the electromagnetic field distribution due to the exposure to radio frequency fields in the vicinity of mobile communication base stations¹. During various indoor measurement campaigns restricted volumes and areas were examined regarding the levels of the BCCH-channels from GSM 900, DCS 1800, a pilot channel of UMTS, VHF (radio channel) and UHF (television channel). The spatial variation as well as the variation in time were evaluated. Due to the results of the measurements, statements about the distribution of the measured electromagnetic field strength were made.

The examination performed during this project showed that in all investigated volumes and areas field strength levels around the global mean appear more often than field strength levels near the maximum value. The examination showed therefore that field strength levels around the mean value can be detected more often compared to field strength levels close to the maximum. It seems that the mean value might be better reproducible compared to the maximum. The factor maximum field strength value to global mean field strength value ($\frac{E_{MAX}}{E_{MEAN}}$) varies between 2.0 and 5.0.

Based on the examined measurement data it can be stated that the electromagnetic field strengths in the investigated volumes and areas are not symmetric distributed.

It can be stated that the electromagnetic field levels in rooms near mobile communication base stations have a large variance in time and space. Although the available measurement data do not allow any sound conclusion about laws of field distribution in certain exposure scenarios like indoor with line of sight, it can be said that the mean value of the field strength is more reliable than the maximum value and could therefore be taken as basis of estimations. The global electromagnetic field strength mean value of all examined measurement campaigns in the GSM 900, DCS 1800 and UMTS frequency bands is in the range between 13.8mV and 956.4mV.

Simulations helped to gain knowledge about the electromagnetic field distribution in indoor scenarios. With this help, a variance of different investigations were made and comparisons with performed measurements were done. A simulation of a scenario similar to one which was measured, offered valuable clues which can be seen in some of the results. By changing the position of a cube within the simulated area, different distribution functions were found. Even by varying the position of a volume in the range of its size different distribution functions were observed. The simulation of an indoor scenario at the GSM 900 frequency band proved to be a good approach for the measurement. Performed measurements delivered factors of the maximum field strength value to the mean value in the range of 1.8 to 3.2 and the simulations delivered values between 2.0 and 3.5.

¹at UMTS base stations are called Node B

Zusammenfassung

Ziel dieser Untersuchungen war es, die Feldverteilung infolge der Exposition gegenüber den elektromagnetischen Feldern von GSM Basisstationen zu bestimmen. In eingeschränkten Volumina in geschlossenen Räumen wurden die Pegel von BCCH - Kanälen von GSM 900 und DCS 1800 Basisstationen, sowie der Pilot Channel einer UMTS Basisstation², bestimmt. Ebenso wurde ein Radio Kanal (VHF) und ein Fernsehkanal (UHF) untersucht. Dabei wurden sowohl die räumlichen als auch die zeitlichen Variationen der Pegel erhoben. Aufgrund der Ergebnisse der Messungen wurden Aussagen über die Wahrscheinlichkeitsverteilungen der erhobenen Feldstärken getroffen.

Die vorliegenden Untersuchungen zeigen, daß in den untersuchten Bereichen in Räumen Feldstärkewerte um den Mittelwert wesentlich häufiger sind, als Feldstärkewerte nahe dem gefundenen Maximum. Die Untersuchungen zeigen daher, daß Feldstärken um den Mittelwert wesentlich besser reproduzierbar sind als Maximalwerte. Der Faktor zwischen der maximal auftretenden Feldstärke und dem globalen Mittelwert aller Messwerte eines untersuchten Bereichs ($\frac{E_{MAX}}{E_{MEAN}}$), ergaben Werte zwischen 2.0 und 5.0.

Aus den durchgeführten Messungen geht hervor, daß die Feldstärkewerte in den untersuchten Volumina keiner symmetrischen Verteilung unterliegen.

Insgesamt zeigt sich, daß die elektromagnetischen Felder in Räumen in deren Umgebung von GSM - Basisstationen sowohl zeitlich wie auch räumlich stark schwanken. Wenn auch die vorliegenden Ergebnisse keine endgültigen Aussagen über die Gesetzmäßigkeiten der Feldstärkeverteilung in bestimmten Expositionsszenarien, wie zum Beispiel Innenräume mit direkter Sicht auf die Sendeanlage, erlauben, kann jedoch aus den vorliegenden Ergebnissen geschlossen werden, daß die lokalen Maximalwerte der Feldstärke nur bedingt geeignet sind um als Basis für Beurteilungen der Exposition herangezogen zu werden, da Feldstärken nahe dem Maximalwert selten auftreten. Der globale Mittelwert der elektromagnetischen Feldstärke des GSM 900, DCS 1800 und des UMTS Frequenzbandes liegt im Bereich zwischen 13.8mV und 956.4mV.

Eine umfangreiche Simulation eines Messszenarios wurde ebenso durchgeführt. Ein weitaus grösserer Feldbereich als der, der in den unterschiedlichen Messkampagnen untersucht wurde, wurde mittels Simulation berechnet und diente als Grundlage für verschiedene weitere Auswertungen. Diese Simulation half Aussagen über die Feldverteilung in abgeschlossenen Räumen in der Nähe einer Basisstation zu treffen. So wurde zum Beispiel festgestellt, daß die Lage eines zu untersuchenden Volumens in einem Raum nicht trivial ist, da bei unterschiedlichen Positionen der Volumen ganz unterschiedliche Feldverteilungen auftreten können. Schon die Verschiebung eines Volumens in der Grössenordnung seiner Abmessungen genügt schon, daß eine ganz andere Feldverteilung auftritt.

²bei UMTS werden die Basisstationen Node B genannt

Introduction

This thesis is a relevant part of the international EUREKA project BASEXPO. This project was endorsed in 2003 and is performed under the leadership of the *ARC Seibersdorf research GmbH* together with France Telekom, Chalmers University, University of Thessaloniki, University of Ghent, ITIS (Foundation for Research on Information Technologies in Society) and OFCOM (Office of Communication). It is dedicated to develop reproducible and reliable methods to determine the electromagnetic field distribution in the vicinity of mobile communication base stations, taking the influence of the environment into account.

Ongoing investigations in this project are supported by the Austrian Mobile Communication Industry, namely Mobilkom Austria, Hutchison, T-Mobile and One. The investigations of the field homogeneity performed by the *ARC Seibersdorf research GmbH* were presented at several international conferences and workshops.

Currently the workgroup 1 of the technical committee TC 106x from CENELEC (European Committee for Electrotechnical Standardization) is creating standards, which will include methods to evaluate the exposure of the population in the vicinity of mobile communication base stations. These standards are based on a mandate of the European Union to standards committees for the implementation of the R&TTE guidelines from 1999. It can be assumed that this standards will be harmonized in near future. The technical committee TC 106x realized, that for future measurement campaigns, the knowledge of laws of electromagnetic field distribution is essential. The result of the available measurement data is an important contribution for the development of comprehensible and therefore creditable methods of exposure assessment. Further investigations are necessary to ensure the development of harmonized standards. In this way, a reproducible and for the population creditable implementation realization of the safety guidelines of the European Committee can be assured.

Entirety and Purpose

The purpose of the following examination was the evaluation of the electromagnetic field distribution near mobile communication base stations. In indoor measurement campaigns in constricted volumes, the levels of Broadcast Control Channels (BCCH) from GSM 900, DCS 1800, a VHF radio channel and a UHF television channel[17] as well as the pilot channel of UMTS were evaluated. The time variance, as well as the spatial variance were taken under consideration. Based on measurement campaigns, also simulations were performed. A model of a measured scenario was created and simulations with a variance of analysis were evaluated and compared with the measurements.

An approach for reliable measurements of the electromagnetic field strength, which deliver a representative statement about the field distribution, was made by

creating averaging procedures. Averaging methods were created to allow a representative statement about the field distribution using only a few examined positions. Some templates (1-dimensional, 2-dimensional and 3-dimensional) were produced and applied to all measured volumes. The deviations of each mean field strength value of a template to the global mean value of each measured volume were calculated and compared to each other.

List Of Symbols

E	electromagnetic field strength [$\frac{V}{m}$]
U	voltage [V]
AF	antenna factor [$\frac{1}{m}$]
t	time [s]
V	volume [m^3]
f	frequency [Hz]
c	light speed [$\frac{m}{s}$]
λ	wavelength [m]
S	power density [$\frac{W}{m^2}$]
P	power [W]
d	distance [m]
α	angle [$^\circ$]

Acronyms

Add3D Addition of three dimensional field components

ARC Austrian Research Center

BCCH Broadcast Control Channel

CENELEC European Committee for Electrotechnical Standardization

COST Cooperation in Science and Technology

DCS Digital Cellular System

GSM General System for Mobile Communication

ICNIRP International Commission on Non-Ionizing Radiation Protection

ITIS Foundation for Research on Information Technologies in Society

LOS Line Of Sight

NLOS Non Line Of Sight

OFCOM Office of Communication

PCD Precision Conical Dipole

RF Radio Frequency

TCH Traffic Channel

UHF Ultra High Frequency

UMTS Universal Mobile Telecommunication System

VHF Very High Frequency

1 Problem Definition

There is a significant increase in the mobile communication in the last few years. From 1996 to 2002 the number of cell phone user in Austria has changed from 0.6 to 6.8 million, thus increased tenfold. The area-wide maintenance in Austria is warranted by about 18,100 mobile communication base stations of 4 GSM and 5 UMTS networks [14]. The radio frequency electromagnetic fields, transmitted by the base stations, are subject of public and private interests.

For the realization of the safety guidelines of the European directive, the European Committee has mandated international standardization institutions for creating harmonized standards. In this context, product standards for mobile communication base stations are under preparation at this time. These standards should guarantee human public health protection in respect of electromagnetic field emission from mobile communication base stations. The exposure in the vicinity of base stations, under consideration of emission from other sources in the area of a base station has to be evaluated using reliable methods. But there are problems in the progression of such methods due to the variation of the field strength in time and space. The variance in time might be in the range of 40 dB [26]. Figure 1 shows the signal behavior of a BCCH (*Broadcast Control Channel*) - GSM 900 base station in a time frame of 1.5 milliseconds as an example.

One of the major reasons for the variance are changes in the environment of the mobile communication base stations due to movements of object like cars which changes their position on the street and thus influences the multipath propagation. But also changes in indoor environments, for example opening and closing of doors and windows or the presence of human beings influences the electromagnetic field distribution. The weather is also a matter of fact, due to the change of humidity, the reflection coefficient may vary and affect the exposure[25]. For example the reflection coefficient on dry grass is different to the reflection coefficient on wet grass[25]. These variances in the propagation path causes variable multipath propagation which is a typical characteristic of a mobile communication channels.

The variance in such a case can be approximately 30 dB, as Figure 1 shows. Also the trace gaps (*Tastlücken*) between the time slots can be seen. Attention should also be paid to the slow-term fading [26]. An example of slow-term fading of a GSM 900 base station can be seen in Figure 2. The level varies within a time frame of 18 hours between $60.2\text{dB}\mu\text{V}/\text{m}$ and $70.7\text{dB}\mu\text{V}/\text{m}$ in this particular case, which is approximately 10dB.

If time extensive measurements (e.g. evaluation of bigger field volumes) are performed, these field level variances must be taken into account. To compensate variations in time, field levels can be normalized by a reference signal measured with an additional antenna.

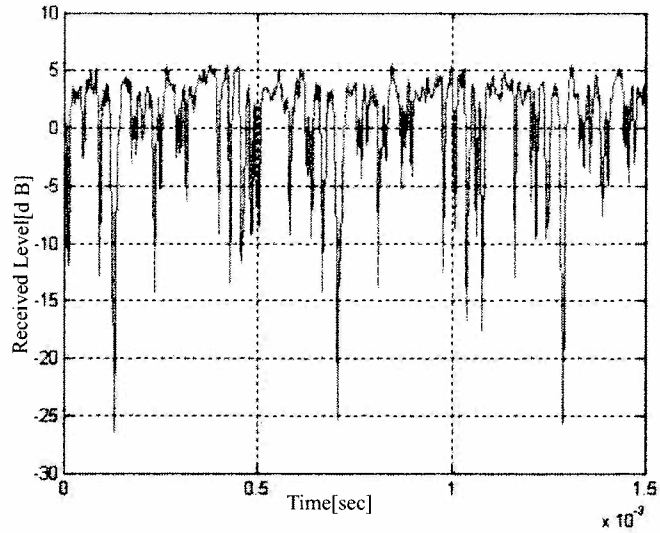


Figure 1: Time dependent characteristics of the field strength of a mobile communication channel (GSM 900), measured at the *ARC Seibersdorf research GmbH* office building (distance to the antenna approximately 60m)[3].

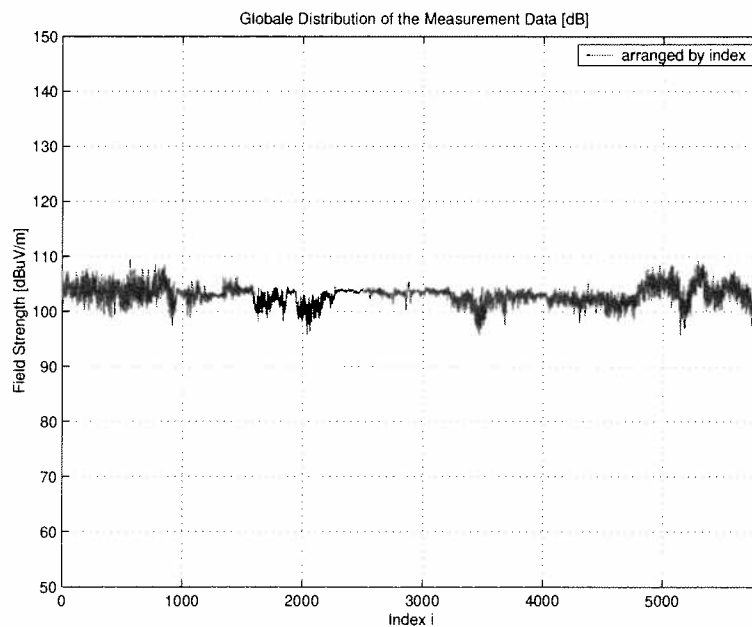


Figure 2: Variance of the signal level of a GSM 900 base station over a period of more than 18 hours (5819 measured samples), measured in Room CC2-12 at the *ARC Seibersdorf research GmbH* office building (distance to the antenna approximately 60m).

The variation in time was already under investigation, but there is a lack on examinations about the spatial variance of mobile communication base stations. To develop reliable methods of the evaluation of exposure assessment with a passable number of measurements, it is necessary to increase the knowledge of the spatial field distribution in complex environments. Already existing exposure assessment methods take the complexity of exposure scenarios only partially into account. Therefore different exposure scenarios were under investigation in this evaluation (e.g. GSM 900, DCS 1800, UMTS, a VHF radio channel and a UHF television channel with LOS or NLOS to the antenna), to gain information about laws of spatial electromagnetic field distribution, which should provide a basis for reliable measurement methods in future.

2 Methods and Measurements

This section describes the measurement set-up as well as the investigated one-dimensional, two-dimensional and three-dimensional figures and in which frequency bands measurements were performed. Each investigated geometrical figure is described in detail. A description of the Add3D measurement method, used for all measurement campaigns, can be found in this chapter as well as the evaluation of the measurement data.

2.1 Measurement Set-Up

The measurement set-up (see Figure 3) was the same in every measurement campaign performed during this project. Each spectrum analyzer was connected to an antenna, the first analyzer was used to record the time varying reference signal and the other was used to measure the field strength with the Add3D method described later in this chapter. The measurement antenna was moved within the area of investigation while the reference antenna was placed at a fixed position in the room. This signal was only used to normalize the measurement signal to take the variance in time of the transmitted signal into account. Both spectrum analyzers were connected to one PC. Each measured position had a time stamp, which means that the time of the measurement was also stored in a file, as well as a reference signal therefore the variance in time could be eliminated.

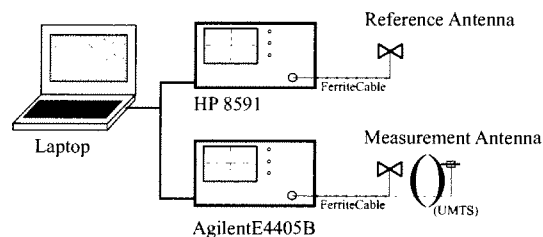


Figure 3: Schematic of the measurement set up including the measurement antenna (PCD 8250), which was moved in the investigated area and the reference antenna (PCD 8250), which was placed on a fixed position. The antenna in brackets was only used for the UMTS measurement with a higher sensitivity (PBA 10200). All antennas were connected to the spectrum analyzers via ferrite cables.

A problem during the measurement was the variation in time of the electromagnetic field strength. Therefore only the BCCH (Broadcast Control Channel) was measured and not the TCH (Traffic Channel), because the TCH has a variable transmission power depending on the volume of traffic. Due to the fading effects, the field level of the BCCH varies within time, see Figure 1. The outcome of this are problems for the investigation of spatial distributions of the field strength because of the measurements on different positions at different times. This yields to over-



Figure 4: Picture of the conference room and the anteroom with the measurement antenna, the reference antenna can not be seen, it is far left behind the wooden wall. The two spectrum analyzers and the Notebook were in the conference room (for the measurements of GSM 900, DCS 1800, UMTS and UHF - ORF2).

lapping of variations in time and space. Within the scope of those measurements, only the spatial variation was of interest.

For a better imagination some pictures were taken from the conference room, the anteroom and the whole building. Figure 4 shows the conference room where the measurement equipment (spectrum analyzers and PC) was set up and a view to the anteroom with the measurement antenna (the reference antenna can not be seen in this picture, it is in the far left corner, covered from the wooden wall). The measurement antenna, mounted on the tripod, with the base station antenna mast in the background can be seen in Figure 5.

The measurement set up of a measurement campaign in Room A07A011 in an office building of the Mobilkom Austria can be seen in Figure 6. The grid was painted on a thin plexiglass plate which was taped to the floor to avoid displacement. In the foreground the measurement antenna with the rotating device and the tripod can be seen. The reference antenna is mounted on a tripod and wasn't changed in its orientation and polarization. Figure 7 shows the antenna mast with the GSM 900, the DCS 1800 and the UMTS antennas. This picture was shot from the open window of the anteroom. A whole outside view of the building's top with the Room A07A011 (conference room and anteroom) on the upper left corner and the base station antenna mast in the background can be seen in Figure 8. Figure 9 and Figure 10 are showing the whole office building of the Mobilkom Austria from

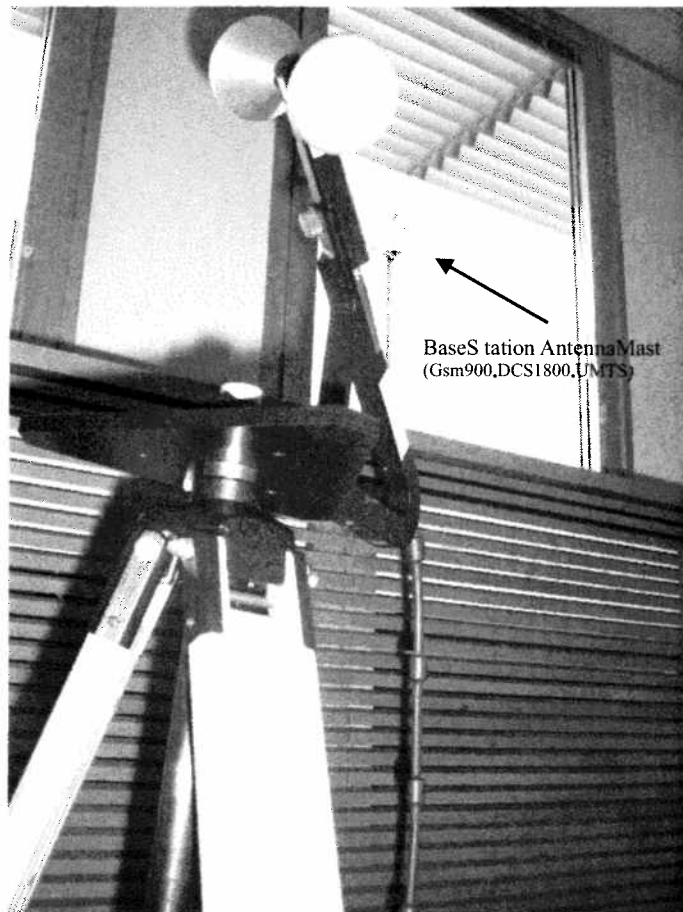


Figure 5: Picture of the measurement antenna with view to the basestation antenna mast.

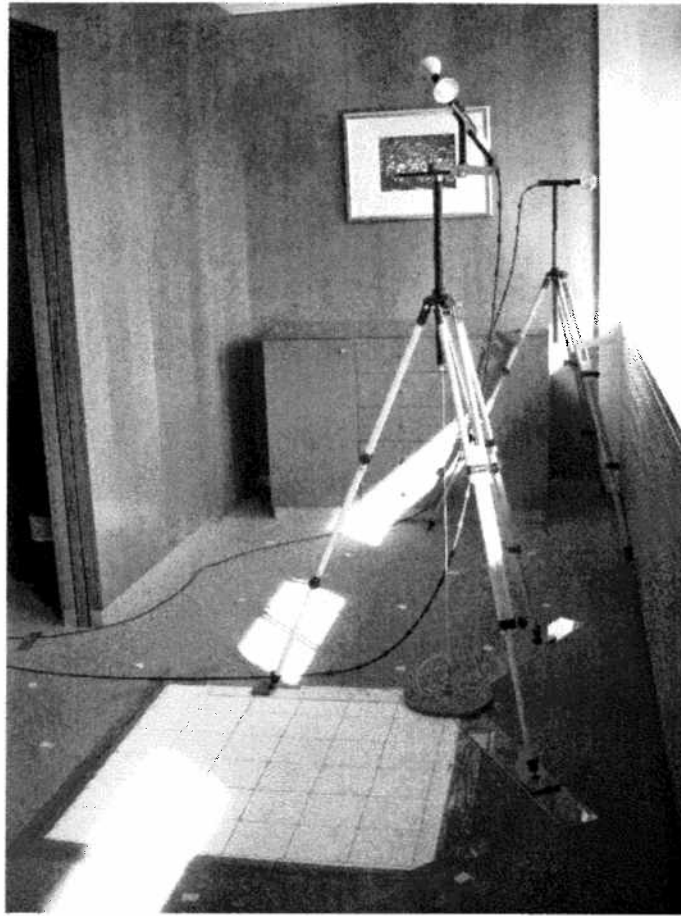


Figure 6: The measurement set up in a Room A07A011 in an office building of the Mobilkom Austria with the grid taped to the floor, the measurement antenna with the rotating device mounted on a tripod and the reference antenna also mounted on a tripod can be seen. The reference antenna wasn't changed in its orientation an positions.

far away, these two pictures should give an idea of the vicinity of the base station and the room under investigation.

Parallel to every measurement of the field strength, performed in max-hold mode, a reference signal was measured, too. The position of the reference antenna was unchanged during the whole measurement campaign. The average of all measured levels obtained with the reference antenna was calculated and further the deviation of every measurement from this mean value was derived. In a next step the measurement data of the measurement antenna was revised with the calculated deviation of the reference data. This was an approach to derive only the spatial variation of the signal level.

Not every measured area had Line-Of-Sight (LOS) to the transmitting antenna,

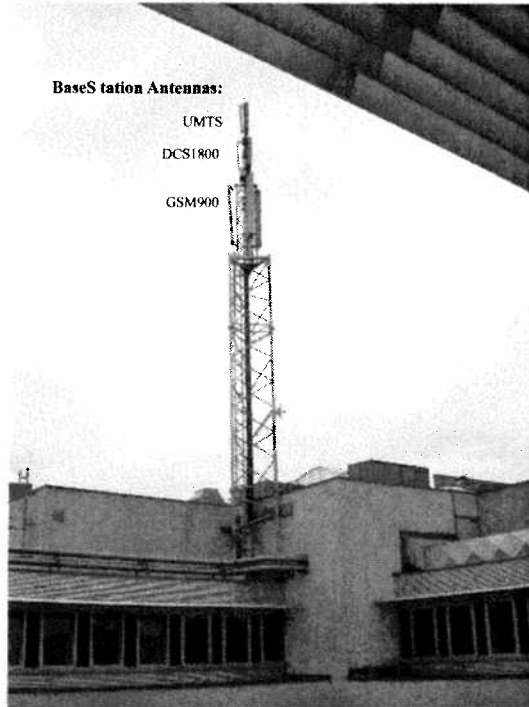


Figure 7: Picture of the basestation antenna mast, shot from one window of the anteroom.

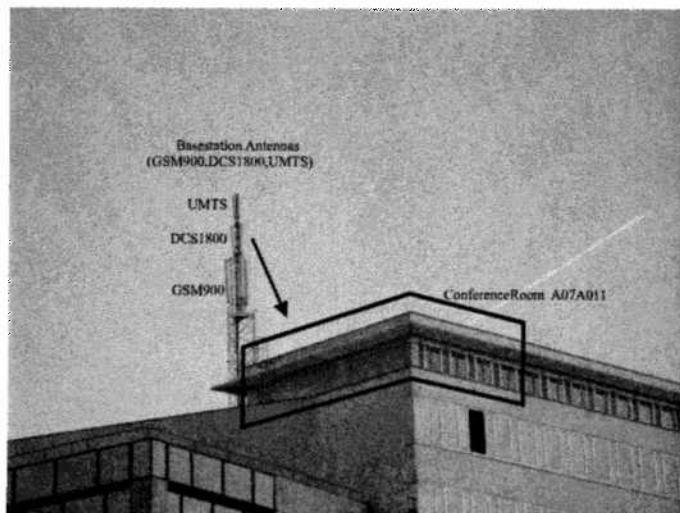


Figure 8: Picture of the Mobilkom Austria office building with the basestation antenna mast. The conference room is located on the top of the building.

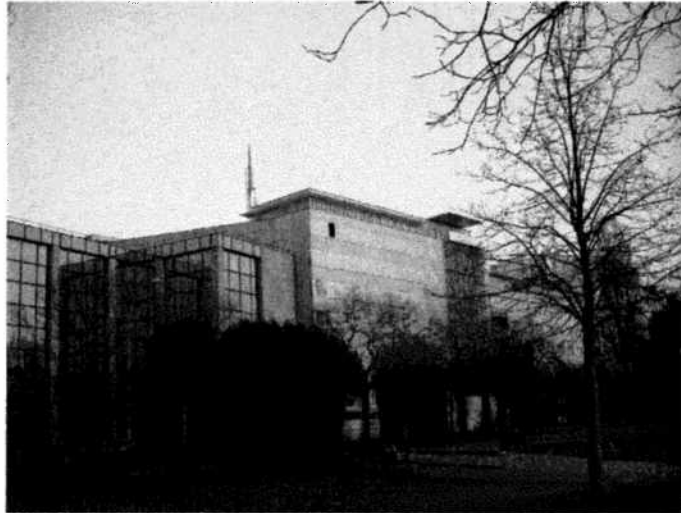


Figure 9: Picture of the Mobilkom Austria office building and the basestation antenna mast.

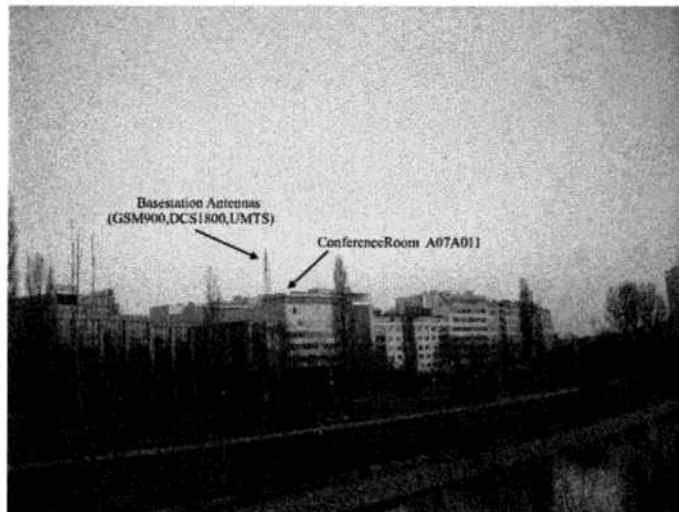


Figure 10: Wide area picture of the Mobilkom Austria office building and the basestation antenna mast.

Name	Frequency	Wavelength λ
GSM 900	944.6 MHz	0.3176m
GSM 900	946.0 MHz	0.3171m
GSM 900	946.6 MHz	0.3169m
DCS 1800	1812.4 MHz	0.1655m
UMTS	2154.7 MHz	0.1392m
UHF - FS ORF 2	575.25 MHz	0.5215m
VHF - RF	105.8 MHz	2.8355m

Table 1: Measured frequencies and their wavelength λ .

also Non-Line-Of-Sight (NLOS) measurements were performed.

2.1.1 Frequencies

Table 1 shows the evaluated frequencies. Measurements in the GSM 900 frequency band were performed at three different frequencies, 946.0MHz were measured at the Mobilkom Austria office building and 944.6MHz, as well as 946.6MHz were measured at the *ARC Seibersdorf research GmbH* office building. Due to a optimization process of the network operator a frequency of the base station in Seibersdorf was changed from 944.6MHz to 946.6MHz but not during a measurement campaign. The wavelength λ can be derived by Equation 1, with light speed c and frequency f :

$$\lambda = \frac{c}{f} \quad [m] \quad \text{with} \quad c = 3 \cdot 10^8 \frac{m}{s} \quad (1)$$

2.1.2 Volumes

The *ICNIRP (International Commission on Non-Ionizing Radiation Protection)* directive requires averaging procedures over a volume corresponding the body of a human being, therefore the volume under investigation should be approximately equal to this size. A cube with an edge length of 90cm was chosen because it is a good compromise between the size of an human being and a easy to measure geometrical Figure with a volume of $0.73m^3$. The distance between each examined position (grid step) is 15cm in each of the three orthogonal directions³.

One level, build by the x -axis and the y -axis, contains 49 measurement positions, a cube consists of 7 horizontal levels which gives a total of 343 measurement positions in the whole cube. The first level is 90cm above the floor and is called

³The grid step of 15cm was chosen because it is short on one half of a wavelength to avoid possible standing wave measurements of e.g. the maximum and therefore generate a wrong impression of constant field strength. On the other hand a relatively big area can be investigated with little expense. With an antenna size of 13cm no overlapping of the integration volume should occur.

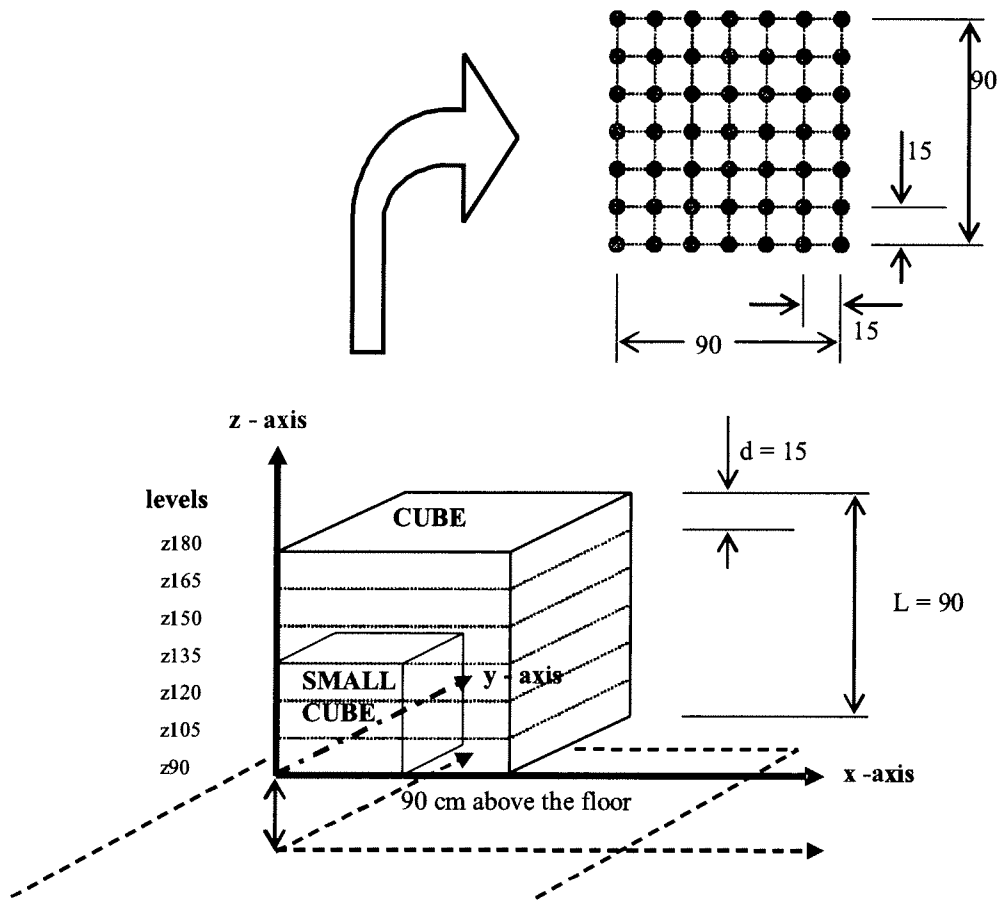


Figure 11: Schematic of the examined positions building the volume under investigation ("CUBE"). The investigated "SMALL CUBE" has its origin at the same position than the cube but is only one eight of the size of the cube.

"Level z90" with a distance of 15cm to the next level called "Level z105" and so on until "Level z180". Therefore the last level is located 180cm above ground. This is similar to the volume occupied by the human body covering the region from the femoral to the head. In every measurement position, three field strength values were measured according to the Add3D method described later. Figure 11 shows a schematic of the examined positions building the three-dimensional Figure which was called a "CUBE".

A cube with edge length of 45cm, which is half of the size of the cube described before, was examined, too. This so called "SMALL CUBE" can be seen in Figure 11. No reduction in the number of measured positions were done but the grid step was half of the grid step of the large cube as described before. With a grid step of 7.5cm the volume of the cube is one eights of the volume of the cube. The first level is located at a height of 90cm above the floor ending in a height of 135cm above the floor with a distance of 7.5cm between each level. This makes again a total of 343 measurement positions. The first measurement position is equal to the

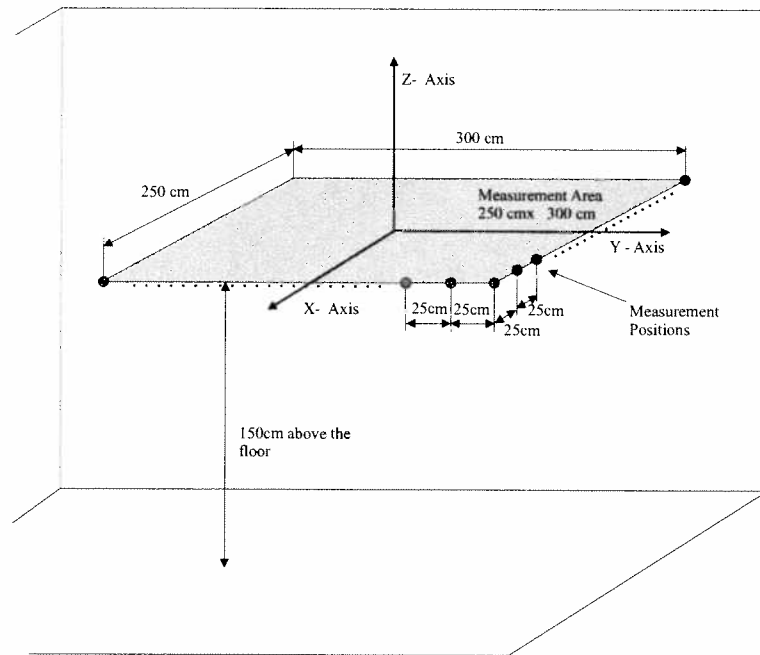


Figure 12: Schematic of the examined positions of the investigated area with a grid step of 25cm and an area size of 250cm times 300cm.

first measurement position of the cube, also the direction in which the measurement antenna was moved is the same as at the cube measurements.

2.1.3 Areas

Not only volumes were under investigation, also areas were measured but only in one room at the *ARC Seibersdorf research GmbH* office building. With an area size of 250cm times 300cm and a grid step of 25cm between each examined position, this makes a total of 143 examined positions. The location of this area was in the middle of a conference room (Room CC2-17) in a height of 150cm above the floor. Figure 12 shows the schematic of the measured area and its examined positions.

2.1.4 Axis

Measurements along a line were also performed but only at the Mobilkom Austria office building. Two axis orthogonal to each other crossing in the center of the cube with a grid step of 1cm were investigated. The center of the cube is 135cm above the floor. In each direction of the x-axis and the y-axis 91 positions were examined, leading to a total of 182 measured positions for each cube measurement. Such axis-measurements of two cubes in the frequency band GSM 900 and DCS 1800 were examined. Figure 13 shows the schematic of the measurement.

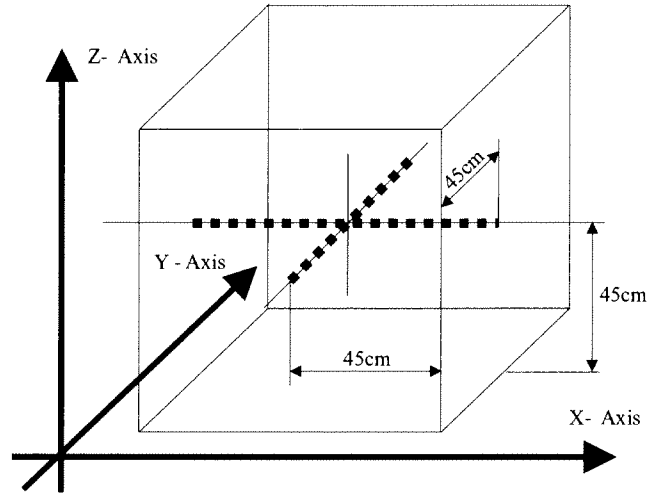


Figure 13: Schematic of the examined positions of the investigated lines along the x-axis and the y-axis with a grid step of 1cm.

2.2 Frequency Selective Measurement Methods - Add3D

A detailed description of the Add3D⁴ measurement method can be found in [11]. The principle of this method is the measurement of the electromagnetic field strength in three axis orthogonal to each other. The antenna is rotated in 120 degree steps around a circle normal to the z-axis. This is shown in Figure 14. A picture of the three positions of the antenna can be seen in Figure 15

It is a frequency selective measurement method with a receiver or a spectrum analyzer and it uses a broadband omnidirectional receive antenna. The directional characteristic of this antenna can be obtained from three voltage measurements with orthogonal orientation of the antenna (PCD 8250) [9].

The physically measured value of this method are the three voltages U_1, U_2 and U_3 . The field strengths E_i are calculated in linear quantities derived by following Equation 2:

$$E_i = U_i \cdot AF \quad \text{with } i = 1, 2, 3 \quad (2)$$

Whereas AF is the antenna factor in the quantity of $[\frac{1}{m}]$ which depends on the frequency and can be read off Figure 16 which is delivered from the manufacturer.

⁴<http://www.arcs.ac.at/gesch/IT/ITR/Productinfodownload/Rffield.pdf>

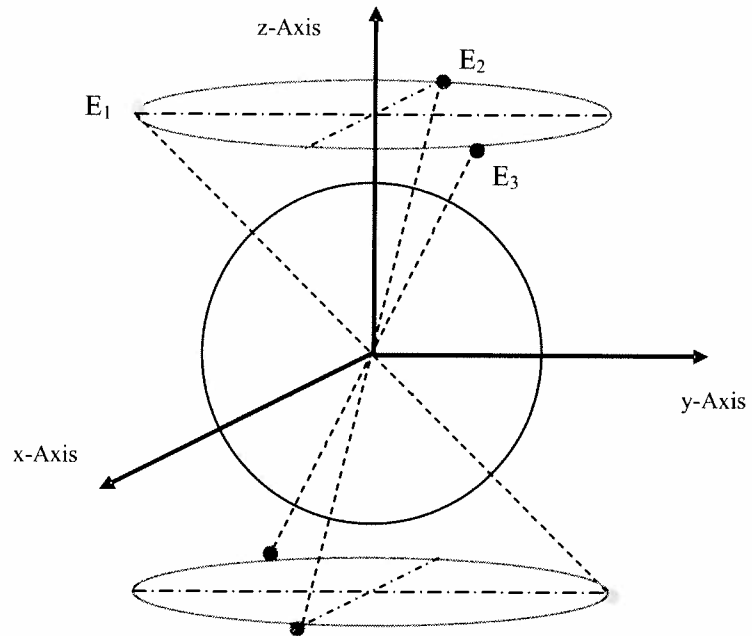


Figure 14: Spherical field volume with the three orthogonal measurement axis.

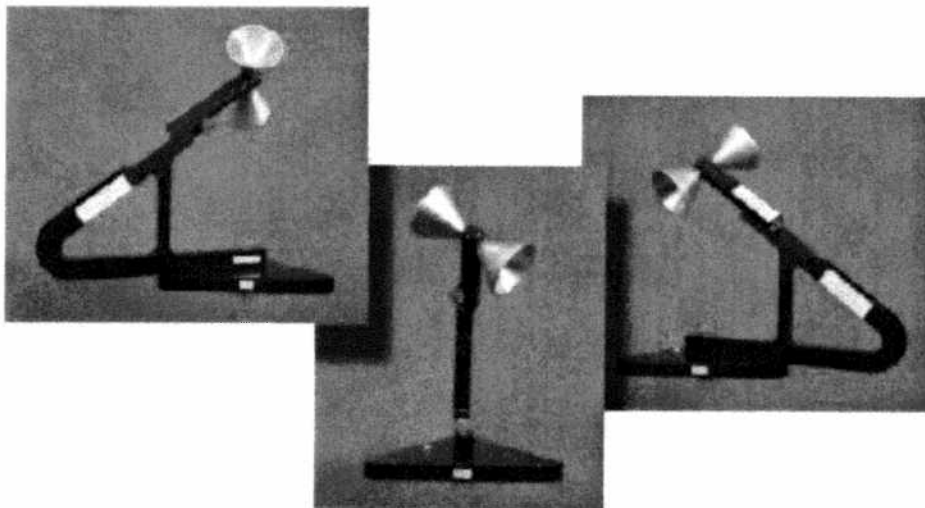


Figure 15: Picture of the three positions build by rotating the antenna around the vertical axis (z-axis).

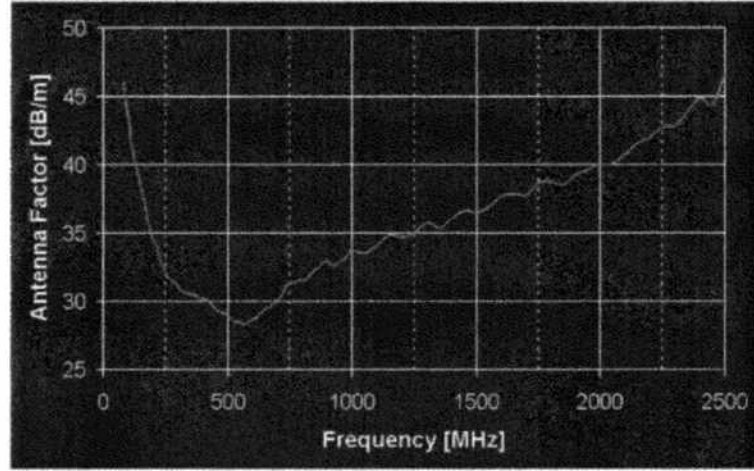


Figure 16: Typical antenna factor diagram of the PCD 8250 antenna which was used as measurement antenna for all frequencies except for UMTS. A more sensitive antenna was used for the UMTS measurements.

For the calculation procedure the cable attenuation, which can be measured for certain frequencies, was included in the antenna factor (see Appendix B). The effective electromagnetic field strength E_{eff} in the unit of $[\frac{V}{m}]$ is calculated by Equation 3:

$$E_{eff} = \sqrt{E_1^2 + E_2^2 + E_3^2} = \sqrt{U_1^2 + U_2^2 + U_3^2} \cdot AF \quad (3)$$

All contributions (U , AF) and therefore also E_{eff} are frequency dependent [9]. Figure 16 shows a typical diagram of the antenna factor of a PCD 8250 antenna which was used as measurement antenna for all frequencies, except UMTS. For the UMTS measurements a more sensitive antenna, the PBA 10200, was used because the signal level was near the noise level.

The antenna factor AF is decreasing with increasing frequency until a minimum is reached (around 600MHz, as can be seen in Figure 16) and is then increasing with increasing frequency. The value of the antenna factor is given by the calibration process of the manufacturer.

To avoid measurement errors due to rapidly changing signals of the transmitter and the time difference between the reading of each direction of the Add3D method all measurements were done in the max-hold mode of the spectrum analyzer within a time period of 10 seconds.

The two spectrum analyzer were measuring the received signal in $[\frac{dB\mu V}{m}]$. Each measured position of the Add3D method was recorded and stored in a file. This file contains six values, one for each of the three direction of the measurement antenna and three values for the reference antenna as well as the time and date of each measured value.

2.3 Evaluation of the Measurement Data

This chapter describes the evaluation of the huge amount of measurement data. Since June 2002 more than 4000 examined positions in defined volumes and areas were measured and in addition over 90000 examined samples in continuous measurement campaigns. The way from the raw measurement data to the total electromagnetic field strength values, which were used for all calculations, is shown in this chapter.

The first step of the evaluation was the compilation of the field strength, the correction with the antenna factor and the attenuation factor of the cable and the conversion in linear values because the data delivered from the two spectrum analyzers were in the unit of $[\frac{dB\mu V}{m}]$.

After the correction of the measured field strength values, described earlier in this section, with the antenna factor and the cable attenuation factor (see Appendix B) all electromagnetic field strength values were converted into linear values. Generally the voltage ratio (A_u) in the unit of $[\frac{dB\mu V}{m}]$ is defined by following Equation 4:

$$A_u = 20 \cdot \log\left(\frac{U_{LIN}}{U_0}\right) \quad \left[\frac{dB\mu V}{m}\right] \quad \text{if} \quad U_0 = 1 \frac{\mu V}{m}. \quad (4)$$

And after converting Equation 4, the linear value can be derived by Equation 5:

$$U_{LIN} = 10^{-6} \cdot 10^{\frac{A_u}{20}} \quad \text{with} \quad U_0 = 1 \frac{\mu V}{m}. \quad (5)$$

The measured field strength value was then converted into linear values by using Equation 5. Now the mean value of all linear field strength values of the reference antenna was build, see Equation 6:

$$\overline{E_{REF}} = \frac{\sum_{i=1}^N E_{REF1\ i} + \sum_{i=1}^N E_{REF2\ i} + \sum_{i=1}^N E_{REF3\ i}}{3 \cdot N} \quad (6)$$

Whereas N is the maximum amount of examined positions per investigated area. For example for the cube: N=343 or the line measurements: N=91.

This global mean value was used to determine the deviation of each measured reference signal value from the global mean value of all reference signals by dividing those two values. Each measured position consists of three values, one for each direction (due to the Add3D method). The calculation of the deviations is shown in

Equation 7). All deviation are in the unity [1] and can be converted into the unity [%] by multiplication with the factor 100.

$$\begin{aligned}
Deviation_{1\ i} &= \frac{E_{REF1\ i}}{E_{REF}} \\
Deviation_{2\ i} &= \frac{E_{REF2\ i}}{E_{REF}} \quad \text{for } i = 1, 2, \dots, N \\
Deviation_{3\ i} &= \frac{E_{REF3\ i}}{E_{REF}}
\end{aligned} \tag{7}$$

We assume that the measured signal varies to the same extent than the reference signal. By dividing the measurement value by its deviation we can normalize the measurement data and the variation in time won't matter anymore. This procedure was used for all measurement data.

The measured signal from the measurement antenna was then corrected with those derived deviation by dividing the measured signal of the measurement antenna with the deviation (see Equation 8). The measured signal of the measurement antenna is so normalized to a constant value.

$$\begin{aligned}
E_{1\ corr\ i} &= \frac{E_{1\ i}}{Deviation_{1\ i}} \\
E_{2\ corr\ i} &= \frac{E_{2\ i}}{Deviation_{2\ i}} \quad \text{for } i = 1, 2, \dots, N \\
E_{3\ corr\ i} &= \frac{E_{3\ i}}{Deviation_{3\ i}}
\end{aligned} \tag{8}$$

For the field strength ($E_{1\ i}$, $E_{2\ i}$ and $E_{3\ i}$) the linearized values were used for deriving the corrected values. These corrected values were then taken for deriving the total field strength in one examined position. Equation 9 shows the calculation of the total field strength value:

$$E_i = \sqrt{E_{1\ corr\ i}^2 + E_{2\ corr\ i}^2 + E_{3\ corr\ i}^2} \quad \text{for } i = 1, 2, \dots, N \tag{9}$$

Those procedures were performed for every measurement data. For each measurement campaign tables were filled with all data described in this section for future calculations.

2.4 Uncertainty Considerations

The presence of objects in the scanned area are influencing the measurement. Due to the fact that the measurement antenna is mounted on a tripod with a few metal parts the measurement is influenced. To reduce the risk of false or incorrect measurements the person who performed all measurements wasn't in the vicinity of the antennas. The distance between the measurement equipment (spectrum analyzers, PC) and the person who performed the measurement was approximately 5m.

2.5 Fading Effects

Scattering and multipath cause fading effects. Signal strength can change rapidly as a function of the location, because the received signal is the sum of potentially numerous signal scattered from nearby objects. As the transmitter, or other objects in the environment move, the scattered signals sometimes add together and sometimes cancel each other. Fading can change significantly over distances of a wavelength or so.

The received signals at the receiver have different phases due to the differences in the propagation path, this means that the distance of the received signals differs, as can be seen in Figure 17. Constructive and destructive interference occurs at the receiver and leads to changes in the signal amplitude with time (because the location of the mobile station changes). The changes in the amplitude, caused by the interference effects, is called *small-scale fading*. For example at 900MHz changes of the location within a distance of 15cm can lead to a change from constructive interference to destructive interference or vice versa. This means that a small change in the location of the mobile station might lead to a tremendous change in the signal amplitude[5][6]. The change of the amplitude due to some shadowing effects is called *large-scale fading*.

Fading also occurs over time as well as location. Even small changes in the environment (for example, people or objects moving) can affect the fading pattern. This means that the received signal strength can also change quite quickly over time, even when the receiver and transmitter are fixed.

Scattering and multipath results in delay spread. The received signal contains several slightly delayed copies of the transmitted signal, as the scatterers signals travel via different physical paths of different lengths.

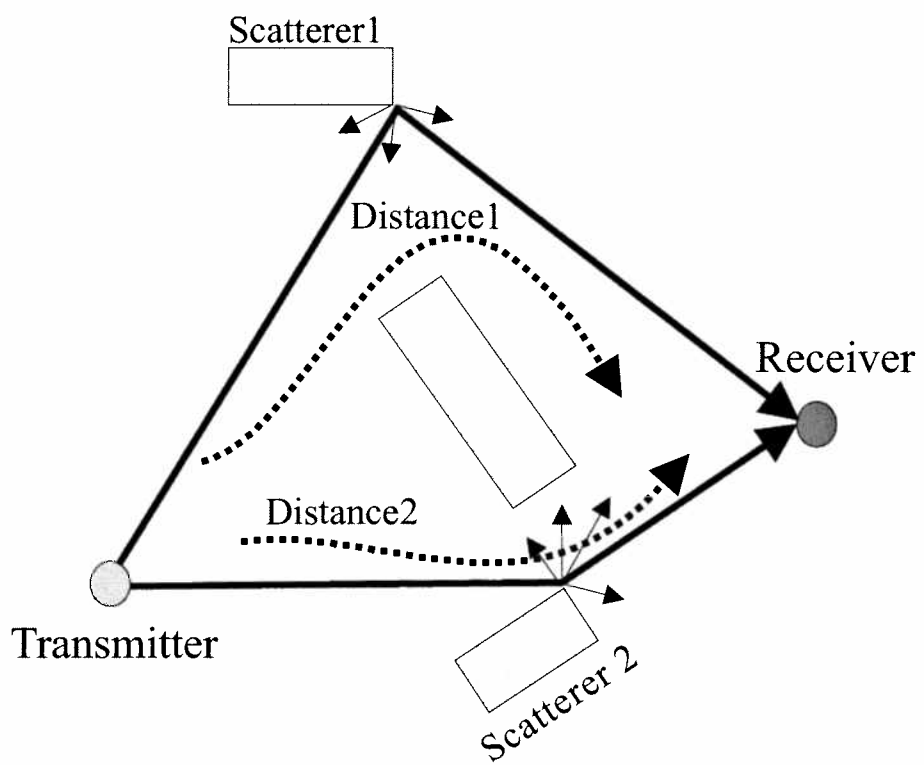


Figure 17: Geometry of the time variant propagation model[5].

3 Measurement Campaign - Mobilkom Austria Room A07A011

This chapter shows the results of all measurement campaigns performed in Room A07A011 at the Mobilkom office building. In the GSM 900, DCS 1800, UMTS, UHF and VHF frequency bands, several cubes, as well as small cubes and axis measurements were performed. The evaluation of the measured data is displayed for each frequency band. It could be seen, that there are no particular field distribution function for a specific scenario.

3.1 Overview

In the course of this project several measurement campaigns were performed at two different locations. First at an office building of the Mobilkom Austria in Vienna and second at the *ARC Seibersdorf research GmbH* office building. The latter is surrounded by a large rural area, therefore two typical scenarios were under investigation. Based on the COST 259 scenarios, we categorized them as General Typical Urban (GTU) for the measurements at the Mobilkom Office building and General Rural Area (GRA) for the *ARC Seibersdorf research GmbH*. A more detailed description of the COST 259 model can be found in Appendix C. Various frequencies were scanned for each location, these frequencies are described later on.

The Mobilkom Austria provided a large conference room in an office building in Vienna. The district where the office building is located is closed to the inner city but has no obvious bigger buildings in the vicinity which could have a deep impact on the propagation path. The room where all measurements were performed, consisted of a small anteroom with an area of $15.6m^2$ and the conference room itself with an area of $42m^2$. A schematic of the conference room (Room A07A011) can be seen in Figure 18. The room is located at the seventh floor close to the mobile communication base station. The distances to each transmitting antenna for each frequency can be found in Table 2. GSM 900, DCS 1800 and UMTS antennas were mounted on one mast on the opposite side of the building front. The antennas were mounted one upon the other, where the GSM 900 antenna was mounted on the bottom, the one on top was the UMTS antenna and the one in the middle was the DCS 1800 antenna.

Concrete walls covered with wood build the structure of the room. Four windows were on the side which was in direction of the transmitting antenna as well as on the opposite side of the room (see Figure 18). Figure 19 shows the position of the transmitting antennas and the location of the Room A07A011 where all measurements were performed.

During the whole measurement campaign, which started on the 11th of March 2003 and ended on the 23rd of March 2003, the room was closed for anybody

Frequency Band	Distance
GSM 900	33 m
DCS 1800	35 m
UMTS	37 m
UHF - FS ORF 2	few km
VHF - RF	few km

Table 2: Distances to the transmitting antenna for each frequency band at the Mobilkom Austria office building.

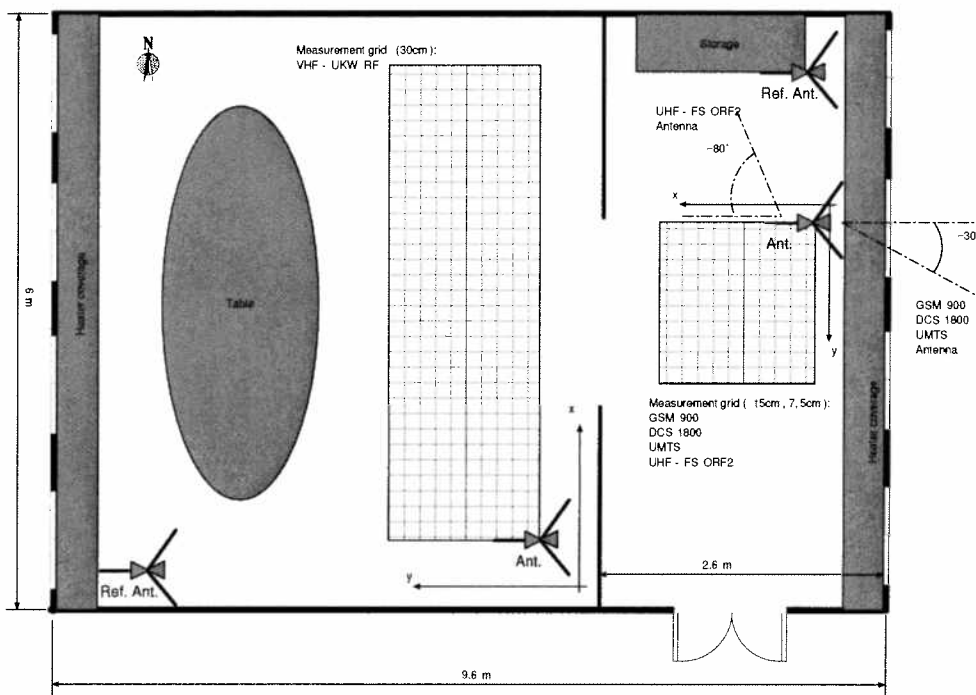


Figure 18: Schematic of the Conference Room A07A011 at the Mobilkom Austria. The smaller room on the right side is the anteroom with an area of $15.6m^2$ and the bigger room on the left side is the conference room with an area of $42m^2$. The measurement grid can be seen in each part of the room with the reference antenna placed on a fixed position in the room and the measurement antenna placed on the first examined position at the investigated area (cube, small cube). The height of the room is 2.5m.

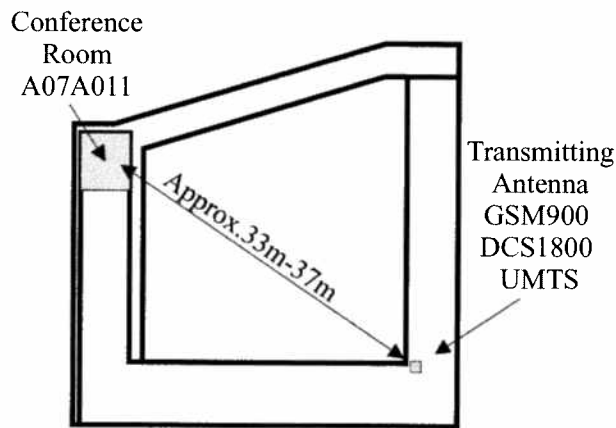


Figure 19: Schematic of the whole building including the conference room and the transmitting antenna.

except for the person who performed the measurements. Other offices were on one side of the conference room where people worked during the week and sometimes on Saturday.

3.2 GSM 900 - Cube Measurements

Measurements at a frequency of 946.0MHz were performed in the anteroom. The investigated areas were a cube, a small cube and line measurements along the x-axis and y-axis through the center of the cube. Continuous measurements during the nighttime delivered also a large amount of data.

In the beginning, global considerations of the measurement data were performed as described in the following section.

3.2.1 Mean, Standard Deviation and Amplitude Distribution

The whole evaluation process will be described in detail starting with the measurement data of the cube. The field measurements were done as described in Section 2.

In a first examination the analysis of the field strength distribution is generally and globally, without considering the spatial positions of the measured field strength in the investigated area.

A statistical description of the measurement data can be found in Table 3. Deviations from the global mean value of the whole examined cube were found from -75% to +218%. This means that the smallest value is 25% and the highest value is 318% of the global mean value. Regarding this, the distribution of the measurement data is not a symmetric distribution and therefore not a Gaussian distribution.

Figure 20 shows the Gaussian distribution function. The standard deviation $\pm s$ for the gaussian distribution function is in a range which contains 68.3% of all

Examined Positions	343
Maximum Value [mV/m]	66.2
Minimum Value [mV/m]	5.2
Global Mean Value [mV/m]	20.8
Standard Deviation [mV/m]	8.9

Table 3: Mean value, minimum and maximum value and standard deviation - GSM 900, Mobilkom Austria Room A07A011.

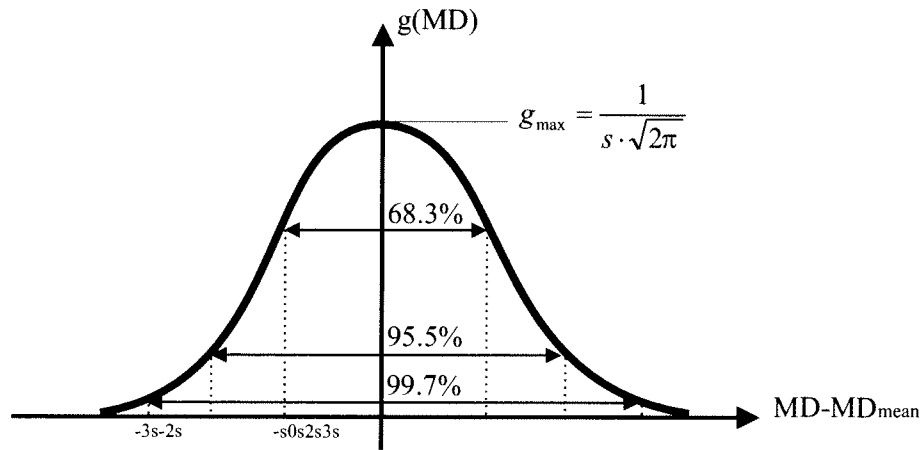


Figure 20: Gaussian distribution density function $g(MD)$; measurement data MD ; mean value of the measurement data MD_{mean} .

measurement data. The standard deviation, included in Table 3, is not equal with the gaussian standard deviation and has therefore to be interpreted in a different way.

In Figure 21 the amplitude distribution of the field strength values is displayed. It confirms what was stated earlier considering the positions of the mean value: the distribution is not uniform nor symmetric distributed over the field strength range. Lower field strength values were found more often than higher values. For many figures, the global mean value is indicated by f_{mean} .

3.2.2 Cumulative Distribution Function and Probability Density Function

The electromagnetic field strength values can be sorted by increasing amplitude. The generated graphical Figure is equal to the cumulative distribution function (see Figure 22). It describes the undershooting or overshooting of the level and if normalized to the maximum value, its numerical value is between 0 and 1 (according to 0% and 100% of the electromagnetic field strength). The mathematical description

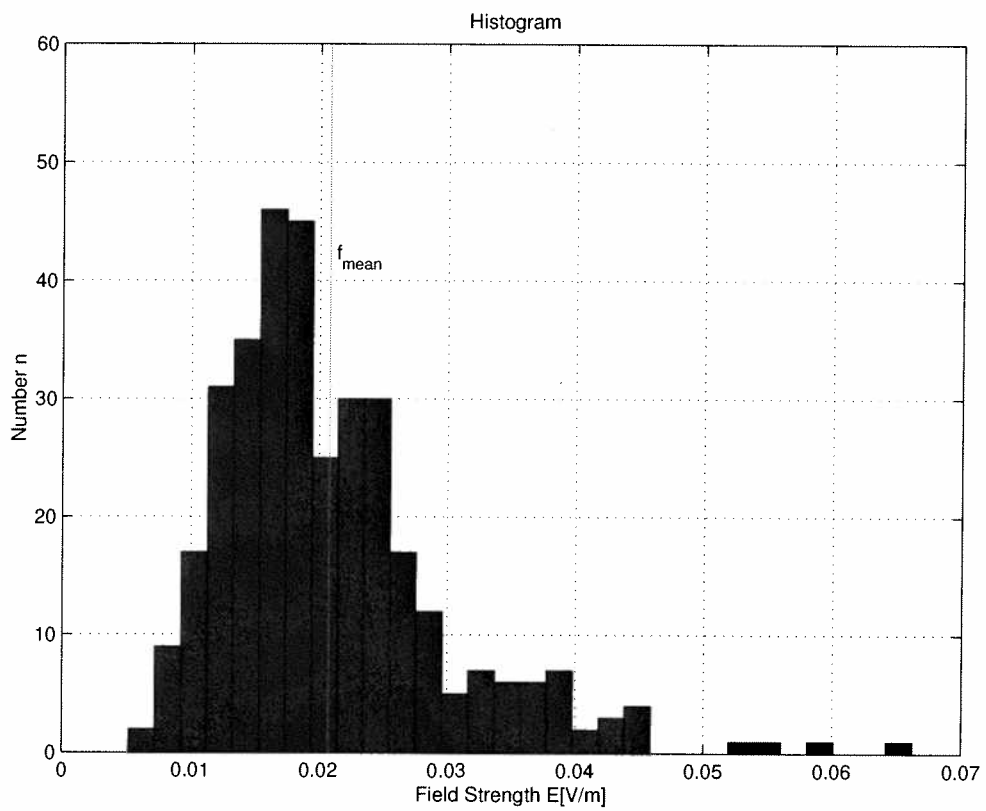


Figure 21: Global distribution of the electromagnetic field strength values disposed in 30 amplitude grades. Measured in Room A07A011 at the Mobilkom Austria office building at a frequency of 944.6MHz, the investigated area was a cube.

of those level rates are:

- undershooting of the field strength rate:

$$F_{under}(E) = P(E \leq E_{boundary}) \quad (10)$$

F_{under} is the probability that the field strength value E is smaller or equal to the boundary value $E_{boundary}$. The level overshooting definition is equal to:

- overshooting of the field strength rate:

$$F_{over}(E) = P(E > E_{boundary}) \quad (11)$$

with $F_{over}(E)$ as the probability that the field strength value E is bigger than the boundary value $E_{boundary}$.

Due to the level undershooting value $F_{under}(E)$ the cumulative distribution function shows that 59.5% of the measured electromagnetic field strength values are lower than the global mean value.

The first differentiation of the cumulative distribution function delivers the probability density function (pdf). It describes the density or how common field strength values are appearing in a specific range. Differentiations of functions can only be derived from continuous functions so that the measured distribution functions (which are discrete functions) must be approximated by a polynomial approximation. The red line in Figure 22 shows the approximation of the measured field strength values. Due to this approximation procedure, it is possible that values higher than 1 (which is equal to 100%) can occur, therefore the cumulative distribution functions (cdf) are not plotted in the range between 0 and 1 (as usual), because if so, it could be possible, that the approximated curve would disappear and reappear after reaching the regions with values around 1.

Using the percentiles for the characterization of the distribution function is helpful. The most commonly used percentiles are the lower and higher quantile ($E_{25\%}$, $E_{75\%}$), lower and higher decile ($E_{10\%}$, $E_{90\%}$) as well as the quintile ($E_{50\%}$) with the variable E as the probability. The percentiles can directly be read off the cumulative distribution function (see Figure 22). Table 4 shows the percentiles of the distribution function, measured in the GSM 900 frequency band, in the Mobilkom Austria office building (Room A07A011).

The percentiles are values in a physical unit $[\frac{V}{m}]$. To make them comparable to others measurement results the right column of Table 4 shows the normalized value (normalized to the maximum electromagnetic field strength). This identification number builds an easily comparable value in the range of 0 to 1. The normalized

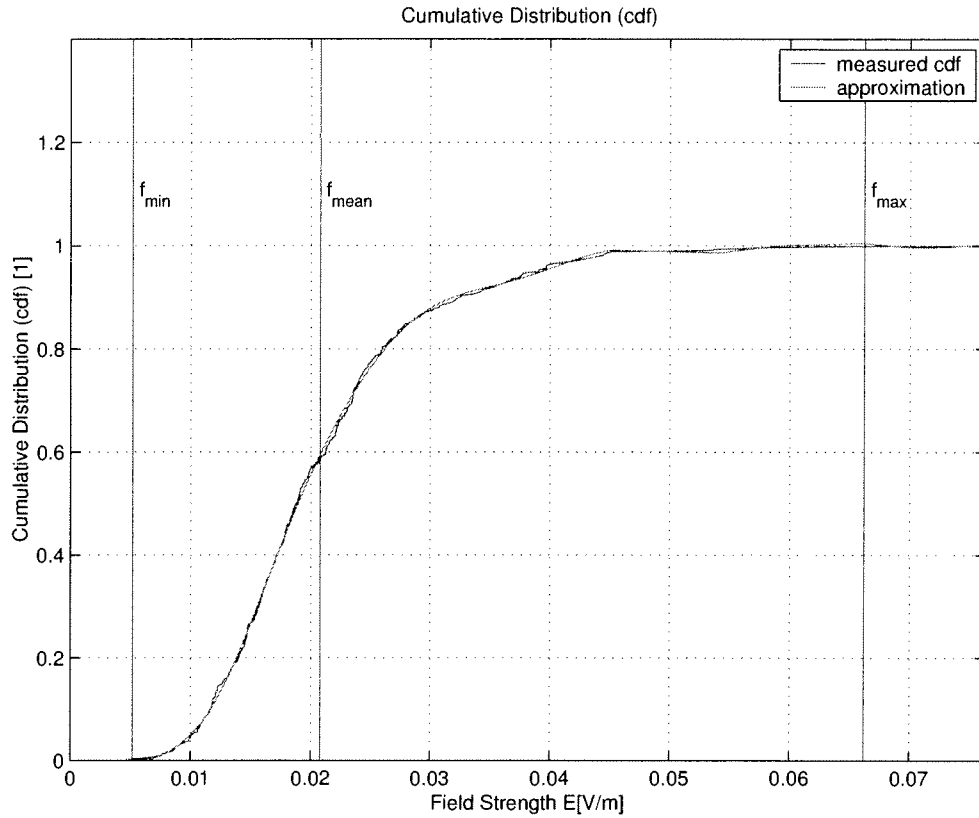


Figure 22: Cumulative distribution function (cdf) of the global field distribution (GSM 900 - Room A07A011 Mobilkom Austria).

Percentiles	Description	Value [$\frac{mV}{m}$]	Normalized to the Maximum [%]
$E_{10\%}$	lower decile	11.6	17.5
$E_{25\%}$	lower quartile	14.8	22.3
$E_{50\%}$	quintile	18.9	28.5
$E_{75\%}$	higher quartile	24.6	37.2
$E_{90\%}$	higher decile	32.7	49.5

Table 4: Lower and higher quartile, lower and higher decile, quintile as well as the relative percentile referring to the maximum of the electromagnetic field strength (Mobilkom Austria Room A07A011 at GSM 900).

percentiles show the information about the partition of the values compared to the maximum value of the field strength. For example Table 4 shows percentile $E_{50\%}$, which means that 50% of all field strength values are smaller than the field strength value at 28.54% of the maximum.

The probability density function can be derived as follows:

$$f_x = \frac{dF_x(x)}{dx} \quad (12)$$

with the characteristics:

$$f_x \geq 0 \quad \text{for} \quad -\infty < x < +\infty \quad (13)$$

and

$$\int_{-\infty}^{+\infty} f_x(x) dx = 1 \quad (14)$$

which means that the sum of the probability over the full range must be equal to 1 or 100%. The probability that a field strength value E is within two boundaries a and b , can be derived by following Equation:

$$P(a < E < b) = F_x(b) - F_x(a) = \int_a^b f_x(x) dx \quad (15)$$

The requirement for the application of this Equation 15 is that the function $f_x(x)$ (which is stated as known) must be integrable and continuous within the boundaries a and b . The probability density function (see Figure 23) can be derived by differentiating the cumulative distribution function according to Equation 12.

The maximum value of the probability density function does not match the arithmetic mean (this would only be the case if the distribution would be a Gaussian-distribution), the maximum is located on the left side of the global mean value. The expressiveness of the cumulative distribution function (cdf) and the probability density function (pdf) is equal but the advantage of the pdf is that the inflection point of the cdf is equal to the maximum at the pdf and is therefore obvious. Considering the maximum, it shows the field strength levels which appears most and are therefore most likely.

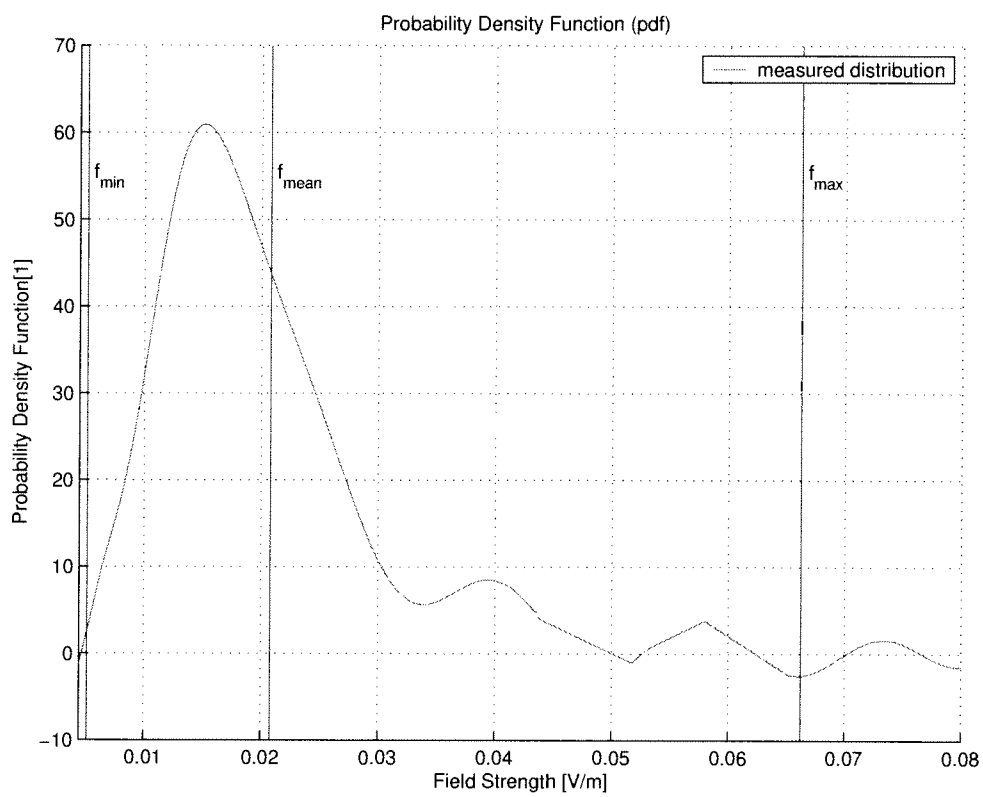


Figure 23: Probability Density function (pdf) of the global field distribution (GSM 900 - Room A07A011 Mobilkom Austria).

3.2.3 Identification of the Probability Density Function

For statistical forecasts and general statements of the field distribution in arbitrary situations it is necessary to have information about the principle structure of the distribution function.

A possible mathematical approximation, of the measured probability density function for the Room A07A011 at GSM 900, could be the LogNormal distribution shown in Figure 24. The LogNormal distribution is described by the following Equation:

$$y = f(x | \mu, \sigma) = \frac{1}{x\sigma\sqrt{2\pi}} \cdot e^{-\frac{(\ln(x)-\mu)^2}{2\sigma^2}} \quad (16)$$

where y is an independent and x is a dependent variable as well as the two variables σ and μ as characteristic location parameter. With this two variables, which have to be fitted to the particular curve progression, the positions of the curve along the field strength can be adjusted.

Figure 24 shows the LogNormal distribution which is fitted to match the polynomial approximated pdf.

3.2.4 Local Distribution of the Measurement Data

After the global examination of the field strength values this chapter considers the spatial variations. For the spatial variations, no coherence could be found, considering recurrent distributions patterns. But there are differences of the field strength values in the different levels, as can be seen in Figure 25.

3.2.4.1 Local Means

The local mean value is defined as the arithmetic mean over the 49 examined positions in one level. The description of a level takes place after the position of the perpendicular axis. For example Level "z180" is the level in direction of the z-axis, which is build by two straight lines, parallel to the x-axis and parallel to the y-axis spanning an area and crossing the point (0/0/180cm). Figure 26 shows this by means of the z-axis.

Figure 27 shows the trend of the local mean increasing in the x, y and z direction. Table 6 shows the mean values of each level in z direction. The arithmetic mean of each level doesn't show a big deviation regarding the global mean with exception of the z-Level. Starting at Level 1, with a value of 152.9% of the global mean (see Figure 27, the global mean value is indicated by the horizontal line f_{mean}), the mean value is tremendous decreasing. In the next level the value decreases to approximately 95.7% of the global mean. The minimum is reached at Level 4 with an value of only 59.1%. After the minimum, the value is increasing till approximately the global mean value and is then nearly constant around this value.

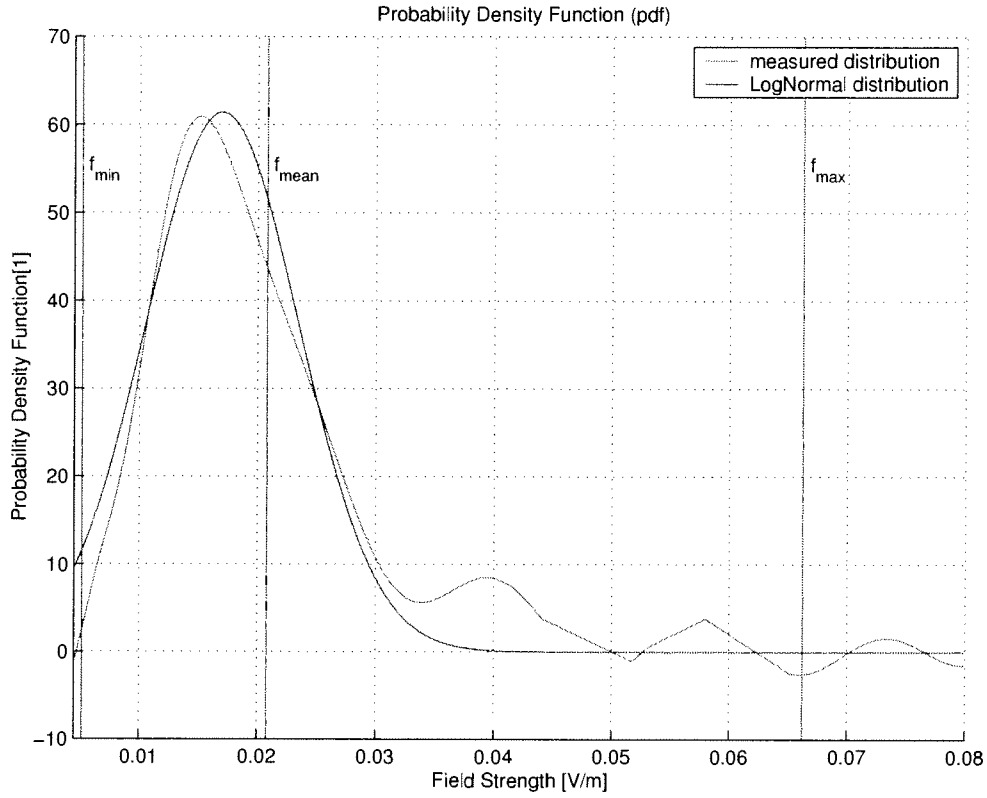


Figure 24: Approximation of the Probability Density function (pdf) with a LogNormal distribution (GSM 900 - Room A07A011 Mobilkom Austria).

Level (Index)	x-axis	y-axis	z-axis
1	x0	y0	z90
2	x15	y15	z105
3	x30	y30	z120
4	x45	y45	z135
5	x60	y60	z150
6	x75	y75	z165
7	x90	y90	z180

Table 5: Index and description of each level.

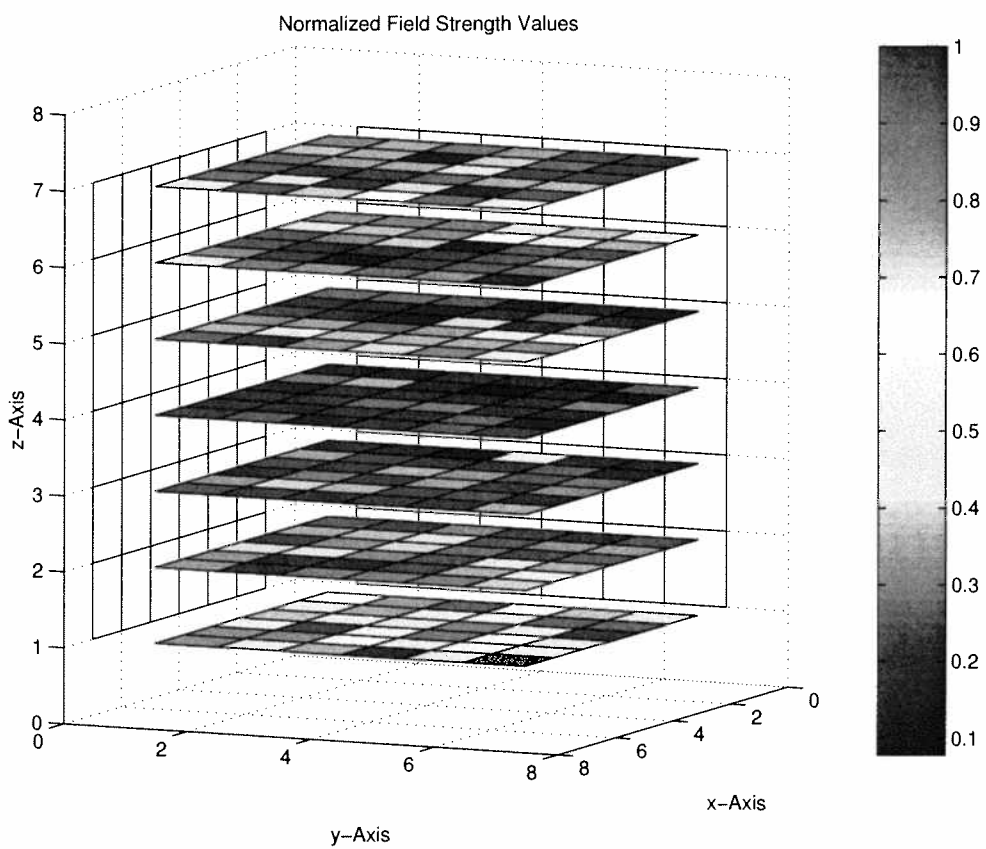


Figure 25: Distribution of the field strength values normalized to the maximum value (GSM 900 - Room A07A011 Mobilkom Austria).

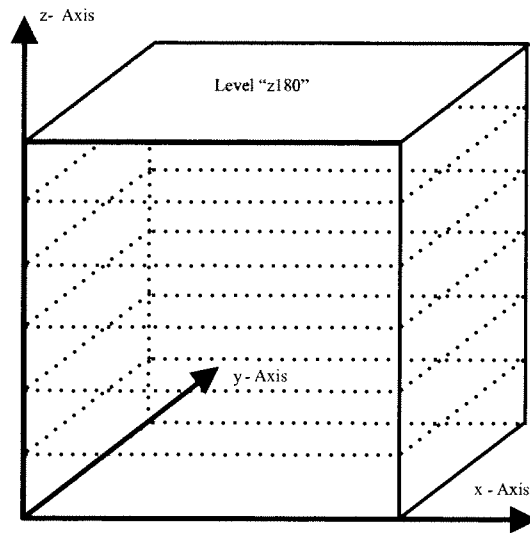


Figure 26: Nomenclature of the z-Level parallel to the area built by the x-axis and the y-axis. The Level z180 is displayed as an example. Analog to this nomenclature the x- and y-Level can be built.

The relative deviations of all local means according to the global mean value can be seen in the right diagram of Figure 27. The level with the minor deviation around the global mean is the x-Level where all deviations are below 10%.

3.2.4.2 Local Minima and Maxima

The variation of the minima and maxima is interesting, too. How is the behavior of the local field strength distribution of each level and can laws be deduced? A partial answer gives Figure 28 where minimum, maximum and the arithmetic mean of the three levels in each direction are displayed - normalized to the global mean. Be-

Level	mean [$\frac{mV}{m}$]	$\frac{localmean}{globalmean}$ [%]
z90	31.8	152.9
z105	19.9	95.7
z120	16.6	79.8
z135	12.3	59.1
z150	19.2	92.3
z165	18.6	89.4
z180	20.0	96.2

Table 6: Local mean of each level (GSM 900 - Room A07A011 Mobilkom Austria).

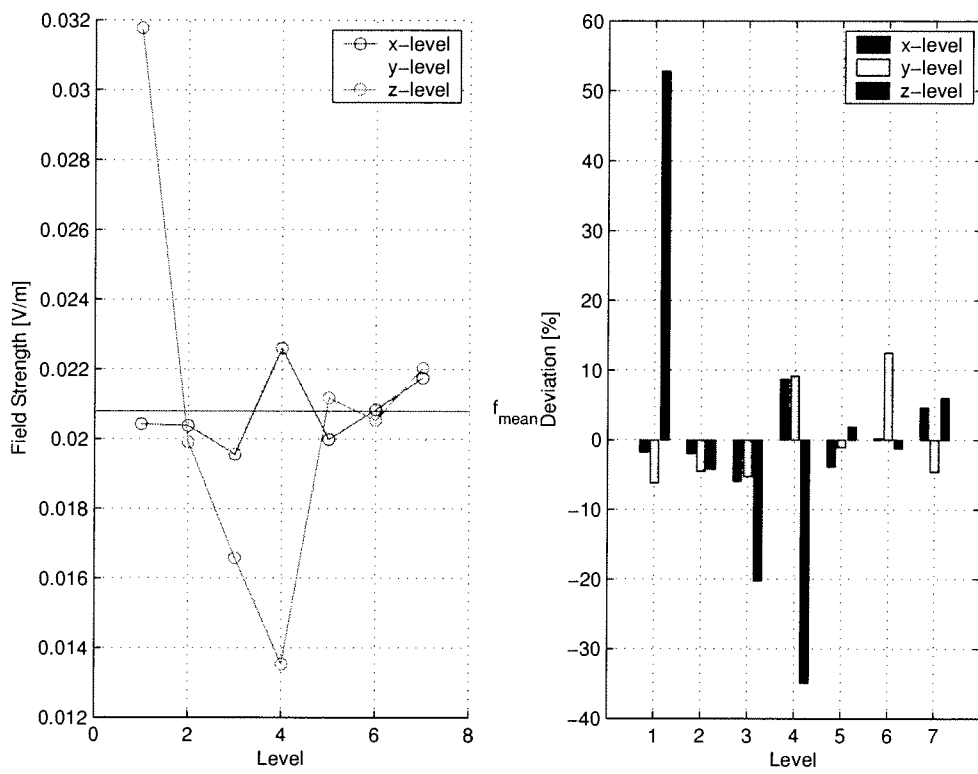


Figure 27: Arithmetic mean of the single levels (GSM 900 - Room A07A011 Mobilkom Austria).

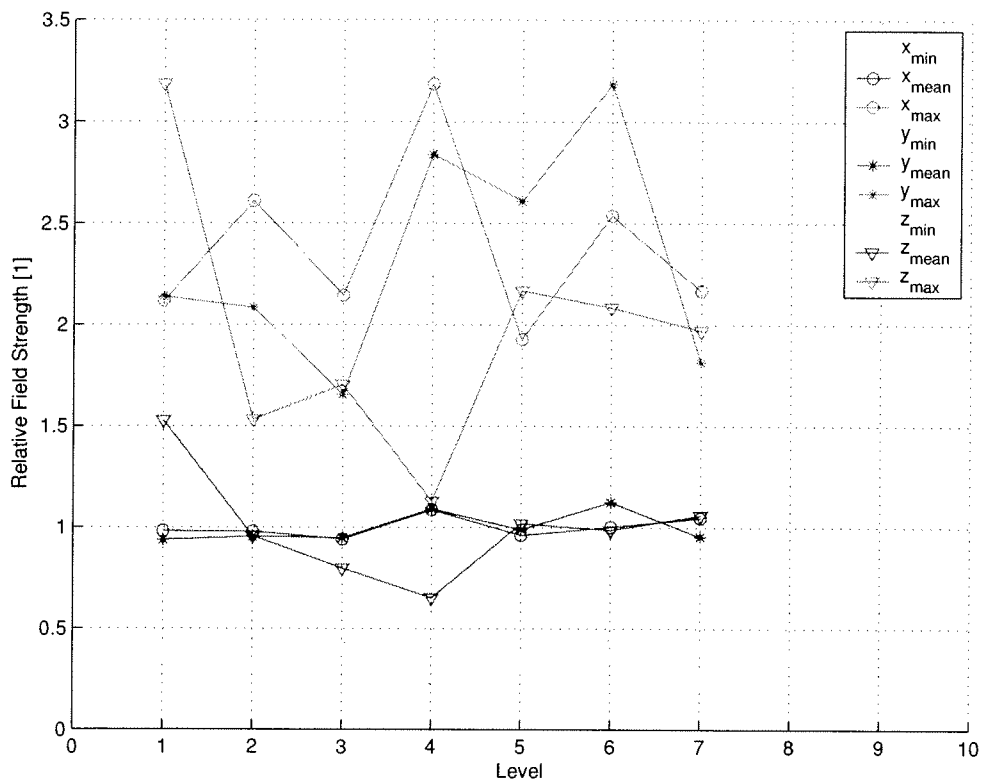


Figure 28: Relative local minimum, maximum and arithmetic mean normalized to the global mean (GSM 900 - Room A07A011 Mobilkom Austria).

cause of the reference to the global mean, the factor how high or low the minimum and maximum are, can directly be read out of the ordinate.

It can be seen that between the maximum, found in the z-Level, and the global mean lies a factor of 3.2. The minimum, found in the x-Level, is by a factor of 0.25 smaller than the global mean value.

The z-Level shows a negative gradient with increasing level index, which means a decreasing of the field strength starting at Level 1 until Level 4. At Level 5, Level 6 and Level 7 the value is nearly constant. This is equal at the minima, maxima and the mean in this level. Level x and Level y doesn't show a similar behavior.

3.3 DCS 1800 - Cube Measurements

Measurements at a frequency of 1812.4MHz were also performed in the same room (Room A07A011 at the Mobilkom Austria Office Building). The measurement set-up was the same as for the measurements described earlier in Section 3.2. Figure 18 shows the room as well as the measurement grid in the anteroom. The mobile communication base station with the transmitting antenna is 35m away from the investigated area. The direction of the antenna can also be seen in Figure 18.

Examined Positions	343
Maximum Value [mV/m]	140.6
Minimum Value [mV/m]	8.7
Global Mean Value [mV/m]	29.0
Standard Deviation [mV/m]	13.4

Table 7: Mean value, minimum and maximum value and standard deviation - DCS 1800, Mobilkom Austria Room A07A011.

Due to the fact that the transmitting antenna is located 2m higher than the GSM 900 antenna the Line Of Sight condition is only partially valid.

As done in the previous measurement campaign (GSM 900), first of all the global considerations were taken into account. The distribution patterns didn't show any regularity.

3.3.1 Mean, Standard Deviation and Amplitude Distribution

The field strength values are statistically described by the values of Table 11. By comparing the maximum value with the maximum value of the GSM 900 cube measurements, it can be seen, that the maximum field strength in the DCS 1800 frequency band is by a factor of 2.12 higher.

Deviations from the global mean value from -70% to +384% were found for the whole examined cube. This means that the smallest value is 30% and the highest value is 484% regarding the global mean value. Regarding this the distribution of the measurement data is not a symmetric distribution and therefore not a Gaussian-distribution. This behavior was already found in the previous measurement campaign (see Section 3.2).

The maximum value is 16.2 times higher then the minimum value. The amplitude distribution is not symmetric because the arithmetic mean is located far left of the center between minimum ($8.7 \frac{mV}{m}$) and maximum ($140.0 \frac{mV}{m}$), as Figure 29 shows.

The amplitude distribution is focused on a very small range between $10.0 \frac{mV}{m}$ and $80.0 \frac{mV}{m}$. The maximum is located on the left side of the global mean. The distribution (in Figure 29) shows a fast rise at the beginning and decreases smoother after reaching the maximum.

3.3.2 Cumulative Distribution Function and Probability Density Function

The cumulative distribution function (see Figure 30) can be build by arranging the field strength with increasing values, as described in Section 3.2.2. Due to the level undershooting value the cumulative distribution function shows that 60% of

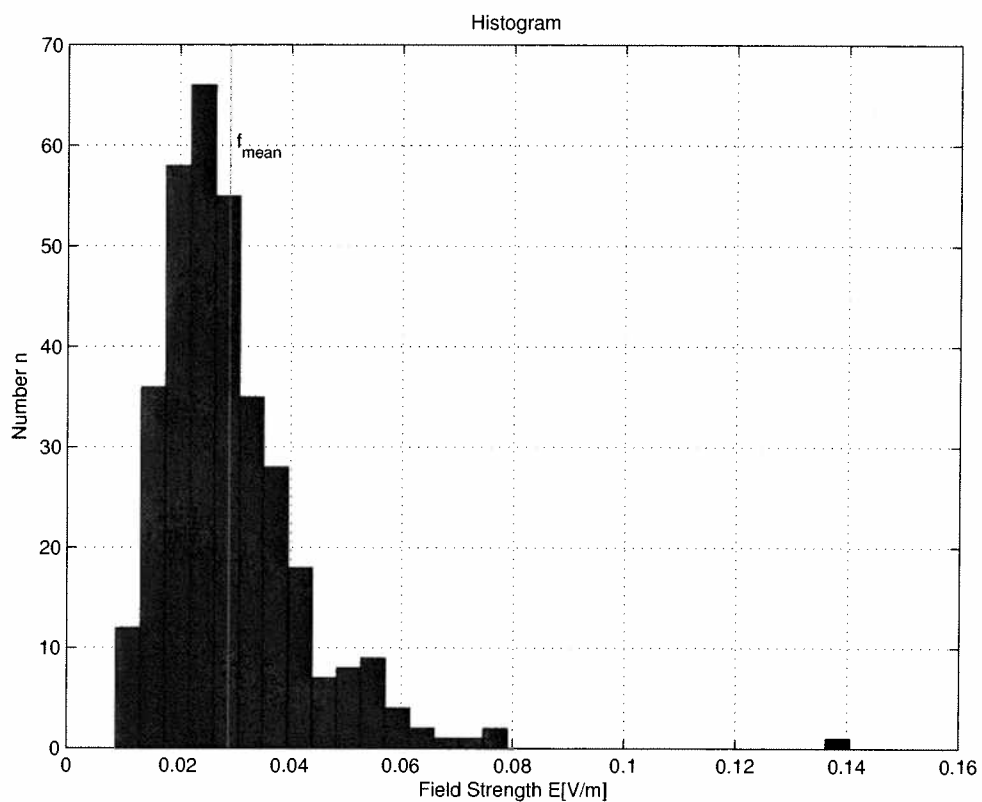


Figure 29: Global distribution of the electromagnetic field strength values disposed in 30 amplitude grades. Measured in Room A07A011 at the Mobilkom Austria office building at a frequency of 1812.4MHz, the investigated area was a cube.

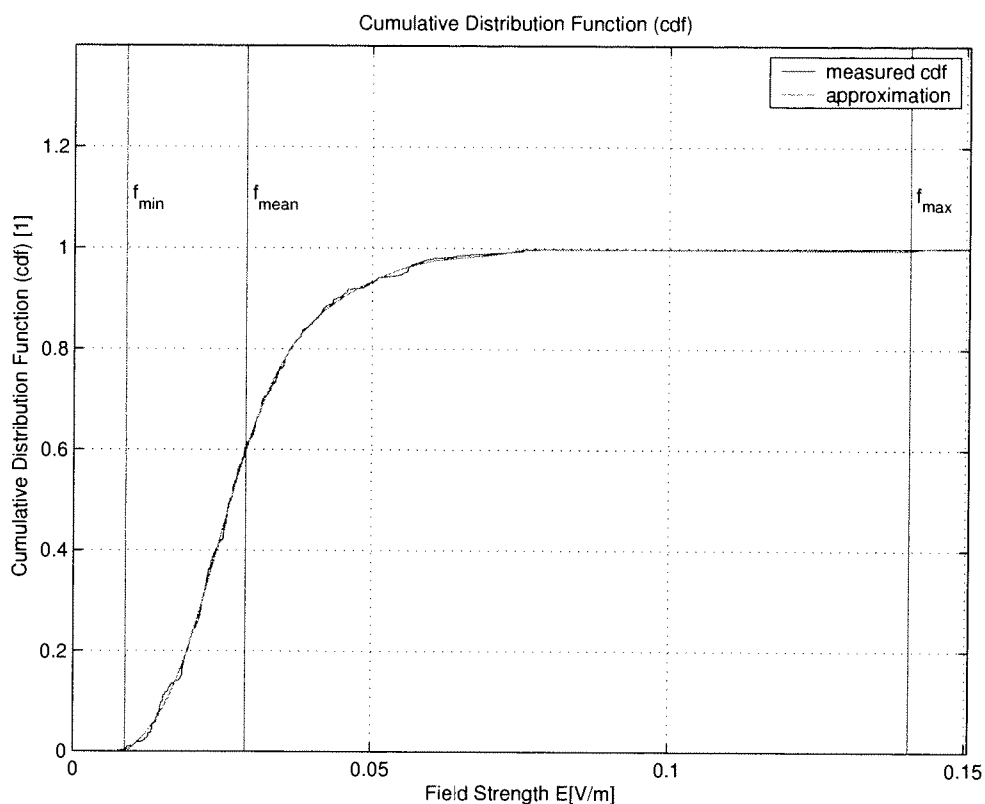


Figure 30: Cumulative distribution function (cdf) of the global field distribution (DCS 1800 - Room A07A011 Mobilkom Austria).

the measured electromagnetic field strength values are lower than the global mean value.

In the range between $40 \frac{mV}{m}$ and $70 \frac{mV}{m}$ a small deviation from the polynomial approximation can be seen. The percentiles of the cumulative distribution function are shown in Table 8, these are values in the physical unit of $[\frac{V}{m}]$. To make them comparable to other distributions the right column of Table 8 shows the normalized value (normalized to the maximum electromagnetic field strength). This value builds an easily comparable value in the range of 0 to 1.

For example Table 8 shows percentile $E_{50\%}$, which means that 50% of all field strength values are smaller than the field strength value at 18.8% of the maximum.

The probability density function (see Figure 31) can be derived by differentiating the cumulative distribution function (see Equation 12). As described in the section before, the probability density function (pdf) describes how common field distribution values appear in a specific range. A polynomial approximation has to be made otherwise the pdf can't be derived. A differentiation is only possible when the function is a continuous function. The red line in Figure 31 shows the approximation of the measured field strength values.

Percentiles	Description	Value [$\frac{mV}{m}$]	Normalized to the Maximum [%]
$E_{10\%}$	lower decile	15.6	11.1
$E_{25\%}$	lower quartile	20.5	14.6
$E_{50\%}$	quintile	26.4	18.8
$E_{75\%}$	higher quartile	34.1	24.3
$E_{90\%}$	higher decile	44.3	31.5

Table 8: Lower and higher quartile, lower and higher decile, quintile as well as the relative percentile referring to the maximum of the electromagnetic field strength (Mobilkom Austria Room A07A011 at DCS 1800).

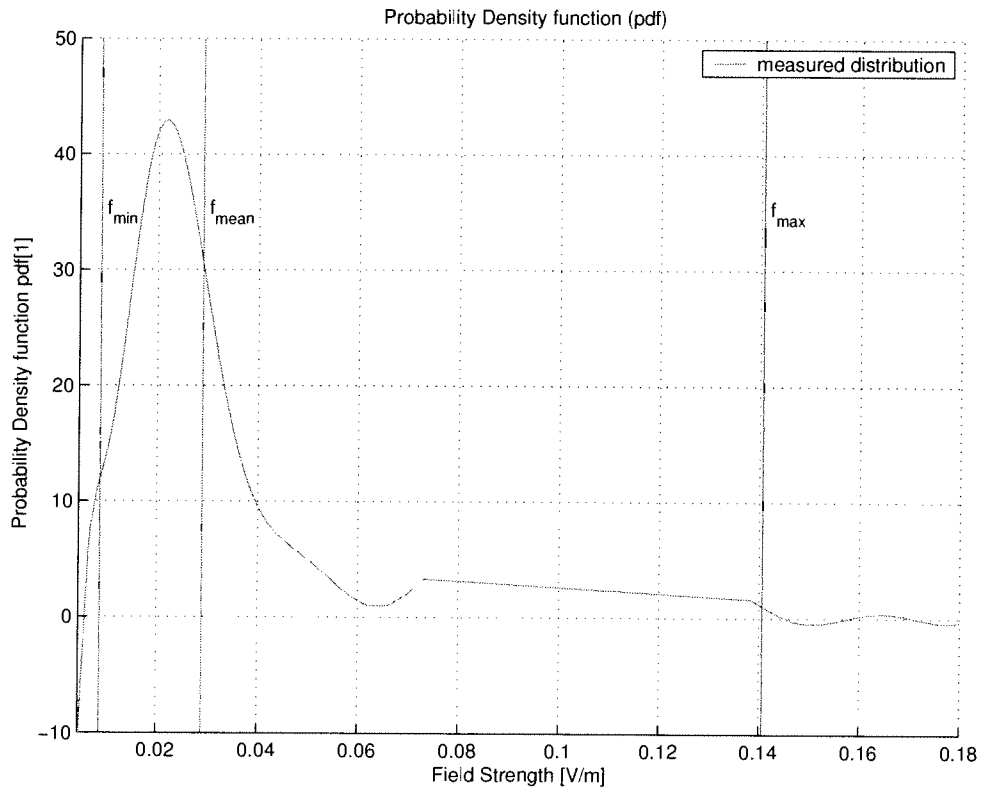


Figure 31: Probability density function (pdf) of the global field distribution (DCS 1800 - Room A07A011 Mobilkom Austria).

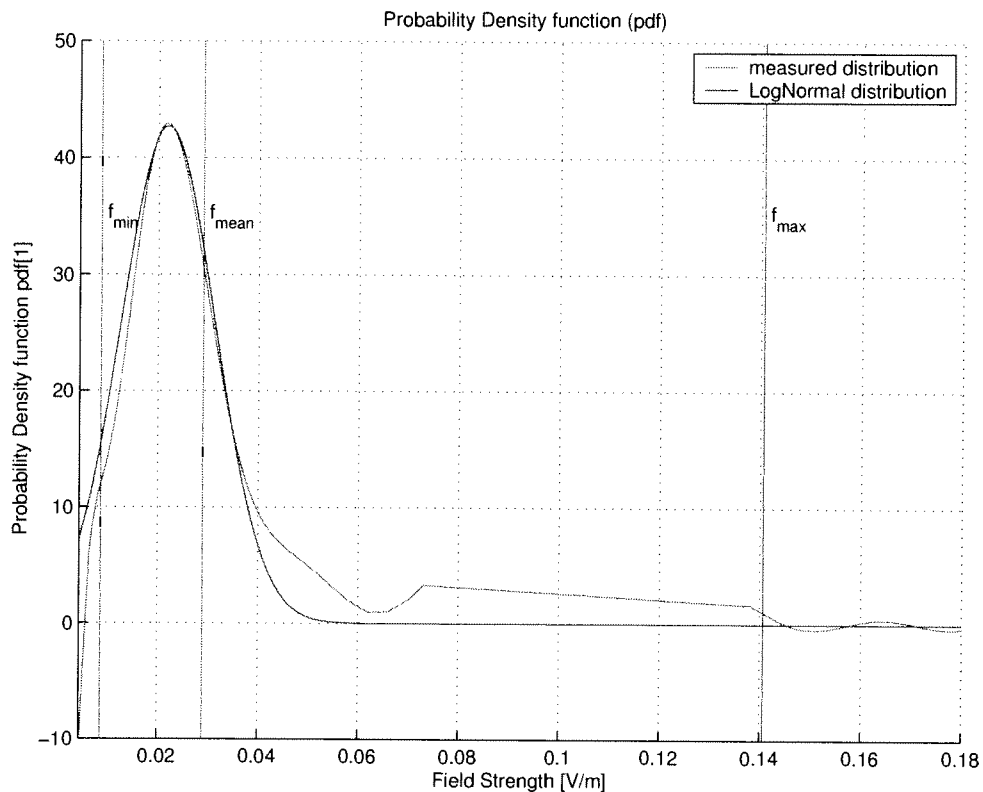


Figure 32: Approximation of the probability density function (pdf) with a LogNormal distribution (DCS 1800 - Room A07A011 Mobilkom Austria).

3.3.3 Identification of the Probability Density Function

A possible approximation for the probability density function is displayed in Figure 32. It is characterized as a LogNormal distribution described by Equation 16 in the section before.

The validity of the polynomial approximation is in the range between minimum and maximum of the electromagnetic field strength.

3.3.4 Local Distribution of the Measurement Data

After the global considerations of the field strength distribution the local demeanor was investigated. The field strength values are very homogenous distributed over the whole cube with only a small maxima in Level z135 (see Table 5 for the nomenclature). Figure 33 shows the spatial variation of the electromagnetic field strength.

3.3.4.1 Local Means

As described at the GSM 900 measurement campaign the local mean value is defined as the arithmetic mean over the 49 examined positions of one level. The description of a level takes place by the direction of the axis which is perpendicular

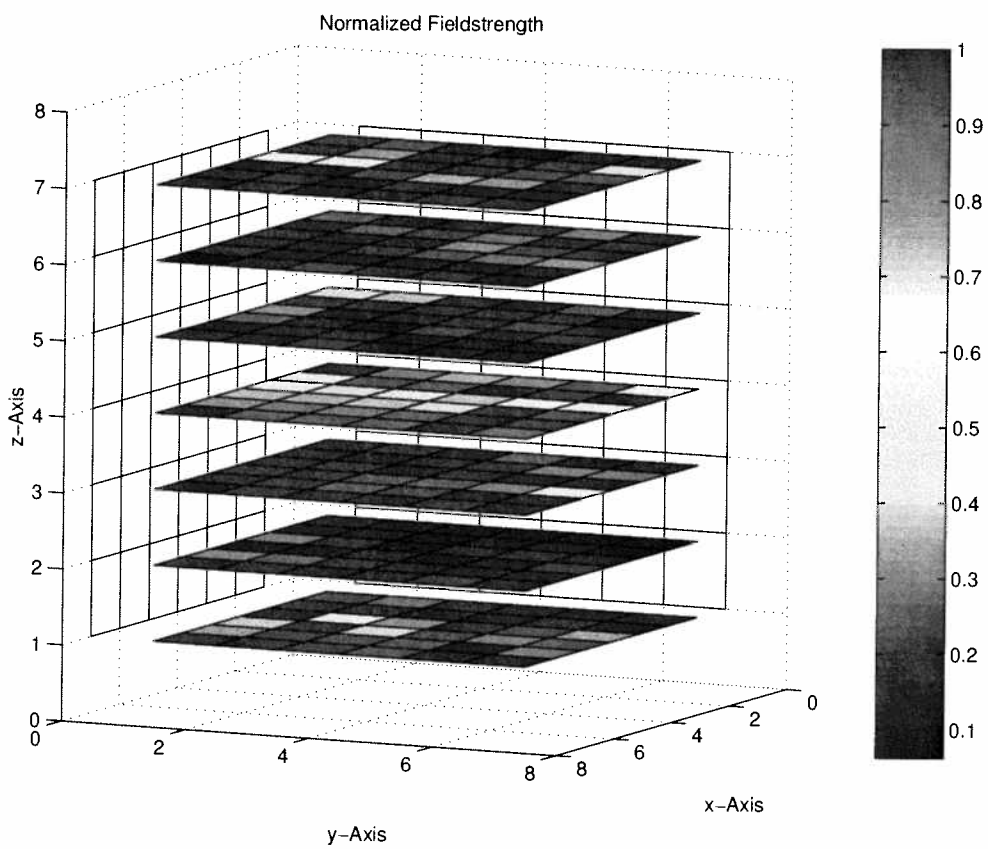


Figure 33: Distribution of the field strength values normalized to the maximum value (DCS 1800 - Room A07A011 Mobilkom Austria).

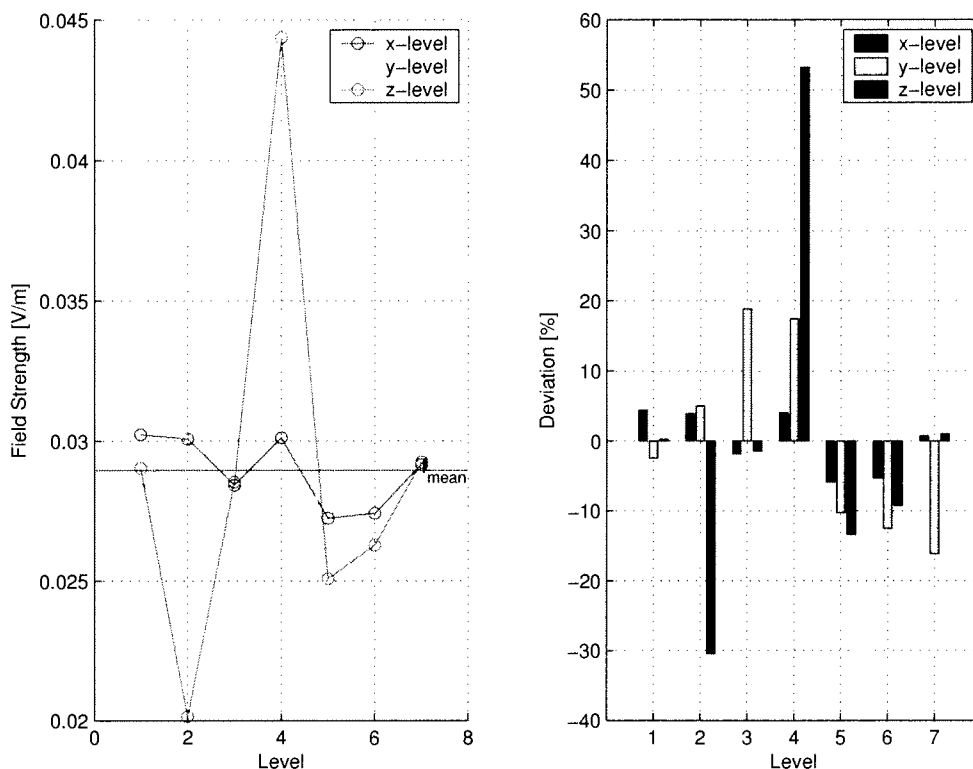


Figure 34: Arithmetic mean of each level and deviations from the global mean in [%] (DCS 1800 - Room A07A011 Mobilkom Austria).

to the plane spanned by the two other axis. Figure 26 shows this by means of the z-axis.

Figure 34 shows the arithmetic mean of each level. The arithmetic mean of the x-Levels doesn't show a big deviation from the global mean, the values in the y-Levels are increasing until Level 3 is reached and are then decreasing starting at Level 3 until Level 7. The maximum deviation occurs in the z-Level, with a minimum at Level 2 and a maximum at Level 4 with values of $20.5 \frac{mV}{m}$ for the minimum and $44.7 \frac{mV}{m}$ for the maximum.

3.3.4.2 Local Minimum and Maximum

Figure 35 shows the variation of the local minimum and maximum of each level normalized to the global mean value. Because of the normalization regarding the global mean global, the factor showing how high or low the minima and maxima are compared to the global mean value, can directly be read off the ordinate. It can be seen that the global maximum is by a factor of 4.7 higher than the global mean value and the global minima is by a factor of 3.1 smaller than the global mean value.

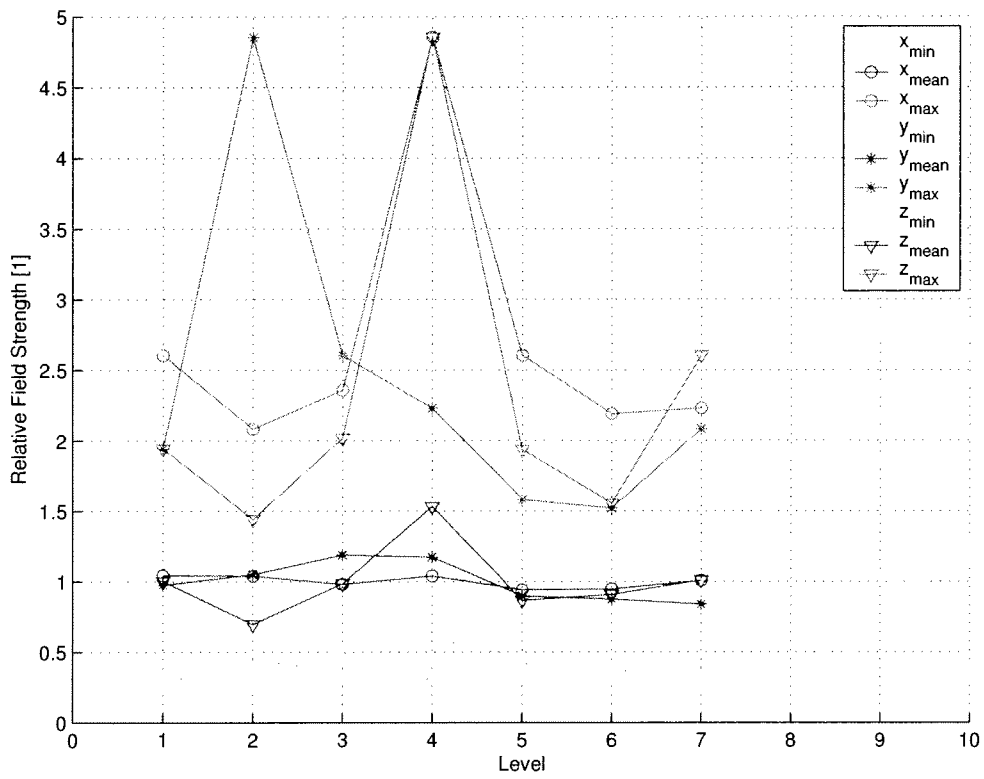


Figure 35: Relative local minima, maxima and arithmetic mean normalized to the global mean value (DCS 1800 - Room A07A011 Mobilkom Austria).

Examined Positions	343
Maximum Value [mV/m]	85.7
Minimum Value [mV/m]	26.8
Global Mean Value [mV/m]	48.0
Standard Deviation [mV/m]	10.1

Table 9: Mean value, minimum and maximum value and standard deviation (Gauß) UMTS, Mobilkom Austria room A07A011.

3.4 UMTS - Cube Measurements

The electromagnetic field distribution of a Universal Mobile Telecommunication System (UMTS) was also under investigation. In order to make measurements possible, the Mobilkom Austria shut an indoor supply unit down so that only the transmitting signal from the antenna mast could be measured. To be able to measure a constant signal, only the pilot channel was transmitted via the antenna. The measurements were performed at a frequency of 2154.7MHz in the same way as described in Section 2.

The received signal was near the noise level so the windows were opened up a bit which raised the signal level for proper measurements. The investigated area was a cube described in Section 2.1.2, which was placed at the same location than in the measurements described before, with a distance between investigated volume and transmitting antenna of 37m. The investigated volume had only partly Line-Of-Sight (LOS) regarding the transmitting antenna due to a small roof above the windows (see Figure 5).

In the following sections the global aspects of this measurement data were taken under consideration.

3.4.1 Mean, Standard Deviation and Amplitude Distribution

Compared to the previous measurement (DCS 1800) the maximum value is only 3.2 times higher than the minimum value. The amplitude distribution is more symmetric than at the previous measurement (DCS 1800) which can be seen in Figure 36.

Deviations from the mean value of the whole examined cube from -79.0% to +78.5% were found. This means that the smallest value is 21.0% and the highest value is 178.5% of the global mean value. Regarding this, the distribution of the measurement data is not a symmetric distribution and therefore not a Gaussian distribution. This behavior was already found in the previous measurement campaigns (see Section 3.2 and Section 3.3).

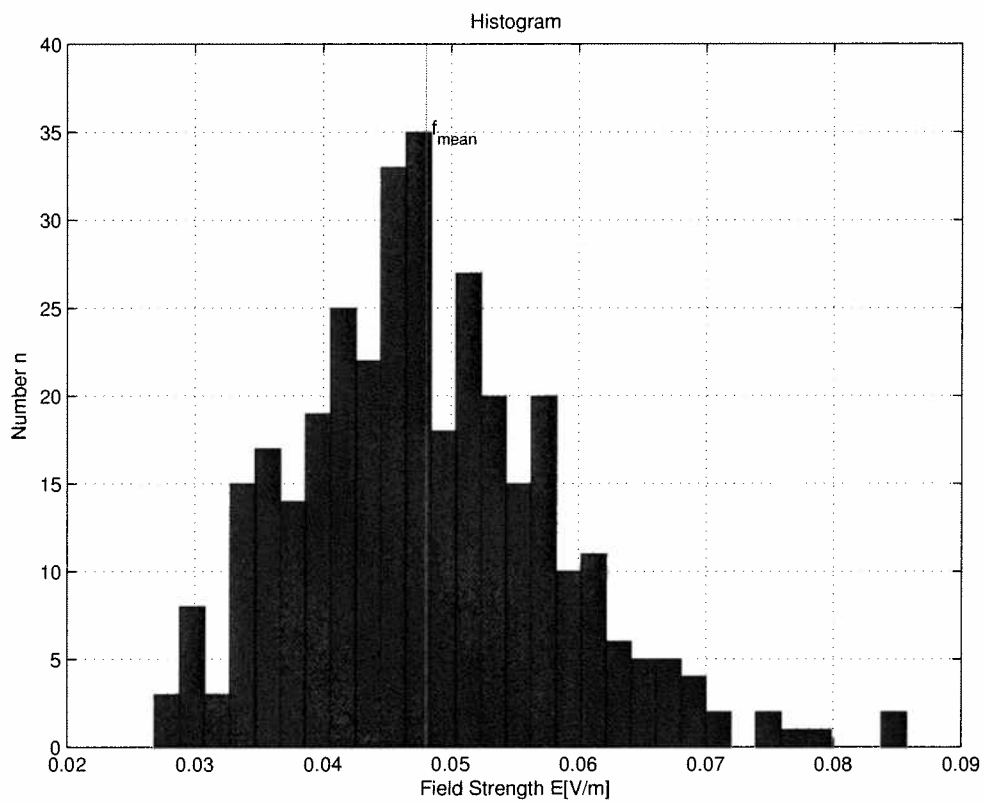


Figure 36: Global distribution of the electromagnetic field strength values disposed in 30 amplitude grades. Measured in Room A07A011 at the Mobilkom Austria office building at a frequency of 2154.7MHz, the investigated area was a cube.

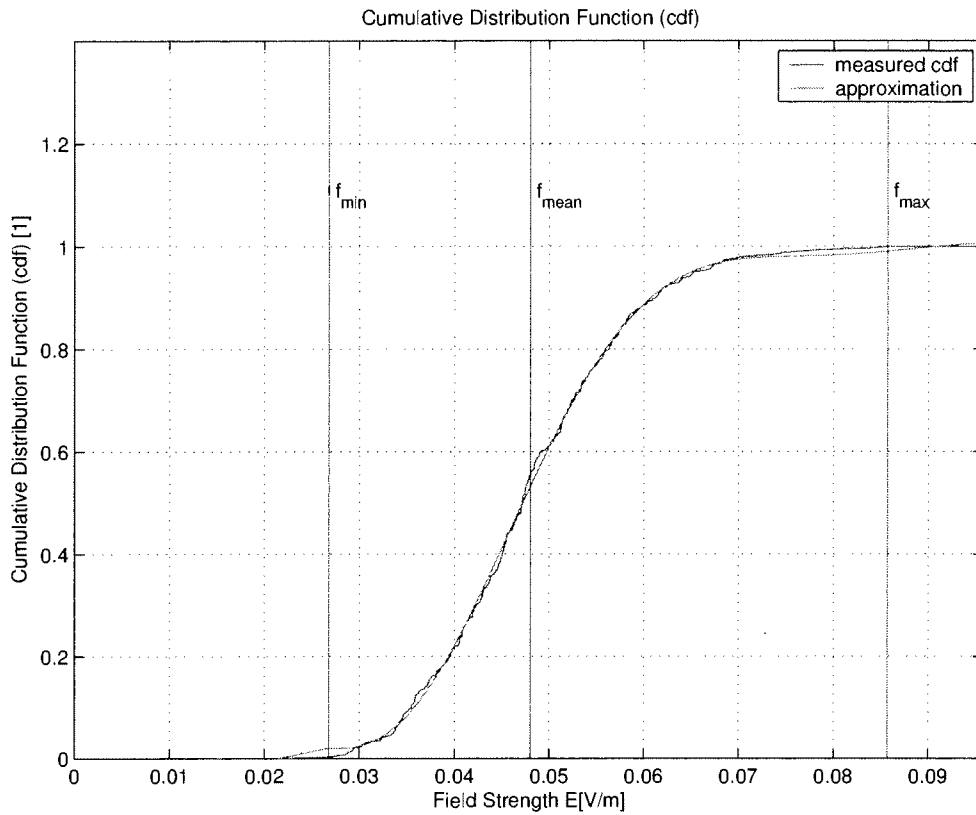


Figure 37: Cumulative distribution function (cdf) of the global field distribution (UMTS - Room A07A011 Mobilkom Austria).

3.4.2 Cumulative Distribution Function and Probability Density Function

The cumulative distribution function (see Figure 37) can be built by arranging the field strength by increasing values as described in Section 3.2.2.

The percentiles of the cumulative distribution function are shown in Table 10. The probability density function (see Figure 38) can be derived by differentiating the cumulative distribution function (see Equation 12).

3.4.3 Identification of the Probability Density Function

A possible approximation for the function is displayed in Figure 39. This approximation is characterized as a Rayleigh distribution described by the following Equation 17.

$$y = f(x | b) = \frac{x}{b^2} \cdot e^{-\frac{x^2}{2b^2}} \quad (17)$$

The variable b characterizes the location of the maximum and is therefore characterized as the location parameter. Compared to the LogNormal distribution (de-

Percentiles	Description	Value [$\frac{mV}{m}$]	Normalized to the Maximum [%]
$E_{10\%}$	lower decile	35.5	41.4
$E_{25\%}$	lower quartile	41.1	47.9
$E_{50\%}$	quintile	47.1	55.0
$E_{75\%}$	higher quartile	54.2	63.2
$E_{90\%}$	higher decile	60.9	71.0

Table 10: Lower and higher quartile, lower and higher decile, quintile as well as the relative percentile referring to the maximum of the electromagnetic field strength (Mobilkom Austria Room A07A011 at UMTS).

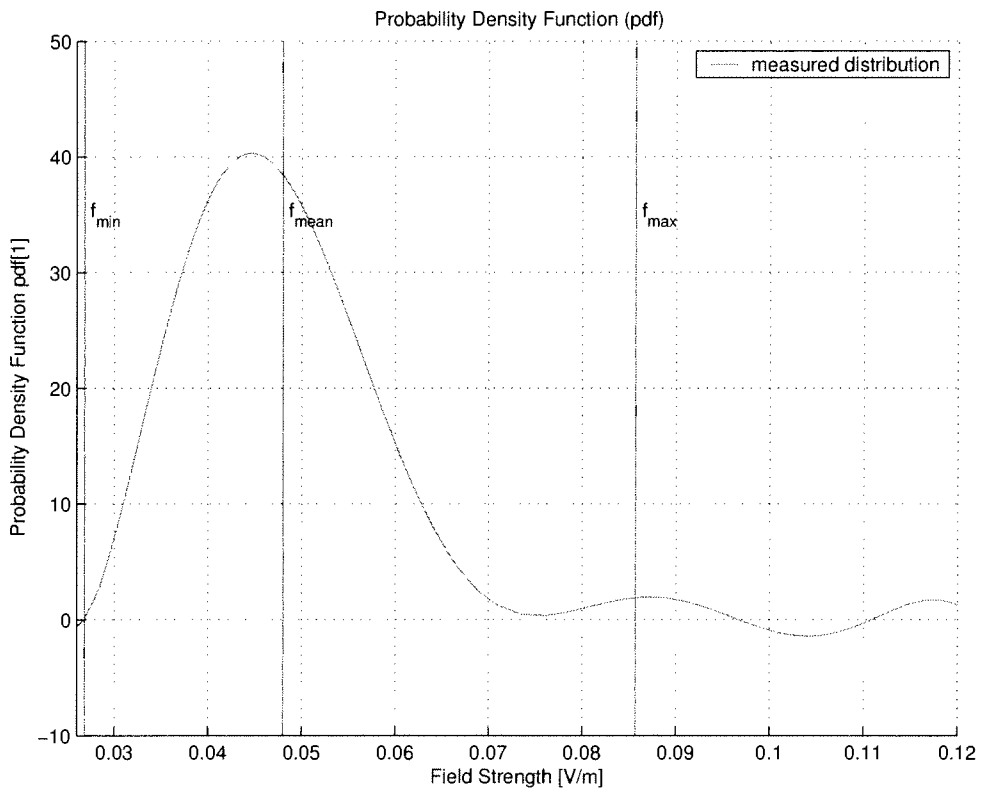


Figure 38: Probability density function (pdf) of the global field distribution (UMTS - Room A07A011 Mobilkom Austria).

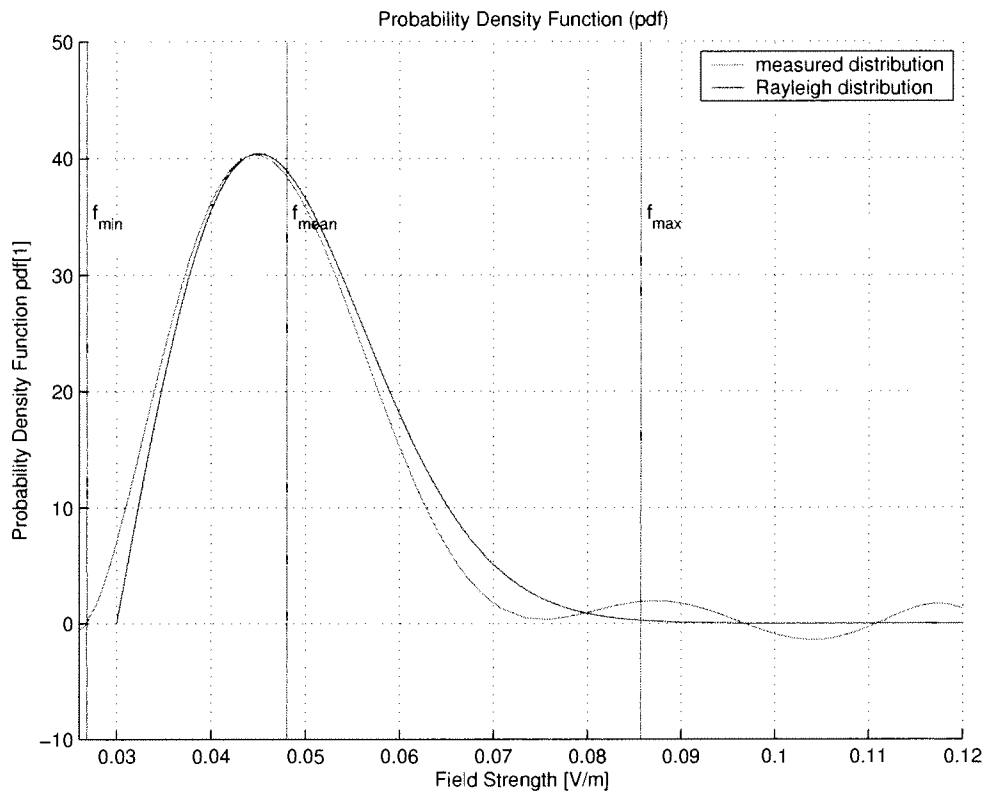


Figure 39: Approximation of the Probability Density function (pdf) with a Rayleigh distribution (UMTS - Room A07A011 Mobilkom Austria).

scribed by Equation 16) the Rayleigh distribution has only one location parameter. The mathematical significance of the Rayleigh distribution for describing a statistical dependency is much stronger as those of the LogNormal distribution because the Rayleigh distribution has only one parameter.

The validity of the polynomial approximation is in the range between minimum and maximum of the electromagnetic field strength.

3.4.4 Local Distribution of the Measurement Data

After the global considerations of the field strength distribution the local behavior was investigated. The field strength values are very homogenous distributed over the whole cube with no particular maxima, as can be seen in Figure 40.

3.4.4.1 Local Means

Figure 41 shows the distribution of the local mean values in each single level.

The maximum deviation from the global mean value occurs in the z-axis. The maximum is reached in Level 7 with an value of $5.5 \frac{mV}{m}$ whereas the minimum is reached in Level 3 with an value of $4.4 \frac{mV}{m}$.

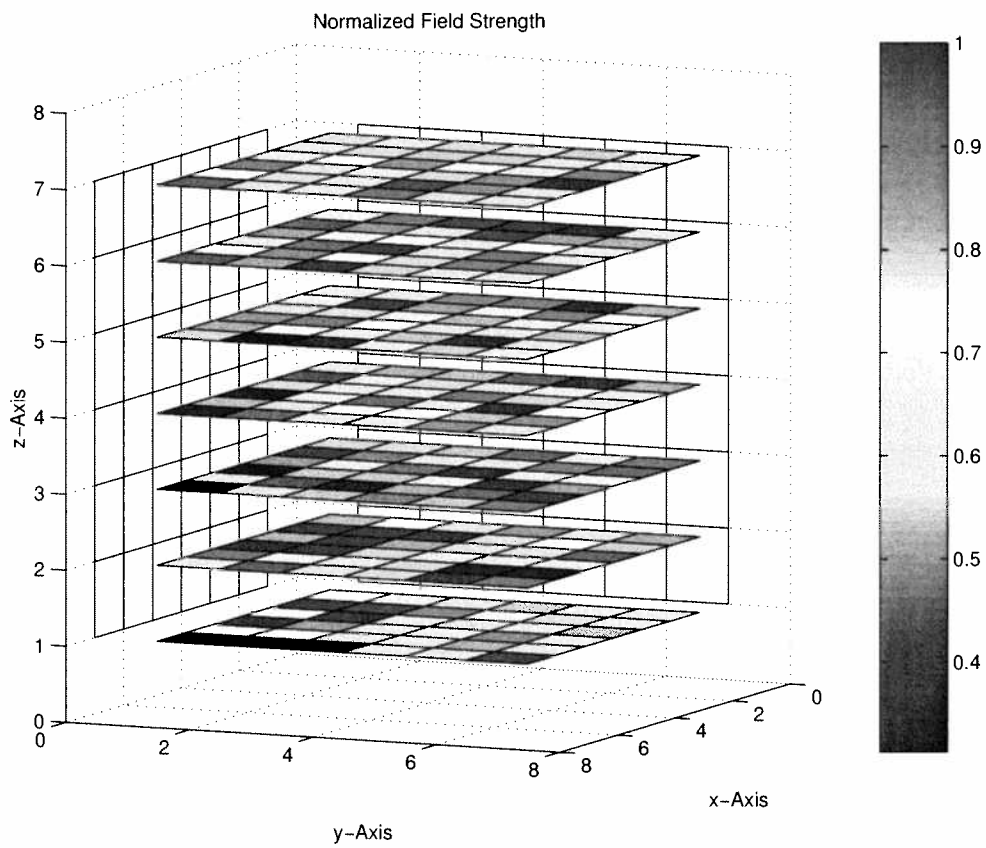


Figure 40: Distribution of the field strength values normalized to the maximum value (UMTS - Room A07A011 Mobilkom Austria).

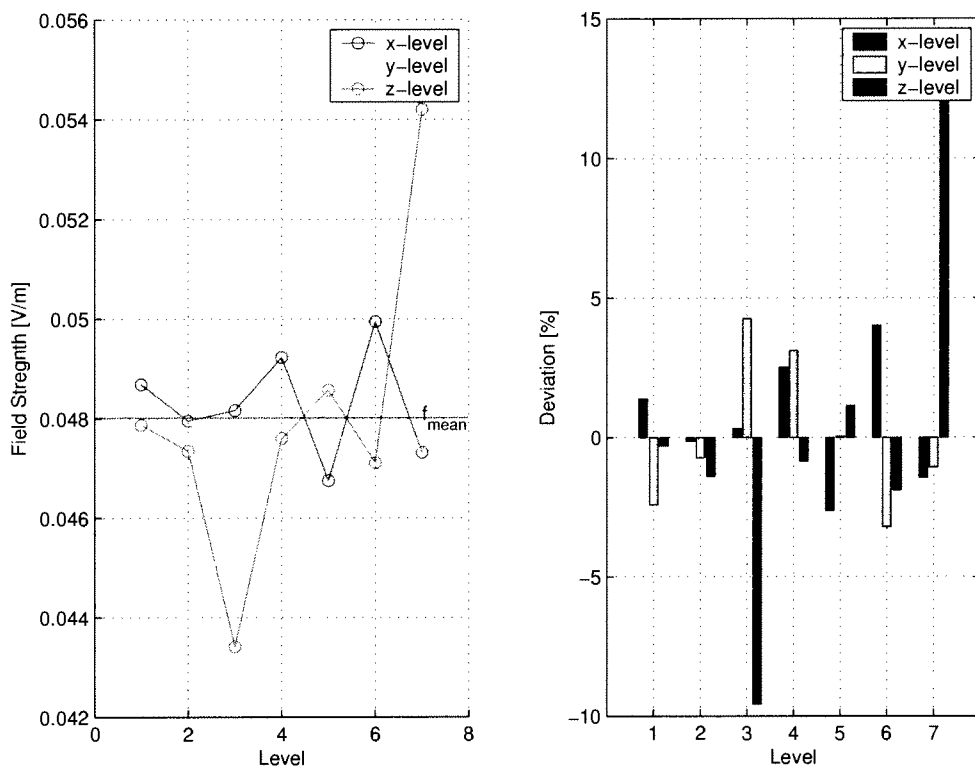


Figure 41: Arithmetic mean of the single levels (UMTS - Room A07A011 Mobilkom Austria).

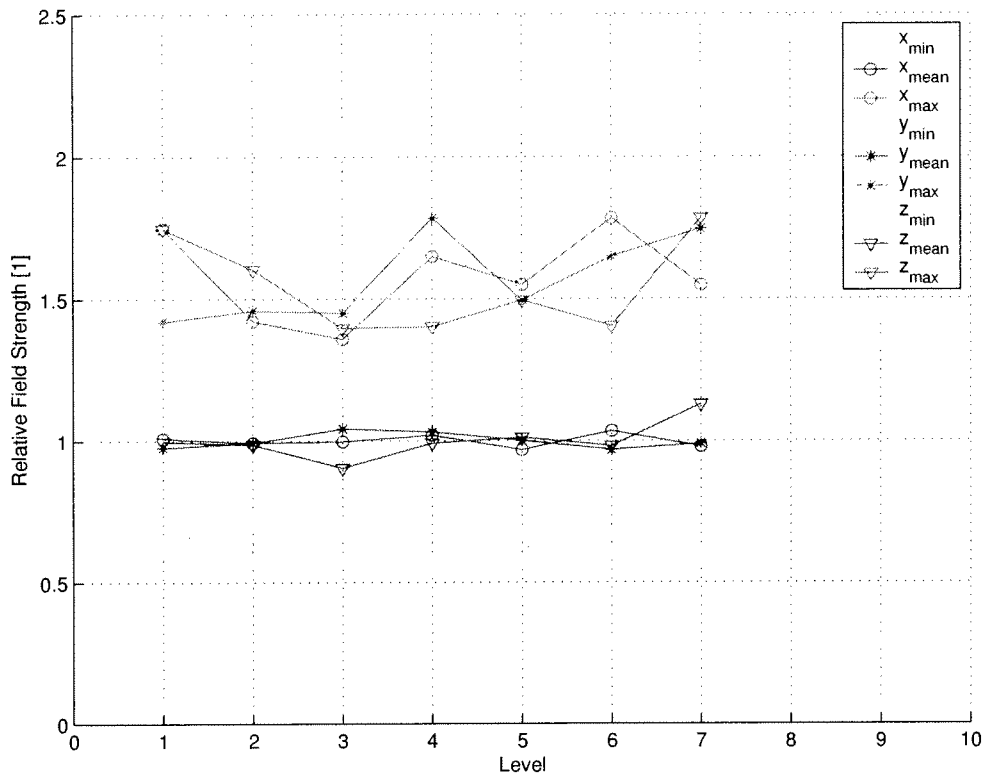


Figure 42: Relative local minima, maxima and arithmetic mean normalized to the global mean (UMTS - Room A07A011 Mobilkom Austria).

3.4.4.2 Local Minimum and Maximum

Figure 42 shows the local minimum and maximum of each level normalized to the global mean. It can be seen, that the minimum, maximum and the mean of each level are nearly in the same range. A reason for this might be, that there are no significant maximums in a single level nor a specific minimum in a single level.

3.5 Ultra High Frequency (UHF) - FS ORF2 - Cube Measurements

Also measurements at a frequency of 575.25MHz, being a television channel (FS ORF2) were performed in the Room A07A011 at the Mobilkom Austria. The transmitting antenna is a few kilometers away from the investigated area. In the north-west direction the transmitting station is located on the Kahlenberg, a small hill in the north west region of Vienna.

The measurement method used was the same like in the other measurement campaigns described in the sections before. A description can be found in Section 2. A cube was examined at the same positions in the anteroom of the conference Room A07A011 as mentioned earlier described in Section 2.1.2. This scenario is catego-

Examined Positions	343
Maximum Value [mV/m]	35.5
Minimum Value [mV/m]	5.0
Global Mean Value [mV/m]	18.3
Standard Deviation [mV/m]	6.1

Table 11: Mean value, minimum and maximum value and standard deviation (Gauß) DCS 1800, Mobilkom Austria Room A07A011.

Percentiles	Description	Value [$\frac{mV}{m}$]	Normalized to the Maximum [%]
$E_{10\%}$	lower decile	10.8	30.4
$E_{25\%}$	lower quartile	13.5	38.2
$E_{50\%}$	quintile	17.5	49.4
$E_{75\%}$	higher quartile	22.8	64.3
$E_{90\%}$	higher decile	26.4	74.7

Table 12: Lower and higher quartile, lower and higher decile, quintile as well as the relative percentile referring to the maximum of the electromagnetic field strength (Mobilkom Austria Room A07A011 at UHF).

alized as Non-Line-Of-Sight (NLOS).

Now the global aspects of this measurement were taken under consideration in the following sections.

3.5.1 Mean, Standard Deviation and Amplitude Distribution

Compared to the previous measurement the maximum value is 7.1 times higher than the minimum value which is much more than in the UMTS measurement campaign. The amplitude distribution has a high peak on the left side of the mean which can be seen in Figure 43.

3.5.2 Cumulative Distribution Function and Probability Density Function

The cumulative distribution function (see Figure 44) can be built by arranging the field strengths by increasing values, as described in Section 3.2.2. The percentiles of the cumulative distribution function are shown in Table 12. By differentiating the cumulative distribution function, the probability density function can be derived which is displayed in Figure 45).

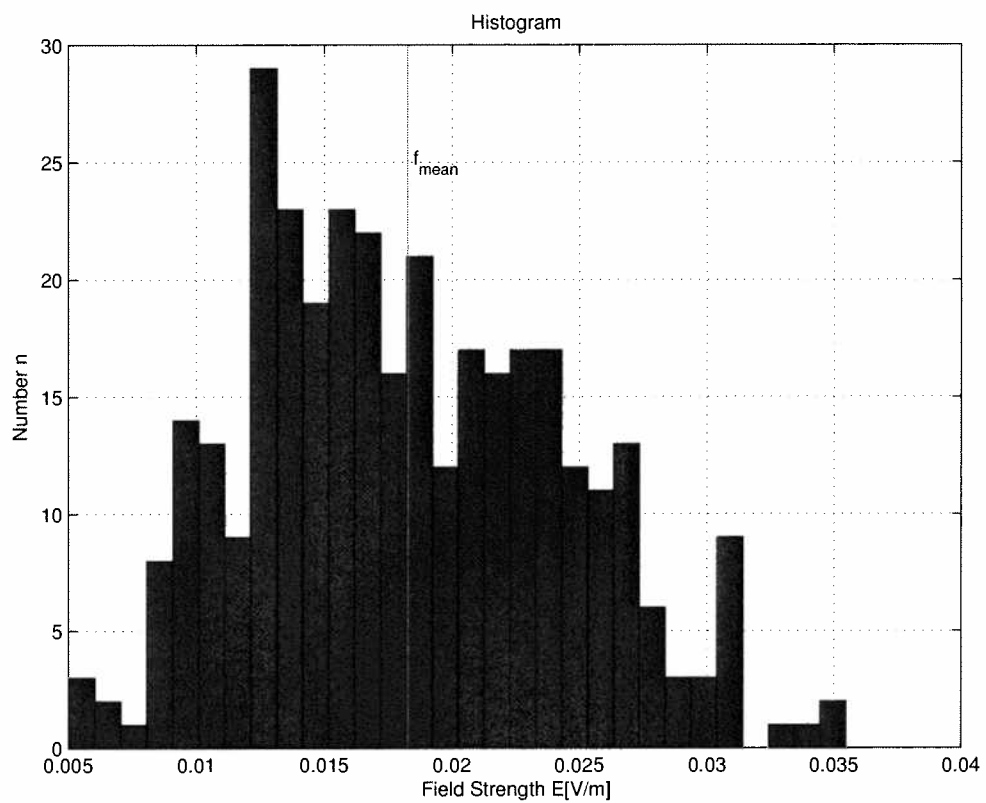


Figure 43: Global distribution of the electromagnetic field strength values disposed in 30 amplitude grades. Measured in Room A07A011 at the Mobilkom Austria office building at a frequency of 575.25MHz, the investigated area was a cube.

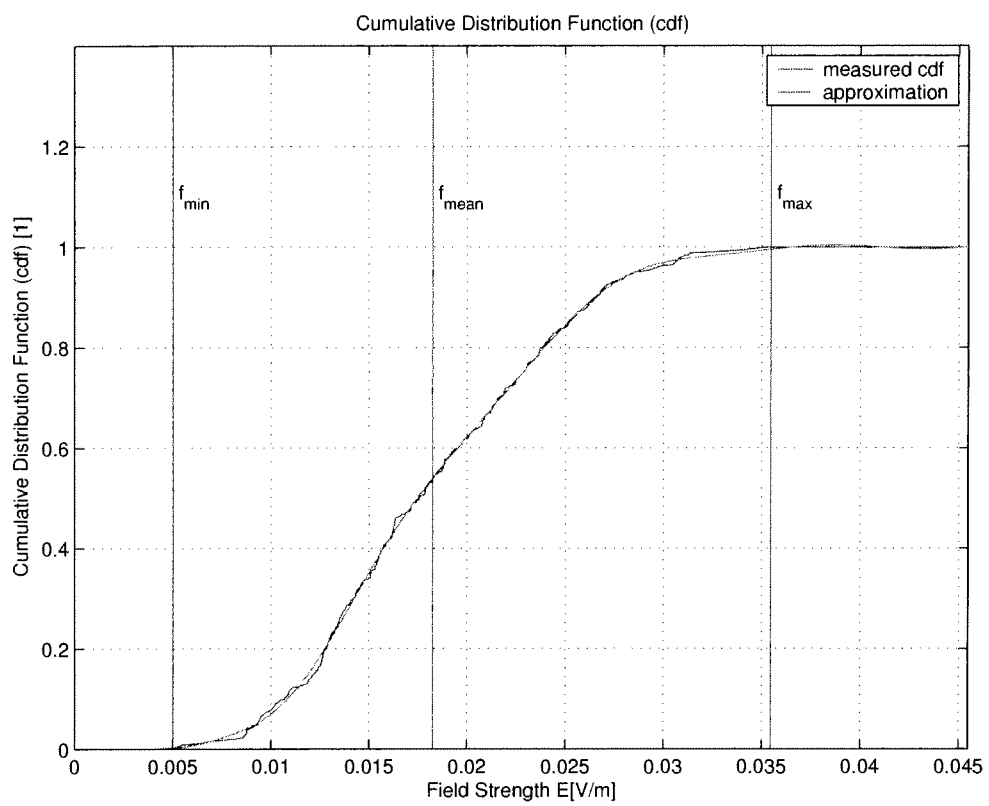


Figure 44: Cumulative distribution function (cdf) of the global field distribution (UHF - Room A07A011 Mobilkom Austria).

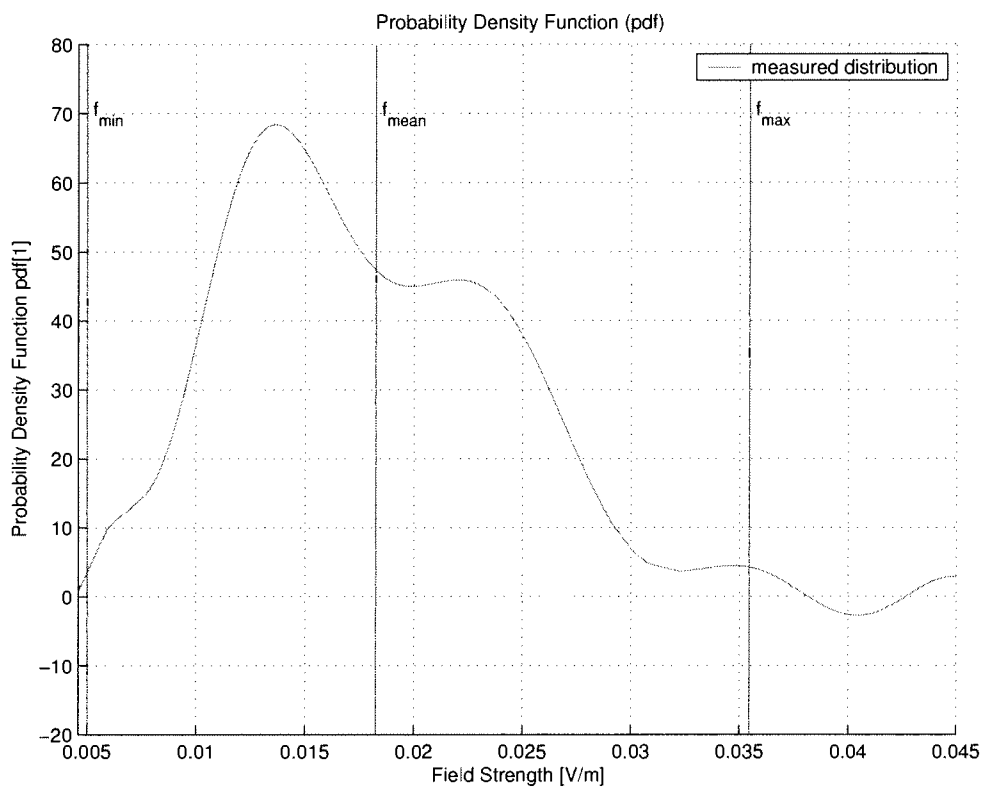


Figure 45: Probability Density function (pdf) of the global field distribution (UHF - Room A07A011 Mobilkom Austria).

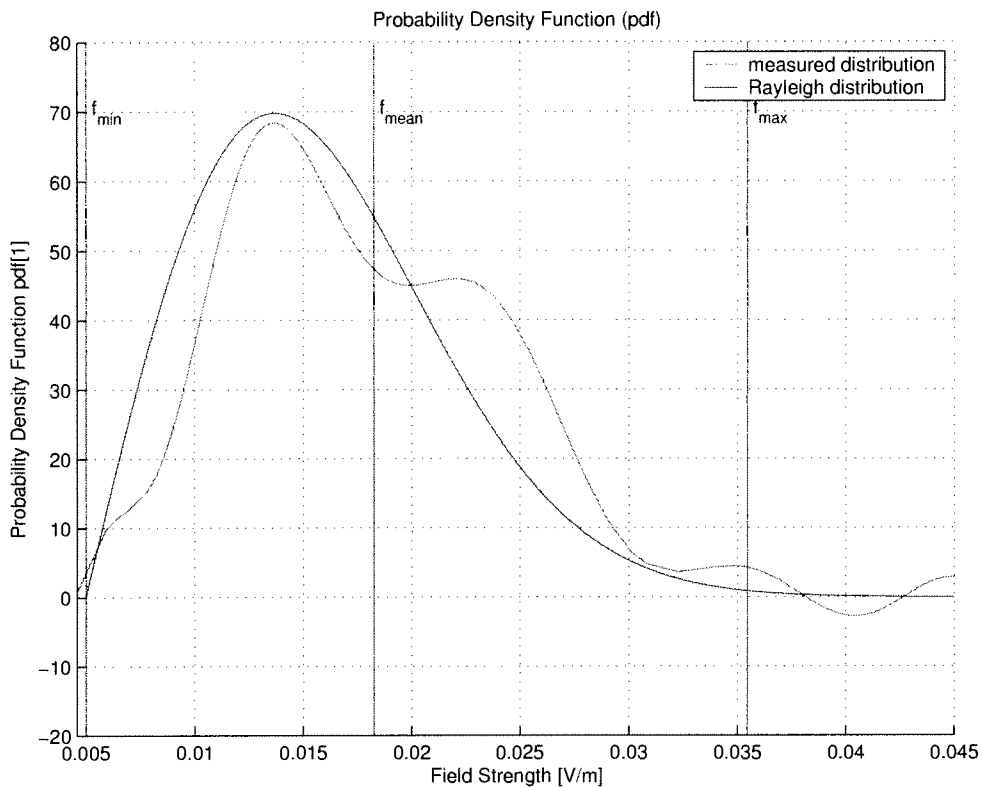


Figure 46: Approximation of the Probability Density function (pdf) with a Rayleigh distribution (UHF - Room A07A011 Mobilkom Austria).

3.5.3 Identification of the Probability Density Function

A possible approximation for the function is displayed in Figure 46. This approximation is characterized as a Rayleigh distribution described by Equation 17. The mathematical significance of the Rayleigh distribution for describing a statistical dependency is much stronger as those of the LogNormal distribution because the Rayleigh distribution has only one parameter.

The validity of the polynomial approximation is in the range between minimum and maximum of the electromagnetic field strength.

3.5.4 Local Distribution of the Measurement Data

After the global considerations of the field strength distribution the local demeanor was investigated. Several higher field strength values were measured in the Levels z135, z150 and z165, as can be seen in Figure 47.

3.5.4.1 Local Means

Figure 48 shows the distribution of the local means in each single level. The maximum deviation from the global mean value occurs in the z-axis. The maximum

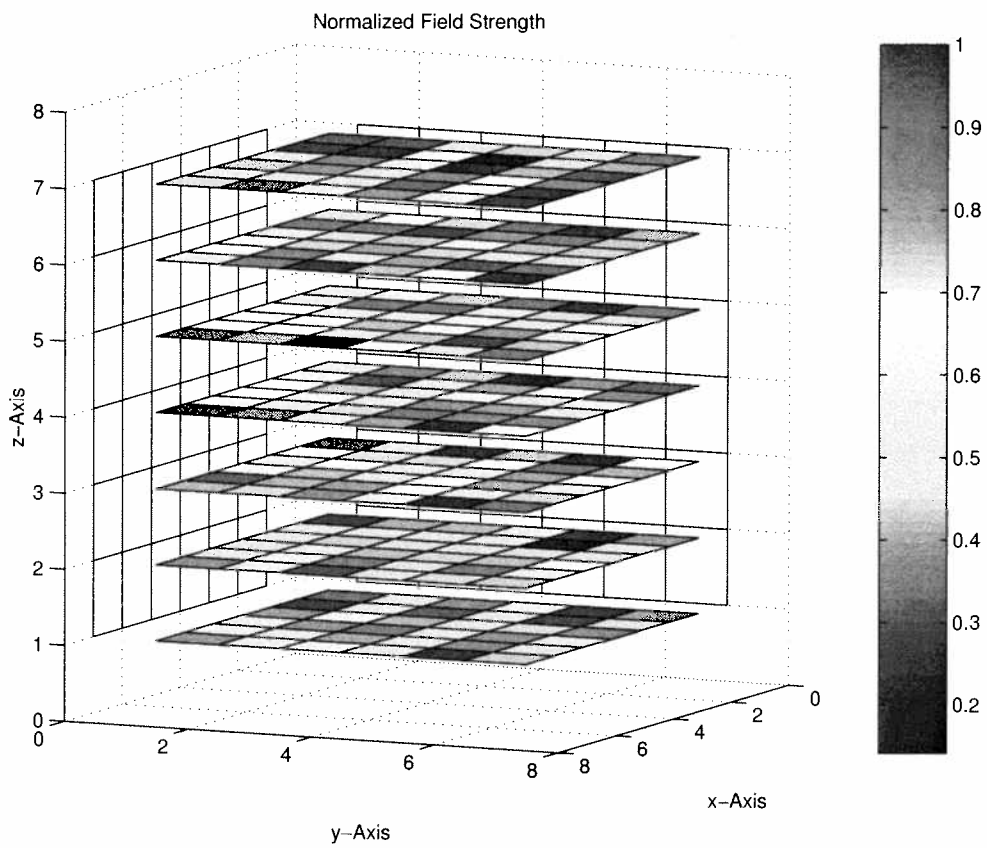


Figure 47: Distribution of the field strength values normalized to the maximum value (UHF - Room A07A011 Mobilkom Austria).

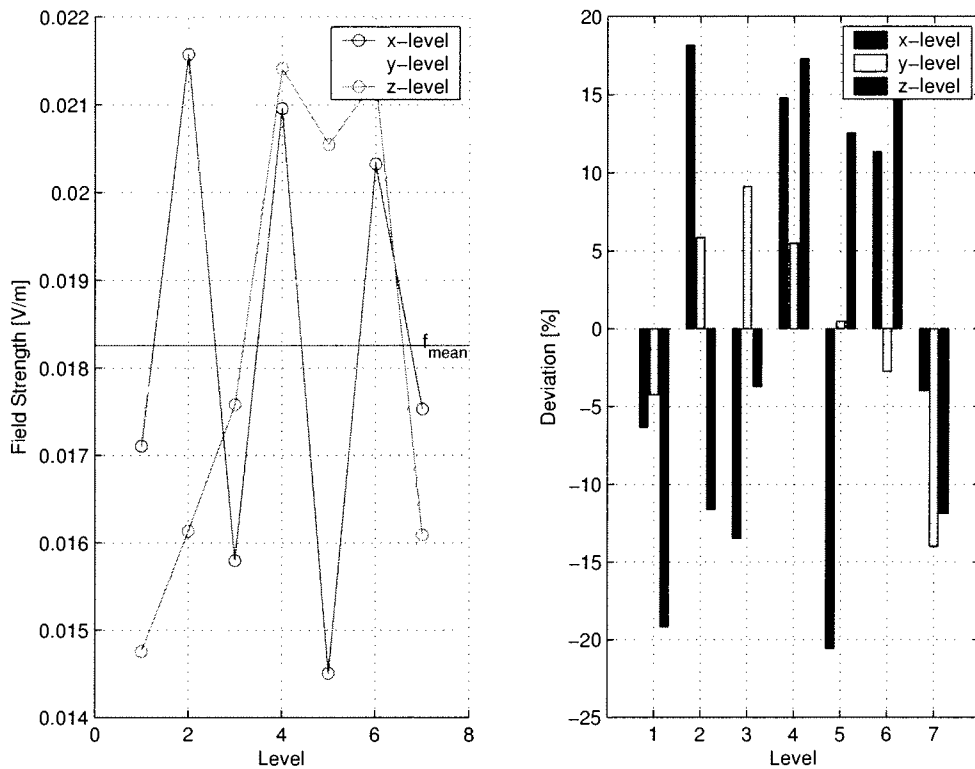


Figure 48: Arithmetic mean of the single levels (UHF - Room A07A011 Mobilkom Austria).

is reached at Level 2 with an value of $21.6 \frac{mV}{m}$ whereas the minimum is reached at Level 5 with an value of $14.5 \frac{mV}{m}$.

3.5.4.2 Local Minimum and Maximum

Figure 49 shows the local minimum and maximum of each level normalized to the global mean value.

3.6 Very High Frequency (VHF) - Cube Measurements

A radio channel at a frequency of 105.8MHz was also measured in the Room A07A011 at the Mobilkom Office Building in Vienna but with a few differences compared to the former measurements. The grid space of the measurement grid was no longer 15cm but 30cm - twice as the grid space in the other measurements. Also the investigated area was no longer a cube. A cuboid with a length of 3.9m and a width of 1.5m, which is equal to 14 x 6 examined positions, this gives a sum of 84 examined positions for each level. Four levels were investigated each separated 30cm, which gives a total of 336 examined positions in this volume. The first level was 90cm above the floor, the last level is 180cm above the floor.

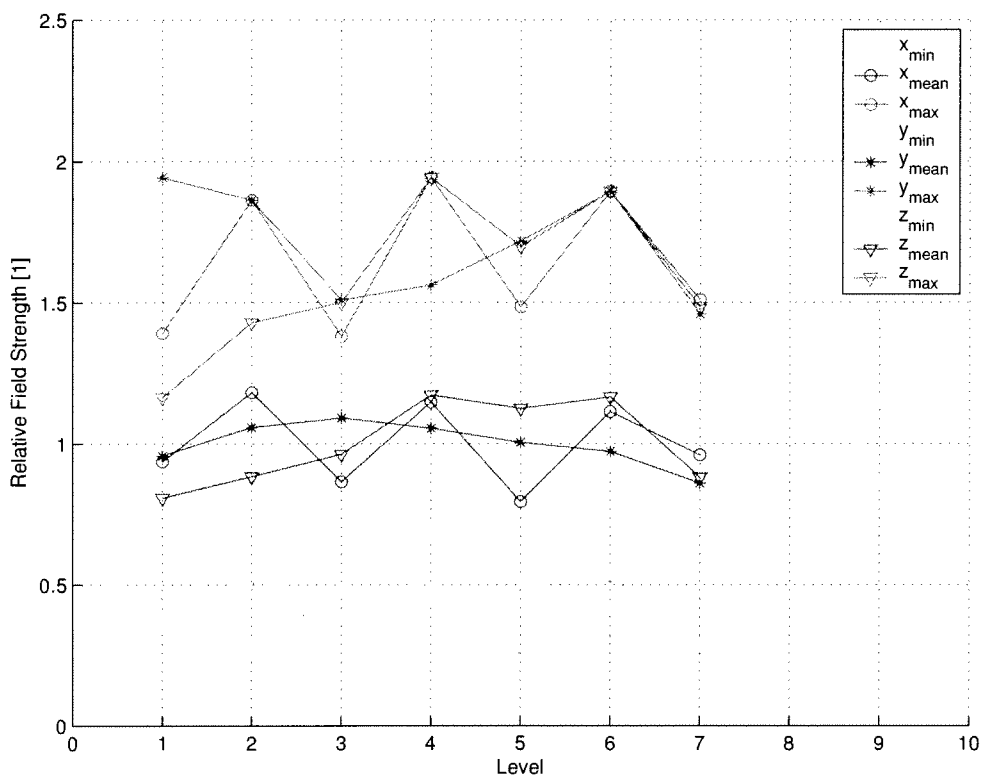


Figure 49: Relative local minima, maxima and arithmetic mean normalized to the global mean (UHF - Room A07A011 Mobilkom Austria).

Examined Positions	343
Maximum Value [mV/m]	8.2
Minimum Value [mV/m]	2.6
Global Mean Value [mV/m]	5.0
Standard Deviation [mV/m]	0.9

Table 13: Mean value, minimum and maximum value and standard deviation (Gauß) VHF, Mobilkom Austria Room A07A011.

The position of the volume was also changed from the anteroom in the conference room, which is in the middle of the whole room. The transmitting antenna was a few kilometers away and the characterization was therefore Non-Line-Of-Sight (NLOS). A schematic of the investigated area shows Figure 18.

Only the measurement method itself was not changed, it was the same like in the other measurement campaigns, described in the sections before. A detailed description can be found in Section 2.

Now the global aspects of this measurement were taken under consideration in the following sections.

3.6.1 Mean, Standard Deviation and Amplitude Distribution

Compared to the previous measurement the ratio between maximum value and minimum value is much smaller, only 1.6. Table 13 shows the minimum value, the maximum value, the mean value and the standard deviation. The amplitude distribution has a smooth rise and a more abrupt decrease after reaching the maximum, this can be seen in Figure 50.

3.6.2 Cumulative Distribution Function and Probability Density Function

The cumulative distribution function (see Figure 51) can be build by arranging the field strength values by increasing values, as described in Section 3.2.2. The percentiles of the cumulative distribution function are shown in Table 14. The probability density function (see Figure 52) can be derived by differentiating the cumulative distribution function (refereing to Equation 12).

3.6.3 Identification of the Probability Density Function

A possible approximation for the function is displayed in Figure 53. This approximation is characterized as a Normal distribution described by following Equation 18.

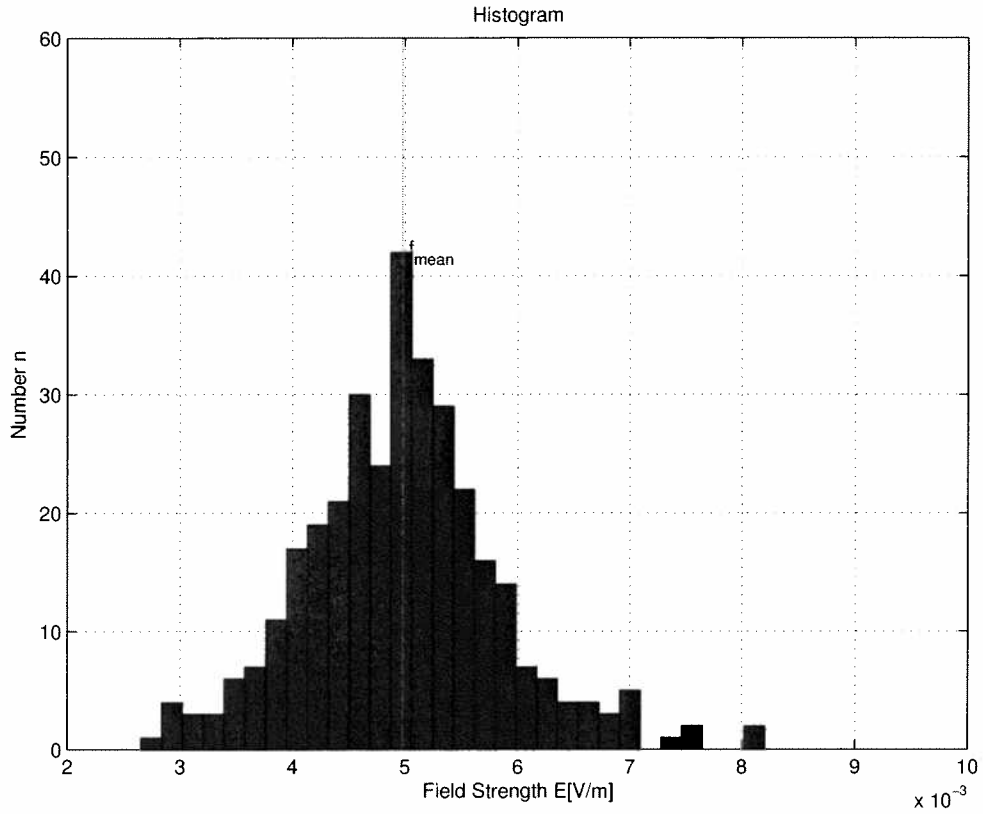


Figure 50: Global distribution of the electromagnetic field strength values disposed in 30 amplitude grades. Measured in Room A07A011 at the Mobilkom Austria office building at a frequency of 105.8MHz, the investigated area was a cuboid with a size of 3.9m x 1.5m x 0.9m, which gives a total of 336 examined positions.

Percentiles	Description	Value [$\frac{mV}{m}$]	Normalized to the Maximum [%]
$E_{10\%}$	lower decile	3.9	47.4
$E_{25\%}$	lower quartile	4.4	54.1
$E_{50\%}$	quintile	5.0	60.5
$E_{75\%}$	higher quartile	5.5	66.4
$E_{90\%}$	higher decile	6.0	73.3

Table 14: Lower and higher quartile, lower and higher decile, quintile as well as the relative percentile referring to the maximum of the electromagnetic field strength (Mobilkom Austria Room A07A011 at VHF).

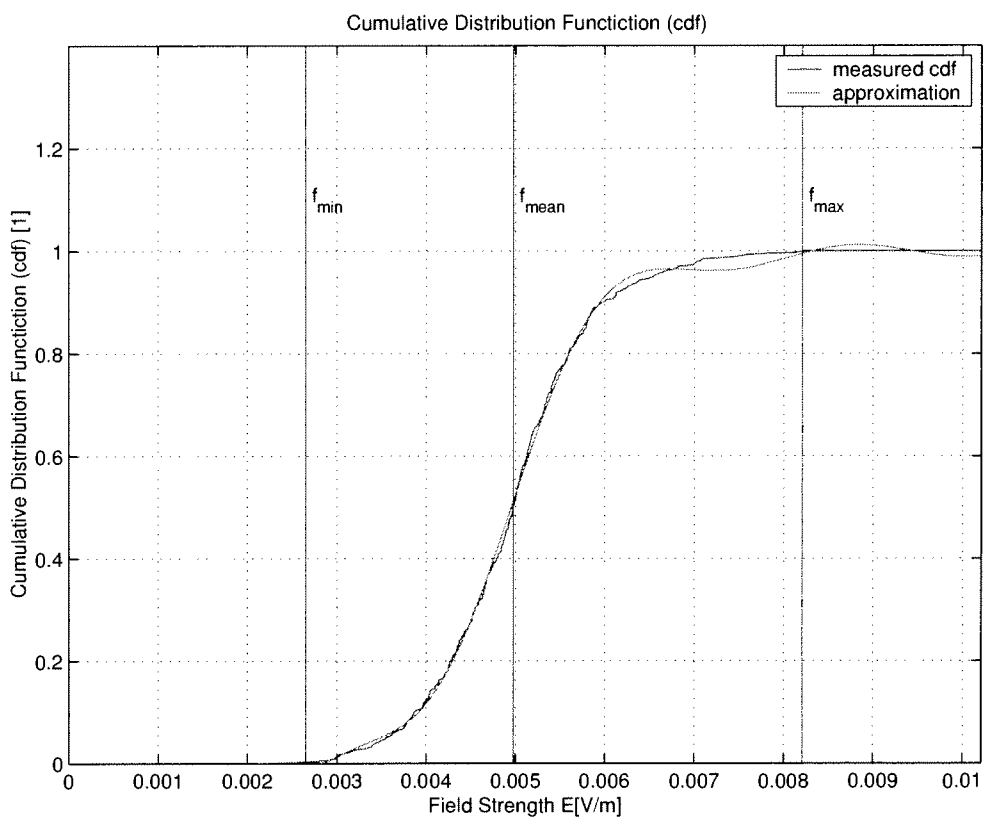


Figure 51: Cumulative distribution function (cdf) of the global field distribution (VHF - Room A07A011 Mobilkom Austria).

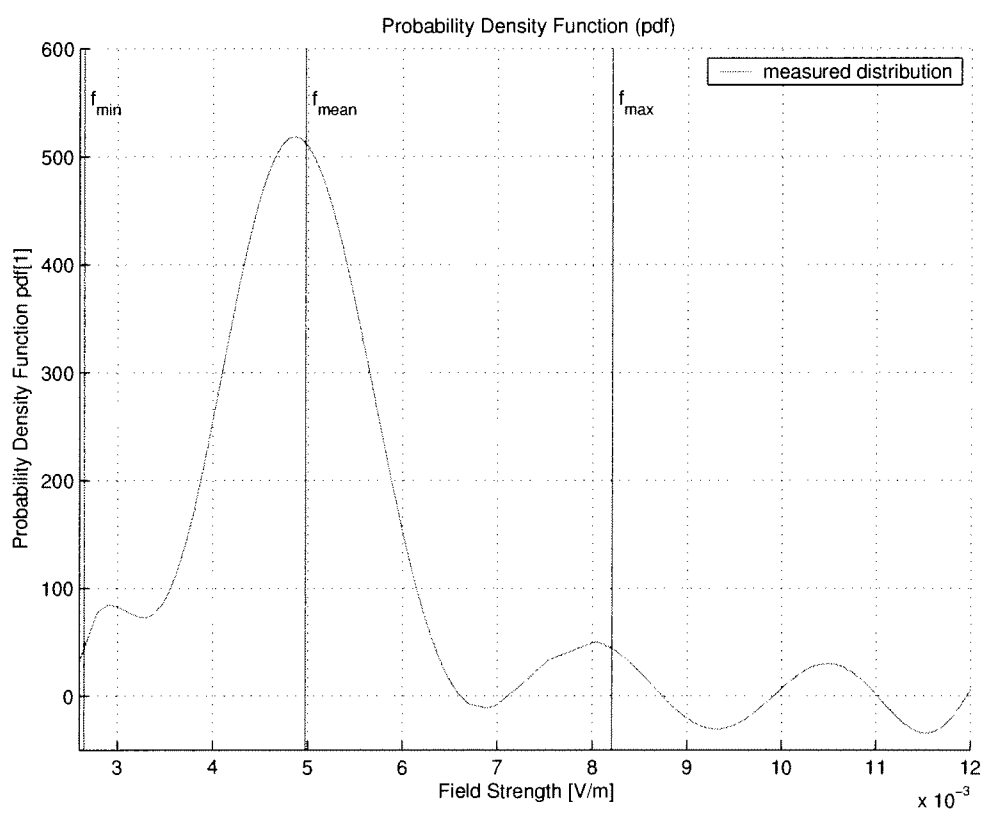


Figure 52: Probability Density function (pdf) of the global field distribution (VHF - Room A07A011 Mobilkom Austria).

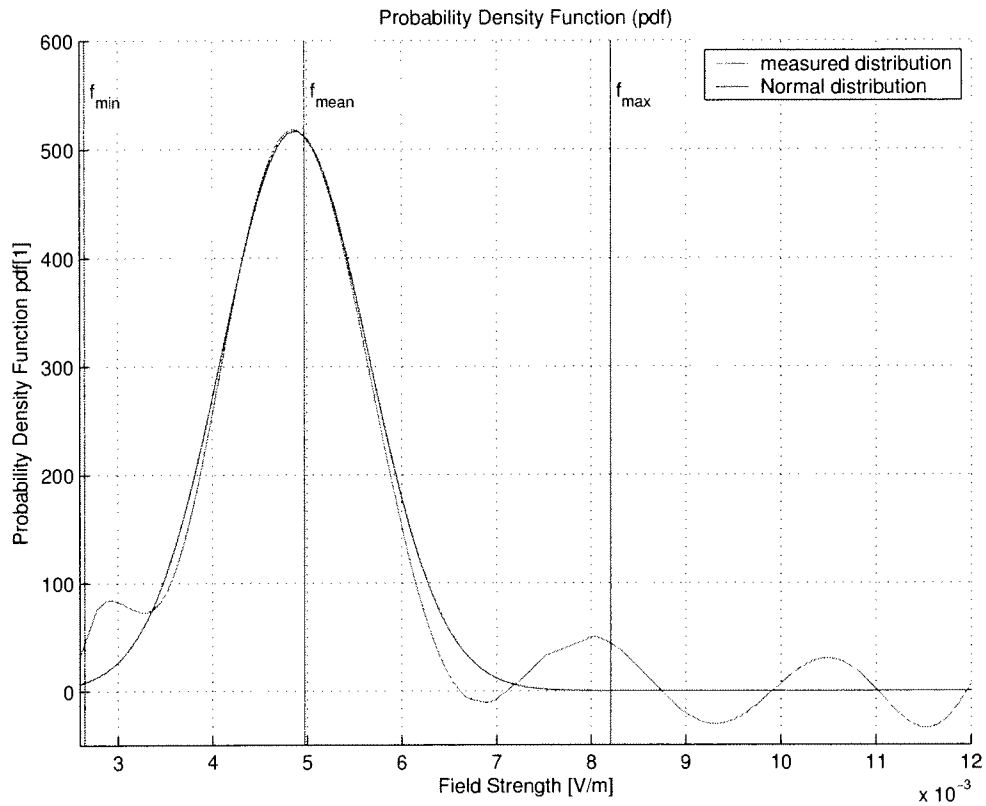


Figure 53: Approximation of the Probability Density function (pdf) with a Normal distribution (VHF - Room A07A011 Mobilkom Austria).

$$y = f(x | \sigma, \mu) = \frac{1}{\sqrt{2\pi}\sigma} \cdot e^{-\frac{1}{2}\left(\frac{x-\mu}{\sigma}\right)^2} \quad (18)$$

The variable μ characterizes the expectation, σ describes the standard deviation.

The validity of the polynomial approximation is in the range between the minimum and the maximum of the electromagnetic field strength.

3.6.4 Local Distribution of the Measurement Data

After the global considerations of the field strength distribution the local demeanor was investigated. Figure 54 shows a clear maximum of the field strength in the highest level, Level z180. The maximum is concentrated over a spot of a few examined positions .

3.6.4.1 Local Means

Figure 55 shows the distribution of the local means in each single level.

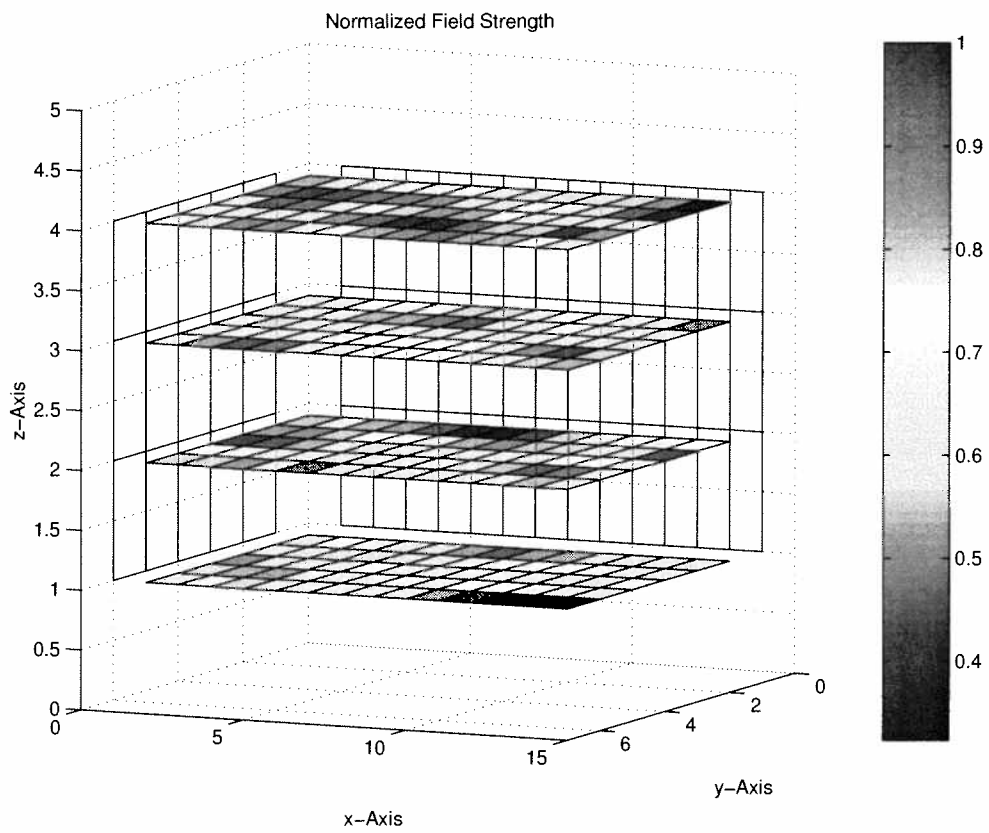


Figure 54: Distribution of the field strength values normalized to the maximum value (VHF - Room A07A011 Mobilkom Austria).

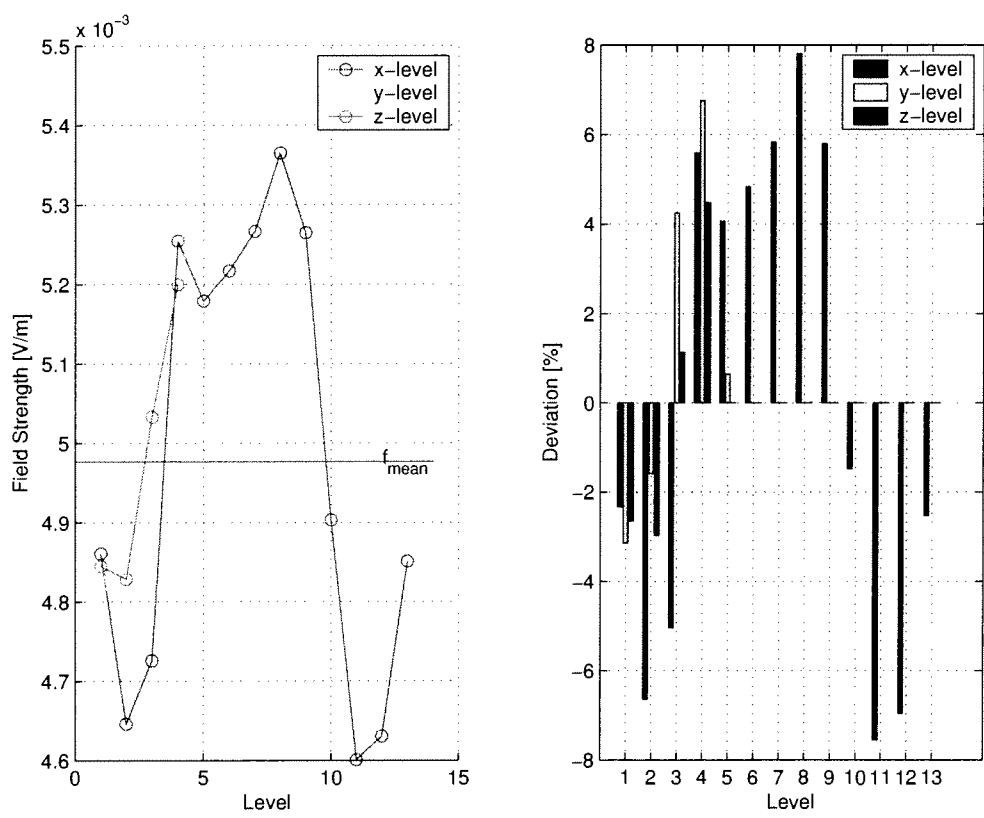


Figure 55: Arithmetic mean of the single levels (VHF - Room A07A011 Mobilkom Austria).

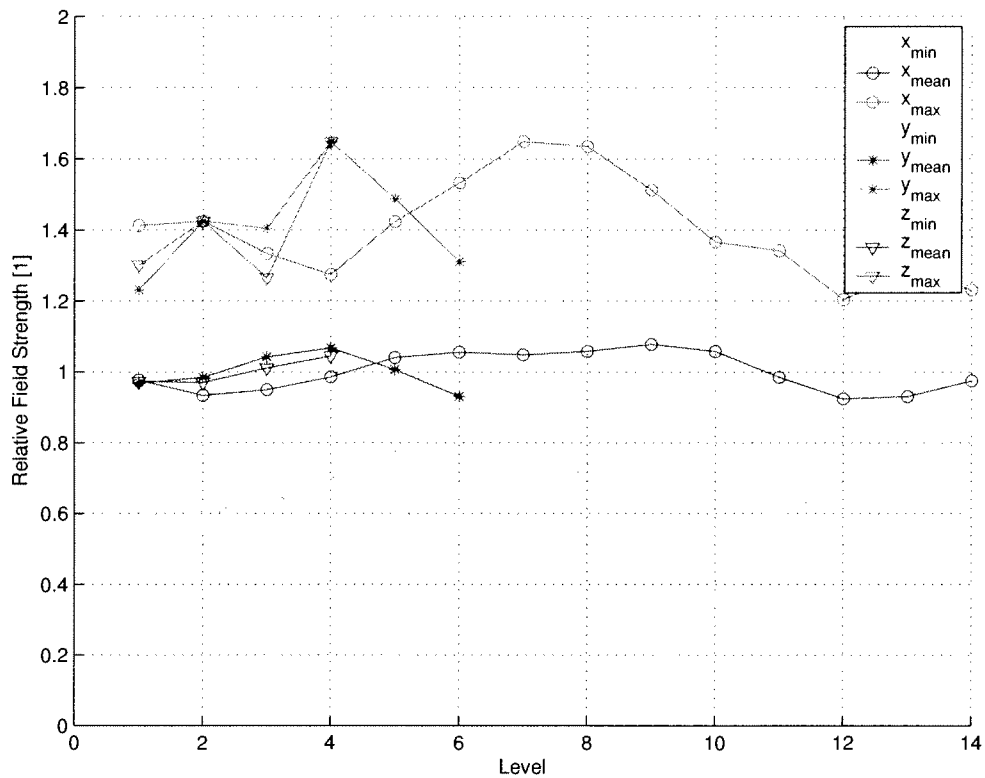


Figure 56: Relative local minima, maxima and arithmetic mean normalized to the global mean (VHF - Room A07A011 Mobilkom Austria).

The maximum deviation from the global mean value occurs in the x-axis. The maximum is reached at x-Level 8 with an value of $5.4 \frac{mV}{m}$ and the minimum is reached at x-Level 11 with an value of $4.6 \frac{mV}{m}$.

3.6.4.2 Local Minimum and Maximum

Figure 56 shows the local minimum and maximum of each level normalized to the global mean.

3.7 GSM 900 - Small Cube Measurements

After finishing the measurement of the cube volumes the same measurement method (refereing to Section 2) was performed within a cube with half of the edge length (45cm), already described in Section 2.1.2. The grid steps were no longer 15cm but 7.5cm in each of the three directions. Like before, 49 examined positions per level were measured over 7 levels, which gives a total of 343 examined positions for each small cube. These measurements were performed in the GSM 900, DCS 1800 and UHF frequency band. The position of the small cube was the same than of the cube starting at position 0 which means [x=0cm, y=0cm and z=90cm] in a height of 90cm

Level (Index)	x-axis	y-axis	z-axis
1	x0	y0	z90
2	x7.5	y7.5	z97.5
3	x15	y15	z105
4	x22.5	y22.5	z112.5
5	x30	y30	z120
6	x37.5	y37.5	z127.5
7	x45	y45	z135

Table 15: Index and description of each level of the small cube with a grid step of 7.5cm instead of a grid step of 15cm.

Examined Positions	343
Maximum Value [mV/m]	45.8
Minimum Value [mV/m]	4.6
Global Mean Value [mV/m]	19.6
Standard Deviation [mV/m]	5.9

Table 16: Mean value, minimum and maximum value and standard deviation (Gauß) at GSM 900 - small cube, Mobilkom Austria Room A07A011.

above the floor. The nomenclature of the small cube is shown in Table 15. Like in all previous measurement campaigns, the global considerations were examined first.

3.7.1 Mean, Standard Deviation and Amplitude Distribution

The field strength values can statistically be described by the values of Table 16. Comparing the maximum value of the small cube with the maximum value of the cube, the cube shows a much higher value. The factor between the maximum of the cube measurement and the maximum of the small cube measurement is 1.4, whereas the maximum value of the small cube is by this factor lower than the maximum of the cube. The global mean value and the minimum value are nearly in the same range, the differences are not so high. The maximum value is 16.2 times higher compared to the minimum value. The amplitude distribution is not symmetric because the arithmetic mean is located on the left side of half of the range, as Figure 57 shows.

The amplitude distribution is nearly uniformly distributed around the mean value with a smooth rise in the beginning and a smooth rise while decreasing on the right

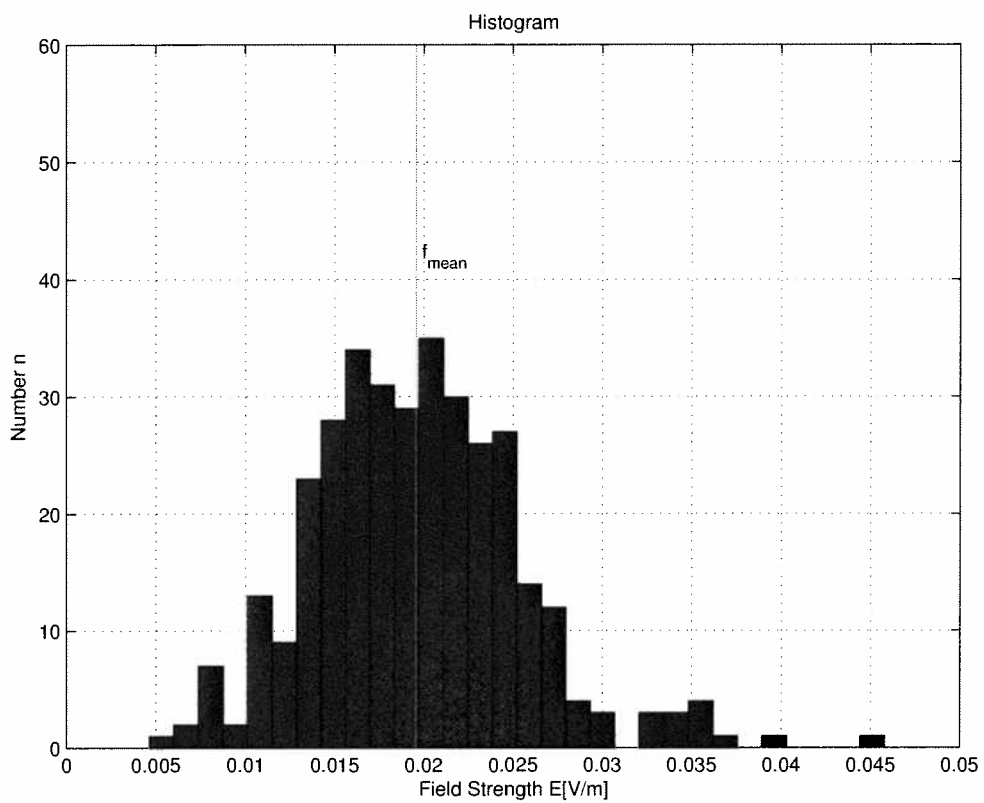


Figure 57: Global distribution of the electromagnetic field strength values disposed in 30 amplitude grades. Measured in Room A07A011 at the Mobilkom Austria office building at a frequency of 944.6MHz, the investigated area was a small cube.

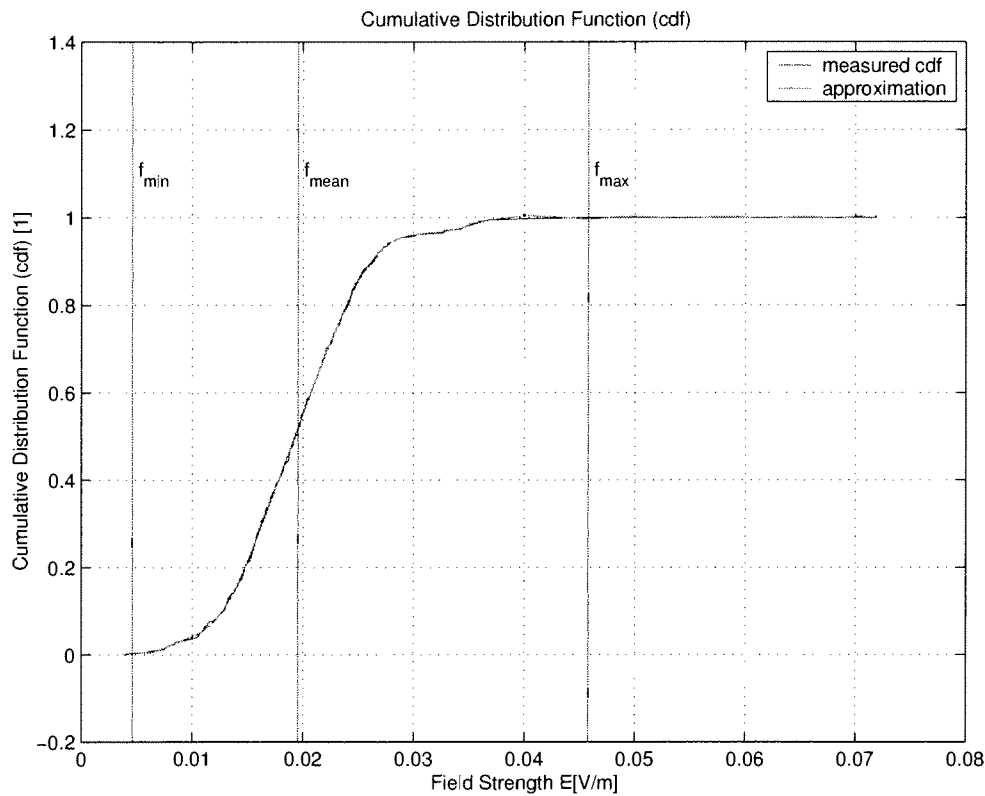


Figure 58: Cumulative distribution function (cdf) of the global field distribution (GSM 900 - small cube - Room A07A011 Mobilkom Austria).

side of the mean value. This could be described as a Rayleigh distribution which was already introduced in a former section (see Equation 17).

3.7.2 Cumulative Distribution Function and Probability Density Function

The cumulative distribution function (see Figure 22) can be derived by arranging the field strength by increasing values, as described in Section 3.2.2. The percentiles of the cumulative distribution function are shown in Table 17.

The probability density function (see Figure 59) can be derived by differentiating the cumulative distribution function (see Equation 12).

3.7.3 Identification of the Probability Density Function

A possible approximation for the function is displayed in Figure 60. It is characterized as a Rayleigh distribution described by Equation 17. The validity of the polynomial approximation is in the range between minimum and maximum of the electromagnetic field strength values.

Percentiles	Description	Value [$\frac{mV}{m}$]	Normalized to the Maximum [%]
$E_{10\%}$	lower decile	12.7	27.8
$E_{25\%}$	lower quartile	15.6	34.0
$E_{50\%}$	quintile	19.3	42.0
$E_{75\%}$	higher quartile	23.0	50.3
$E_{90\%}$	higher decile	26.2	57.2

Table 17: Lower and higher quartile, lower and higher decile, quintile as well as the relative percentile referring to the maximum of the electromagnetic field strength (Mobilkom Austria Room A07A011 at GSM 900 - small cube).

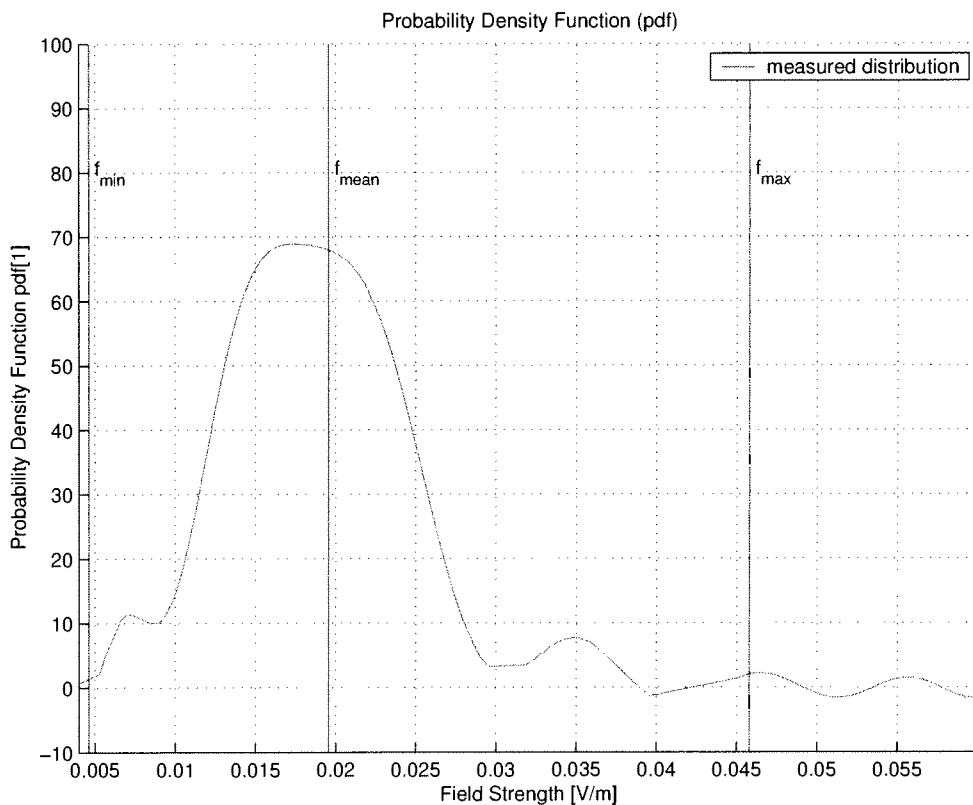


Figure 59: Probability Density function (pdf) of the global field distribution (GSM 900 - small cube - Room A07A011 Mobilkom Austria).

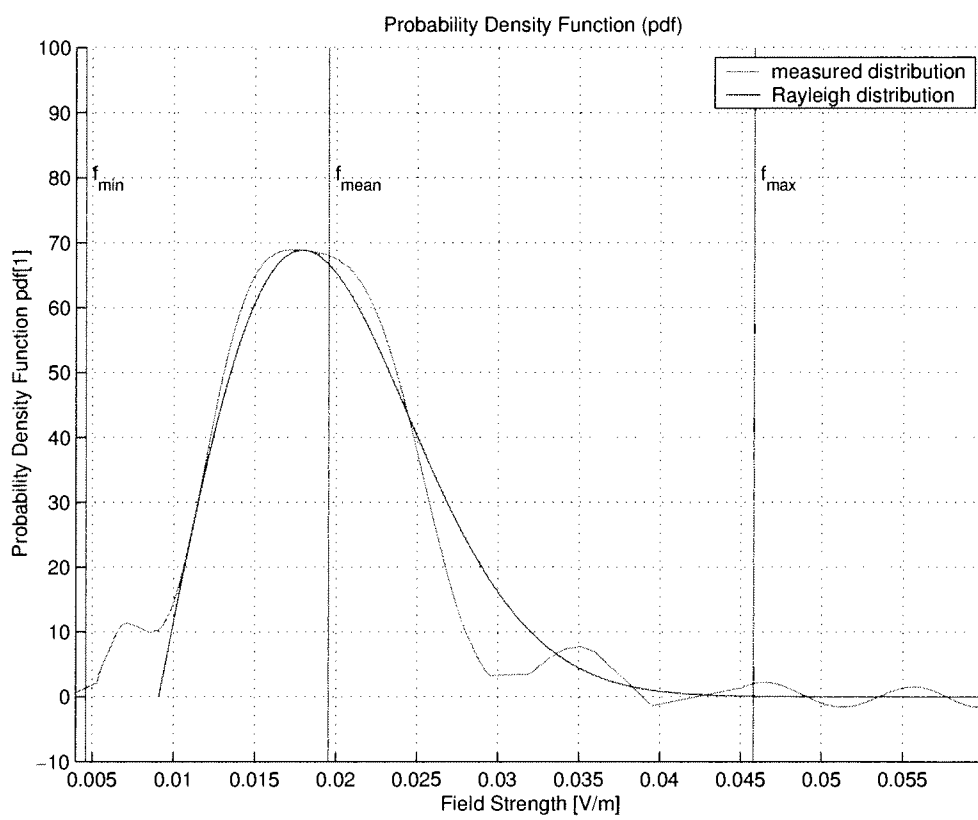


Figure 60: Approximation of the Probability Density function (pdf) with a Rayleigh distribution (GSM 900 - small cube - Room A07A011 Mobilkom Austria).

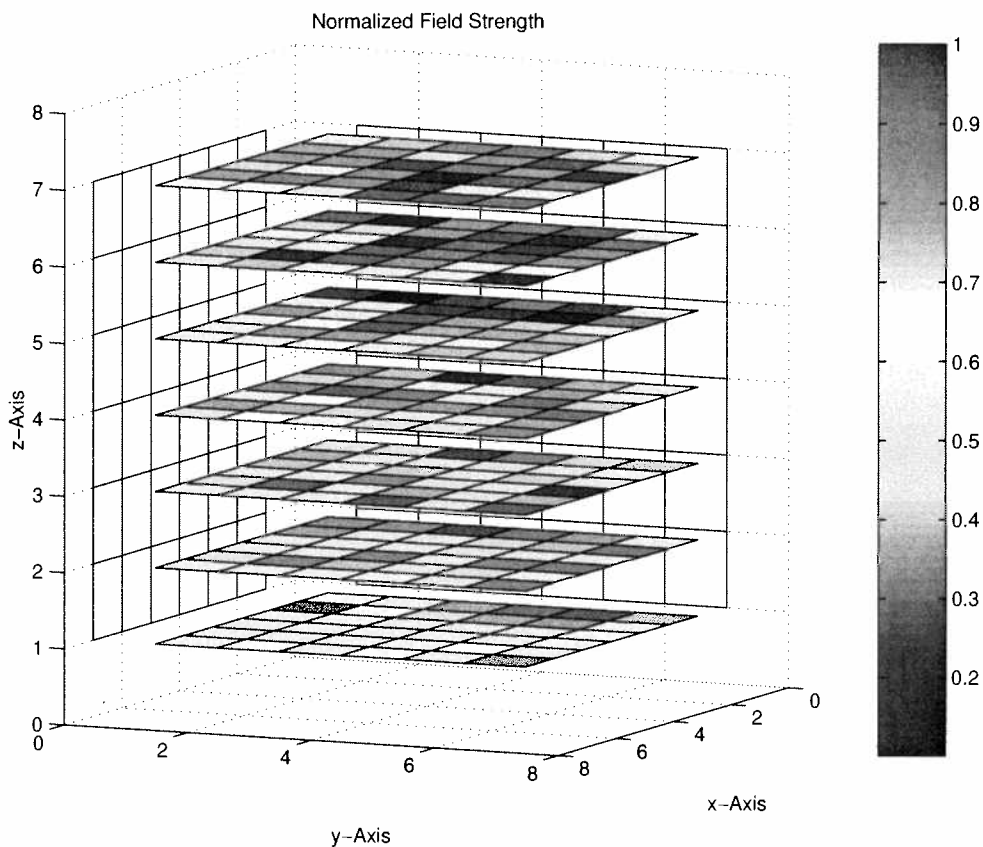


Figure 61: Distribution of the field strength values normalized to the maximum value (GSM 900 - small cube - Room A07A011 Mobilkom Austria).

3.7.4 Local Distribution of the Measurement Data

After the global considerations of the field strength distribution the local behavior was investigated. The field strength values are very homogenous distributed over the whole cube which can be seen in Figure 61 with a little bit higher field strengths values in the lower levels.

3.7.4.1 Local Means

Figure 62 shows the distribution of the local mean value in each single level. The maximum deviation from the global mean value occurs in the z-axis. The maximum is reached in Level 1 with a value of $23.3 \frac{mV}{m}$, while the minimum is reached in the y-Level 1 with a value of $16.7 \frac{mV}{m}$.

3.7.4.2 Local Minimum and Maximum

Figure 63 shows the local minimum and maximum of each level normalized to the global mean.

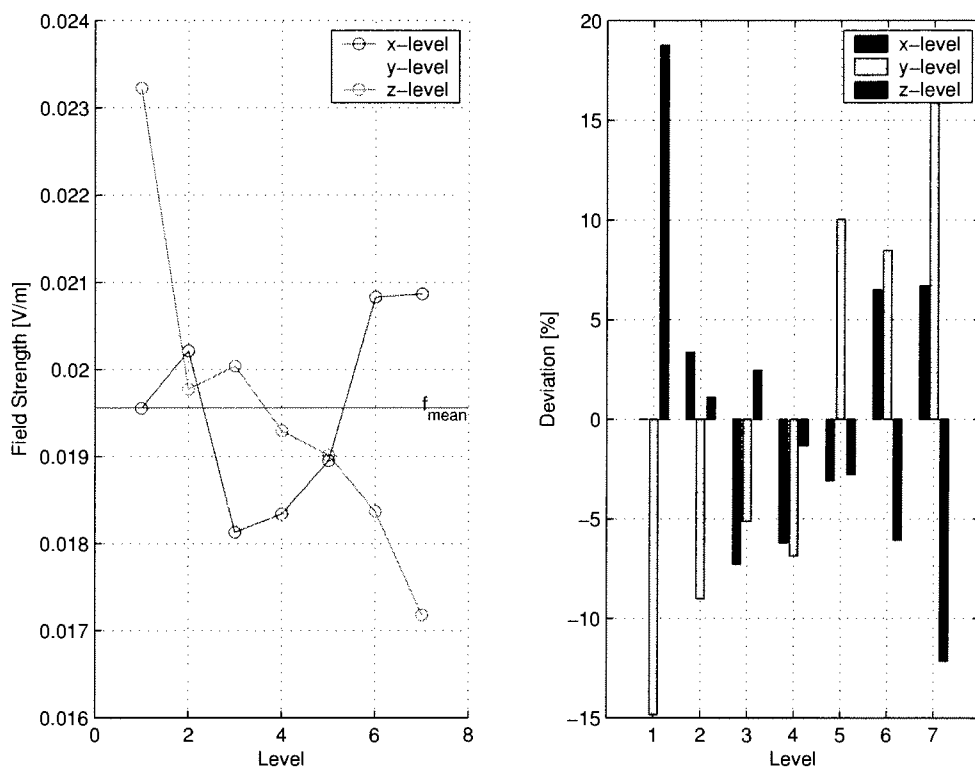


Figure 62: Arithmetic mean of the single levels (GSM 900 - small cube - Room A07A011 Mobilkom Austria).

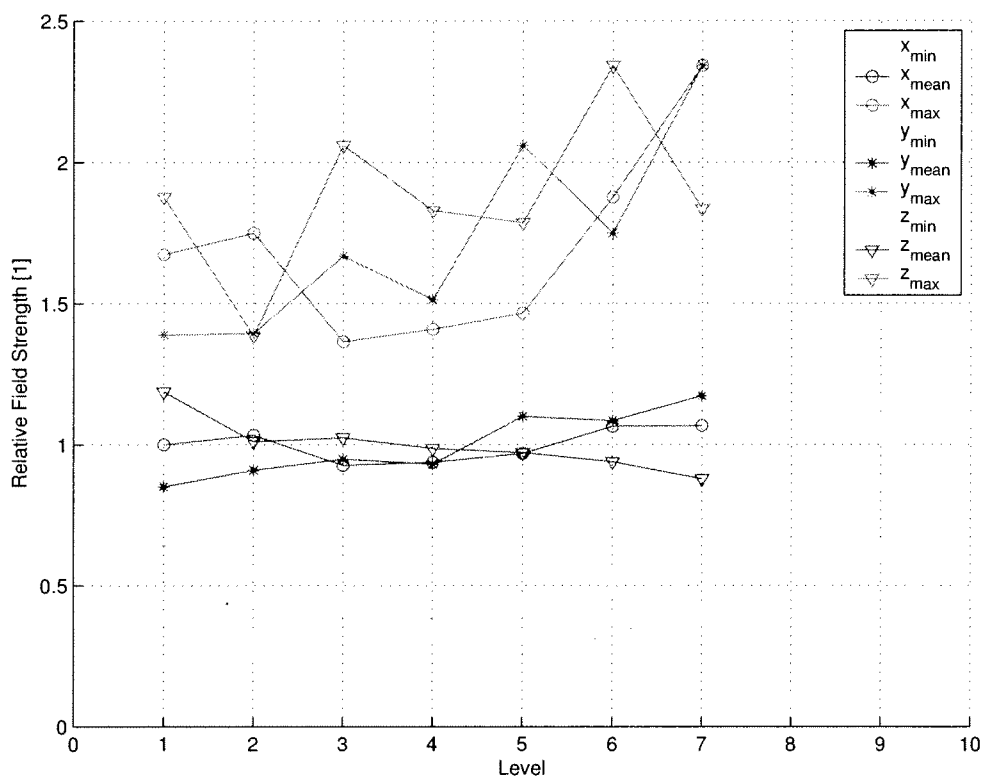


Figure 63: Relative local minima, maxima and arithmetic mean normalized to the global mean (GSM 900 - small cube - Room A07A011 Mobilkom Austria).

Examined Positions	343
Maximum Value [mV/m]	61.6
Minimum Value [mV/m]	8.6
Global Mean Value [mV/m]	27.1
Standard Deviation [mV/m]	9.3

Table 18: Mean value, minimum and maximum value and standard deviation (Gauß) at DCS 1800 - small cube, Mobilkom Austria Room A07A011.

3.8 DCS 1800 - Small Cube Measurements

As mentioned before, also a small cube was examined in the DCS 1800 frequency band, using the same measurement set up than in all other measurements (except for UMTS, a more sensitive antenna was used to measure the field strength values). First of all the global considerations were evaluated like in all previous measurement campaigns before.

3.8.1 Mean, Standard Deviation and Amplitude Distribution

The field strength values can statistically be described by the values of Table 18. The maximum value of the small cube shows higher values compared to the measurement of the cube in the DCS 1800 frequency band. The difference between the maximum value of the cube measurement and the maximum value of the small cube measurement is a factor 2.3, whereas the maximum value of the cube measurement is higher than the small cube measurement. Mean value and minimum value are nearly in the same range, the differences compared to the cube measurement are not so high.

The maximum value is 7.2 times higher than the minimum value. The amplitude distribution is not symmetric because the arithmetic mean is located on the left side of the center between minimum value and maximum value, as Figure 64 shows.

The fast rise in the beginning and the more smoother fall while decreasing on the right side of the mean value could be characterized by a LogNormal-distribution. This was already introduced in a former section (see Equation 16).

3.8.2 Cumulative Distribution Function and Probability Density Function

The cumulative distribution function (see Figure 65) can be build by arranging the field strength values with increasing amplitude, as described in Section 3.2.2. The percentiles of the cumulative distribution function are shown in Table 19.

The probability density function (see Figure 66) can be derived by differentiating the cumulative distribution function (see Equation 12).

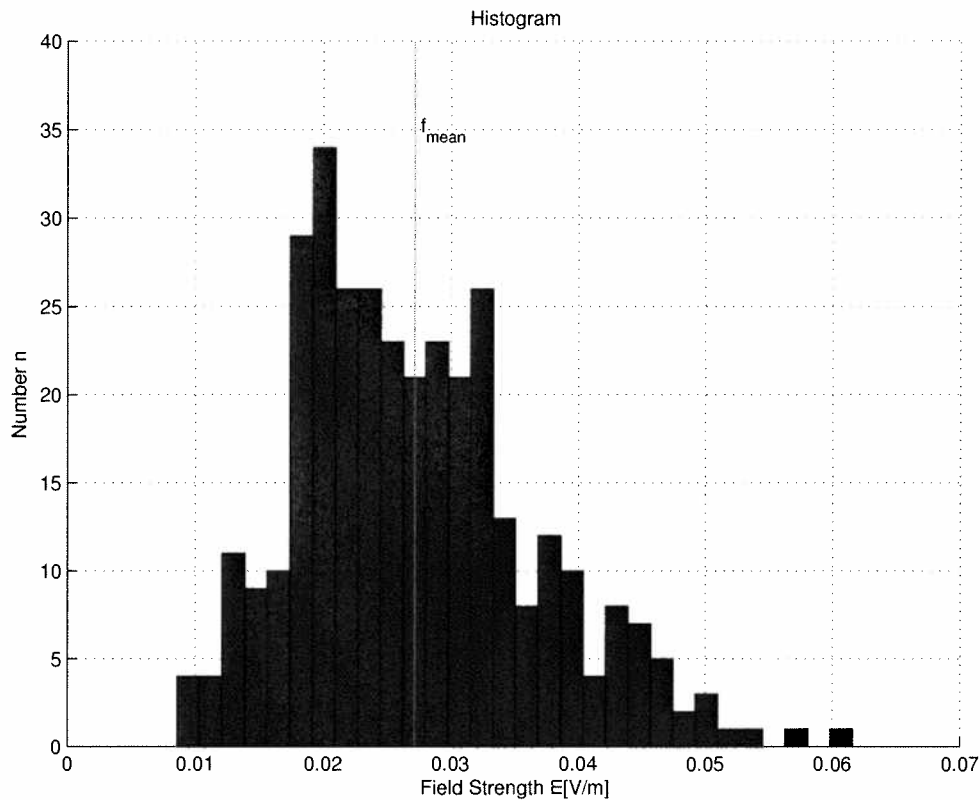


Figure 64: Global distribution of the electromagnetic field strength values disposed in 30 amplitude grades. Measured in Room A07A011 at the Mobilkom Austria office building at a frequency of 1812.4MHz, the investigated area was a small cube.

Percentiles	Description	Value [$\frac{mV}{m}$]	Normalized to the Maximum [%]
$E_{10\%}$	lower decile	16.6	27.0
$E_{25\%}$	lower quartile	20.1	32.7
$E_{50\%}$	quintile	25.9	42.0
$E_{75\%}$	higher quartile	32.7	53.1
$E_{90\%}$	higher decile	40.3	65.5

Table 19: Lower and higher quartile, lower and higher decile, quintile as well as the relative percentile referring to the maximum of the electromagnetic field strength (Mobilkom Austria Room A07A011 at DCS 1800 - small cube).

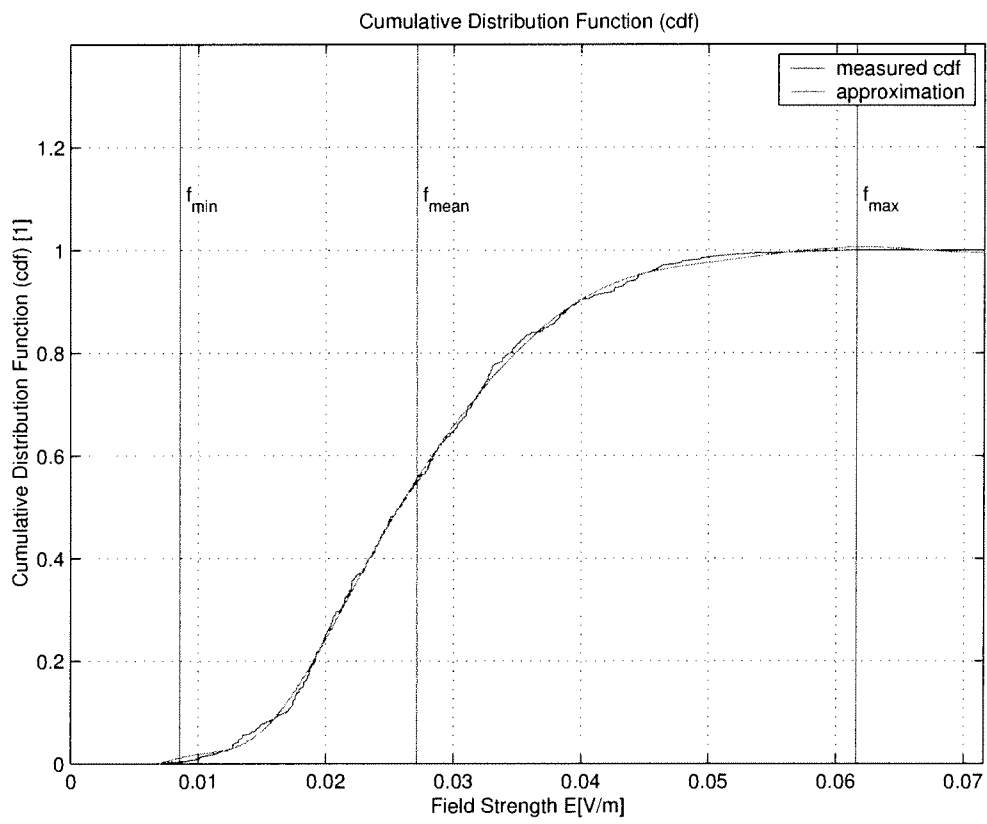


Figure 65: Cumulative distribution function (cdf) of the global field distribution (DCS 1800 - Room A07A011 Mobilkom Austria).

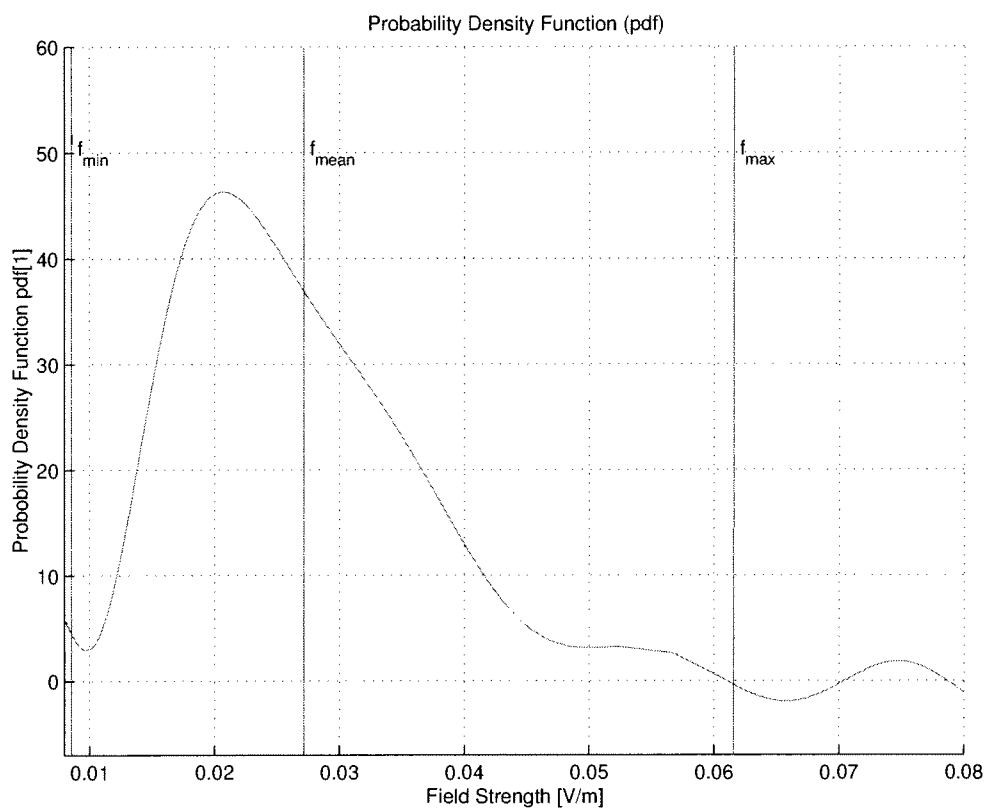


Figure 66: Probability Density function (pdf) of the global field distribution (DCS 1800 - Room A07A011 Mobilkom Austria).

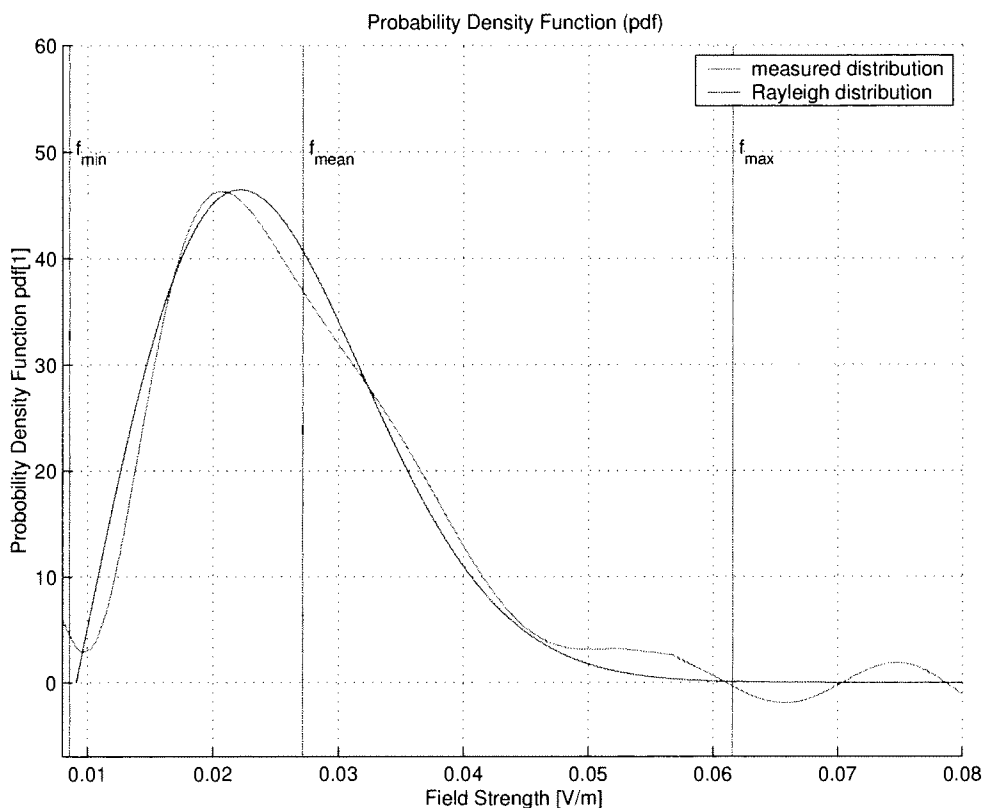


Figure 67: Approximation of the Probability Density function (pdf) with a LogNormal distribution (DCS 1800 - small cube - Room A07A011 Mobilkom Austria).

3.8.3 Identification of the Probability Density Function

A possible approximation for the function is displayed in Figure 67. It is characterized as a LogNormal distribution described by Equation 16. The polynomial approximation is valid in the range from minimum to maximum of the electromagnetic field strength.

3.8.4 Local Distribution of the Measurement Data

After the global considerations of the field distribution the local demeanor was investigated. The field strength values are very homogenous distributed over the whole cube with only a small maxima at Level z120 and z135, as Figure 68 shows (see Table 5 for the nomenclature).

3.8.4.1 Local Means

Figure 69 shows the distribution of the local mean values in each single level.

The maximum deviation from the global mean value occurs in the z-axis. The maximum is reached in Level 7 with an value of $31.9 \frac{mV}{m}$ and the minimum is

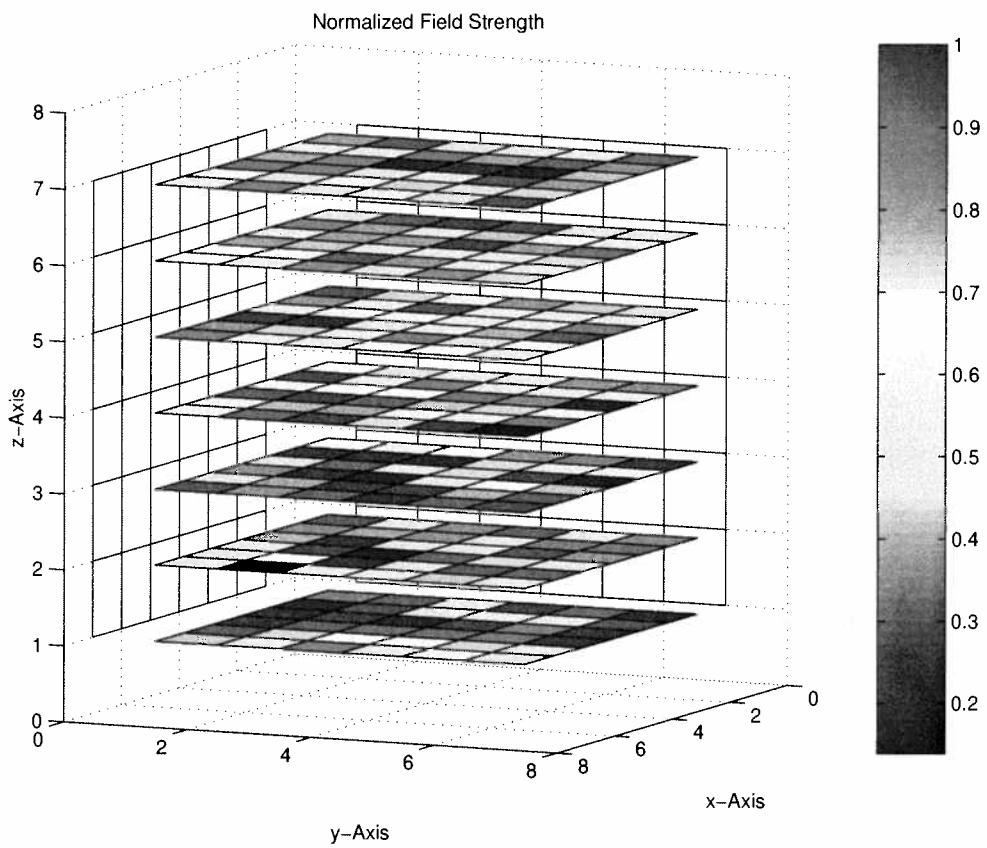


Figure 68: Distribution of the field strength values normalized to the maximum value (DCS 1800 - small cube - Room A07A011 Mobilkom Austria).

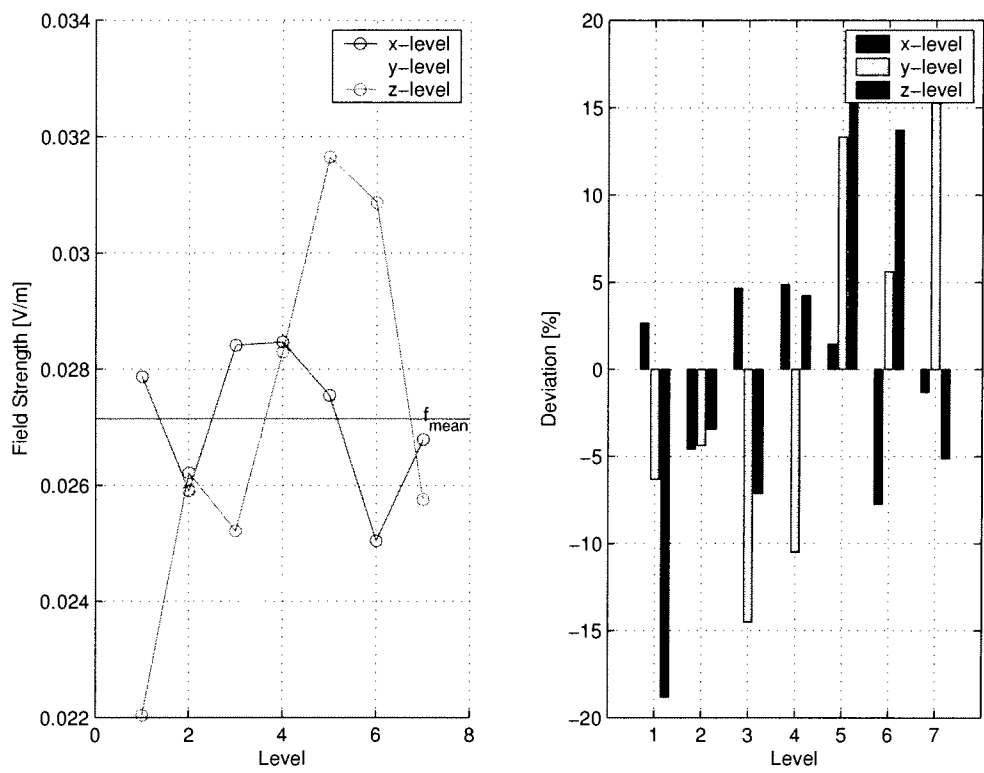


Figure 69: Arithmetic mean of the single levels (DCS 1800 - small cube - Room A07A011 Mobilkom Austria).

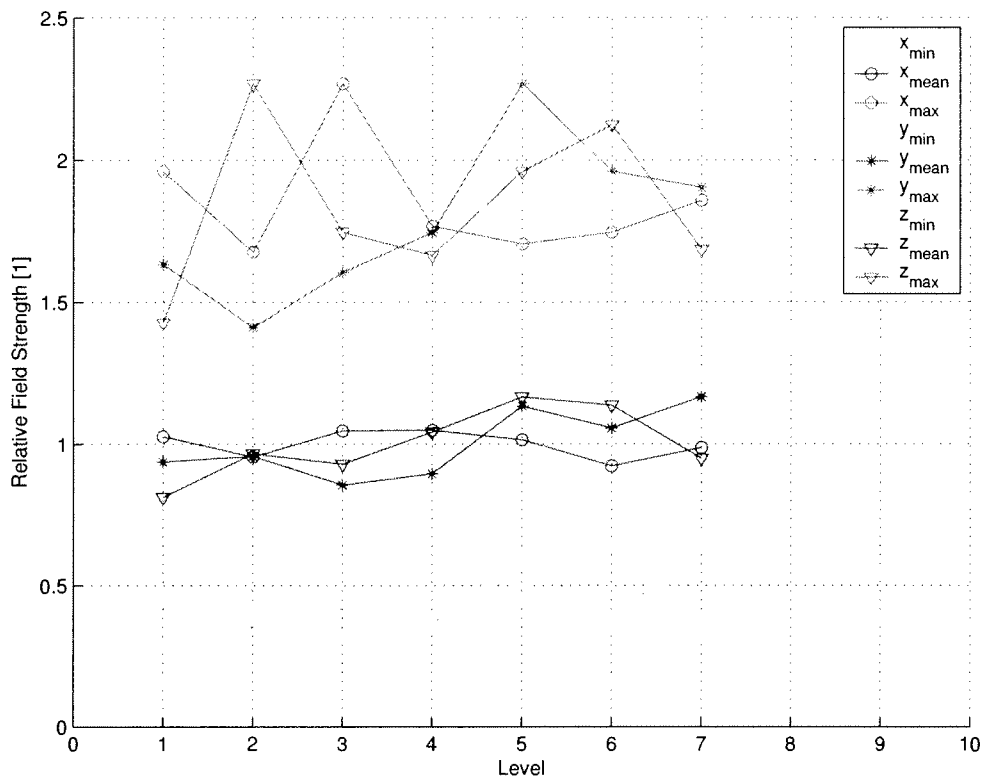


Figure 70: Relative local minima, maxima and arithmetic mean normalized to the global mean (DCS 1800 - small cube - Room A07A011 Mobilkom Austria).

reached at the z-Level 1 with an value of $22.0 \frac{mV}{m}$ which is equivalent to a factor of 14.5 between minimum and maximum.

3.8.4.2 Local Minimum and Maximum

Figure 70 shows the local minimum and maximum of each level normalized to the global mean value.

3.9 Ultra High Frequency - Small Cube Measurements

The last small cube measurement campaign was performed at a frequency of 575.25MHz, in the so called Ultra High Frequency (UHF) band. Like in all previous measurement campaigns first of all the global considerations were evaluated.

3.9.1 Mean, Standard Deviation and Amplitude Distribution

The field strength values can statistically be described by the values of Table 20. Comparing the maximum value with the maximum value of the UHF (cube measurement) measurement campaign, it shows values nearly in the same range.

Examined Positions	343
Maximum Value [mV/m]	35.8
Minimum Value [mV/m]	5.4
Global Mean Value [mV/m]	17.0
Standard Deviation [mV/m]	5.1

Table 20: Mean value, minimum and maximum value and standard deviation (Gauß) at UHF - small cube, Mobilkom Austria Room A07A011.

Percentiles	Description	Value [$\frac{mV}{m}$]	Normalized to the Maximum [%]
$E_{10\%}$	lower decile	11.0	30.6
$E_{25\%}$	lower quartile	13.3	37.0
$E_{50\%}$	quintile	16.4	45.7
$E_{75\%}$	higher quartile	19.8	55.2
$E_{90\%}$	higher decile	23.7	66.1

Table 21: Lower and higher quartile, lower and higher decile, quintile as well as the relative percentile referring to the maximum of the electromagnetic field strength (Mobilkom Austria Room A07A011 at UHF - small cube).

The maximum value is 6.6 times higher than the minimum value. The amplitude distribution is not symmetric because the arithmetic mean is located on the left side of the center between minimum and maximum of the field strength, as Figure 71 shows.

A smooth rise in the beginning and a smooth fall while decreasing on the right side of the global mean value can be observed. This could be described by a Rayleigh distribution which was already introduced in a former section (see Equation 17).

3.9.2 Cumulative Distribution Function and Probability Density Function

The cumulative distribution function (see Figure 72) can be build by arranging the field strength values by increasing amplitudes, as described in Section 3.2.2. The percentiles of the cumulative distribution function are shown in Table 21.

The probability density function (see Figure 73) can be derived by differentiating the cumulative distribution function (see Equation 12).

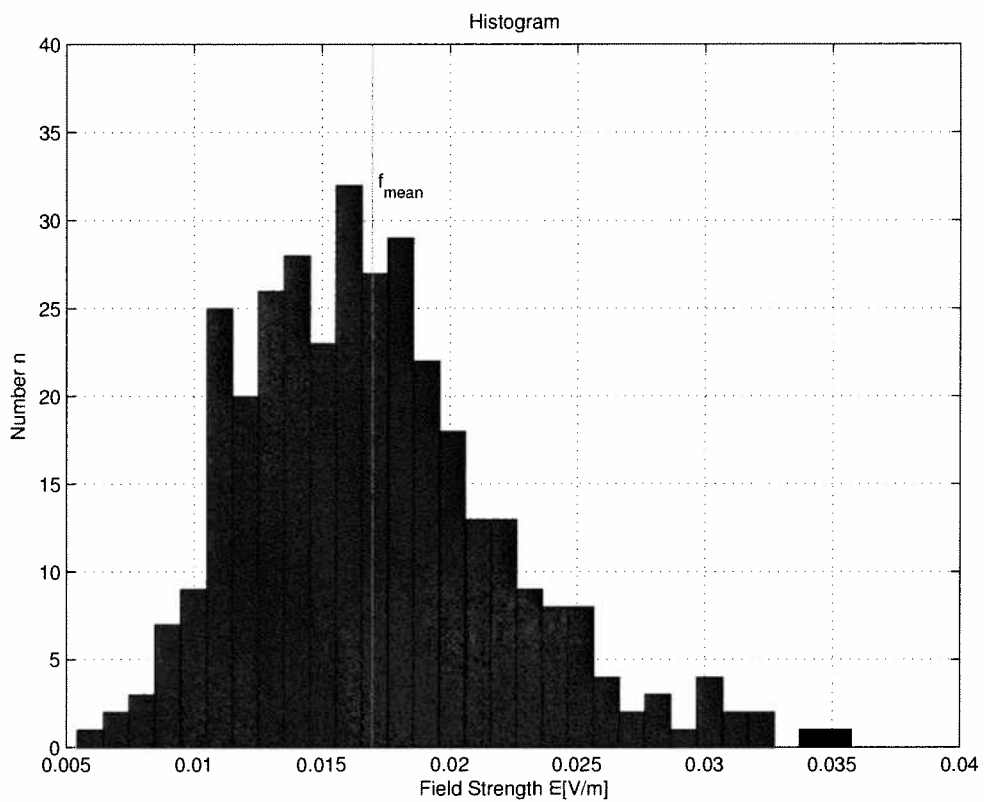


Figure 71: Global distribution of the electromagnetic field strength values disposed in 30 amplitude grades. Measured in Room A07A011 at the Mobilkom Austria office building at a frequency of 575.25MHz, the investigated area was a small cube.

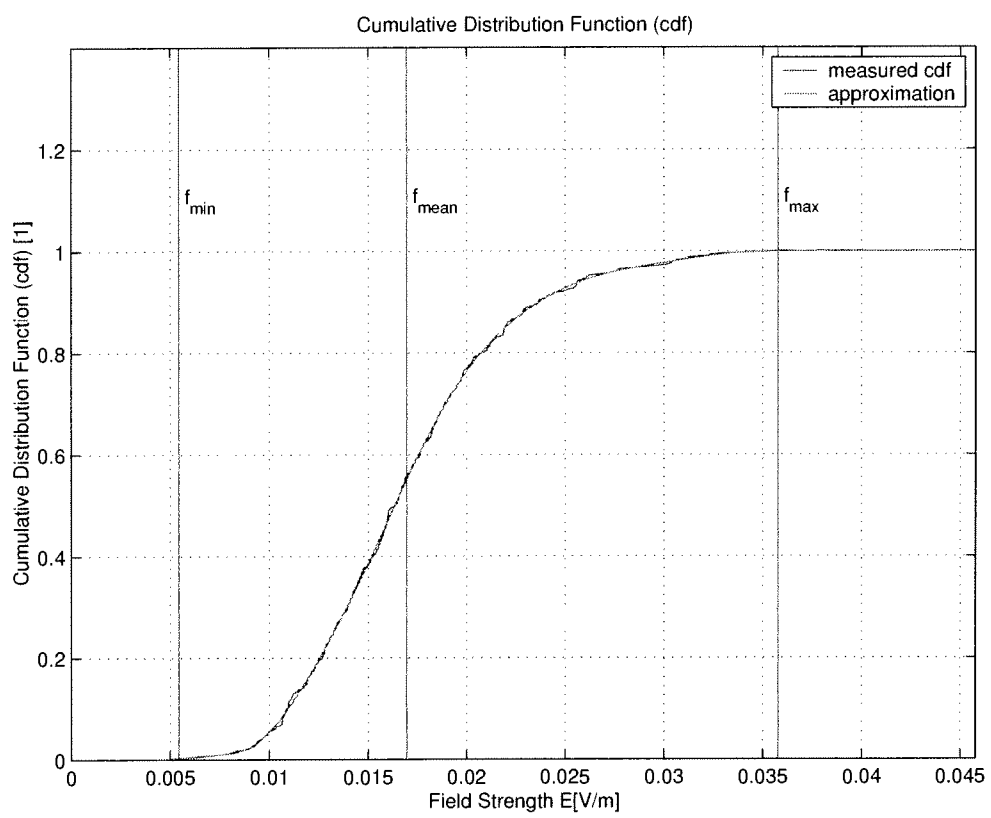


Figure 72: Cumulative distribution function (cdf) of the global field distribution (UHF - small cube - Room A07A011 Mobilkom Austria).

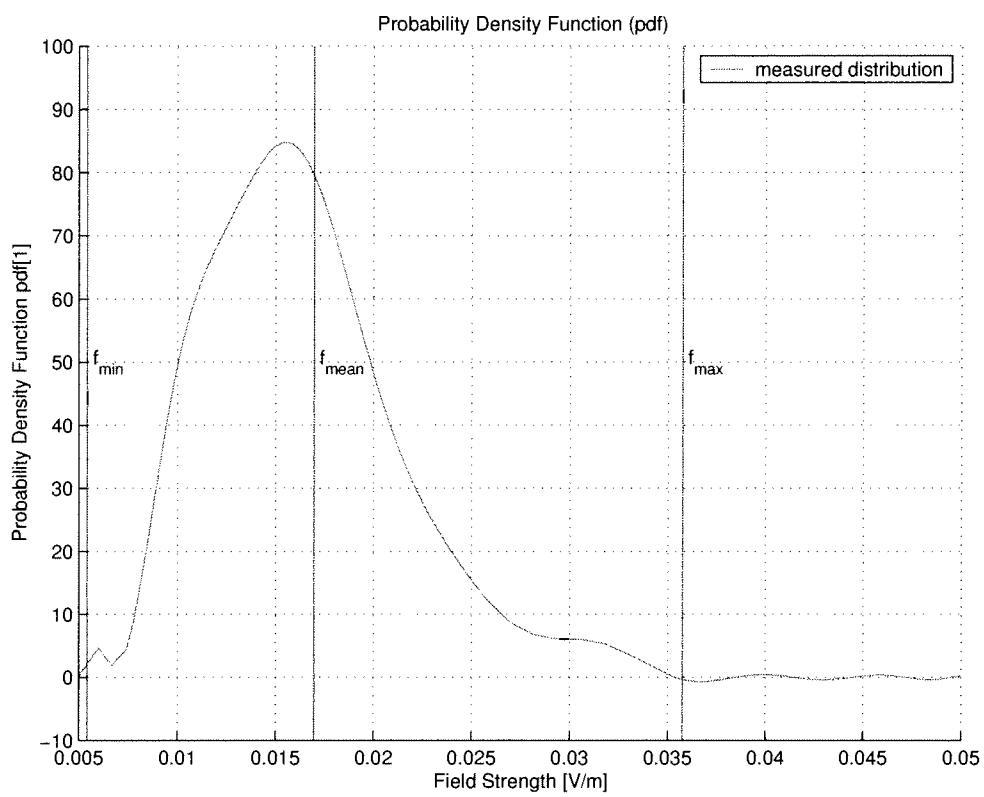


Figure 73: Probability Density function (pdf) of the global field distribution (UHF - small cube - Room A07A011 Mobilkom Austria).

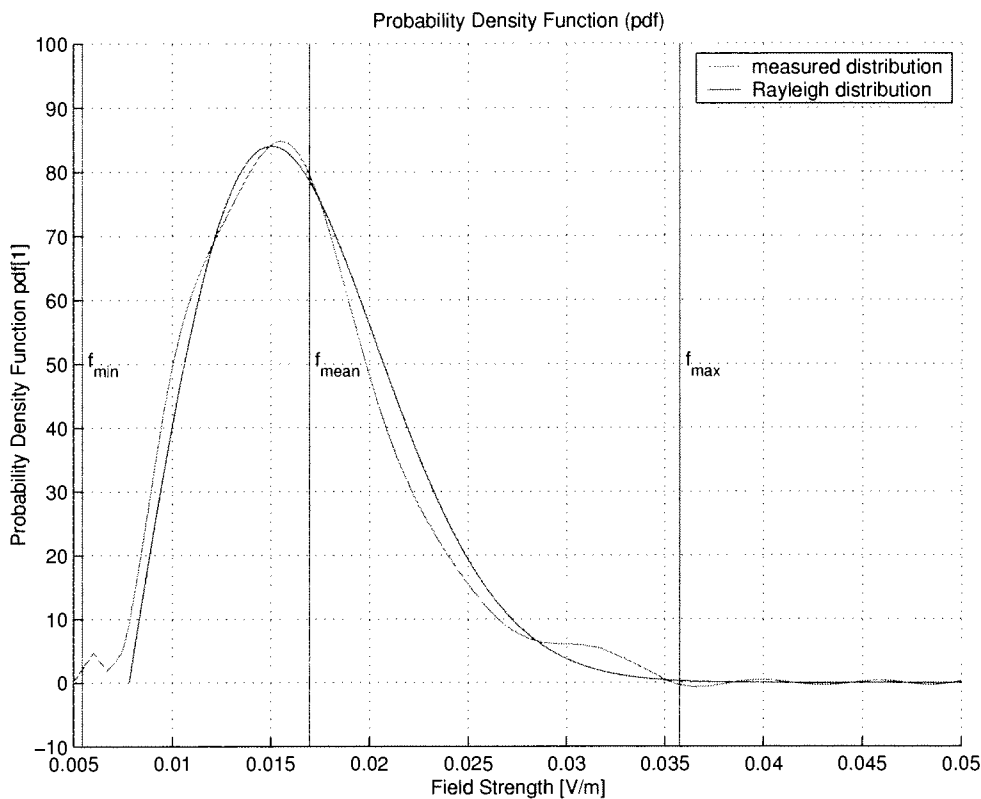


Figure 74: Approximation of the Probability Density function (pdf) by a Rayleigh distribution (UHF - small cube - Room A07A011 Mobilkom Austria).

3.9.3 Identification of the Probability Density Function

A possible approximation for the pdf is displayed in Figure 74. It is characterized as a Rayleigh distribution described by Equation 17. The polynomial approximation is valid in the range from minimum to maximum of the electromagnetic field strength.

3.9.4 Local Distribution of the Measurement Data

After the global considerations of the field strength distribution the local demeanor was investigated. The field strength values are not very homogenous distributed over the whole cube, with maximum spots distributed in Level z135, z150 and z165 as can be seen in Figure 75 (see Table 5 for the nomenclature).

3.9.4.1 Local Means

Figure 76 shows the distribution of the local mean values in each single level. The maximum deviation from the global mean value occurs in the z-axis. The maximum is reached in z-Level 7 with an value of $41.9 \frac{mV}{m}$, the minimum is reached in the z-Level 4 with an value of $24.8 \frac{mV}{m}$.

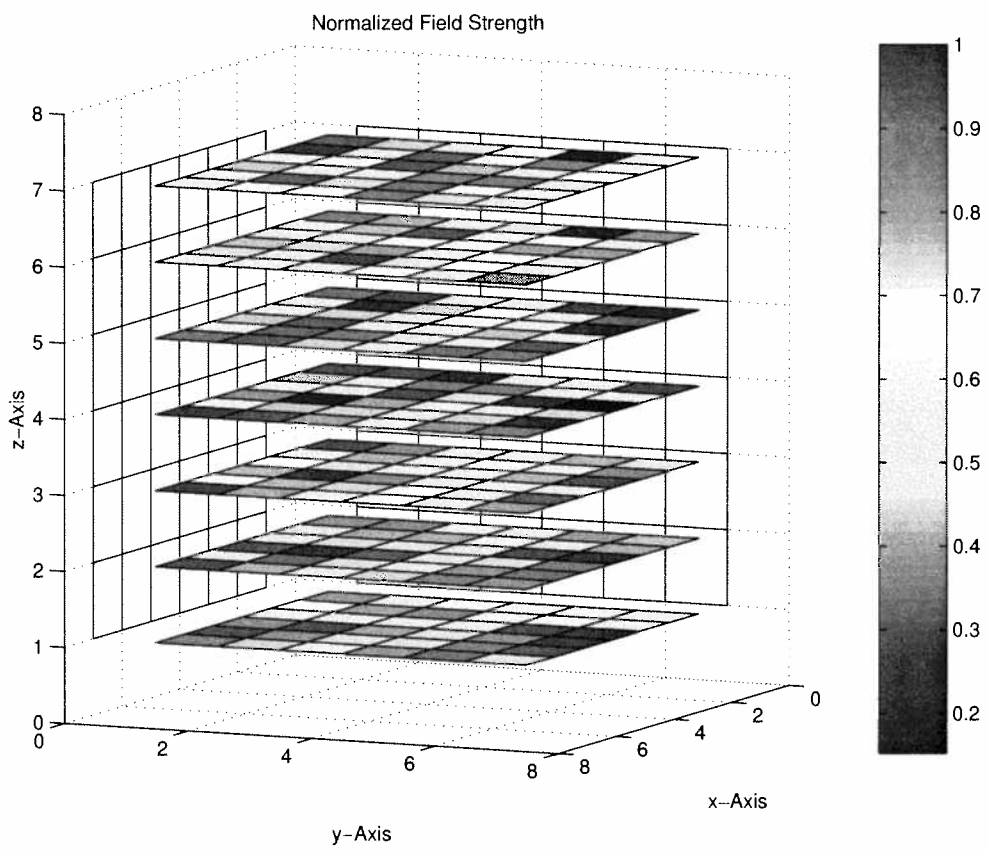


Figure 75: Distribution of the field strength values normalized to the maximum value (UHF - small cube - Room A07A011 Mobilkom Austria).

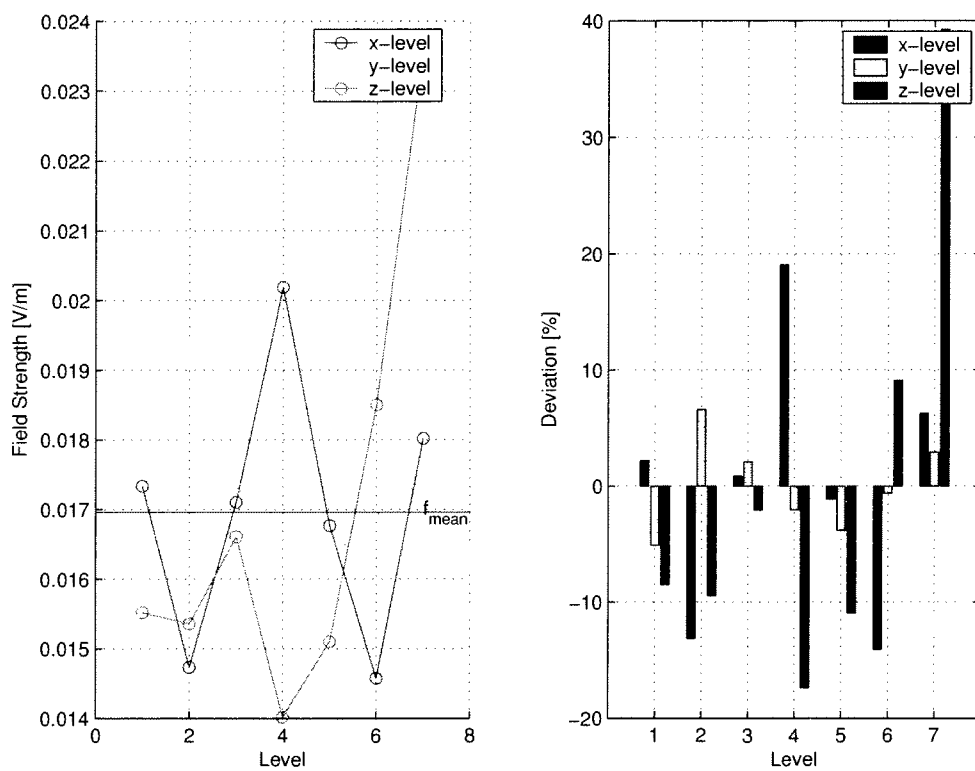


Figure 76: Arithmetic mean of the single levels (UHF - small cube - Room A07A011 Mobilkom Austria).

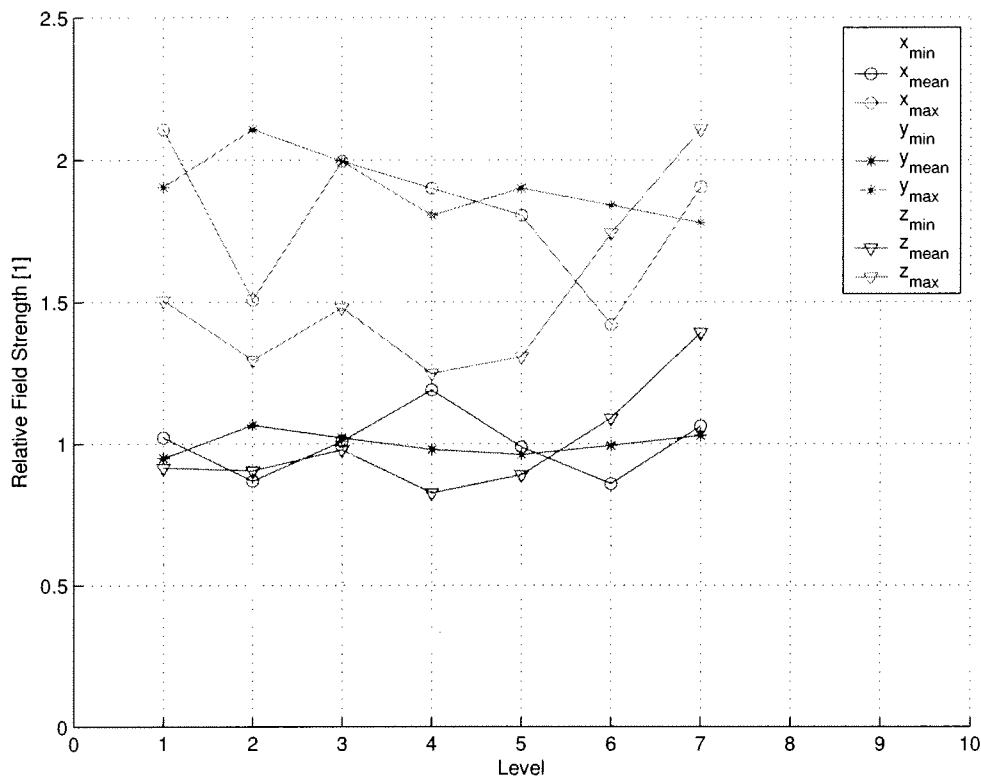


Figure 77: Relative local minima, maxima and arithmetic mean normalized to the global mean (UHF - small cube - Room A07A011 Mobilkom Austria).

3.9.4.2 Local Minimum and Maximum

Figure 77 shows the local minimum and maximum of each level normalized to the global mean.

3.10 GSM 900 - Axis Measurements

In addition to the cube and the small cube measurements, in the office building of the Mobilkom Austria, axis measurements in two different frequency bands (GSM 900 and DCS 1800) were performed, too. The axis measurement is described in Section 2.1.4 and the measurement method is the same as described in Section 2. Measurements along the x-axis and y-axis, which are orthogonal to each other, crossing the center of a cube were performed in the anteroom of the Mobilkom Austria office building (Room A07A011). In each axis 91 positions were examined which gives a total of 182 examined positions for GSM 900 and 182 examined positions for DCS 1800.

Like in all previous measurement campaigns first of all the global considerations were evaluated.

	x - axis	y - axis
Examined Positions	91	91
Maximum Value [mV/m]	41.7	33.9
Minimum Value [mV/m]	14.5	8.6
Global Mean Value [mV/m]	23.6	18.0
Standard Deviation [mV/m]	7.3	6.2

Table 22: Mean value, minimum and maximum value and standard deviation (Gauß) at GSM 900 - axis, Mobilkom Austria office building.

3.10.1 Mean, Standard Deviation and Amplitude Distribution

The field strength values can statistically be described with the values of Table 22.

The values measured along the y-axis are smaller, this can be observed at the maximum value, the minimum value, the global mean value and the standard deviation. The factor between maximum of the x-axis and maximum of the y-axis is 1.2, the factor between minimum value of the x-axis and minimum of the y-axis is 1.7 and the factor between the global mean value of the x-axis and the global mean value of the y-axis is 1.3.

The factor between the maximum value and minimum value of the x-axis is 2.9 and the factor between maximum value and minimum value of the y-axis is 3.9. The amplitude distribution is not symmetric because the arithmetic mean is located on the left side of the center between minimum and maximum of the field strength, which can be seen in Figure 78 for the x-axis and in Figure 79 for the y-axis.

The global distribution of the electromagnetic field strength values doesn't show a clear LogNormal-distribution nor a Rayleigh distribution, a possible reason for this could be the amount of measured positions which is much smaller (91 positions) compared to the cube measurement (343 positions).

3.10.2 Cumulative Distribution Function and Probability Density Function

The cumulative distribution function (see Figure 80 and Figure 81) can be build by arranging the field strength with increasing values, as described in Section 3.2.2. The percentiles of the cumulative distribution function are shown in Table 23. The probability density function (see Figure 82 and Figure 83) can be derived by differentiating the cumulative distribution function (see Equation 12).

3.10.3 Identification of the Probability Density Function

Unless stated earlier in this section, a possible approximation for the probability density function could be a LogNormal-distribution, described by Equation 16. This approximated LogNormal-distribution is displayed in Figure 84 and Figure 85. The

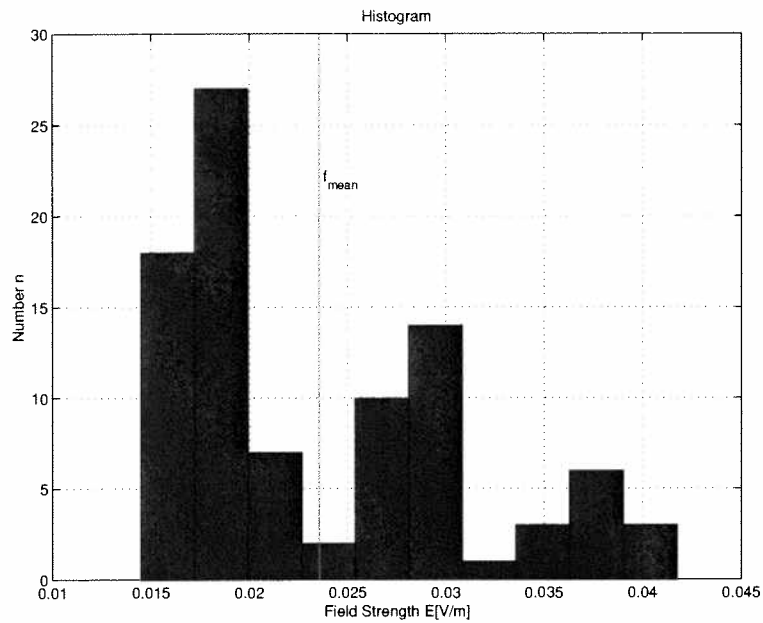


Figure 78: Global distribution of the electromagnetic field strength values disposed in 10 amplitude grades. Measured in Room A07A011 at the Mobilkom Austria office building at a frequency of 944.6MHz, the investigated area was a line along the x-axis.

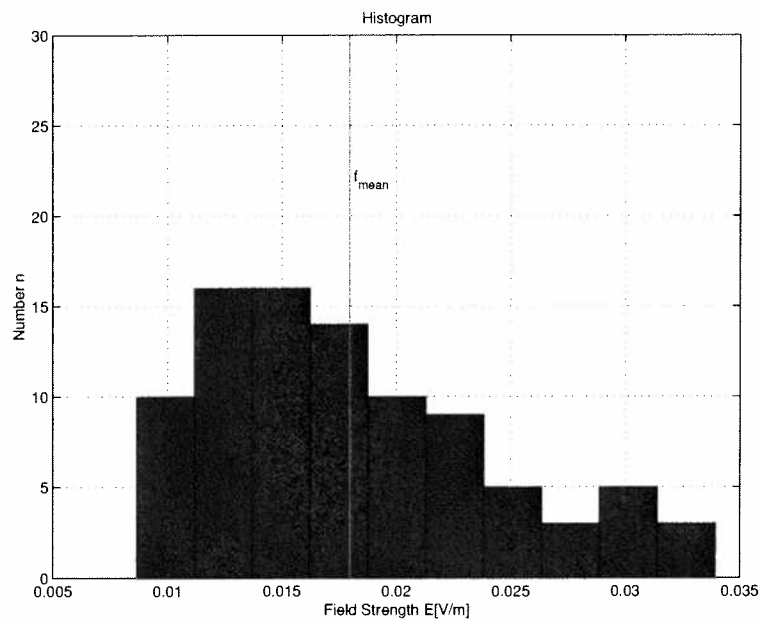


Figure 79: Global distribution of the electromagnetic field strength values disposed in 10 amplitude grades. Measured in Room A07A011 at the Mobilkom Austria office building at a frequency of 944.6MHz, the investigated area was a line along the y-axis.

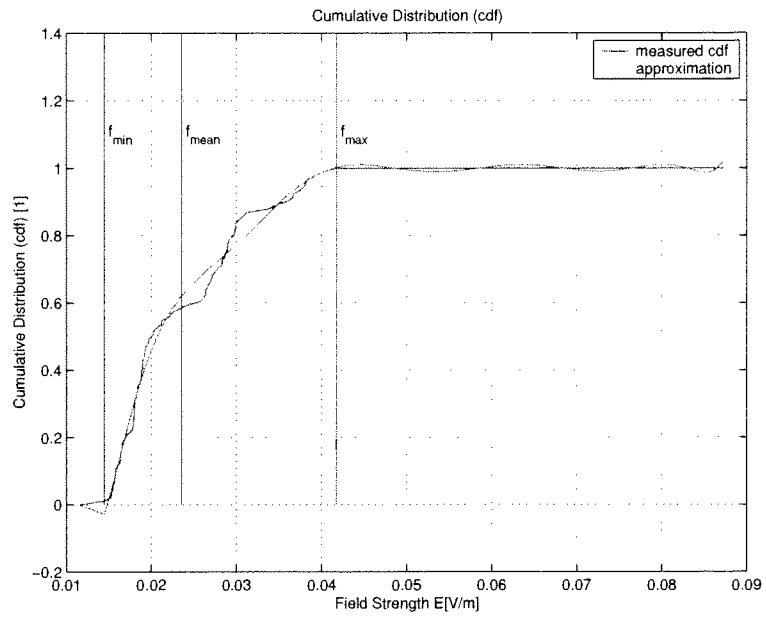


Figure 80: Cumulative distribution function (cdf) of the global field distribution (GSM 900 - x-axis, Room A07A011 Mobilkom Austria).

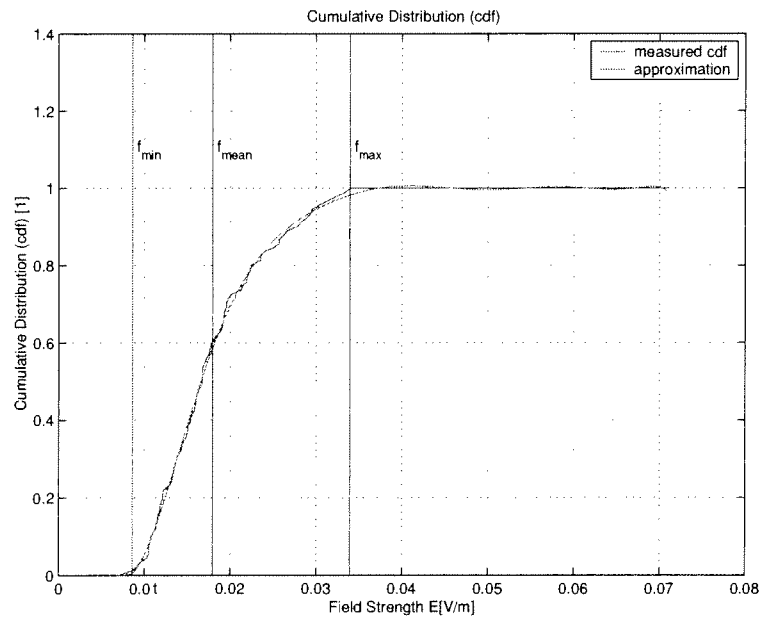


Figure 81: Cumulative distribution function (cdf) of the global field distribution (GSM 900 - y-axis, Room A07A011 Mobilkom Austria).

Percentiles	Value [$\frac{mV}{m}$]	Norm. to Max.	Value [$\frac{mV}{m}$]	Norm. to Max.
	x - axis	[%]	y - axis	[%]
$E_{10\%}$	15.9	38.1	10.9	32.2
$E_{25\%}$	17.4	41.7	13.1	38.6
$E_{50\%}$	20.7	49.6	16.6	49.0
$E_{75\%}$	29.0	69.5	21.3	62.8
$E_{90\%}$	35.2	84.4	26.8	79.1

Table 23: Lower and higher quartile, lower and higher decile, quintile as well as the relative percentile referring to the maximum of the electromagnetic field strength (Mobilkom Austria Room A07A011 at GSM 900 - x-axis and y-axis).

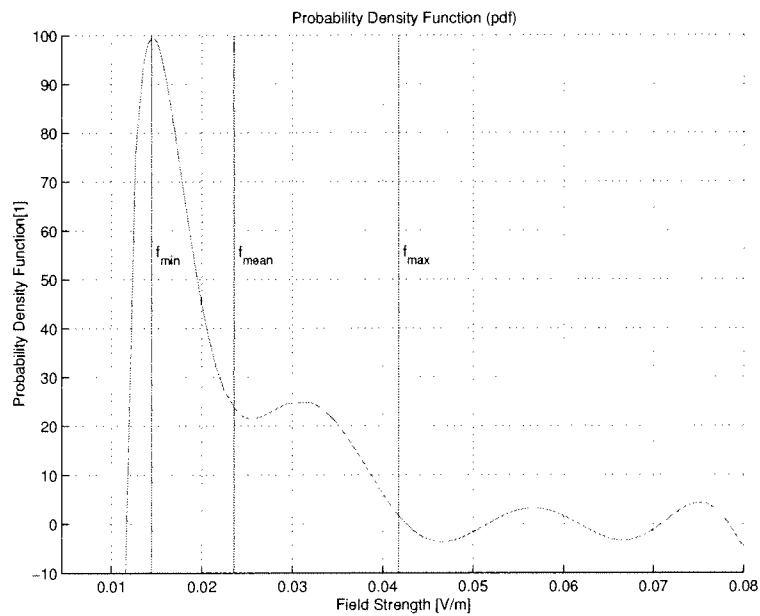


Figure 82: Probability Density function (pdf) of the global field distribution (GSM 900 - x-axis, Room A07A011 Mobilkom Austria).

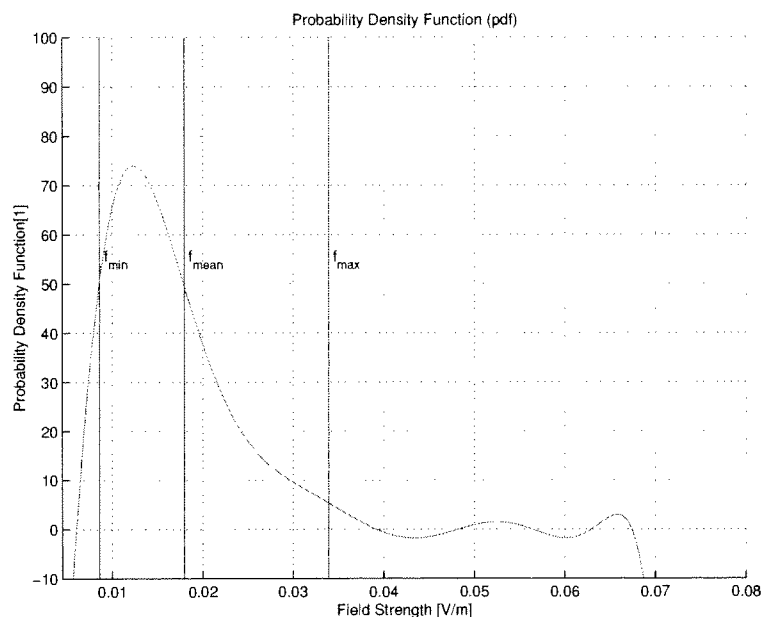


Figure 83: Probability Density function (pdf) of the global field distribution (GSM 900 - y-axis, Room A07A011 Mobilkom Austria).

polynomial approximation is valid in the range from the minimum value to the maximum value of the electromagnetic field strength.

Because the investigated area is only one dimensional local considerations do not make any sense and were therefore not evaluated.

3.11 DCS 1800 - Axis Measurements

As mentioned in the section before, also the DCS 1800 frequency band was under investigation. Like described earlier 91 examined positions along the x-axis and 91 examined positions along the y-axis, which are orthogonal to each other crossing in the center of the cube, were measured. Like in all previous measurement campaigns, first of all the global considerations were evaluated.

3.11.1 Mean, Standard Deviation and Amplitude Distribution

The field strength values can statistically be described by the values of Table 24.

The maximum value, the minimum value, the mean value and the standard deviations are nearly in the same range in both measurements (along the x-axis and along the y-axis). The factor between maximum of the x-axis and maximum of the y-axis is 1.1, the factor between minimum value of the x-axis and minimum of the y-axis is 0.6 and the factor between mean value of the x-axis and mean value of the y-axis is 1.4.

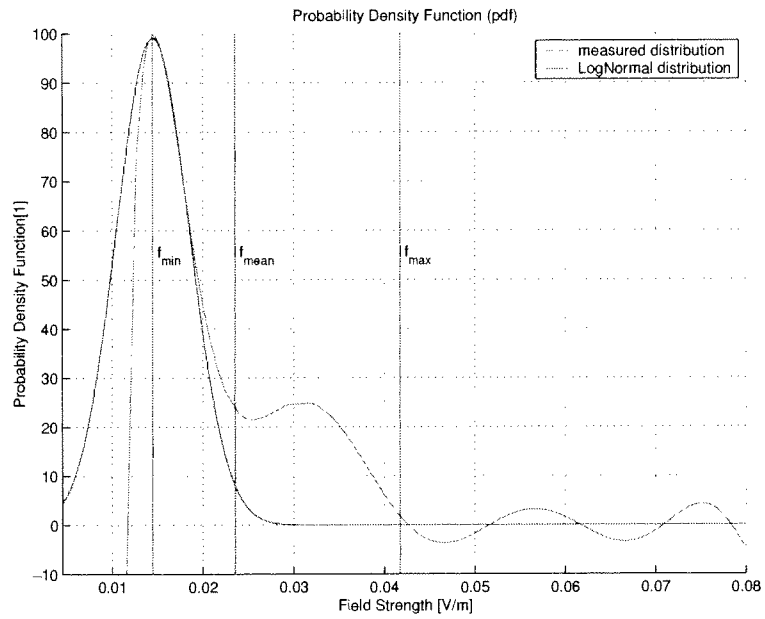


Figure 84: Approximation of the Probability Density function (pdf) by a LogNormal distribution (GSM 900 - x-axis, Room A07A011 Mobilkom Austria).

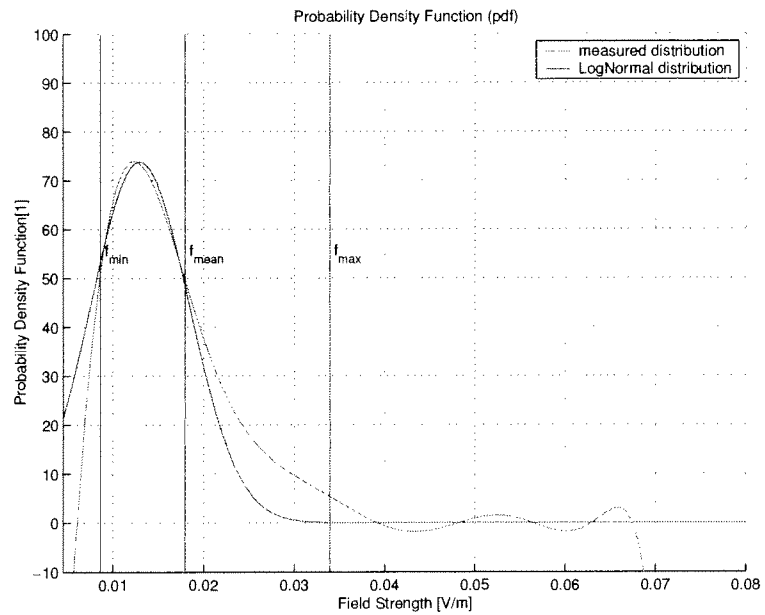


Figure 85: Approximation of the Probability Density function (pdf) by a LogNormal distribution (GSM 900 - y-axis, Room A07A011 Mobilkom Austria).

	x - axis	y - axis
Examined Positions	91	91
Maximum Value $[\frac{mV}{m}]$	41.2	36.7
Minimum Value $[\frac{mV}{m}]$	8.3	13.6
Global Mean Value $[\frac{mV}{m}]$	27.2	26.6
Standard Deviation $[\frac{mV}{m}]$	7.0	5.1

Table 24: Mean value, minimum and maximum value and standard deviation (Gauß) at DCS 1800 - axis, Mobilkom Austria office building.

Percentiles	Value $[\frac{mV}{m}]$	Norm. to Max.	Value $[\frac{mV}{m}]$	Norm. to Max.
	x - axis	[%]	y - axis	[%]
$E_{10\%}$	18.9	45.9	19.7	53.8
$E_{25\%}$	22.2	53.9	23.0	62.7
$E_{50\%}$	26.7	64.8	26.7	72.8
$E_{75\%}$	32.0	77.7	30.3	82.6
$E_{90\%}$	36.7	89.1	33.2	90.5

Table 25: Lower and higher quartile, lower and higher decile, quintile as well as the relative percentile referring to the maximum of the electromagnetic field strength (Mobilkom Austria Room A07A011 at DCS 1800 - x-axis and y-axis).

The factor between the maximum value and minimum value of the x-axis is 4.9 and the factor between maximum value and minimum value of the y-axis is 2.7. The amplitude distribution is not symmetric because the arithmetic mean is located on the left side of the center between minimum and maximum of the field strength, which can be seen in Figure 86 for the x-axis and in Figure 87 for the y-axis.

The global distribution of the electromagnetic field strength doesn't show a clear LogNormal distribution nor a Rayleigh distribution, because the examined positions are only one fourth of the examined positions of a cube and therefore not so representative (91 positions vs. 343 positions).

3.11.2 Cumulative Distribution Function and Probability Density Function

The cumulative distribution function (see Figure 88 and Figure 89) can be build by arranging the field strength with increasing values, as described in Section 3.2. The percentiles of the cumulative distribution function are shown in Table 25.

The probability density function (see Figure 82 and Figure 83) can be derived by differentiating the cumulative distribution function (see Equation 12).

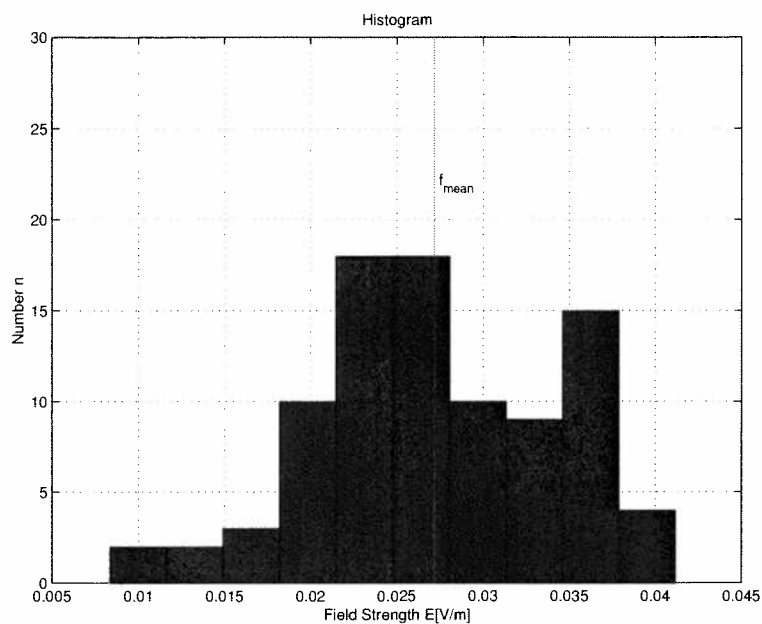


Figure 86: Global distribution of the electromagnetic field strength values disposed in 10 amplitude grades. Measured in Room A07A011 at the Mobilkom Austria office building at a frequency of 944.6MHz, the investigated area was a line along the x-axis.

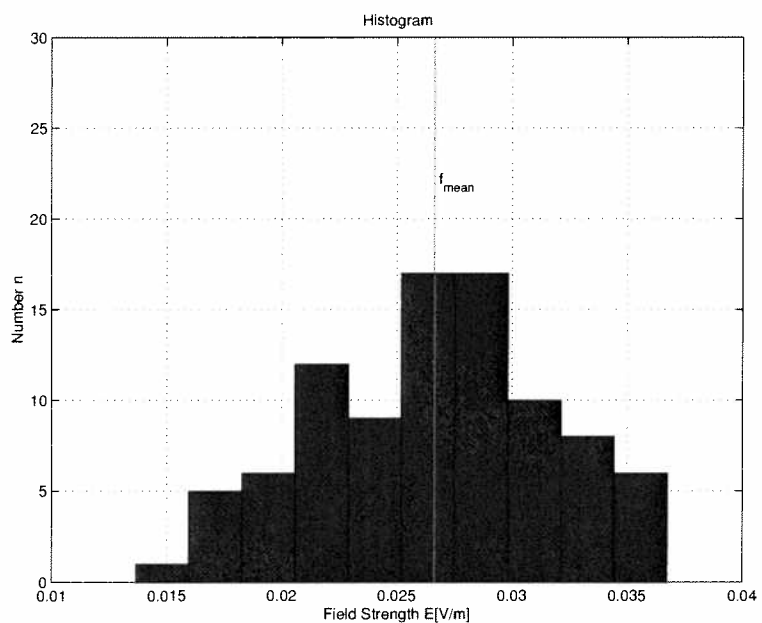


Figure 87: Global distribution of the electromagnetic field strength values disposed in 10 amplitude grades. Measured in Room A07A011 at the Mobilkom Austria office building at a frequency of 944.6MHz, the investigated area was a line along the y-axis.

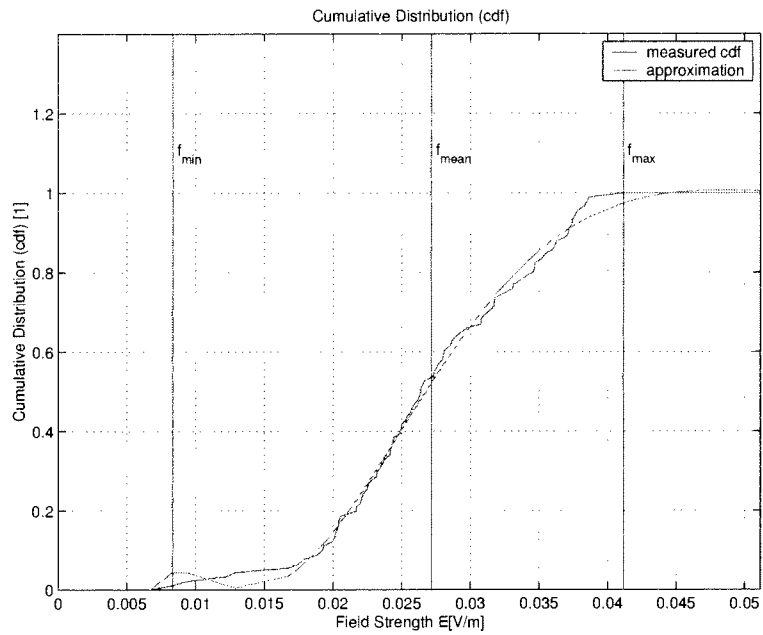


Figure 88: Cumulative distribution function (cdf) of the global field distribution (DCS 1800 - x-axis, Room A07A011 Mobilkom Austria).

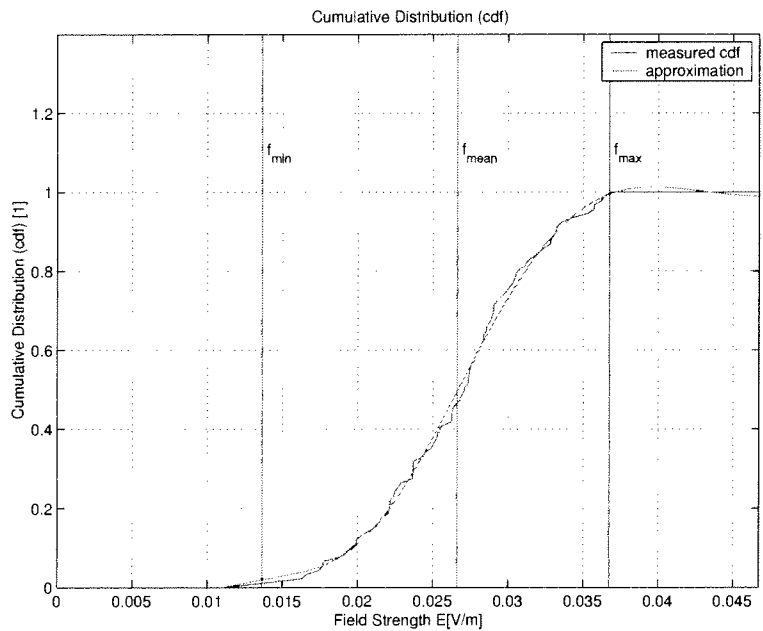


Figure 89: Cumulative distribution function (cdf) of the global field distribution (DCS 1800 - y-axis, Room A07A011 Mobilkom Austria).

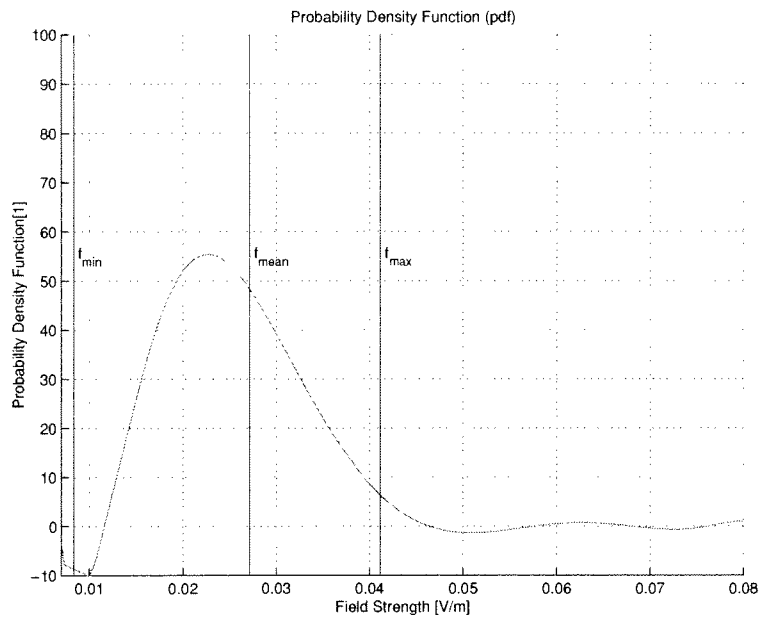


Figure 90: Probability Density function (pdf) of the global field distribution (DCS 1800 - x-axis, Room A07A011 Mobilkom Austria).

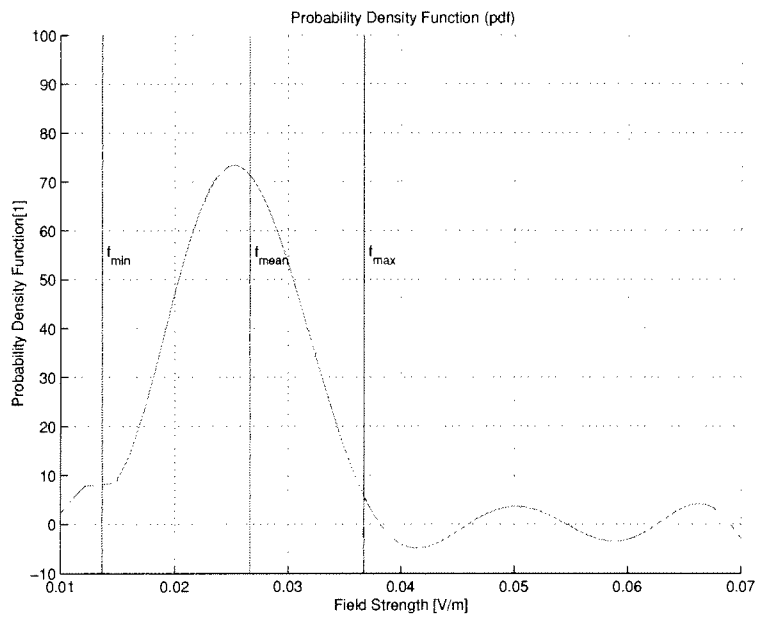


Figure 91: Probability Density function (pdf) of the global field distribution (DCS 1800 - y-axis, Room A07A011 Mobilkom Austria).

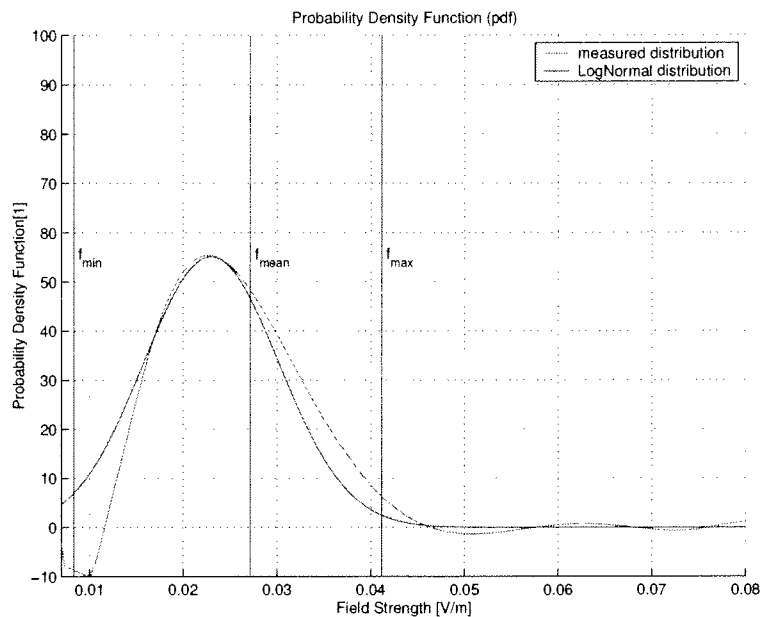


Figure 92: Approximation of the Probability Density function (pdf) by a LogNormal distribution (DCS 1800 - x-axis, Room A07A011 Mobilkom Austria).

3.11.3 Identification of the Probability Density Function

Unless stated earlier in this section a possible approximation for the probability density function could be a LogNormal distribution, described by Equation 16. This approximated LogNormal distribution is displayed in Figure 92 and Figure 93. The polynomial approximation is valid in the range from minimum value to maximum value of the electromagnetic field strength.

Because the investigated area is only one dimensional local considerations do not make any sense and were therefore not evaluated.

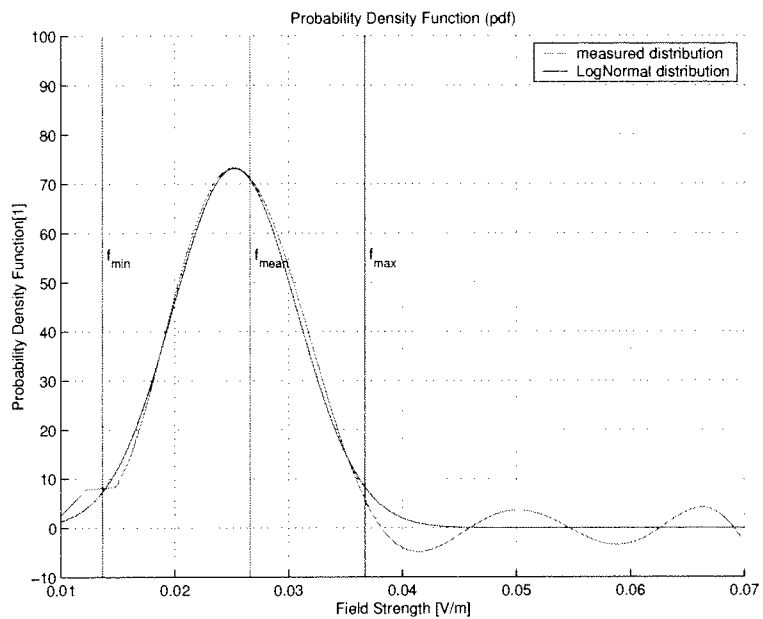


Figure 93: Approximation of the Probability Density function (pdf) by a LogNormal distribution (DCS 1800 - y-axis, Room A07A011 Mobilkom Austria).

4 Measurement Campaign - *ARC Seibersdorf research GmbH* office building

With the same measurement method (described in Section 2), volumes and areas were examined at the *ARC Seibersdorf research GmbH* office building. On the premises a GSM 900 Base Station is located as shown in Figure 94. Two different rooms were under investigation with different characteristics. The Room TOX 7 had Non-Line-Of-Sight (NLOS) to the transmitting antenna while Room CC2-17 had Line-Of-Sight (LOS), only a tree is partly in the direction to the transmitting antenna.

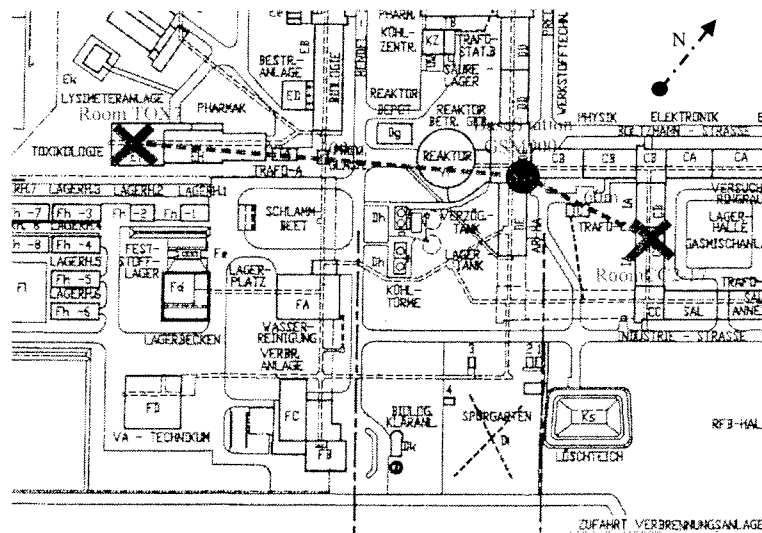


Figure 94: Map of the two rooms - Room TOX 7 and Room CC2-17, as well as the location of the mobile communication base station.

4.1 GSM 900 - Room TOX 7 - Cube Measurements

At a frequency of 946.6MHz measurements were performed in Room TOX 7 in the *ARC Seibersdorf research GmbH* office building. This room had no windows and therefore represented a typical Non-Line-Of-Sight scenario. The transmitting antenna was 200m away from the examined volume. A map of the area around the room and the transmitting antennas is shown in Figure 94. The measurement method used was the same than at the Mobilkom Austria measurement campaign described in Section 2, also the set-up and the used equipment was the same.

Now the global aspects of this measurement were taken under consideration in the following sections.

Examined Positions	343
Maximum Value [mV/m]	4.6
Minimum Value [mV/m]	1.0
Global Mean Value [mV/m]	2.3
Standard Deviation [mV/m]	0.6

Table 26: Mean value, minimum and maximum value and standard deviation (Gauß) at GSM 900 - cube, *ARC Seibersdorf research GmbH* Room TOX 7.

4.1.1 Mean, Standard Deviation and Amplitude Distribution

Compared to the former measurement campaign (GSM 900) of the cube in the Mobilkom Austria office building the maximum value is tremendously lower. The factor between the maximum of the cube measurement in the Mobilkom Austria and the maximum of the cube measurement in Room TOX 7 in Seibersdorf is 14.4, whereas the measured value in Seibersdorf is by this factor lower. Comparing the behavior of the global mean and minimum of those two measurements, it doesn't show any differences. The minimum value in Room TOX 7 is by a factor of 5.4 smaller and the global mean value is by the factor of 9.0 smaller than the value measured in the Mobilkom Austria office building (Room A07A011). The reason are the circumstances where the measurement was performed, the room had Non-Line-Of-Sight, no windows, thick walls and was located in the middle of a building complex, also the distance to the transmitting antenna was with 200m much higher than at the Mobilkom Austria. The amplitude distribution can be seen in Figure 95.

4.1.2 Cumulative Distribution Function and Probability Density Function

The cumulative distribution function (see Figure 96) can be built by arranging the field strength with increasing values, as described in Section 3.2.2. The percentiles of the cumulative distribution function are shown in Table 27. The probability density function (see Figure 97) can be derived by differentiating the cumulative distribution function (see Equation 12).

4.1.3 Identification of the Probability Density Function

A possible approximation for the function is displayed in Figure 98. This approximation is characterized as a Rayleigh distribution described by Equation 17. The validity of the polynomial approximation is in the range between minimum and maximum of the electromagnetic field strength.

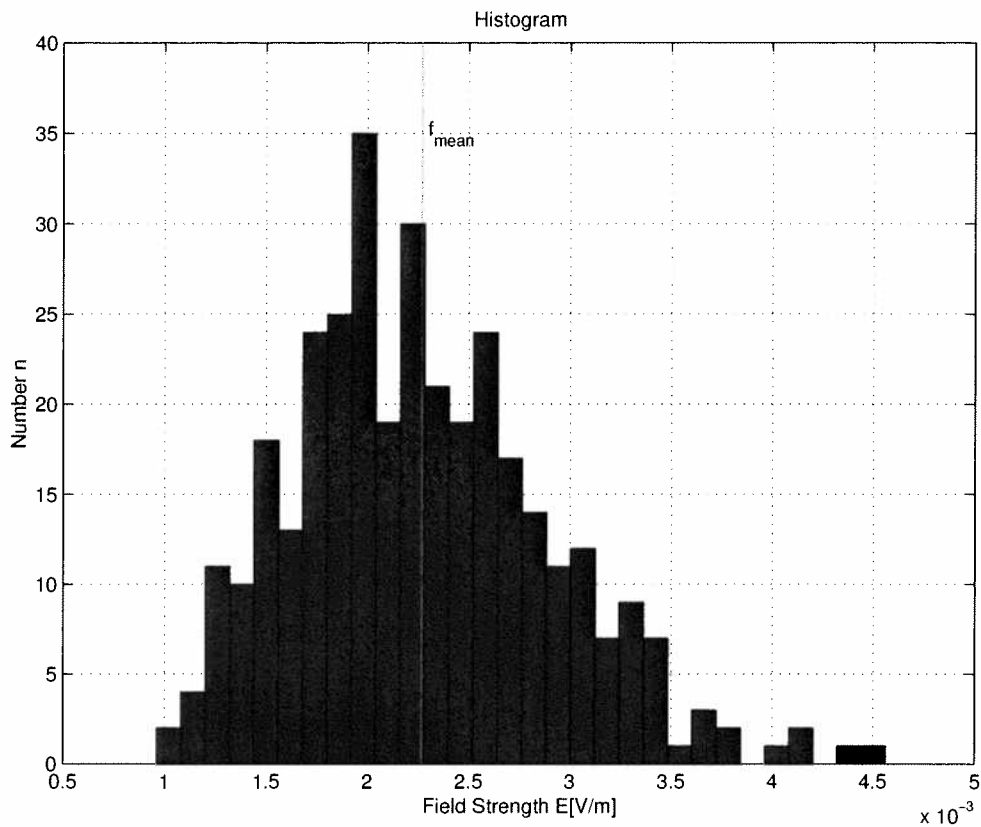


Figure 95: Global distribution of the electromagnetic field strength values disposed in 30 amplitude grades. Measured in Room TOX 7 at the *ARC Seibersdorf research GmbH* office building at a frequency of 944.6MHz, the investigated area was a cube.

Percentiles	Description	Value [$\frac{mV}{m}$]	Normalized to the Maximum [%]
$E_{10\%}$	lower decile	15.0	32.6
$E_{25\%}$	lower quantile	18.0	39.1
$E_{50\%}$	quintile	22.0	47.8
$E_{75\%}$	higher quartile	27.0	58.7
$E_{90\%}$	higher decile	31.0	67.4

Table 27: Lower and higher quartile, lower and higher decile, quintile as well as the relative percentile referring to the maximum of the electromagnetic field strength (*ARC Seibersdorf research GmbH* at GSM 900 - cube, Room TOX 7).

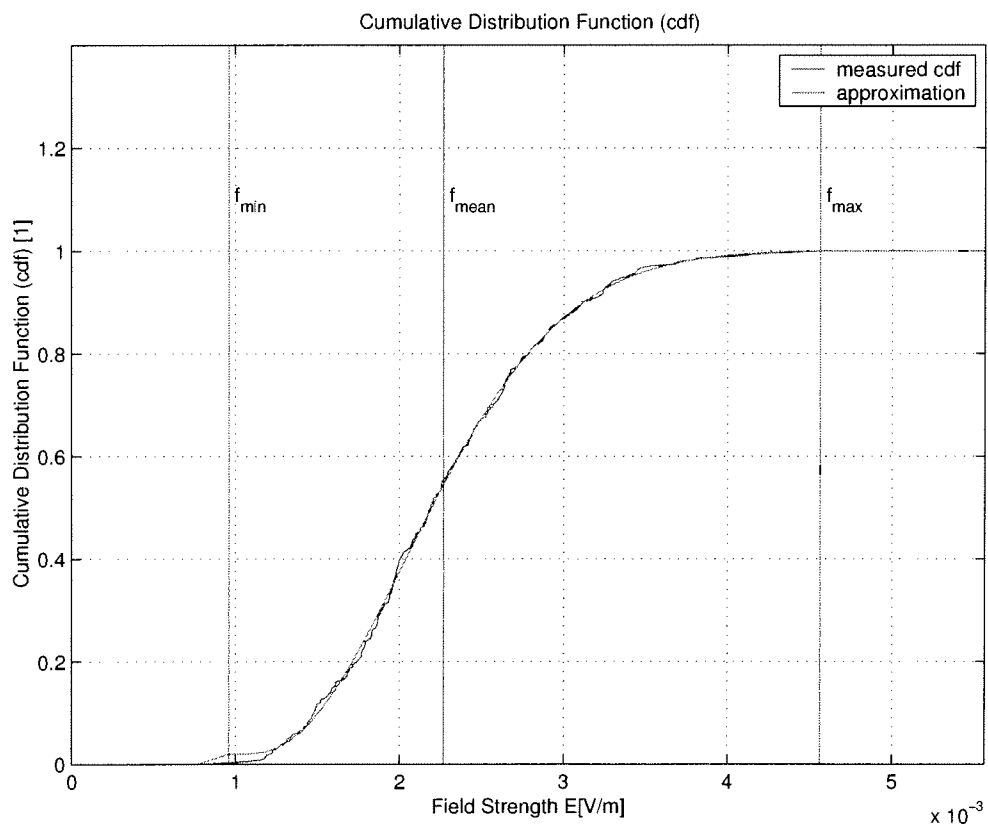


Figure 96: Cumulative distribution function (cdf) of the global field distribution (GSM 900 - Room TOX 7 ARC Seibersdorf research GmbH office building).

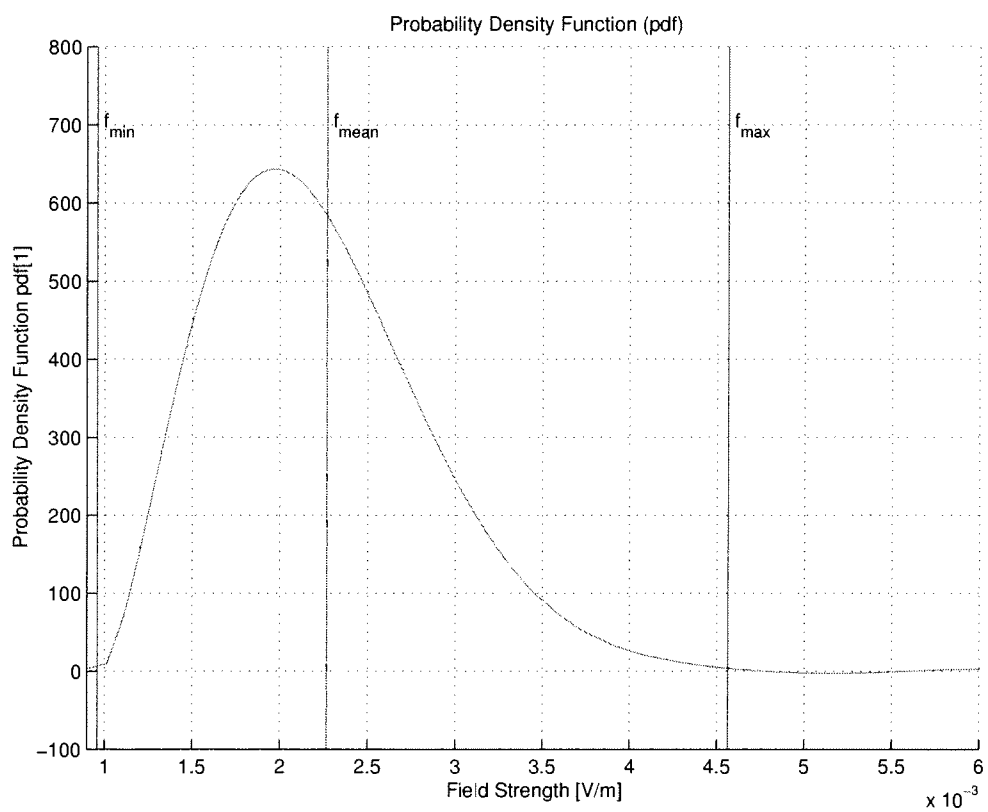


Figure 97: Probability Density function (pdf) of the global field distribution (GSM 900 - Room TOX 7 ARC Seibersdorf research GmbH office building).

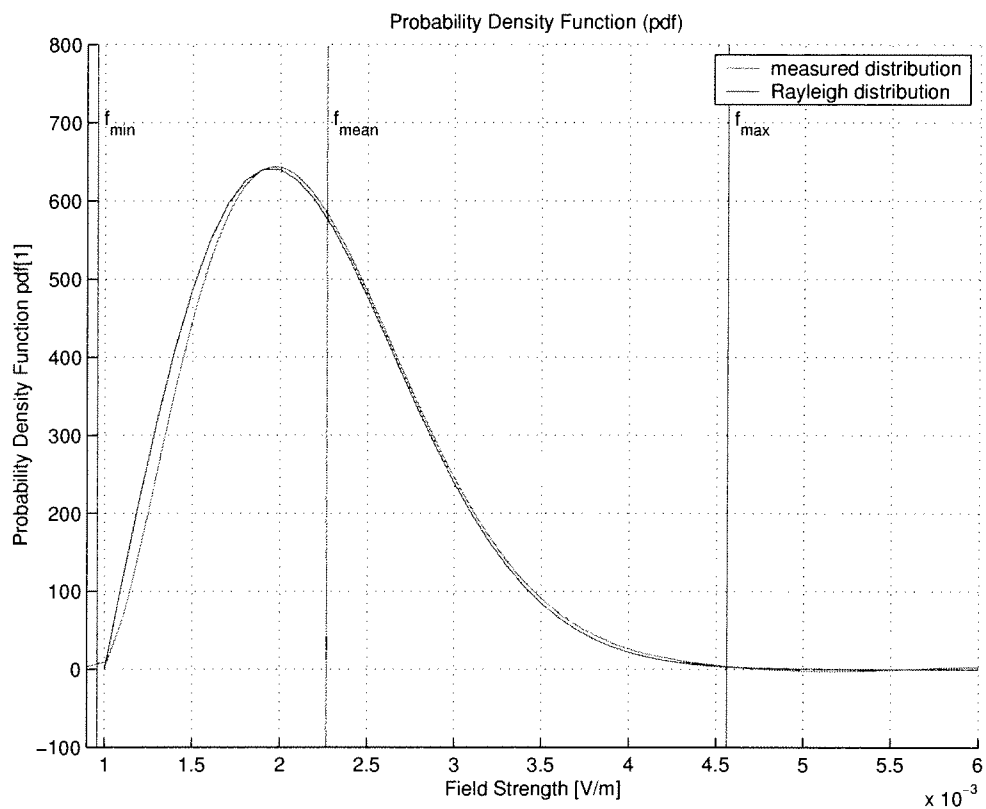


Figure 98: Approximation of the Probability Density function (pdf) by a Rayleigh distribution (GSM 900 - Room TOX 7 ARC Seibersdorf research GmbH office building).

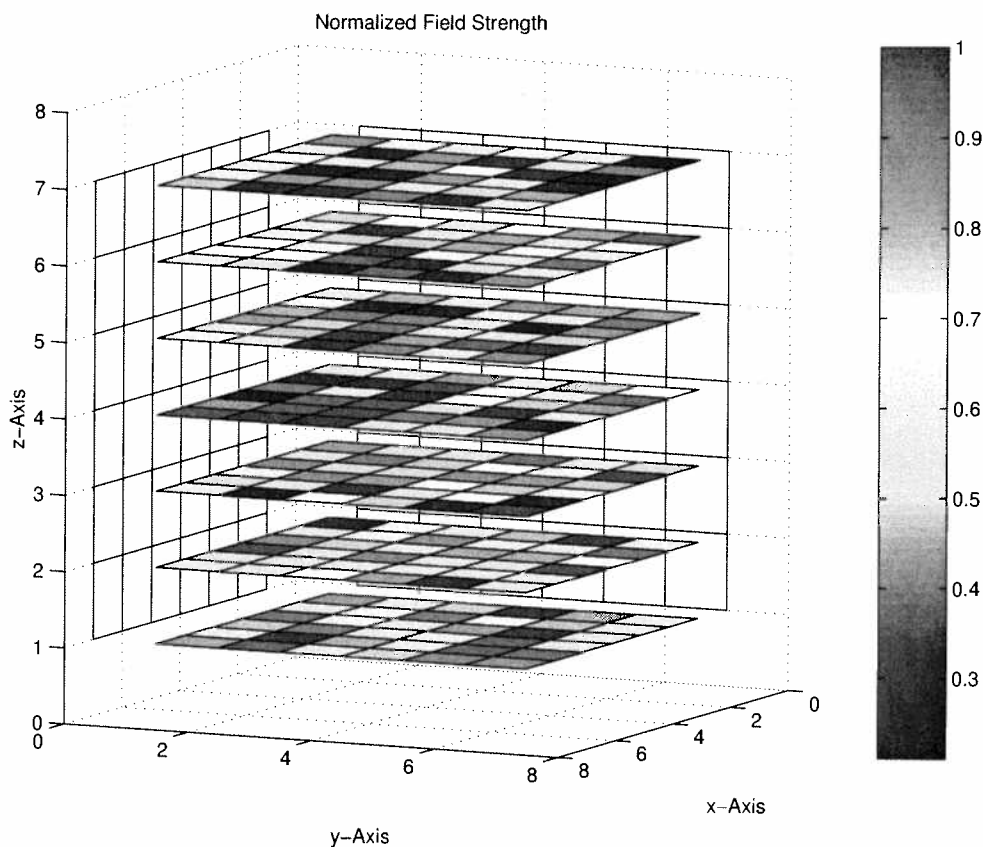


Figure 99: Distribution of the field strength values normalized to the maximum value (GSM 900 - Room TOX 7 ARC Seibersdorf research GmbH office building).

4.1.4 Local Distribution of the Measurement Data

After the global considerations of the field strength distribution, the local demeanor was investigated. The field strength values are very homogeneously distributed over the whole cube with no particular maxima, as can be seen in Figure 99.

4.1.4.1 Local Means

Figure 100 shows the distribution of the local means in each single level. The maximum deviation from the global mean value occurs in the z-axis. The maximum is reached in x-Level 4 with an value of $2.7 \frac{mV}{m}$ whereas the minimum is reached in z-Level 4 with an value of $2.0 \frac{mV}{m}$.

4.1.4.2 Local Minimum and Maximum

Figure 101 shows the local minimum and maximum of each level normalized to the global mean value.

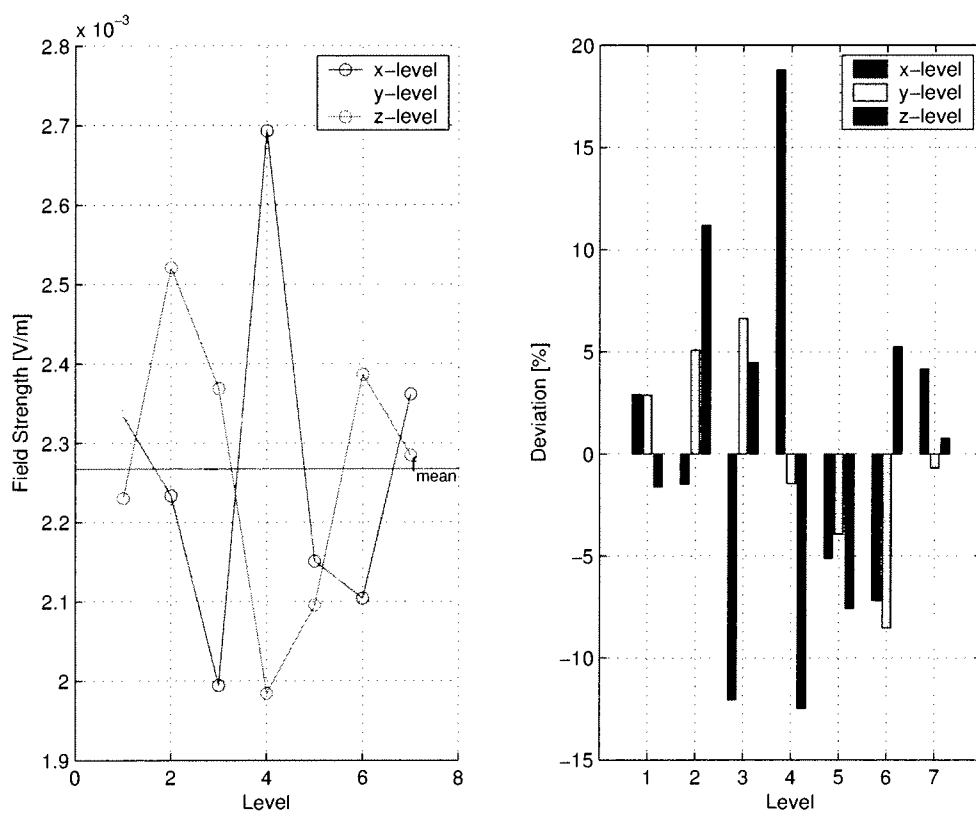


Figure 100: Arithmetic mean of the single levels (GSM 900 - cube - Room TOX 7 ARC Seibersdorf research GmbH office building).

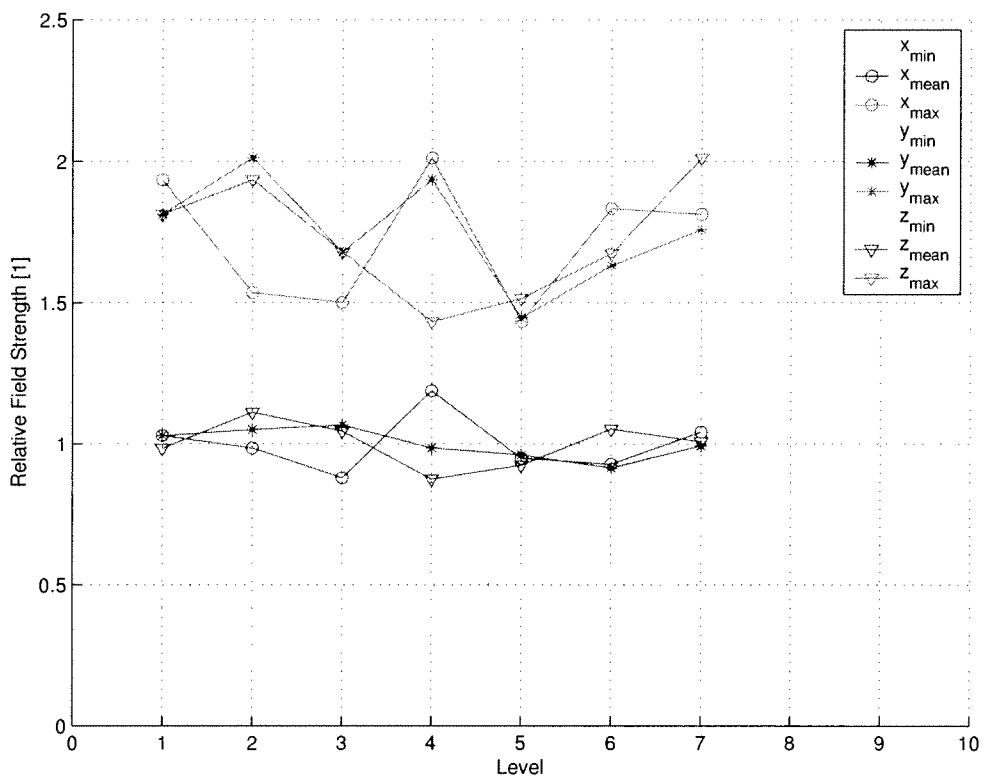


Figure 101: Relative local minima, maxima and arithmetic mean normalized to the global mean (GSM 900 - Room TOX 7 ARC Seibersdorf research GmbH office building).

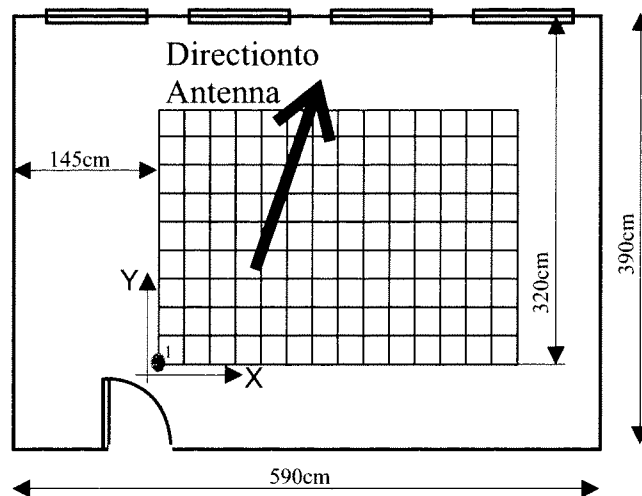


Figure 102: Schematic of the conference Room CC2-17 at the *ARC Seibersdorf research GmbH* office building. The grey area shows the area which was under investigation with the origin in the lower left corner. The height of the room is 3m.

4.2 GSM 900 - Room CC2-17 - Area Measurements

The Room CC2-17 is a conference room with 4 windows on one side, which are facing the transmitting antenna. A schematic of this room can be found in Figure 102. The base station antenna is 60m away from the room under investigation. At a frequency of 946.6MHz measurements within an area (described in Section 2.1.3) were performed. A map of the area around the room and the transmitting antennas is shown in Figure 94. To generate a better imagination of the measurement scenario, some pictures were shot from the Room CC2-17 as well as from outside the building. Figure 103 shows the Room CC2-17 with the measurement antenna, the reference antenna, the measurement equipment and the grid taped to the floor. The green arrow shows the direction to the base station antenna. The base station antenna, partly hidden by the leaves of the tree can be seen in Figure 104. An outside view of the base station antenna, mounted on the building, shows Figure 105. A view of the whole area between base station antenna and Room CC2-17, which was under investigation, can be seen in Figure 106. A front view of the four windows of Room CC2-17 and the direction to the base station antenna can be seen in Figure 107. Figure 108 shows the view of the base station antenna through the open window of Room CC2-17. It can be seen, that the antenna is partly hidden behind the leaves of the tree.

This measurement was repeated two days after the first measurement took place. The first measurement was on a Saturday afternoon (in this context called "day 1") and the second on a Monday afternoon (called "day 2"). So the exact same measurement was performed on two different days.

The measurement method used, was the same than in the Mobilkom Austria



Figure 103: Picture of the measurement antenna, the reference antenna, the measurement equipment (spectrum analyzers and Notebook) and the grid. The grid steps of 25cm was taped on the floor.



Figure 104: A view of the Room CC2-17 with the measurement antenna and the base station antenna hidden behind the leaves of the tree marked with the red circle.



Figure 105: Outside view of the base station antenna mounted on the front of the building (marked with a red cycle) and the direction to the Room CC2-17 which was under investigation.

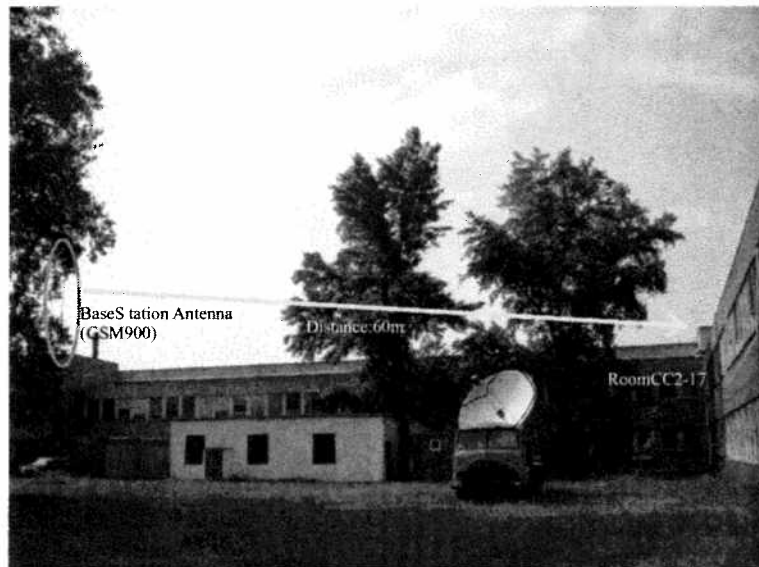


Figure 106: Outside view of the base station antenna and the opposite building where the Room CC2-17 was under investigation. The distance between the base station antenna and the Room CC2-17 is 60m.



Figure 107: A view of the building front and the four windows of Room CC2-17. The direction to the base station antenna is marked by the green arrow.

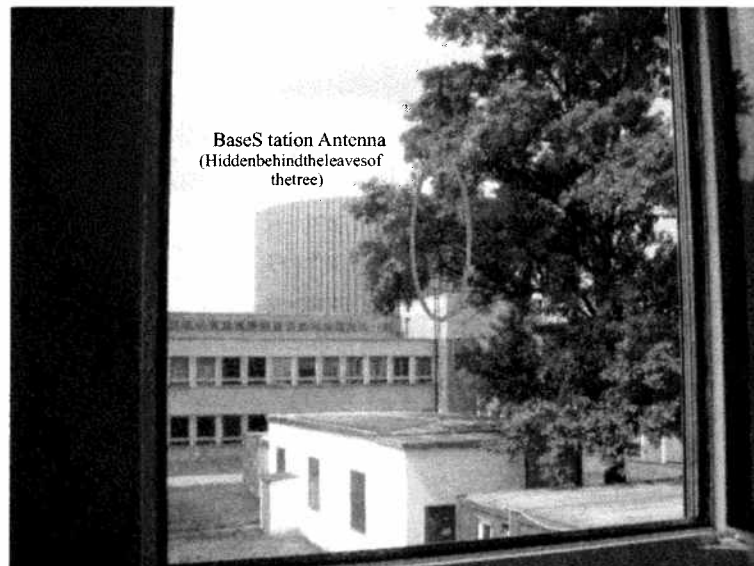


Figure 108: A view through the open window to the base station antenna (marked with a red circle) which was partly hidden behind the leaves of the tree.

	Area (day 1)	Area (day 2)	Factor $\frac{\text{day1}}{\text{day2}}$ [%]
Examined Positions	143	143	
Maximum Value [V/m]	0.82	0.89	7.5
Minimum Value [V/m]	0.14	0.12	-15.5
Global Mean Value [V/m]	0.39	0.33	-15.1
Standard Deviation [V/m]	0.16	0.15	-8.4

Table 28: Mean value, minimum and maximum value and standard deviation (Gauß) at GSM 900 - area, *ARC Seibersdorf research GmbH* Room CC2-17 on two different days. The first area was measured on a Saturday afternoon and the second measurement was on a Monday afternoon. The last row shows the differences of those two measurements in %.

measurement campaign, described in Section 2. The set-up and the used equipment was also the same, only the examined area is different to the previous measurements. A 2.5m x 3m area with a grid step of 25cm was examined which gives a total of 143 positions, this are 200 measurement positions less compared to the cube measurements. The area was located in a height of 150cm above the floor in the middle of the room (see Figure 102).

The global aspects of this measurement were taken under consideration in the following sections. In the following, both measurement results are compared in each section, this gives a better overview of the measurement data.

4.2.1 Mean, Standard Deviation and Amplitude Distribution

Comparing the two measurements, performed on two different days, is interesting. The differences between the measured values is very low. Comparing the global mean value, which is more representative than the minimum or maximum because the global mean value contains all measured positions of both measurements, shows a difference of -15.1%, which means that the global mean value on day 2 is 15.1% lower than the global mean value on day 1. The difference of the maximum of day 1 and day 2 is 7.9%, whereas the maximum on day 2 is 7.9% higher than on day 1. The difference of the minimum is -15.5%, whereas the minimum on day 2 is 15.5% lower than on day 1 and the difference of the standard deviation is -8.4%, whereas the standard deviation on day 2 is 8.4% lower than on day 1. Table 28 shows the values and the factor between the two measurements. The amplitude distribution of the area measured on two different days can be seen in Figure 109 and Figure 110.

Due to the fact, that only 143 positions were examined, both histograms (the histogram of day 1 - Figure 109 and the histogram of day 2 - Figure 109) doesn't show the same characteristics. Only 15 amplitude grades were disposed, which do not allow any conclusions regarding distribution functions like the LogNormal-

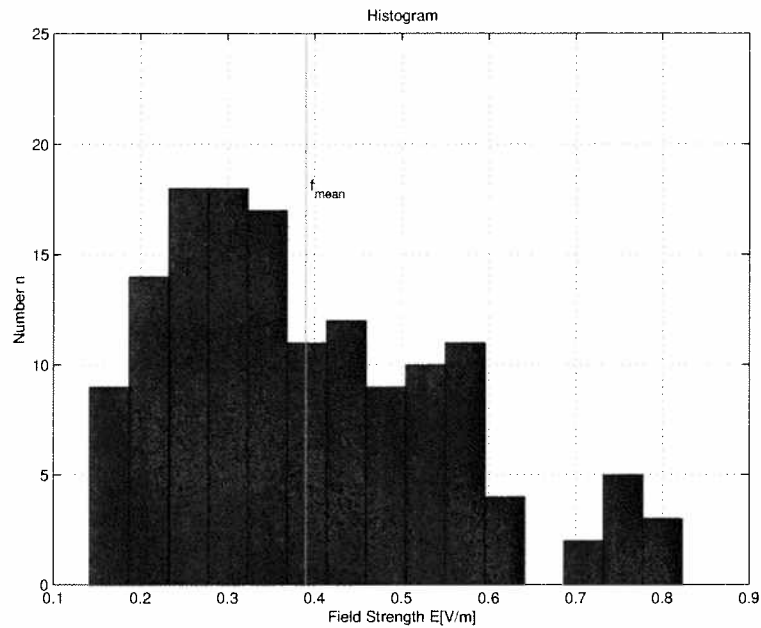


Figure 109: Global distribution of the electromagnetic field strength values disposed in 15 amplitude grades. Measured in Room TOX 7 at the *ARC Seibersdorf research GmbH* office building at a frequency of 946.6MHz, the investigated area was a plane. This diagram shows the measurement on Saturday afternoon.

distribution or the Rayleigh-distribution.

4.2.2 Cumulative Distribution Function and Probability Density Function

The cumulative distribution function (see Figure 111 and Figure 112) can be build by arranging the field strength values by increasing amplitudes, as described in Section 3.2.2. The percentiles of the cumulative distribution function are shown in Table 29 and can be compared to each other.

The probability density function (see Figure 113 and Figure 114) can be derived by differentiating the cumulative distribution function (see Equation 12).

4.2.3 Identification of the Probability Density Function

A possible approximation for both functions is displayed in Figure 115 and Figure 116. This approximation is characterized as a Rayleigh distribution, described by Equation 17. The polynomial approximation is valid in the range between minimum and maximum of the electromagnetic field strength.

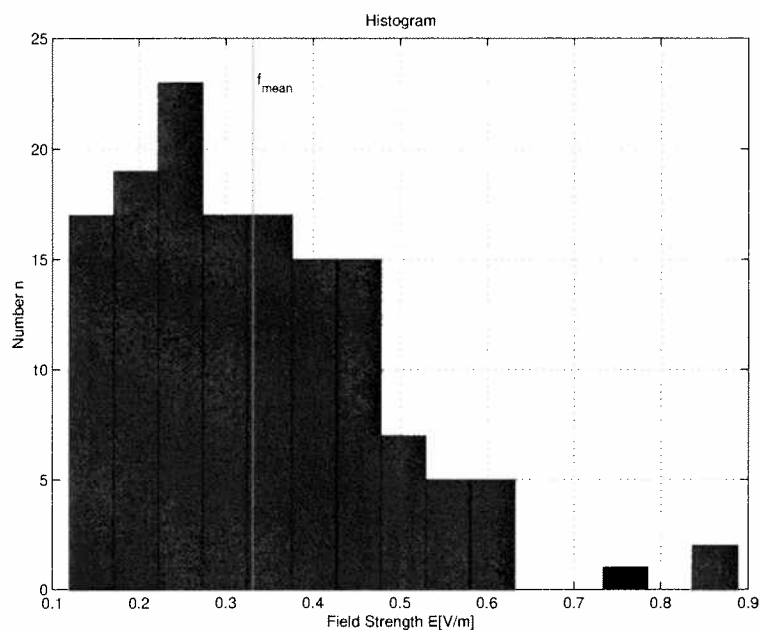


Figure 110: Global distribution of the electromagnetic field strength values disposed in 15 amplitude grades. Measured in Room TOX 7 at the *ARC Seibersdorf research GmbH* office building at a frequency of 946.6MHz, the investigated area was a plane. This diagram shows the measurement on Monday afternoon.

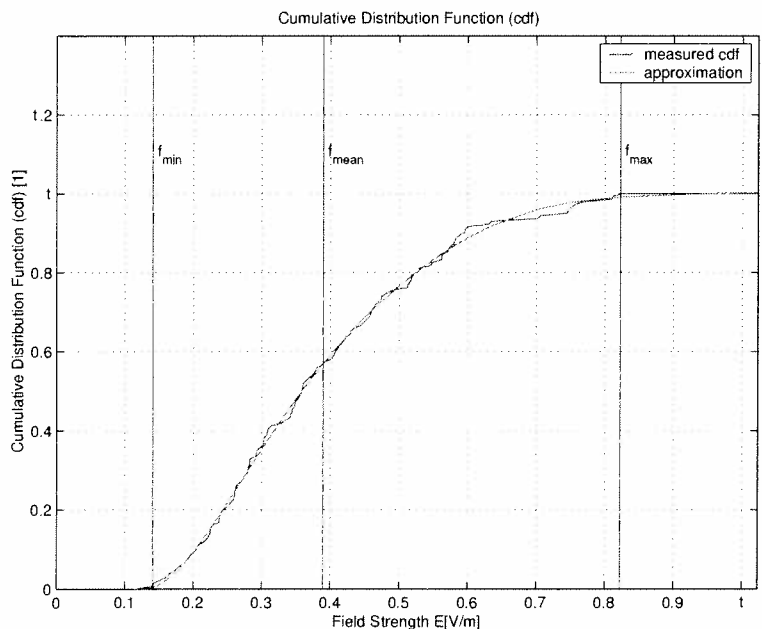


Figure 111: Cumulative distribution function (cdf) of the global field distribution (GSM 900 - Room CC2-17 *ARC Seibersdorf research GmbH* office building, area measured on day 1).

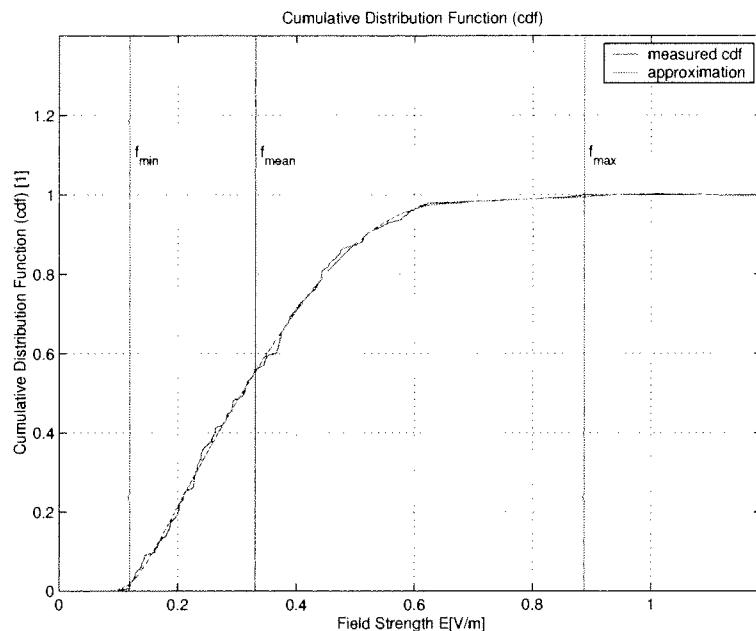


Figure 112: Cumulative distribution function (cdf) of the global field distribution (GSM 900 - Room CC2-17 *ARC Seibersdorf research GmbH* office building, area measured on day 2).

Percentiles	Value [$\frac{mV}{m}$]	$\frac{E}{E_{MAX}}$ [%]	Value [$\frac{mV}{m}$]	$\frac{E}{E_{MAX}}$ [%]
	Area (day 1)		Area (day 2)	
$E_{10\%}$	0.21	25.0	0.16	17.7
$E_{25\%}$	0.26	31.9	0.21	24.2
$E_{50\%}$	0.36	43.8	0.31	34.7
$E_{75\%}$	0.49	59.9	0.42	47.2
$E_{90\%}$	0.60	72.6	0.52	58.6

Table 29: Lower and higher quartile, lower and higher decile, quintile as well as the relative percentile referring to the maximum of the electromagnetic field strength (*ARC Seibersdorf research GmbH* at GSM 900 - area on day 1 and day 2, Room CC2-17).

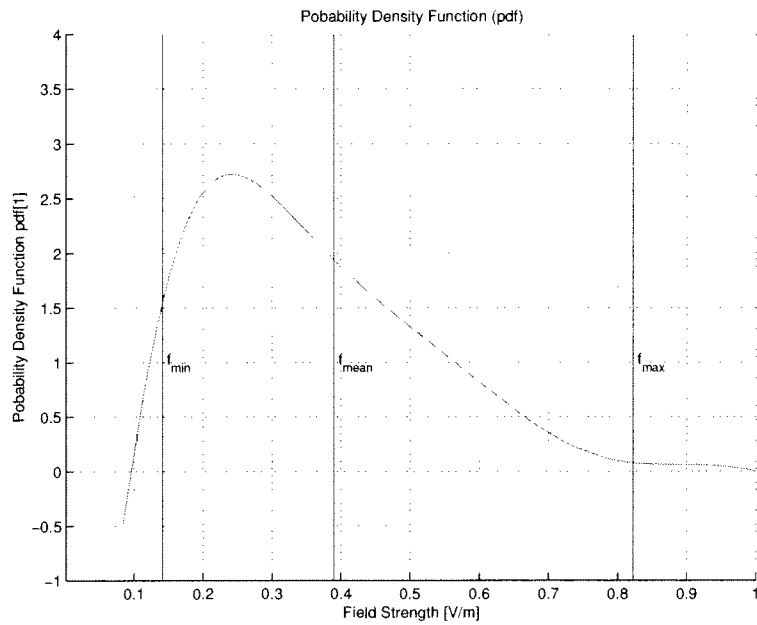


Figure 113: Probability Density function (pdf) of the global field distribution (GSM 900 - Room CC2-17 *ARC Seibersdorf research GmbH* office building, area measured on day 1).

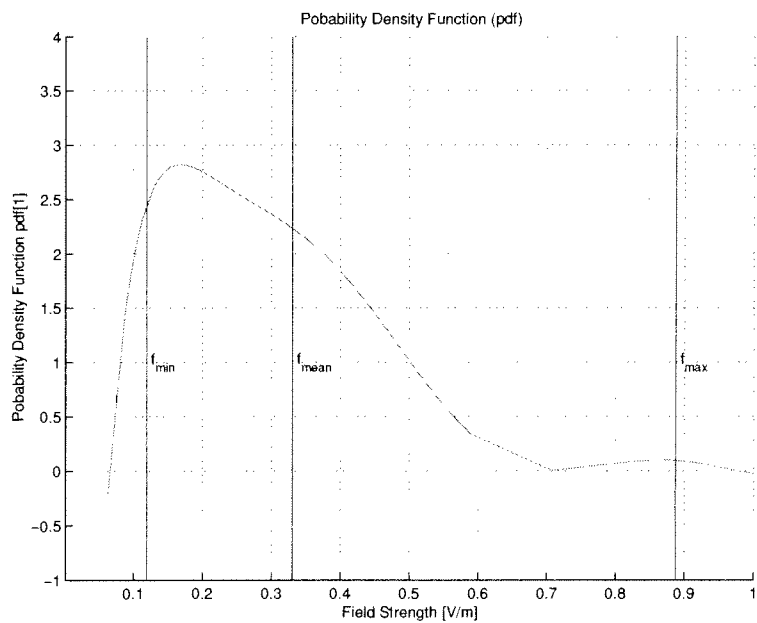


Figure 114: Probability Density function (pdf) of the global field distribution (GSM 900 - Room CC2-17 *ARC Seibersdorf research GmbH* office building, area measured on day 2).

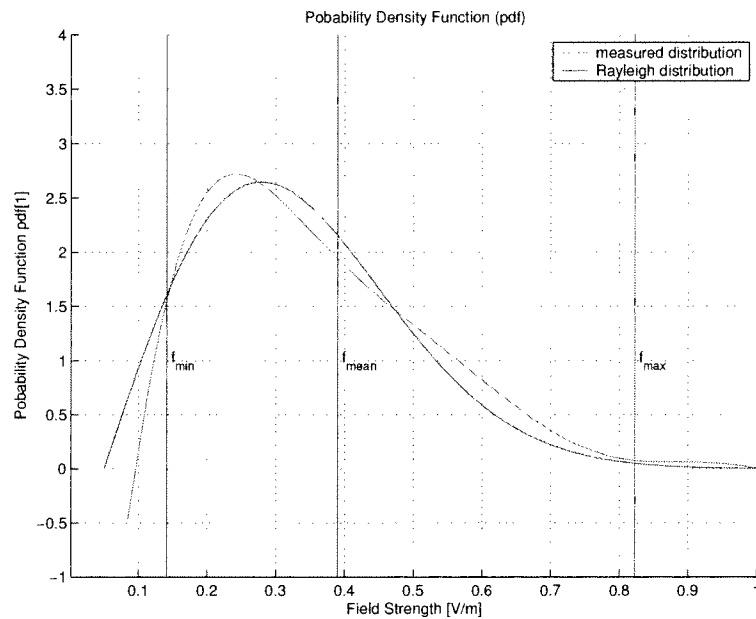


Figure 115: Approximation of the Probability Density function (pdf) with a Rayleigh distribution (GSM 900 - Room CC2-17 ARC Seibersdorf research GmbH office building, area measured on day 1).

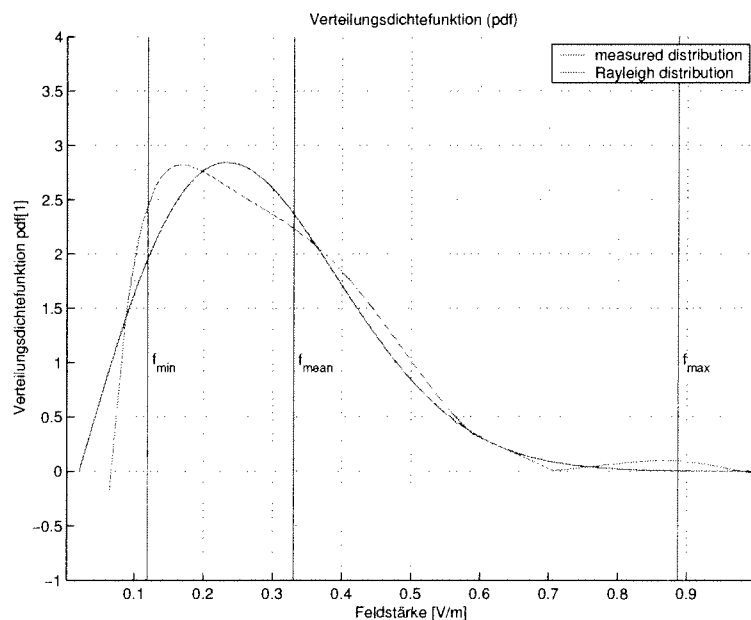


Figure 116: Approximation of the Probability Density function (pdf) with a Rayleigh distribution (GSM 900 - Room CC2-17 ARC Seibersdorf research GmbH office building, area measured on day 2).

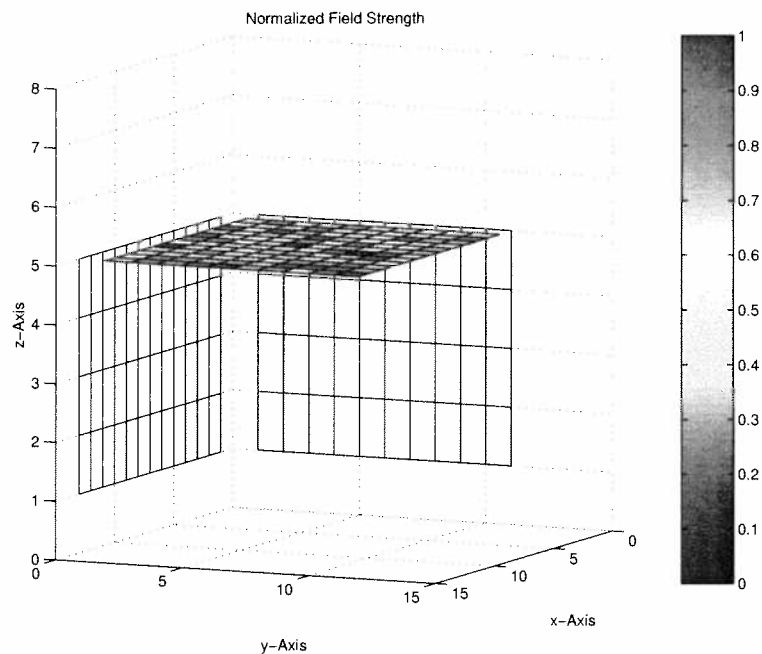


Figure 117: Distribution of the field strength values normalized to the maximum value (GSM 900 - Room CC2-17 *ARC Seibersdorf research GmbH* office building, area measured on day 1).

4.2.4 Local Distribution of the Measurement Data

After the global considerations of the field strength distribution, the local demeanor was investigated. The field strength distribution shows higher field strength values in the center of the area in Figure 117, which was the first measurement, performed on day 1. Figure 118, the area which was measured on day 2, shows a more homogeneous distribution of the field strength with only a small spot with higher field strength values in the far left corner.

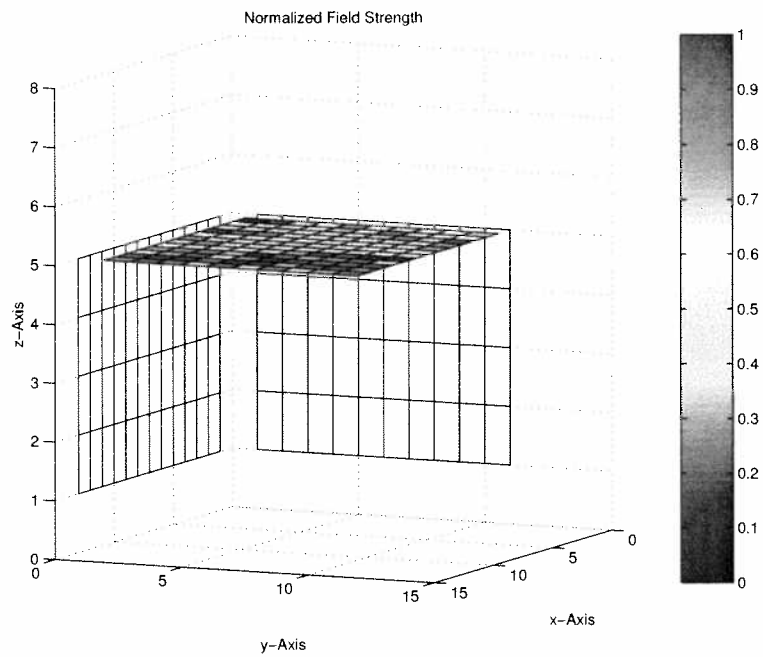


Figure 118: Distribution of the field strength values normalized to the maximum value (GSM 900 - Room CC2-17 *ARC Seibersdorf research GmbH* office building, area measured on day 2).

5 Variation in Time

Continuous measurements were performed at several locations. The measurement set up was the same like the set up used for the measurements of volumes and areas (described in Section 2) but with one difference: the variations in time was examined. For this purpose the measurement antenna was not moved within a restricted area like in the measurements described in the previous sections. Both antennas, the reference antenna and the measurement antenna, were mounted at the same height but with different polarization because the reference antenna was mounted on a different holder which didn't allow the same orientation as the measurement antenna. The polarization of the reference antenna was horizontal, whereas the measurement antenna was still mounted on the Add3D antenna holder and had therefore a different polarization as the reference antenna.

The measurement process was the same as described earlier, the BCCH (Broadcast Control Channel) was scanned over 20 sweeps in max-hold mode of the spectrum analyzers and stored in files. The time and date was also recorded and stored in the same files so statements regarding the time of a measurement could be made. This could be useful for investigations of the relation between the changing of the weather condition (if the weather was recorded for the time of the measurement) and the field levels for example.

A large amount of data was measured in different scenarios like the office building of the Mobilkom Austria (but only during nighttime) as well as the *ARC Seibersdorf research GmbH* office building (in two different rooms). The largest measurement campaign was performed in a conference room (Room CC2-17) at the *ARC Seibersdorf research GmbH* office building. Over a period of 6 days a continuous measurement delivered over 45000 measured samples. Table 30 gives an overview of the performed measurements and the amount of measurement data.

In the following sections, the electromagnetic field strength is displayed in figures, where the x-axis shows the number of the measured samples and the y-axis shows the electromagnetic field strengths. The maximum value, global mean value, minimum value and the standard deviation were also derived and displayed in tables for comparison with the volume, area and axis measurements.

5.1 Continuous Measurements at the Mobilkom Austria Office Building

5.1.1 GSM 900

Figure 119 and Figure 120 are showing the field strength values for each measured sample of two continuous measurements, performed during the night time. Starting at 20:24 on the 12th of March and ending on the 13th at 8:28 the first measurement delivered 4031 samples. The second measurement started at 22:31 on the 19th of March and ended at 8:34 on the 20th of March and delivered 3391 examined positions.

Description	Date		Time			Samples (N)
	from	to	from	to	min.	
Room A07A011						
GSM 900	11.03.2003	12.03.2003	20:24	08:28	724	4031
946.0MHz	19.03.2003	20.03.2003	22:31	08:34	603	3391
DCS 1800	12.03.2003	13.03.2003	17:23	08:47	924	5091
1812.4MHz	13.03.2003	14.03.2003	22:54	08:54	600	3390
	20.03.2003	21.03.2003	20:01	08:44	763	4711
UHF - FS ORF2	21.03.2003	22.03.2003	21:42	08:20	638	794
575.25MHz						
VHF - UKW RF	17.03.2003	18.03.2003	20:50	08:33	703	3878
105.8MHz						
UMTS	22.03.2003	23.03.2003	19:26	09:30	844	4637
2154.7MHz						
Room CC2-17						
GSM 900						
944.6MHz	26.05.2003	27.05.2003	16:12	10:19		5815
946.6MHz	15.07.2003	21.07.2003	14:00	12:40	10000	46410
Room TOX 7						
GMS 900	09.07.2003	10.07.2003	14:50	15:40	1490	8200
946.6MHz						

Table 30: Overview of the measurement data and the investigated frequency bands. This gives a total of more than 90000 examined samples.

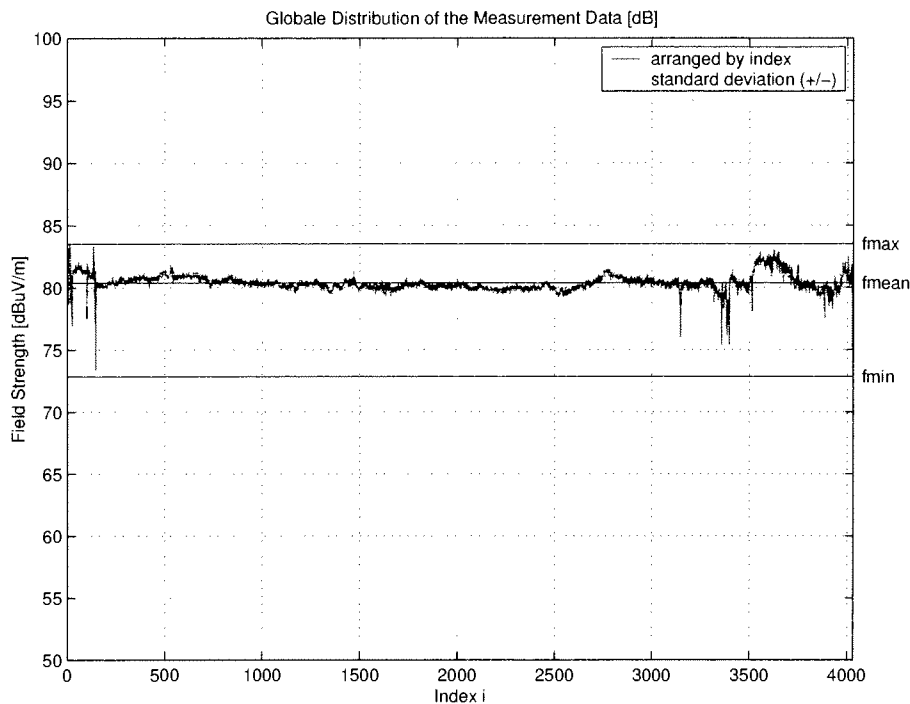


Figure 119: Distribution of the field strength amplitude (GSM 900 - Room A07A011 Mobilkom Austria, measured on the 11th of March 2003).

In each figure a singularity can be observed. At the end of the two Figures the level varies in a larger range than at the beginning. At approximately position 3400, in Figure 119, the level varies in a much larger range, in Figure 120 this behavior can be observed, starting with examined position number 2400. The time for those particular positions can be calculated with the help of the time stamp which were recorded as well. For Figure 119 it is approximately 6:30 in the morning, for Figure 120 it is approximately 5:45 in the morning. This effect can also be seen at the continuous measurement of the DCS 1800 frequency band and in a more smaller impact at the measurement of the UHF and VHF frequency band, as described in the following sections.

Table 31 shows the maximum value, the minimum value, the global mean value as well as the standard deviation (Gauß) of each continuous measurement. It can be observed, that the values between those two measurements do not vary in a large range. The difference between the measurement on day 1 and day 2 is very low. The global mean value of day 2 is by a factor of 1.39 higher than the global mean value on day 1, as can be seen in Table 31. With this measurements, an interesting aspect can be examined: the variance between the measurement antenna and the reference antenna. Comparing the measurement data of the measurement antenna with the measurement data of the reference antenna could verify, if the chosen normalization method is valid.

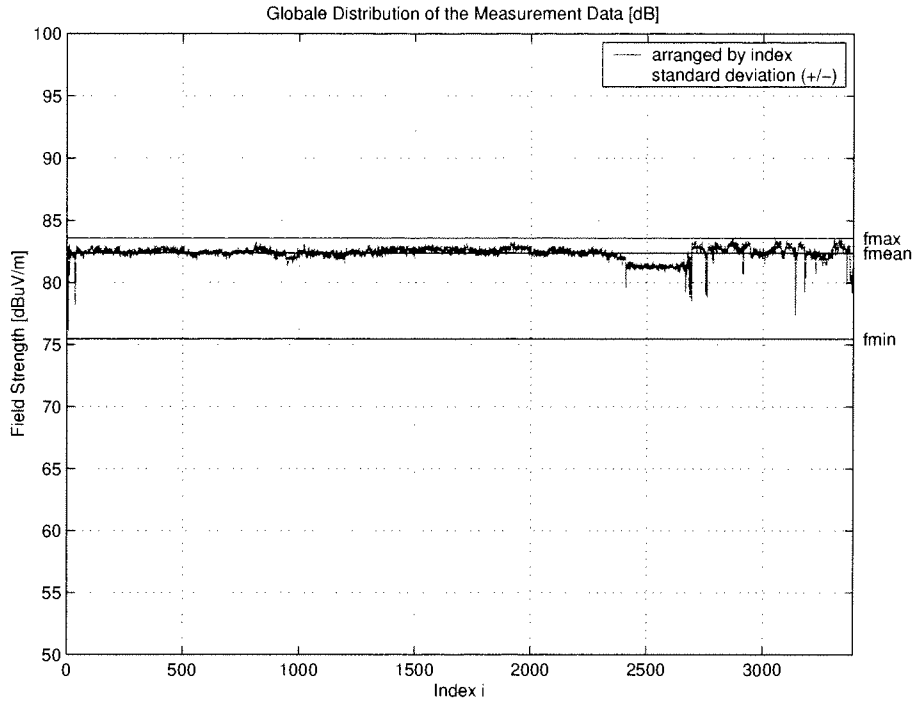


Figure 120: Distribution of the field strength amplitude (GSM 900 - Room A07A011 Mobilkom Austria, measured on the 19th of March 2003).

	11.3.2003	19.3.2003
Examined Positions	4031	3391
Maximum Value [mV/m]	13.6	15.1
Minimum Value [mV/m]	4.0	5.9
Global Mean Value [mV/m]	9.5	13.2
Standard Deviation [mV/m]	0.7	0.8

Table 31: Mean value, minimum and maximum value and standard deviation at GSM 900 - continuous measurements, Mobilkom Austria Office Building Room A07A011 on two different days. All measurements were performed during the night time.

The first window in Figure 121 displays the absolute electromagnetic field strength values, measured with the measurement antenna (red curve) and the absolute field strength values of the reference antenna (green curve). The second window shows the deviations of the field strengths values to the global mean value of the measurement data of the reference antenna while the third window shows the same diagram but with the measurement data of the measurement antenna. The fourth and last window shows the difference between the deviation of the measurement data of the measurement antenna to its global mean value and the deviation of the measurement data of the reference antenna to its global mean value. The following equations are showing how the fourth curve can be derived. With Equation 19 and Equation 20 the global mean value of the measurement data of the measurement antenna and the global mean value of the measurement data of the reference antenna was built. The index "M" indicates that all values were measured with the measurement antenna and the index "R" indicates that all values were measured with the reference antenna.

$$Mean_M = \frac{\sum_{i=1}^N E_M(i)}{N} \quad (19)$$

$$Mean_R = \frac{\sum_{i=1}^N E_R(i)}{N} \quad (20)$$

The deviation of the field strength of each measured sample to the global mean value of the measurement data of the measurement antenna was derived by Equation 21 and is displayed in window 2. With Equation 22 the deviations of the field strength of each measured sample to the global mean value of the measurement data of the reference antenna was derived and is displayed in window 3.

$$Deviation_M(i) = \frac{E_M(i)}{Mean_M} \quad (21)$$

$$Deviation_R(i) = \frac{E_R(i)}{Mean_R} \quad (22)$$

Deriving the difference of the results of Equation 21 and the results of Equation 22 delivers the values for building the curve in the fourth window (see Equation 23).

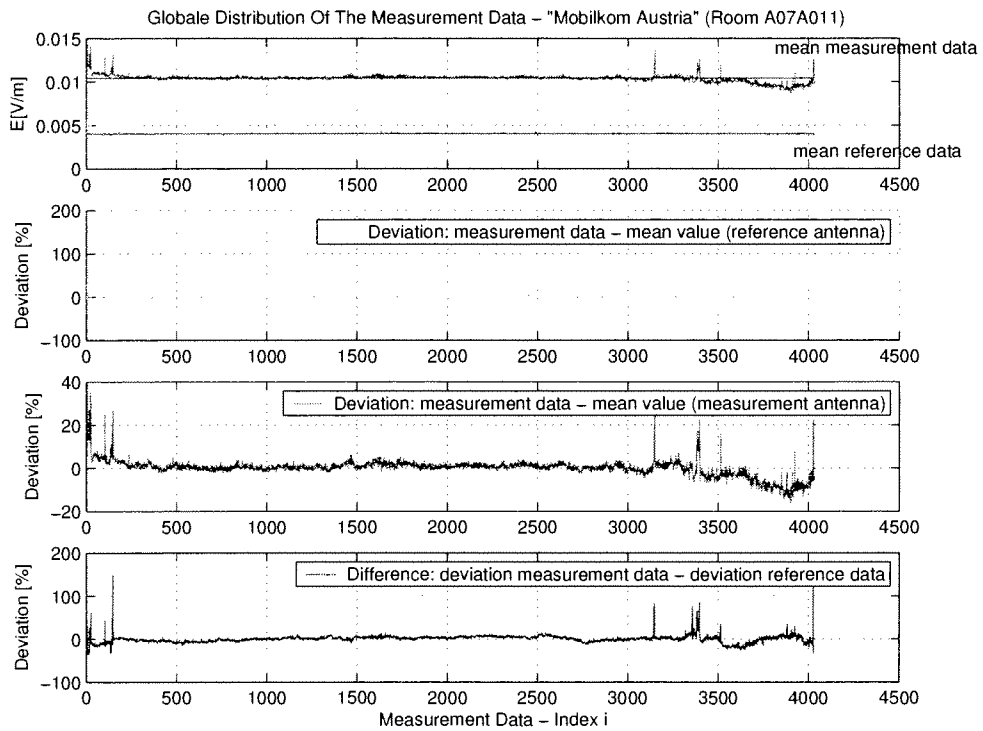


Figure 121: Comparison of the measurement data of the measurement antenna and the reference antenna. The first window shows both, the distribution of the field strength amplitude of the measurement antenna and the reference antenna. The second window shows the deviation of the filed strength values to the mean value of the measurement data measured with the reference antenna. The third window shows the same deviation but with the measurement data of the measurement antenna. The fourth and last window shows the deviation between the measurement data of the measurement antenna and the measurement data of the reference antenna. (GSM 900 - Room A07A011 Mobilkom Austria, measured on the 11th of March 2003).

$$Difference_{M-R}(i) = Deviation_M(i) - Deviation_R(i) \quad (23)$$

Whereas i is the number of a sample and is in the range from 1 up to N . N is the number of examined positions, $E(i)$ is the electromagnetic field strength of one examined sample.

Figure 122 shows the same comparison of the measurement antenna and the reference antenna from the continuous measurement on the 19th of March 2003.

Both Figures (Figure 121 and Figure 122) show very little deviations between the measurement data of the measurement antenna to its global mean value and the

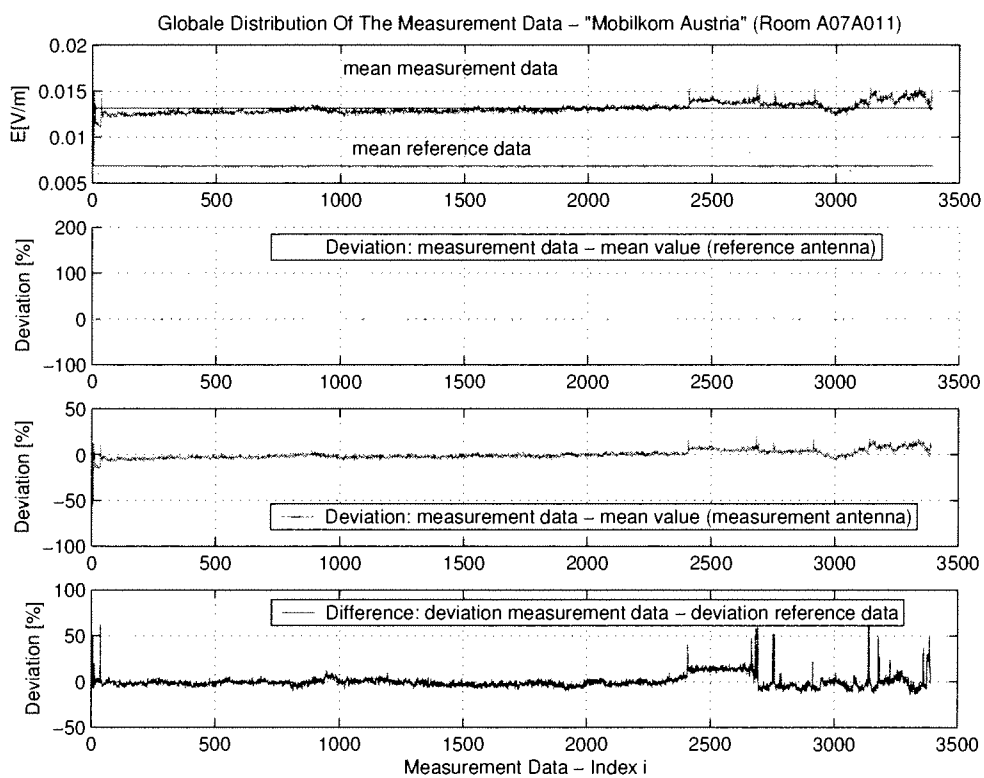


Figure 122: Comparison of the measurement data of the measurement antenna and the reference antenna. (GSM 900 - Room A07A011 Mobilkom Austria, measured on the 19th of March 2003).

GSM 900		
Date:	11.3.2003	19.3.2003
MAX dev. (pos.) [%]	149.7	89.0
MAX dev. (neg.) [%]	-35.2	-14,7
MEAN dev. (abs.) [%]	5.3	4.4
MAX dev. (abs.) [%]	149.7	89.0
MIN dev. (abs.) [%]	0.004	0.001

Table 32: Comparison of the measurement data of the measurement antenna with the measurement data of the reference antenna at GSM 900. Maximum deviation in positive direction of the y-axis, maximum deviation in the negative direction of the y-axis, mean value of the absolute values of the deviations, maximum and minimum of the absolute values of the deviations.

measurement data of the reference antenna to its global mean value, only a few peaks occur over the whole measurement period. Higher deviation occur at the end of both figures which is equal to the region described earlier were irregularities in the distribution of the amplitudes occur. Table 32 shows the maximum deviation in the positive direction of the y-axis, the maximum deviation in the negative direction of the y-axis. The global mean value of the absolute values of the deviations is derived as well as the minimum value of the absolute values of the deviations.

The maximum deviation occurs at both measurements in the positive direction of the y-axis, which means that the measured sample of the measurement antenna is higher than the measured sample of the reference antenna. As Table 32 shows, nearly 150% deviation between the measurement data of the measurement antenna and the measurement data of the reference antenna on the 11th of March and with nearly 90% on the 19th of March 2003.

5.1.2 DCS 1800

The same measurements were performed in the DCS 1800 frequency band. Table 33 shows the maximum value, the minimum value, the global mean value and the standard deviation from measurements in three different nights. A comparison of the three global mean values shows, that those three values are nearly in the same range. Comparing the three global mean values, it can be seen that the variation of those three values isn't high. The global mean value of the measurement on day 2 shows the highest value, by a factor of 1.6 higher than the global mean value of day 1 and by a factor of 1.7 higher than the global mean value on day 3. The continuous measurement of the 13th of March has also the highest maximum of those three measurements. The maximum value is by a factor of 2.0 higher than

	12.3.2003	13.3.2003	20.3.2003
Examined Positions	5091	3390	4711
Maximum Value [mV/m]	24.2	47.3	23.8
Minimum Value [mV/m]	4.4	5.7	7.5
Global Mean Value [mV/m]	12.0	18.8	11.0
Standard Deviation [mV/m]	2.6	3.9	1.7

Table 33: Mean value, minimum and maximum value and standard deviation at DCS 1800 - continuous measurements, Mobilkom Austria Office Building Room A07A011 on three different days. All measurements were performed during the night time.

the measurement on the 12th of March (day 1) an by a factor of 2.0 higher than the measurement on the 20th of March (day 3).

As described in the section before the figures of the global distribution of the measurement data of each continuous measurement are showing the same behavior at the end of the curves. The deviations of each measured sample compared to the global mean value at the end of each curve is much higher than at the beginning. Figure 123 shows this behavior at sample number 1800 (approximately), first, which is equal to about 23:00 in the evening and at the end at sample number 3900 (approximately) which is equal to about 5:30 in the morning. Figure 124 shows the same behavior starting at sample number 2300, which is equal to about 6:00 in the morning but after more than half an hour later the disruption seems to disappear. The third figure, Figure 125, also shows this behavior starting at sample 3500 (approximately) which is equal to 5:30 in the morning. At this point of the project no sound conclusion of this phenomena can be made.

The deviation between the measurement data of the measurement antenna and the measurement data of the reference antenna was investigated and displayed in figures as well. Figure 126, Figure 127 and Figure 128 are showing those deviations. At the end of each figure the deviations between the field strength of each sample to the global mean value of the measurement data are higher than in the region before, which was already observed in the GSM 900 frequency band.

Refereing to Table 34, the continuous measurements on the 12th and 13th of March shows, that the highest deviations occur in direction of the positive y-axis with 155.5% and 141.8%. The third measurement shows a lower deviation with only 56% in direction of the negative y-axis, which means that the value of the measured sample of the measurement antenna is lower than the measured sample of the reference antenna. The global mean value of the absolute values of the measurement data shows the highest deviation at the first measurement performed, the second and third measurement have very similar values, below 10%.

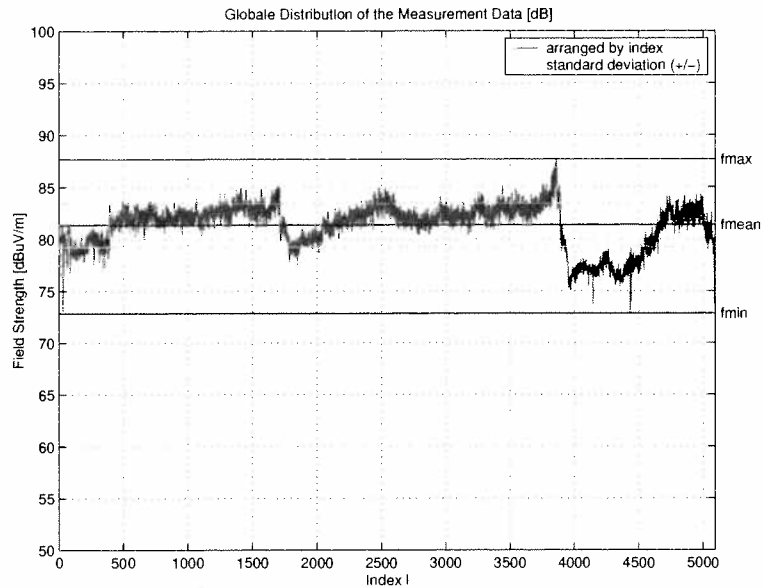


Figure 123: Distribution of the field strength amplitude (DCS 1800 - Room A07A011 Mobilkom Austria, measured on the 12th of March 2003).

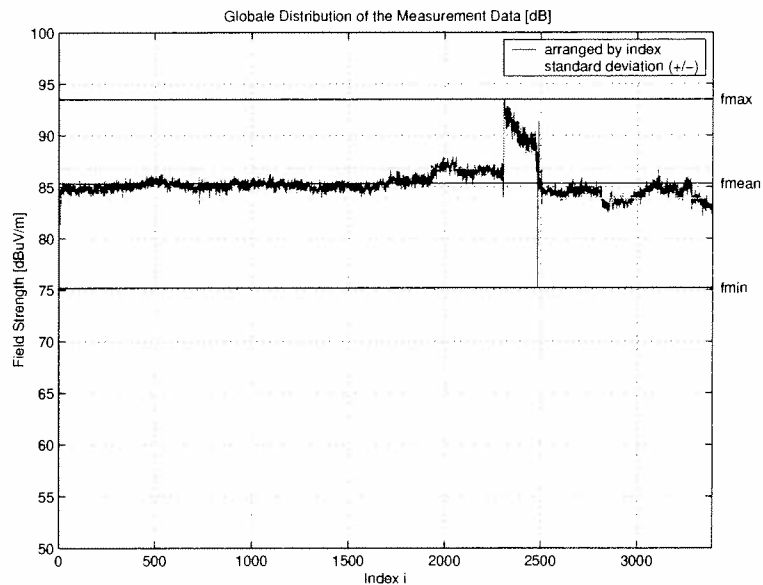


Figure 124: Distribution of the field strength amplitude (DCS 1800 - Room A07A011 Mobilkom Austria, measured on the 13th of March 2003).

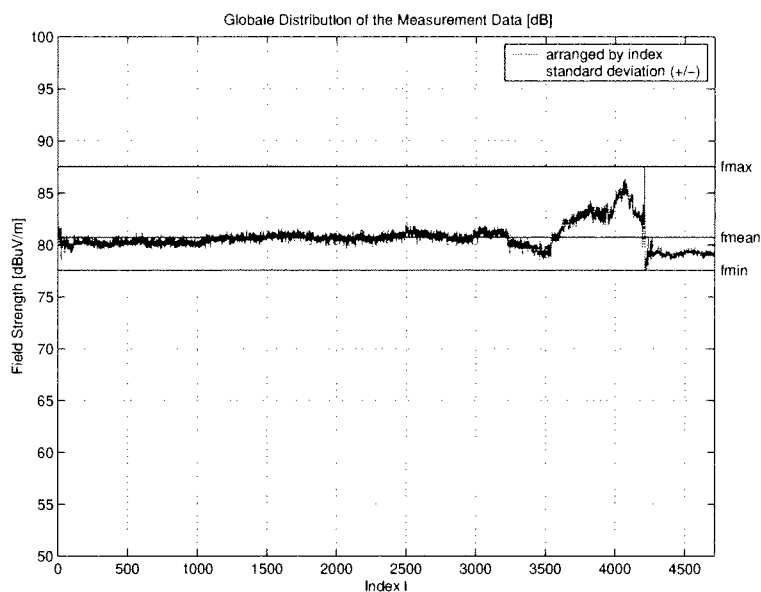


Figure 125: Distribution of the field strength amplitude (DCS 1800 - Room A07A011 Mobilkom Austria, measured on the 20th of March 2003).

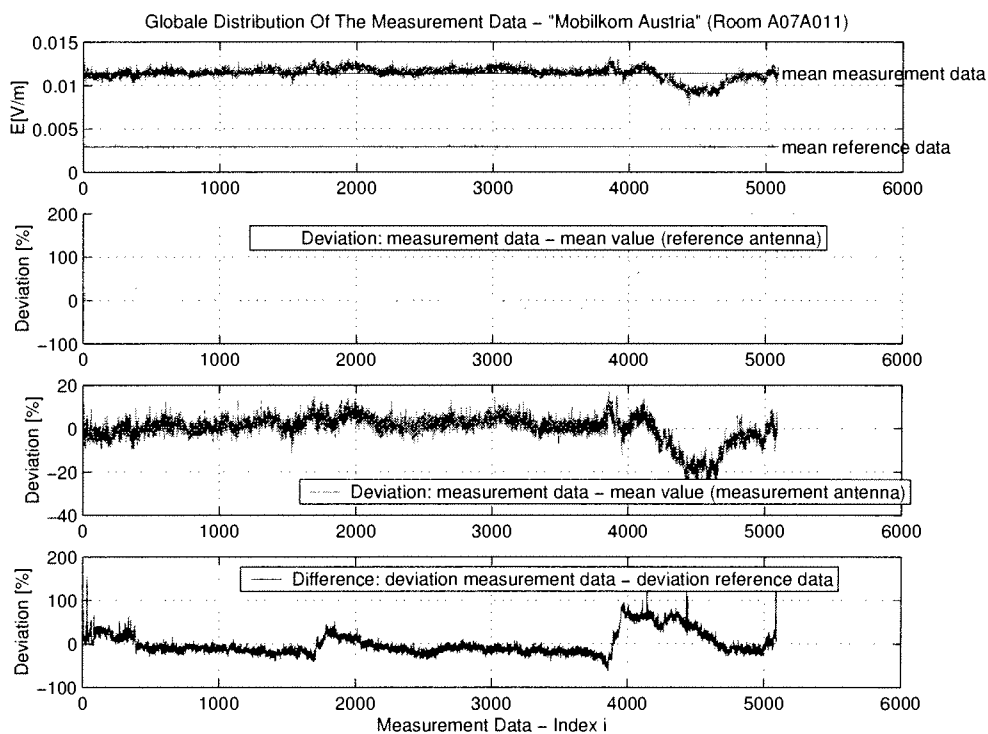


Figure 126: Comparison of the measurement data of the measurement antenna and the reference antenna. (DCS 1800 - Room A07A011 Mobilkom Austria, measured on the 12th of March 2003).

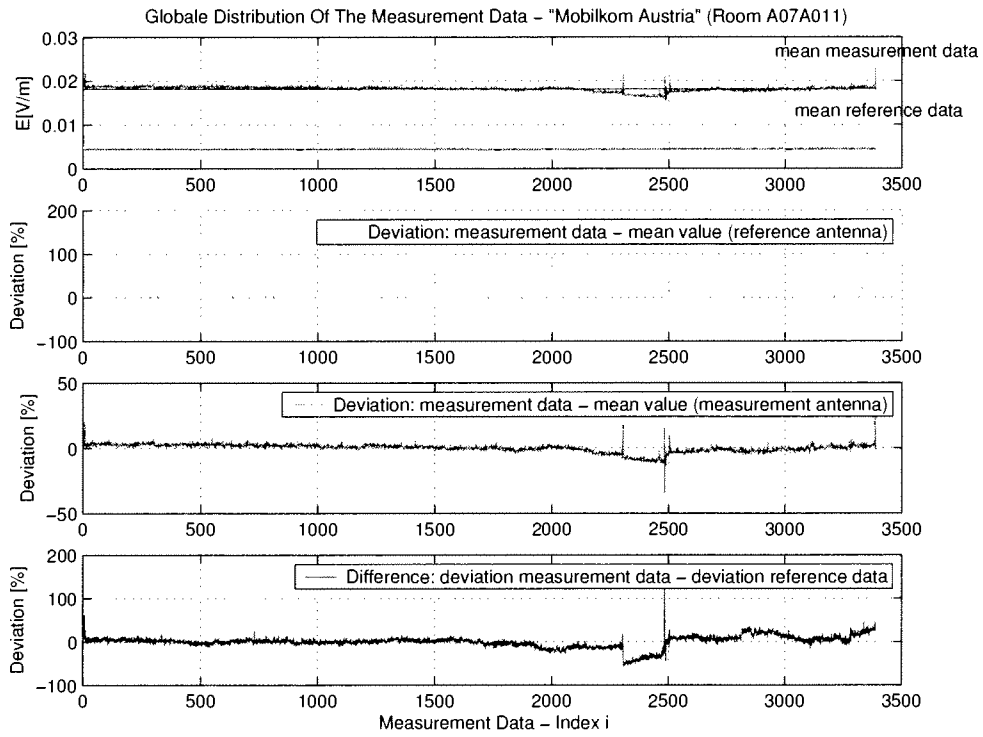


Figure 127: Comparison of the measurement data of the measurement antenna and the reference antenna. (DCS 1800 - Room A07A011 Mobilkom Austria, measured on the 13th of March 2003).

DCS 1800			
Date:	12.3.2003	13.3.2003	20.3.2003
MAX dev. (pos.) [%]	155.5	141.8	29.1
MAX dev. (neg.) [%]	-62.7	-57.7	-56.0
MEAN dev. (abs.) [%]	20.4	9.2	8.1
MAX dev. (abs.) [%]	155.5	141.8	56.0
MIN dev. (abs.) [%]	0.009	0.009	0.005

Table 34: DCS 1800: maximum deviation in positive direction of the y-axis, maximum deviation in the negative direction of the y-axis, mean value of the absolute values of the deviations, maximum and minimum of the absolute values of the deviations.

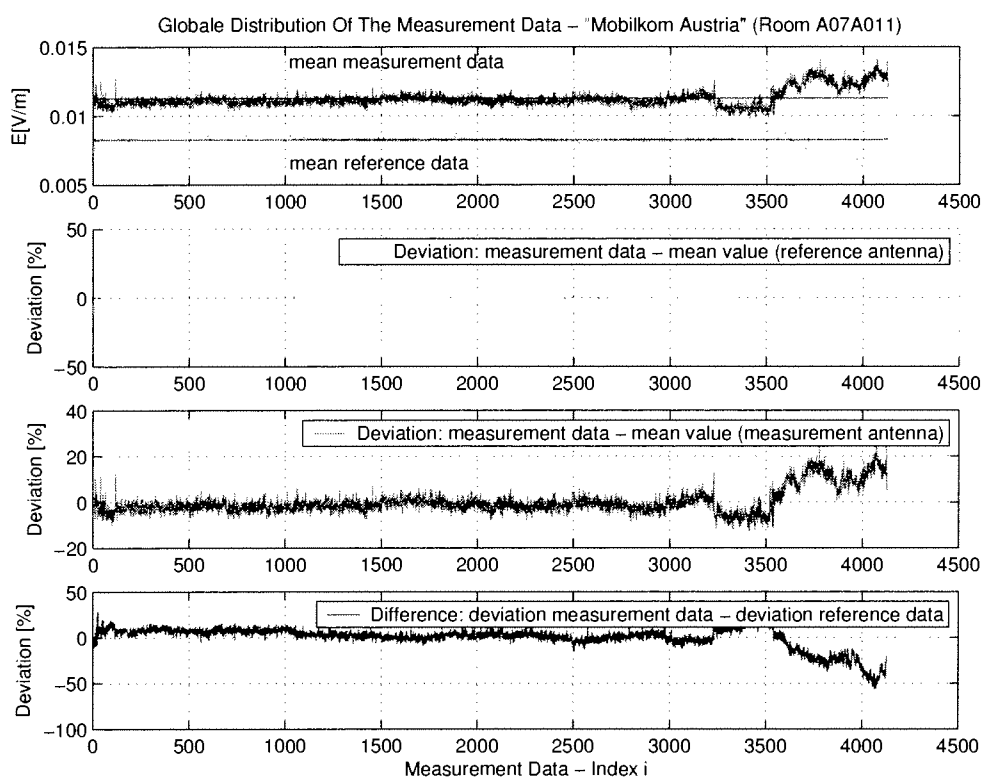


Figure 128: Comparison of the measurement data of the measurement antenna and the reference antenna. (DCS 1800 - Room A07A011 Mobilkom Austria, measured on the 20th of March 2003).

	22.3.2003
Examined Positions	4637
Maximum Value [$\mu V/m$]	332.0
Minimum Value [$\mu V/m$]	19.9
Global Mean Value [$\mu V/m$]	26.3
Standard Deviation [$\mu V/m$]	1.6

Table 35: Mean value, minimum and maximum value and standard deviation at UMTS - continuous measurements, Mobilkom Austria Office Building Room A07A011. The measurement was performed during the night time.

5.1.3 UMTS

At UMTS only one continuous measurement was performed during the night. This measurement was done from Saturday evening (22nd of March) to Sunday morning. As described in Section 3.4, only the pilot channel was measured and the UMTS indoor supply unit was shut down from the Mobilkom Austria, so that measurements with the spectrum analyzer could be performed. Table 35 shows the maximum value, the minimum value, the mean value and the standard deviation.

Figure 129 shows a much smaller deviation at the end of the curve compared to the previous measurements (GSM 900 and DCS 1800). The disturbance also begins early in the morning at about 6:30.

Comparing the measurement data of the measurement antenna with the measurement data of the reference antenna shows the deviation of both measured signals and gives an idea how accurate the normalization is. Figure 130 shows the comparison of those two measurements. It can be seen, that the deviation between the two measured signals is very low in the whole range. The highest deviation is below 30% and occurs in the positive direction of the y-axis, as can be seen in Table 36. Compared to the previous continuous measurements in the GSM 900 and DCS 1800 frequency band, the deviation at UMTS shows the lowest deviation from them all.

5.1.4 UHF - FS ORF2

In the night from 21st of March to 22nd of March, a continuous measurement in the UHF frequency band was performed, delivering only 794 measured samples because the interval between two measured samples was increased. This means, that the measurement was also performed from the evening until the morning of the next day. Table 37 shows the maximum value, the minimum value, the global mean value and the standard deviation.

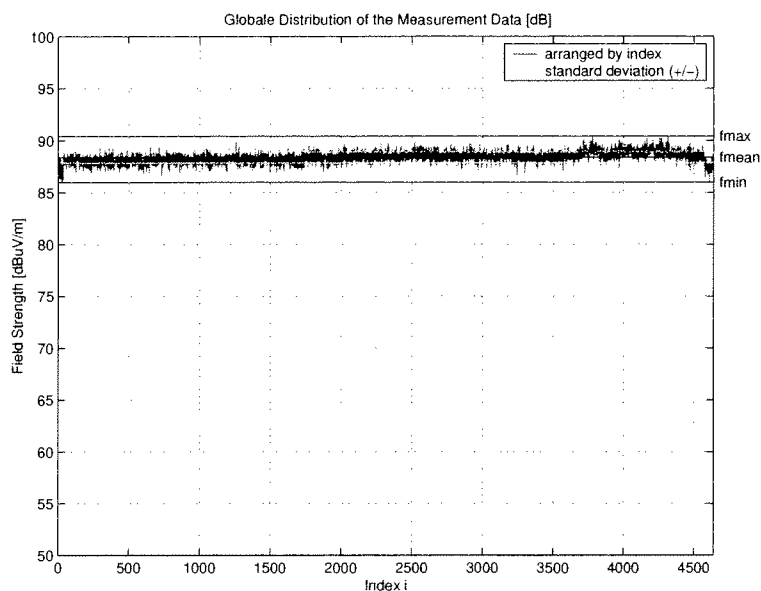


Figure 129: Distribution of the field strength amplitude (UMTS - Room A07A011 Mobilkom Austria, measured on the 22nd of March 2003).

UMTS	
Date:	22.3.2003
MAX dev. (pos.) [%]	26.7
MAX dev. (neg.) [%]	-24.2
MEAN dev. (abs.) [%]	4.8
MAX dev. (abs.) [%]	26.7
MIN dev. (abs.) [%]	0.0010

Table 36: UMTS: maximum deviation in positive direction of the y-axis, maximum deviation in the negative direction of the y-axis, mean value of the absolute values of the deviations, maximum and minimum of the absolute values of the deviations.

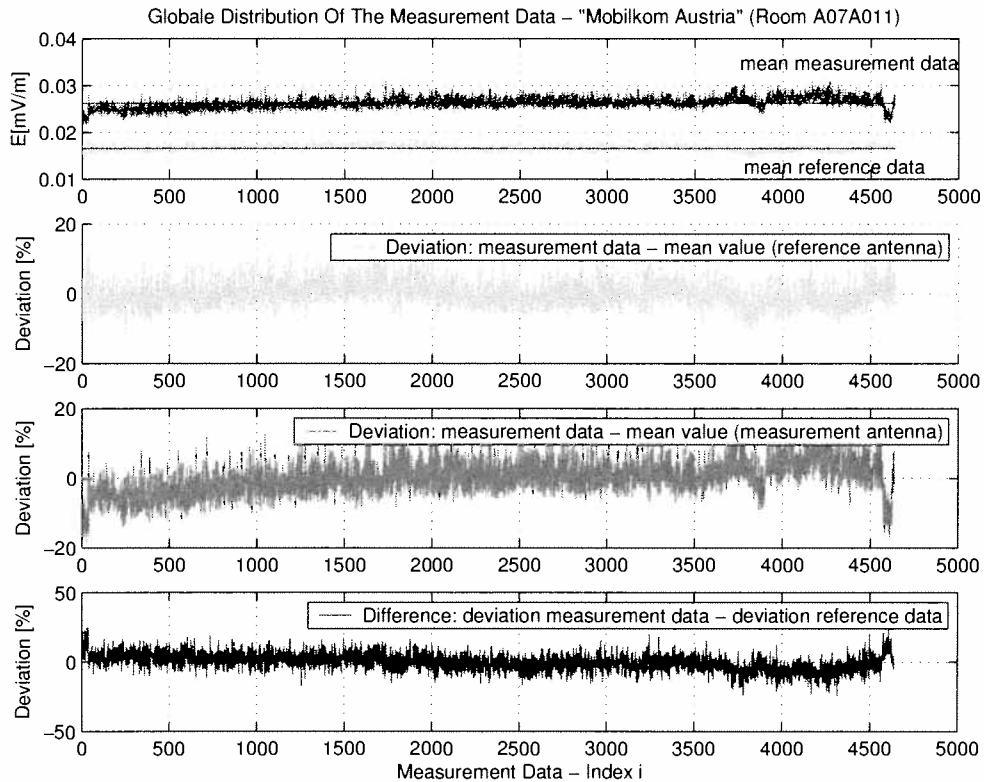


Figure 130: Comparison of the measurement data of the measurement antenna and the reference antenna. (UMTS - Room A07A011 Mobilkom Austria, measured on the 22nd of March 2003).

	21.3.2003
Examined Positions	794
Maximum Value [mV/m]	18.7
Minimum Value [mV/m]	6.3
Global Mean Value [mV/m]	16.1
Standard Deviation [mV/m]	1.2

Table 37: Mean value, minimum and maximum value and standard deviation at UHF - continuous measurements, Mobilkom Austria Office Building Room A07A011. The measurement was performed during the night time.

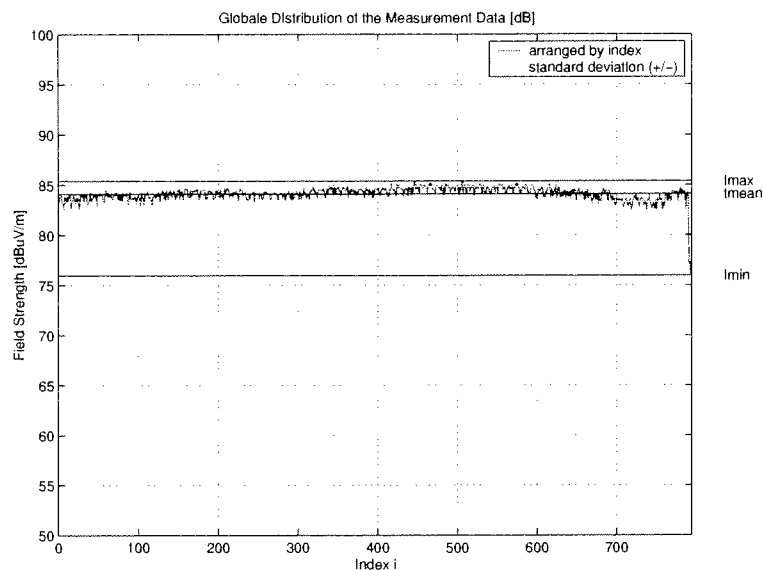


Figure 131: Distribution of the field strength amplitude (UHF - FS ORF2 - Room A07A011 Mobilkom Austria, measured on the 21st of March 2003.

Only a small deviation at the end of the curve can be observed in Figure 131, starting at approximately sample 700, which is equal to about 7:00 in the morning. The measurement was performed during the week. Figure 132 shows the comparison of the measurement data of the measurement antenna with the measurement data of the reference antenna. Table 38 displays the deviations between the measurement data of the measurement antenna and the measurement data of the reference antenna. The maximum deviation occurs in the positive direction with a value of nearly 20%. The global mean value of the absolute values of the measurement data shows a deviation of 5% between the measurement data of the measurement antenna and the measurement data of the reference antenna.

5.1.5 VHF - UKW

One continuous measurement was performed at the VHF frequency band. This measurement was performed during the week and delivered 3928 measured samples. Table 39 shows the maximum value, the minimum value, the global mean value and the standard deviation.

Figure 133 shows only a very small deviation from each measured sample compared to the global mean value at the end of the curve. At about sample number 3700, which is equal to about 8:00 in the morning, the disturbance starts. Like mentioned earlier no sound conclusion for this effect could be found.

Again the measurement data from the measurement antenna and from the reference antenna was compared to each other and the deviation between them was

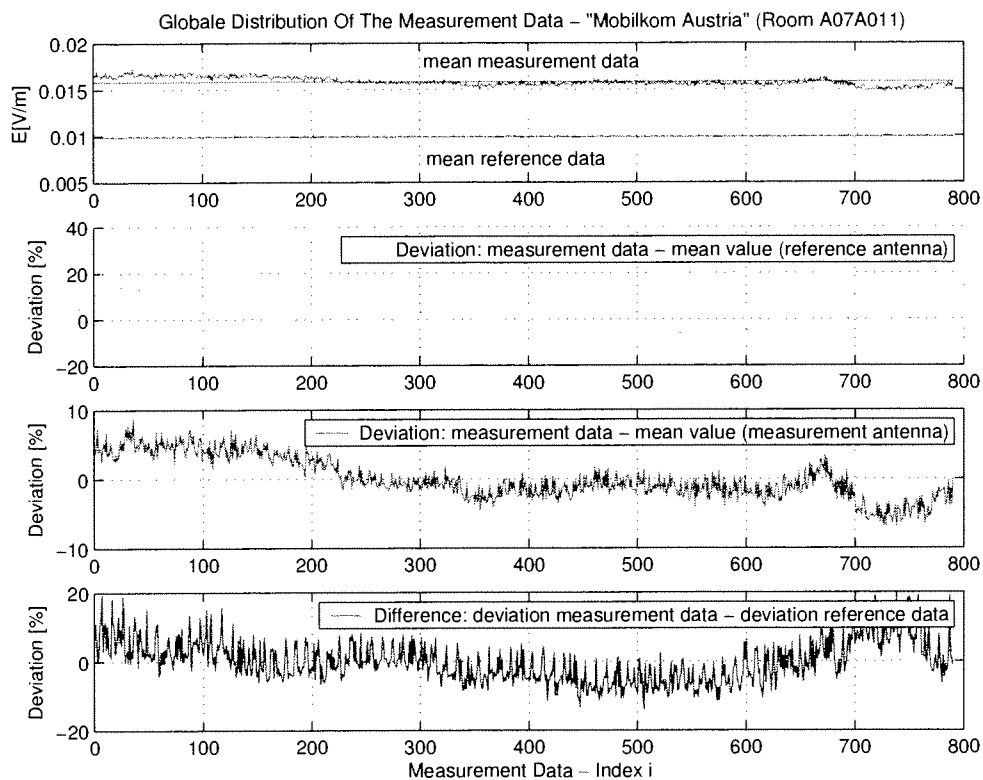


Figure 132: Comparison of the measurement data of the measurement antenna and the reference antenna. (UHF - Room A07A011 Mobilkom Austria, measured on the 21st of March 2003).

UHF	
Date:	21.3.2003
MAX dev. (pos.) [%]	19.7
MAX dev. (neg.) [%]	-13.9
MEAN dev. (abs.) [%]	5.0
MAX dev. (abs.) [%]	19.7
MIN dev. (abs.) [%]	0.026

Table 38: UHF: maximum deviation in positive direction of the y-axis, maximum deviation in the negative direction of the y-axis, mean value of the absolute values of the deviations, maximum and minimum of the absolute values of the deviations.

	17.3.2003
Examined Positions	3878
Maximum Value [mV/m]	4.8
Minimum Value [mV/m]	1.8
Global Mean Value [mV/m]	2.7
Standard Deviation [mV/m]	0.3

Table 39: Mean value, minimum and maximum value and standard deviation in the VHF frequency band - continuous measurements, Mobilkom Austria Office Building Room A07A011. The measurement was performed during the night time.

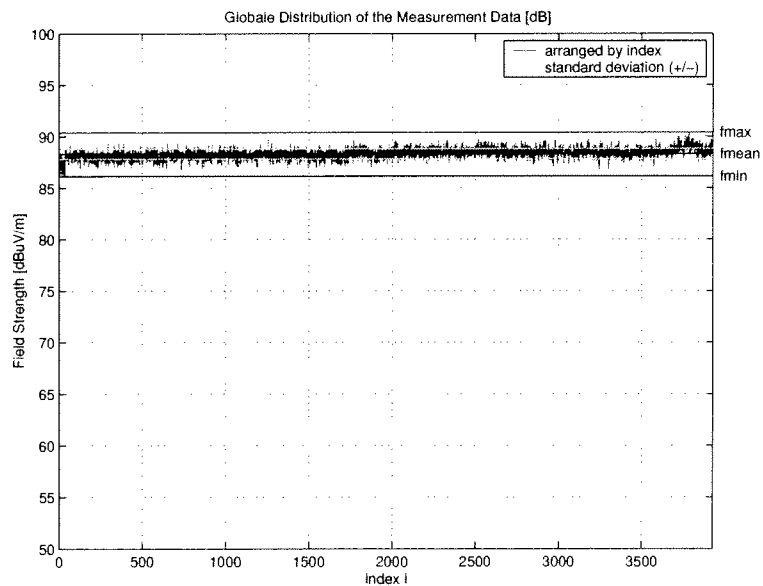


Figure 133: Distribution of the field strength amplitude (VHF - RF UKW - Room A07A011 Mobilkom Austria, measured on the 17th of March 2003).

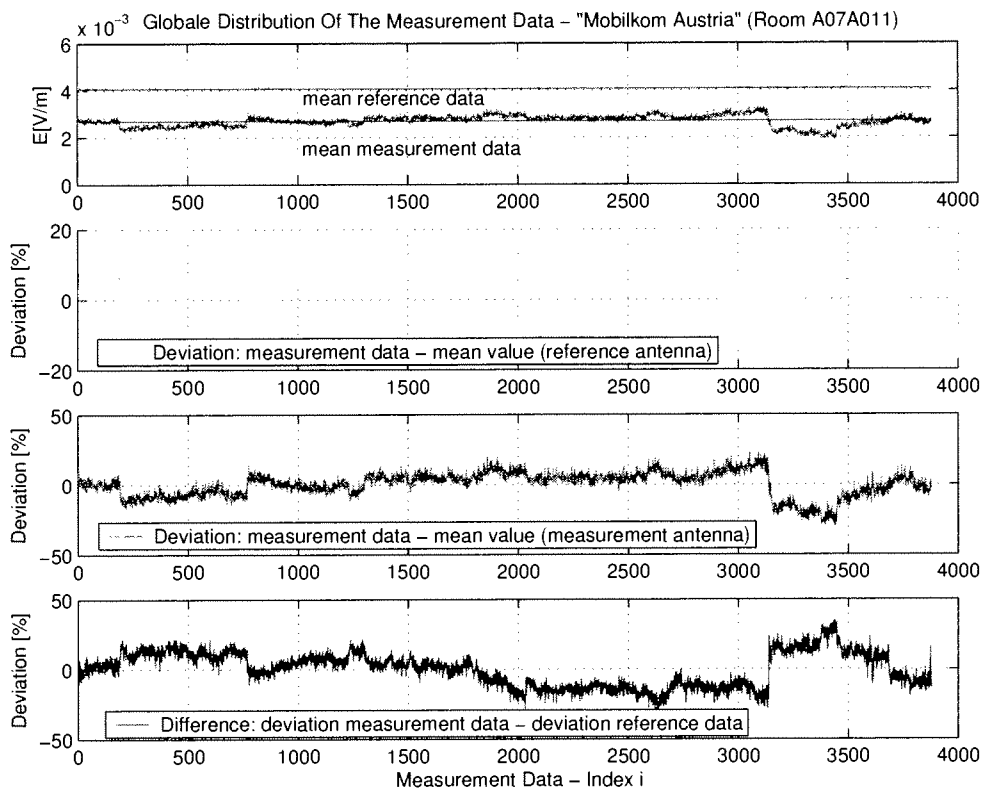


Figure 134: Comparison of the measurement data of the measurement antenna and the reference antenna. (VHF - Room A07A011 Mobilkom Austria, measured on the 17th of March 2003).

evaluated. Figure 134 shows the result. In the end, starting at about measured sample 3150, higher deviations occur, this is equal to the region described where the amplitude values are also starting to vary in a wider range. Table 40 shows the maximum deviation of 34.8% in the positive direction and a mean value of the deviation between the absolute values of the measurement data of the measurement antenna and the absolute values of the measurement data of the reference antenna of 10.7%.

5.2 Continuous Measurements at the *ARC Seibersdorf research GmbH* office building

Continuous measurements were also performed at the *ARC Seibersdorf research GmbH* office building in two different rooms. One room is the conference Room CC2-17 with Line-Of-Sight to the transmitting antenna and the other one, Room TOX 7, is a room characterized as Non-Line-Of-Sight. At the GSM 900 frequency band measurements were performed and are described in the following sections.

VHF	
Date:	17.3.2003
MAX dev. (pos.) [%]	34.8
MAX dev. (neg.) [%]	-29.8
MEAN dev. (abs.) [%]	10.7
MAX dev. (abs.) [%]	34.8
MIN dev. (abs.) [%]	0.002

Table 40: VHF: maximum deviation in positive direction of the y-axis, maximum deviation in the negative direction of the y-axis, mean value of the absolute values of the deviations, maximum and minimum of the absolute values of the deviations.

5.2.1 GSM 900 - Room CC2-17

As mentioned before, the biggest measurement campaign of continuous measurements was performed in a conference room (Room CC2-17) at the *ARC Seibersdorf research GmbH* office building. Over a period of 6 days, measurement data was recorded and delivered more than 45000 single field strength values. The measurement started on a Tuesday afternoon and ended the following Monday at mid-day. This means, that both, weekdays where employees were working as well as a weekend was included in the measurement data. At a frequency of 946.6MHz the measurement was performed. Figure 135 shows the amplitude distribution.

Tremendous variations of the amplitude values occur over the whole measurement period. Although the days are marked specifically with lines in Figure 135, no recurrent behavior could be reported. The variations seems to occur more randomly than with a specific behavior. Table 41 shows the maximum value, the minimum value, the global mean value and the standard deviation of the 46410 examined samples during this 6 day measurement campaign. As described in an earlier section the transmitting antenna is about 60m away from the investigated Room CC2-17. This room can be characterized as Line-Of-Sight only a tree is partly in the propagation path. This room has 4 windows on one side and a corridor on the opposite, office rooms are located on the two other sides. A schematic of this room can be seen in Figure 102.

This large amount of measurement data was also investigated separately, which means that the measurement data of the measurement antenna was plotted in a diagram as well as the measurement data of the reference antenna. In a next step a comparison of those two data was made which is shown in Figure 136. In the range of measured sample 17500 up to about sample 25000 large deviations occur between the measurement data of the measurement antenna and the measurement data of the reference antenna, reaching approximately 300% and again in the range

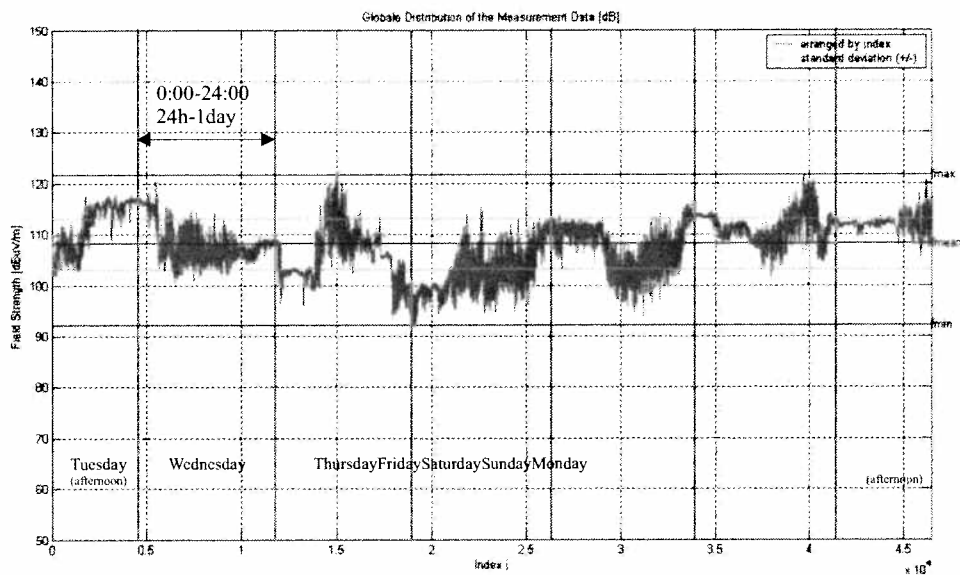


Figure 135: Distribution of the field strength amplitude (GSM 900 - Room CC2-17 *ARC Seibersdorf research GmbH* office building, measured on 15th to 21st of July 2003).

	15.7. - 21.7.2003
Examined Positions	46410
Maximum Value [V/m]	1.2
Minimum Value [mV/m]	41.1
Global Mean Value [mV/m]	299.6
Standard Deviation [mV/m]	162.4

Table 41: Mean value, minimum and maximum value and standard deviation at GSM 900 - continuous measurements, *ARC Seibersdorf research GmbH* Room CC2-17 from the 15th to the 21st of July 2003.

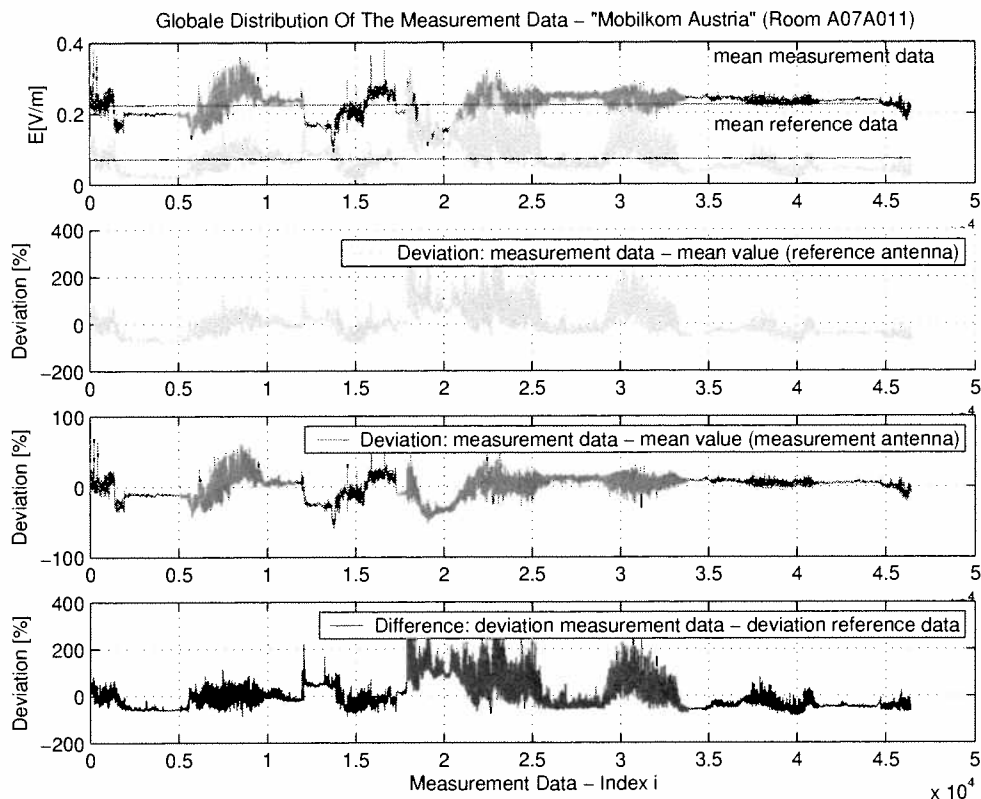


Figure 136: Comparison of the measurement data of the measurement antenna and the reference antenna. (GSM 900 - Room CC2-17 ARC Seibersdorf research GmbH office building, measured on the 15th to the 21st of July 2003).

of sample 29000 up to approximately sample 33500, crossing the 200% level.

A smaller measurement campaign was performed two month earlier in the same room. At a frequency of 944.6MHz the measurement was performed. The difference of the frequency between the former measurement might come from a network optimization process of the network organization. Figure 137 shows the amplitude distribution. The maximum value, the minimum value, the mean value and the standard deviation of this continuous measurement can be seen in Table 42.

The deviation between the measurement data of the measurement antenna and the measurement data of the reference antenna was compared to each other which can be seen in Figure 138. The deviation is nearly constant over the whole range, no particular higher deviations occur. Table 43 shows the values of the deviations between the measurement data of the measurement antenna and the measurement data of the reference antenna. It can be seen, that the highest deviation from the continuous measurement on the 26th of May 2003 occurs in the negative direction of the y-axis with a little over 100%. The highest deviation of all continuous measurements occurs at the 6th measurement from the 15th to the 21st of July with a

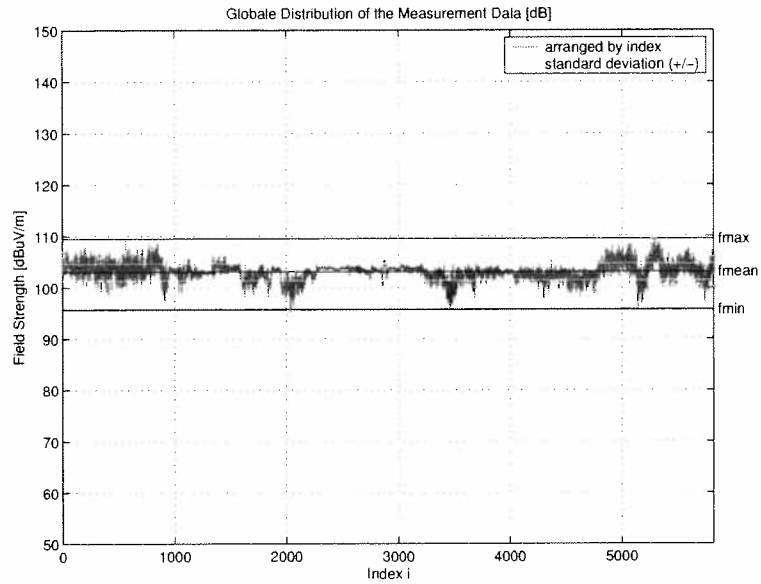


Figure 137: Distribution of the field strength amplitude (GSM 900 - Room CC2-17 *ARC Seibersdorf research GmbH* office building, measured on the 26th of May 2003).

	26.5.2003
Examined Positions	5815
Maximum Value [mV/m]	299.1
Minimum Value [mV/m]	61.0
Global Mean Value [mV/m]	145.4
Standard Deviation [mV/m]	27.7

Table 42: Mean value, minimum and maximum value and standard deviation at GSM 900 - continuous measurements, *ARC Seibersdorf research GmbH* Room CC2-17 from the 26th of May 2003.

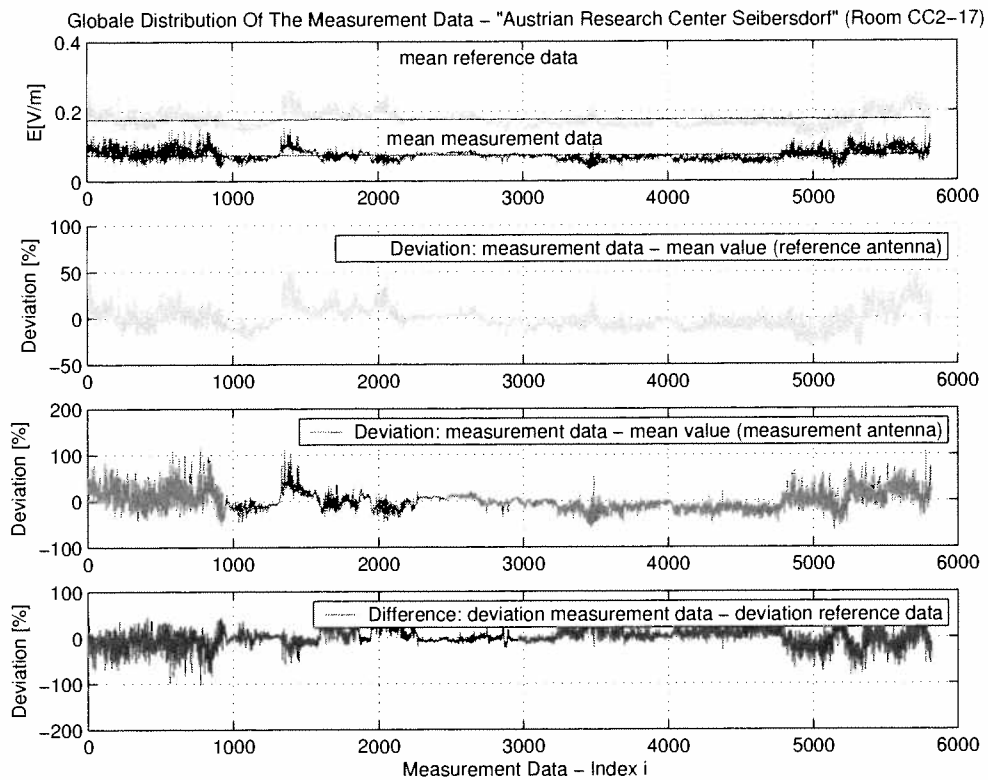


Figure 138: Comparison of the measurement data of the measurement antenna and the reference antenna. (GSM 900 - Room CC2-17 ARC Seibersdorf research GmbH office building, measured on the 26th of May 2003).

value of over 320%. The global mean value of the absolute values of the measurement data is also the highest one compared to all other continuous measurements with a value of 46.1%.

5.2.2 GSM 900 - Room TOX 7

In another room of the *ARC Seibersdorf research GmbH* office building continuous measurements were performed in the GSM 900 frequency band (946.6MHz). As described earlier, this room was characterized as Non-Line-Of-Sight, because it had no windows and the location of the room was in the center of a building complex, with other rooms at all four sides.

The amplitude distribution of the 8200 examined samples is displayed in Figure 139. The maximum value, the minimum value, the global mean value and the standard deviation of this continuous measurement can be seen in Table 44. All field strength values are significant lower compared to the previous measurement campaign because of the Non-Line-Of-Sight scenario.

The evaluation of the measurement data of the measurement antenna and the

GSM 900		
Date:	26.5.2003	15.-21.7.2003
MAX dev. (pos.) [%]	74.2	324.9
MAX dev. (neg.) [%]	-101.9	-87.3
MEAN dev. (abs.) [%]	14.1	46.1
MAX dev. (abs.) [%]	102.0	324.9
MIN dev. (abs.) [%]	0.007	0.003

Table 43: GSM 900: Maximum deviation in positive direction of the y-axis, maximum deviation in the negative direction of the y-axis, mean value of the absolute values of the deviations, maximum and minimum of the absolute values of the deviations.

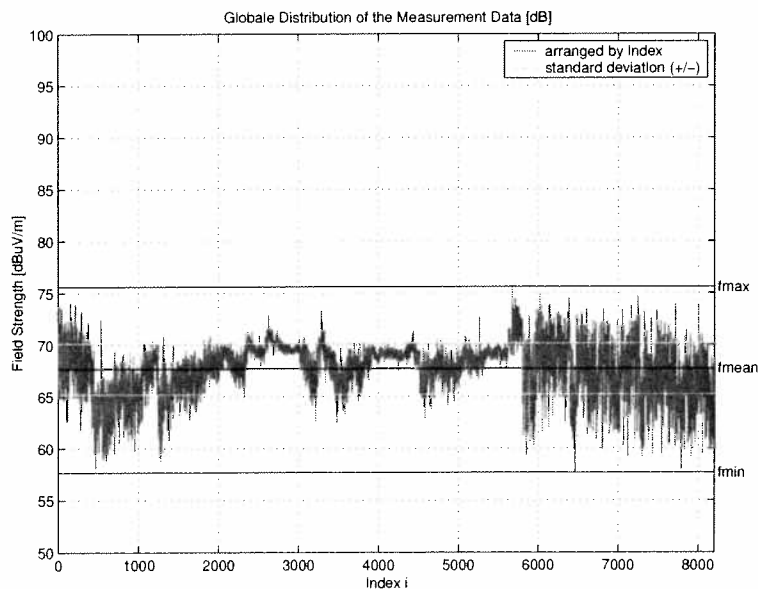


Figure 139: Distribution of the field strength amplitude (GSM 900 - Room TOX 7 ARC Seibersdorf research GmbH office building, measured on the 10th of July 2003).

	10.7.2003
Examined Positions	8200
Maximum Value [mV/m]	6.0
Minimum Value [mV/m]	0.8
Global Mean Value [mV/m]	2.5
Standard Deviation [mV/m]	0.7

Table 44: Mean value, minimum and maximum value and standard deviation at GSM 900 - continuous measurements, Austrian Research Center Seibersdorf Room TOX 7 from the 10th of July 2003.

GSM 900	
Date:	10.7.2003
MAX dev. (pos.) [%]	134.6
MAX dev. (neg.) [%]	-118.6
MEAN dev. (abs.) [%]	23.1
MAX dev. (abs.) [%]	134.6
MIN dev. (abs.) [%]	0.02

Table 45: GSM 900: Maximum deviation in positive direction of the y-axis, maximum deviation in the negative direction of the y-axis, mean value of the absolute values of the deviations, maximum and minimum of the absolute values of the deviations.

measurement data of the reference antenna is shown in Figure 140. Higher deviations occur in the beginning until approximately measurement sample 1500 and in the end starting at about measurement sample 5800 until the end. Table 45 shows the maximum deviation between the measurement data of the measurement antenna and the measurement data of the reference antenna with a value of more than 130% in the negative direction of the y-axis and a mean value of the deviation of more than 20%.

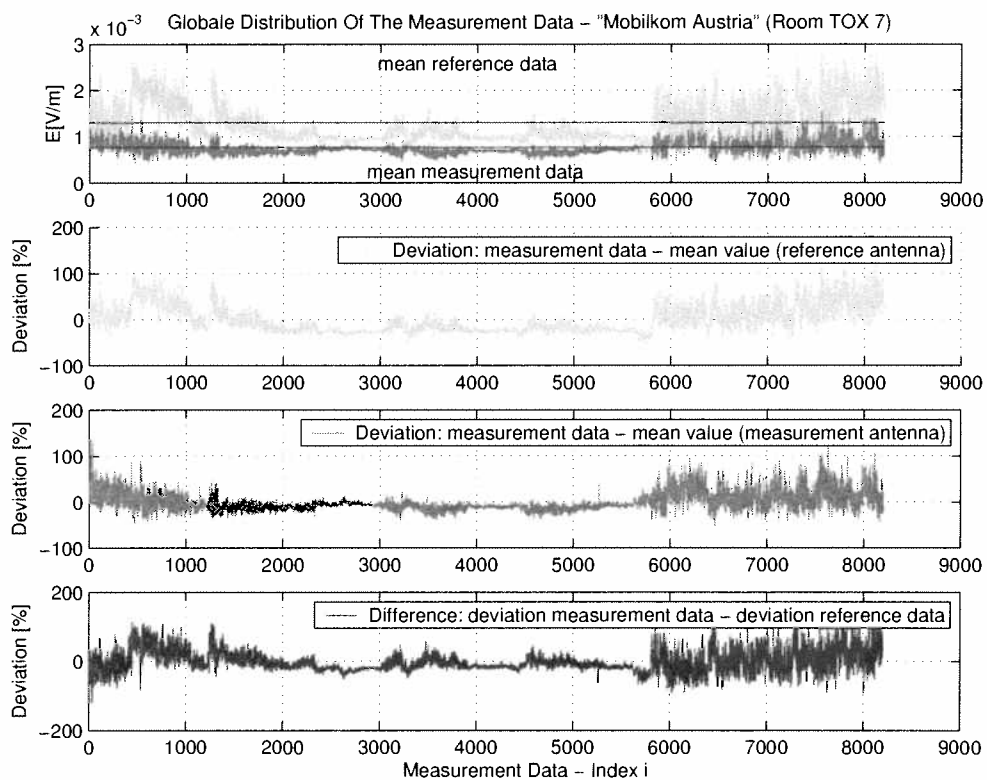


Figure 140: Comparison of the measurement data of the measurement antenna and the reference antenna. (GSM 900 - Room TOX 7 ARC Seibersdorf research GmbH office building, measured on the 10th of July 2003).

6 Simulation

To gain additional knowledge about the electromagnetic field distribution a simulation of the Mobilkom Austria measurement scenario was performed. With the help of the simulation tool *WirelessInsite*[27] from *REMCOM* the simulation was performed. *WirelessInsite* is a simulation tool working with optical ray tracing. Figure 141 shows the scenario designed for simulations. The original dimensions couldn't be realized due to the limited memory of the PC, therefore the height of the building was reduced which shouldn't have any significant effect to the simulation results.

6.1 Simulation of the "Mobilkom Austria - Scenario"

Table 46 gives a short overview of a few significant parameters used in the simulation. The distance to the transmitting antenna was equal to the measurement campaign. The red region in Figure 141 shows the investigated area with a grid step of 15cm. This figure shows only one level, the Level z90, in a height of 90cm above the floor. Six additional levels with a distance of 15cm between each other were calculated but not displayed. The transmitting antenna is in a distance of 33m away from the investigated area. Its antenna pattern was imported from a Kathrein product CD, the frequency for the simulation was 946.0MHz, similar to the antenna on the Mobilkom Austria office building rooftop. To have insight into the room which was under investigation, the ceiling of the building was not displayed but was included in the simulation procedure.

The field pattern at different locations within the investigated area can easily be calculated and so various situations can be observed. In the following sections results from six cubes at different positions within the investigated area were calculated and the histogram, the cumulative distribution function, the probability density function as well as the local distribution of the electromagnetic field strength were displayed. The locations of those six cubes are shown in Figure 142. Seven measured positions in each direction of the three axes were used to calculate the representative values of a cube. The 7 levels in direction of the z-axis are 'z90' (90cm above the floor), 'z105' (105cm above the floor), 'z120' (120cm above the floor), 'z135' (135cm above the floor), 'z150' (150cm above the floor), 'z165' (165cm above the floor) and 'z180' (180cm above the floor). Table 47 shows the location of the six cubes with the first positions in direction of the x-axis and the y-axis of each simulated cube.

In the following sections the global aspects of this simulation and the six cubes on certain locations were taken under consideration.

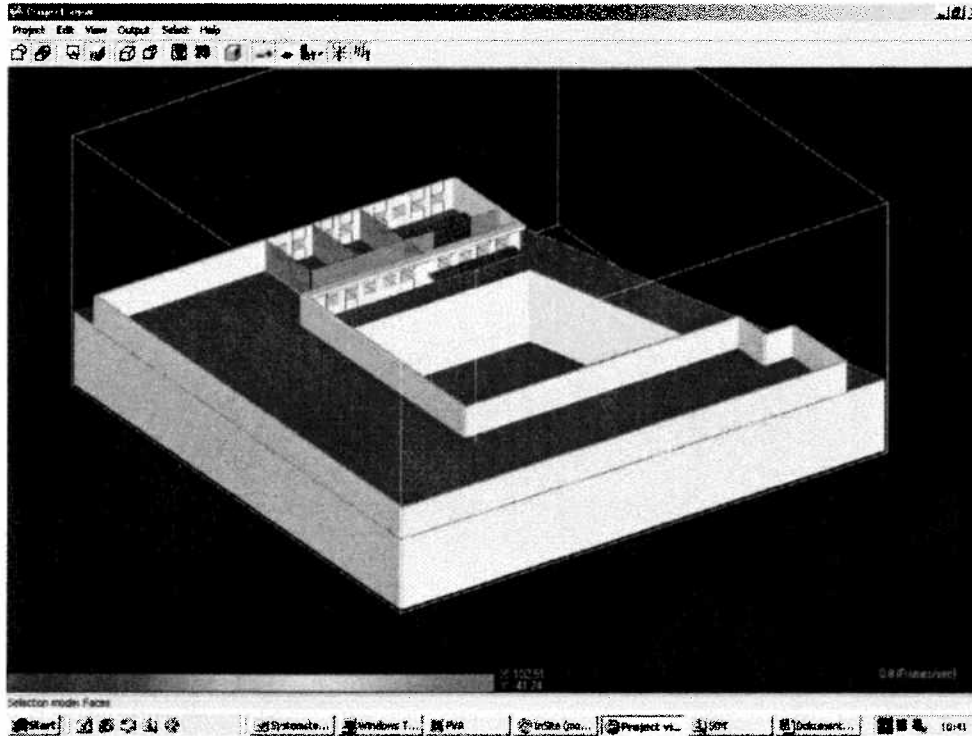


Figure 141: Scenario of the simulated Mobilkom Austria measurement campaign in the GSM 900 frequency band (946MHz) . The red area is the investigated area with a grid step of 15cm equal to the grid step of the measured cubes. Seven layers were measured with a distance of 15cm to each other starting at Level 'z90' which is 90cm above the ground. 60 times 60 examined positions in each level were calculated which gives a total of 3600 positions per level. The small green cube is the transmitting antenna. The yellow cuboid around the whole building is the study area, which represents the area under investigation.

Frequency	GSM 900 - 944.6MHz
Grid Step	15cm
Examined Positions per level	3600 (60 x 60)
Levels	7 (z90, z105, ..., z180)
Examined Positions total	25200
Distance	33m

Table 46: Parameters of the Mobilkom Austria simulation.

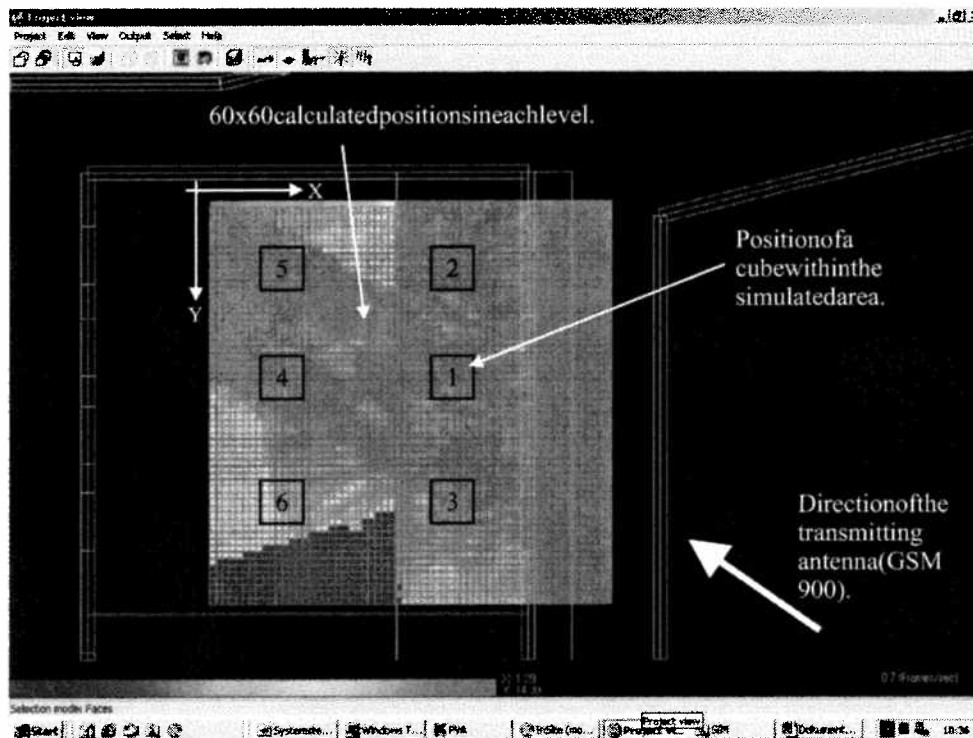


Figure 142: This is a schematic of the six cubes and their locations within the simulated area. The cube with the number 1 (SIM 1) is approximately the positions of the cube measured in the Room A07A011 at the Mobilkom Austria office building. Seven positions in each direction of the three axis were used to calculate the representative values of each cube. In direction of the z-axis the first level is level 'z90', located 90cm above the floor the last level is 'z180', located 180cm above the floor.

Cube	Location
Sim 1	(35/27)
Sim 2	(35/10)
Sim 3	(35/43)
Sim 4	(15/27)
Sim 5	(15/10)
Sim 6	(15/43)

Table 47: Positions of the cubes within the simulated area. The numbers in brackets show the coordinates in direction of the x-axis and y-axis. The first level in direction of the z-axis was z90, which is located 90cm above the floor.

	Exam. Pos.	Max.	Min.	Mean	Std. Dev.
		[mV/m]	[mV/m]	[mV/m]	[mV/m]
Total	25200	5.2	0.01	0.99	0.87
Sim 1	343	4.4	0.16	0.25	0.75
Sim 2	343	3.3	0.23	0.93	0.52
Sim 3	343	2.5	0.09	0.95	0.54
Sim 4	343	4.5	0.02	0.22	0.08
Sim 5	343	3.2	0.01	1.90	0.66
Sim 6	343	1.6	0.03	0.59	0.38

Table 48: Mean value, minimum and maximum value and standard deviation - GSM 900, simulation of the Mobilkom Austria Room A07A011. The first row shows the results for the whole measurement data and the other rows are showing the results for 6 cubes on different locations within the whole area.

6.1.1 Mean, Standard Deviation and Amplitude Distribution

Table 48 shows the maximum value, the minimum value, the global mean value as well as the standard deviation of the whole investigated area as well as for each of the six cubes at different locations within the area of interest. Figure 143 shows the histogram of the whole measurement data.

For each of the six cubes the histogram was derived and can be seen in the following figures. Figure 144 was the first evaluation and the location of this cube should be approximately equal to the location of the cube measured in Room A07A011 at the Mobilkom Austria office building. For the comparison of different simulation results five more cubes were evaluated on different locations within the simulated volume. Figure 145 shows the histogram of a second cube (SIM 2), Figure 146 shows the histogram of a third cube (SIM 3), Figure 147 shows the histogram of a fourth cube (SIM 4), Figure 148 shows the histogram of a fifth cube (SIM 5) and Figure 149 shows the histogram of the last cube (SIM 6).

6.1.2 Cumulative Distribution Function and Probability Density Function

The cumulative distribution function can be build by arranging the field strength values by increasing amplitudes, as described in Section 3.2.2. Figure 150 shows the cumulative distribution function of the whole simulated area. Figure 151 shows the cumulative distribution function of the first simulated cube (SIM 1) which is approximately at the same location than the cube measured in Room A07A011 at the Mobilkom Austria, further Figure 152, Figure 153, Figure 154, Figure 155, Figure 156 are showing the cumulative distribution function of the other evaluated cubes (SIM 2, SIM 3, SIM 4, SIM 5, SIM 6).

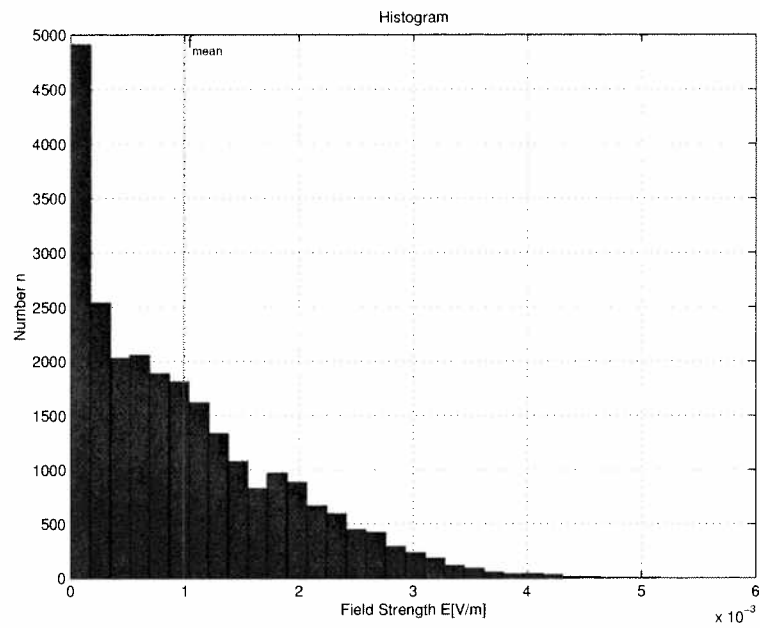


Figure 143: Global distribution of the electromagnetic field strength values disposed in 30 amplitude grades. Simulation of the Mobilkom Austria office building Room A07A011 at a frequency of 946MHz.

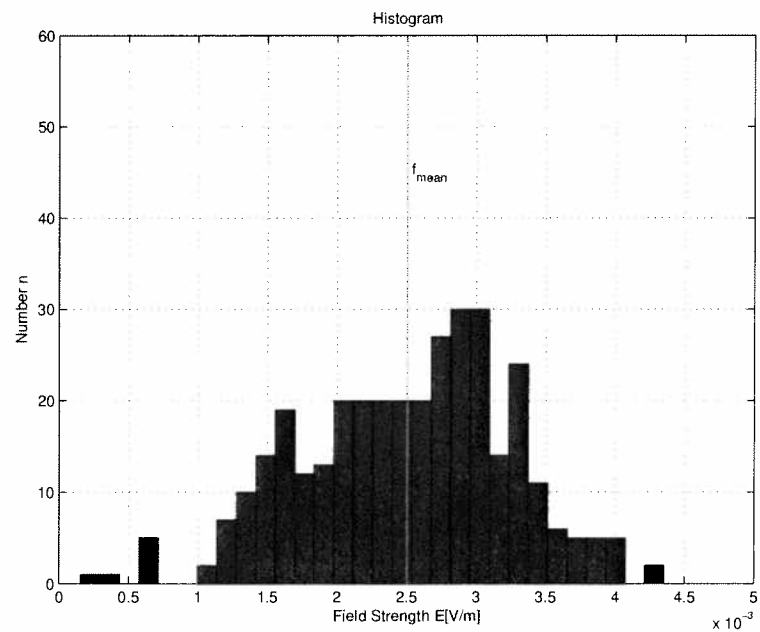


Figure 144: Global distribution of the electromagnetic field strength values disposed in 30 amplitude grades. Simulation of a cube at approximately the same positions (SIM 1) than a cube measured at the Mobilkom Austria office building Room A07A011 at a frequency of 946MHz.

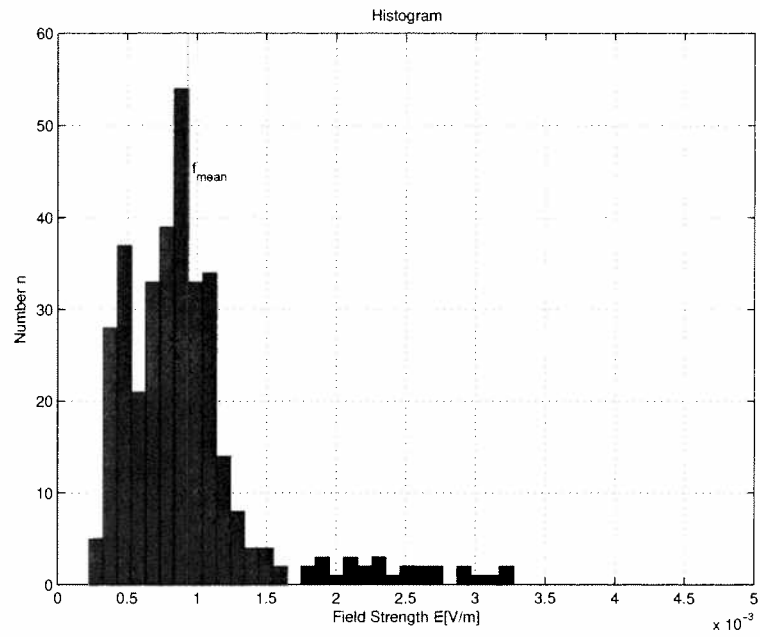


Figure 145: Global distribution of the electromagnetic field strength values disposed in 30 amplitude grades. Simulation of a second cube (SIM 2) at a frequency of 946MHz.

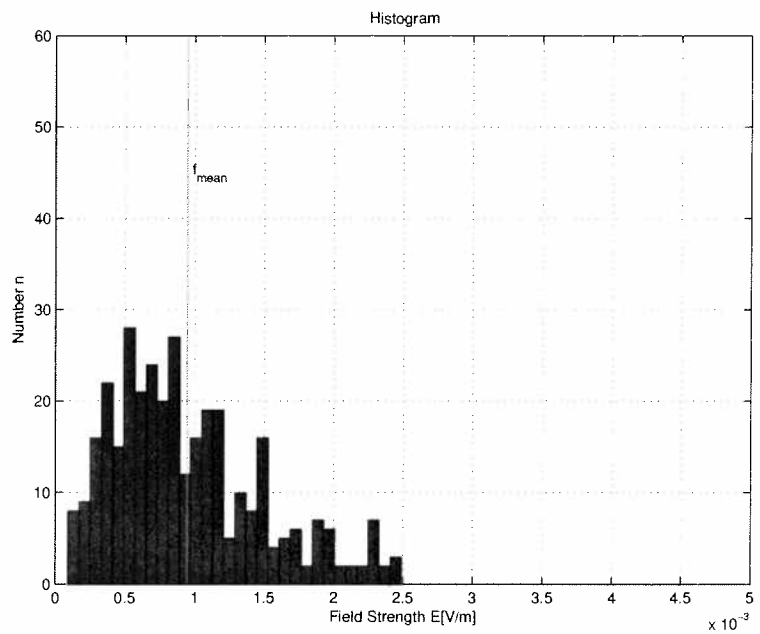


Figure 146: Global distribution of the electromagnetic field strength values disposed in 30 amplitude grades. Simulation of a third cube (SIM 3) at a frequency of 946MHz.

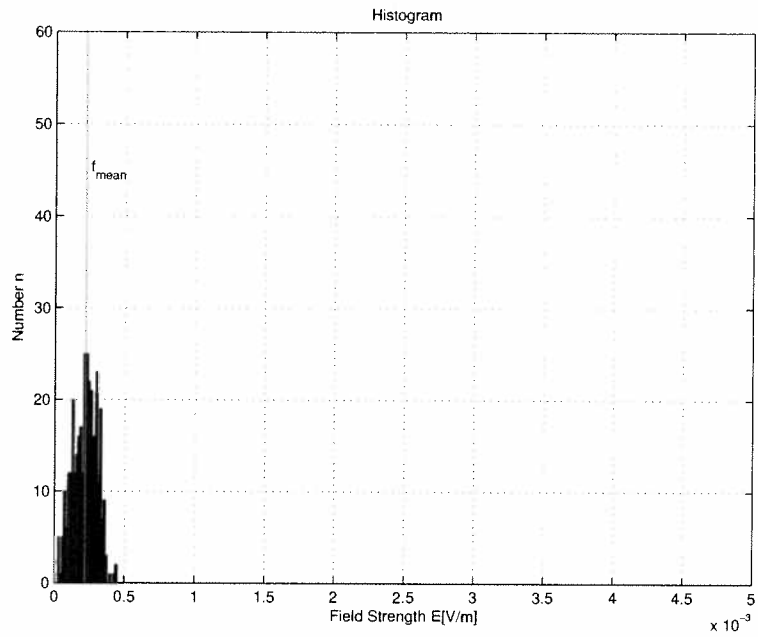


Figure 147: Global distribution of the electromagnetic field strength values disposed in 30 amplitude grades. Simulation of a fourth cube (SIM 4) at a frequency of 946MHz.

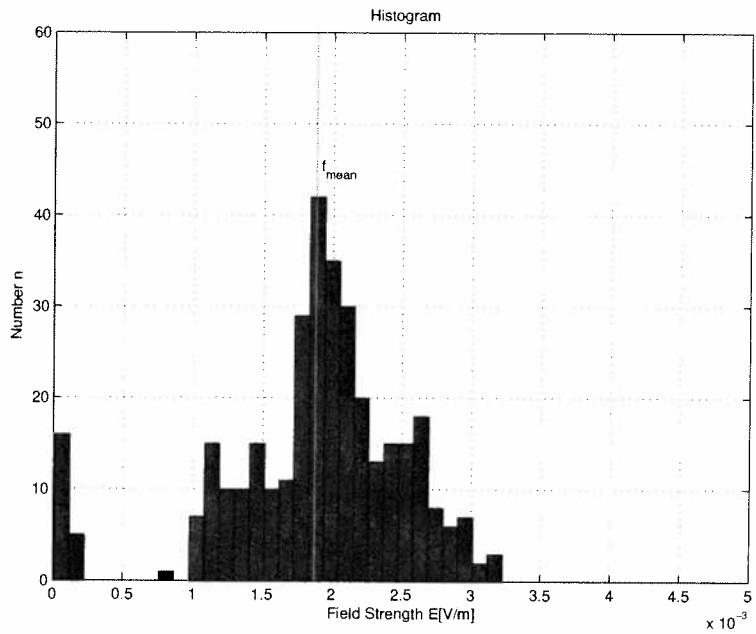


Figure 148: Global distribution of the electromagnetic field strength values disposed in 30 amplitude grades. Simulation of a fifth cube (SIM 5) at a frequency of 946MHz.

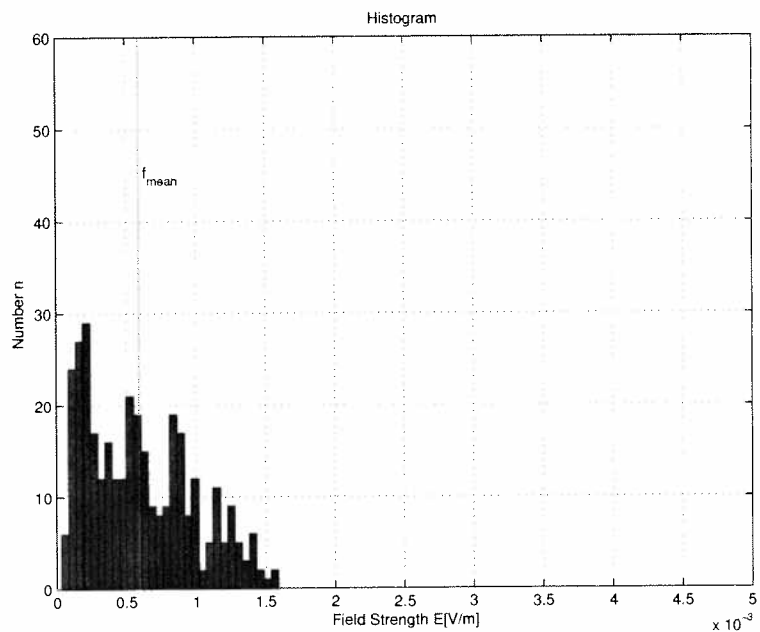


Figure 149: Global distribution of the electromagnetic field strength values disposed in 30 amplitude grades. Simulation of a sixth cube (SIM 6) at a frequency of 946MHz.

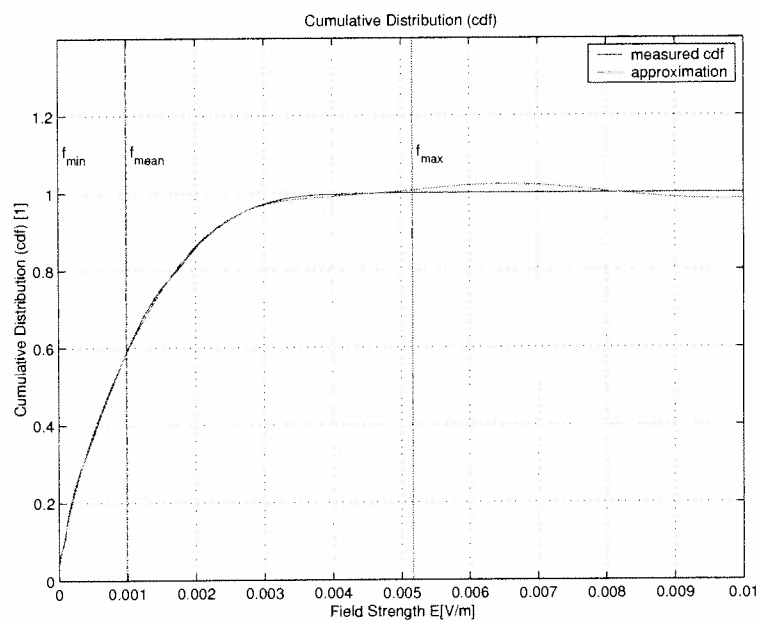


Figure 150: Cumulative distribution function (cdf) of the global field distribution of the whole simulated area (GSM 900 - Simulation of Room A07A011 Mobilkom Austria).

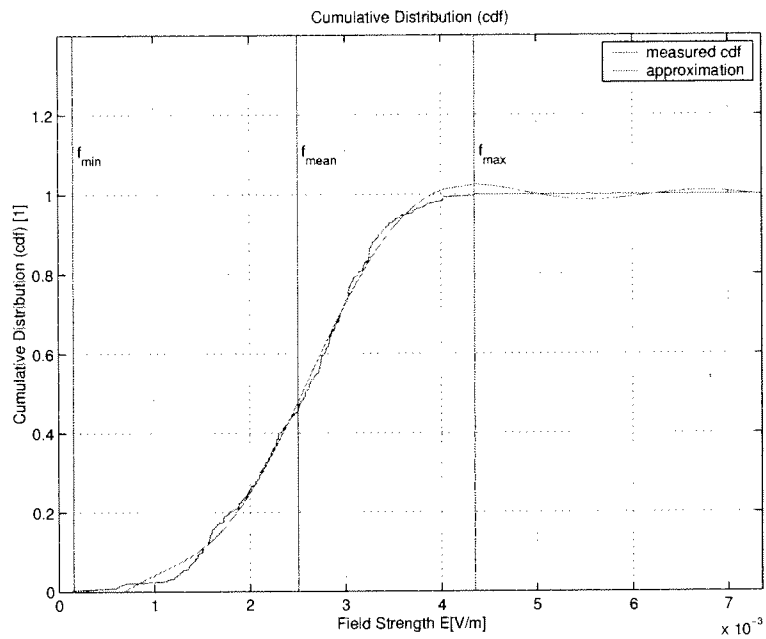


Figure 151: Cumulative distribution function (cdf) of the global field distribution of the first cube (SIM 1 - GSM 900 - Simulation of Room A07A011 Mobilkom Austria).

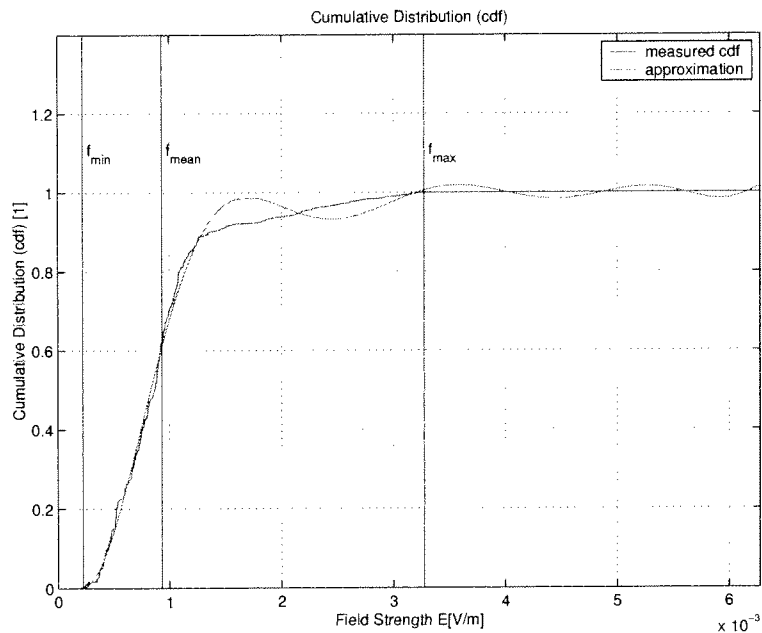


Figure 152: Cumulative distribution function (cdf) of the global field distribution of the second cube (SIM 2 - GSM 900 - Simulation of Room A07A011 Mobilkom Austria).

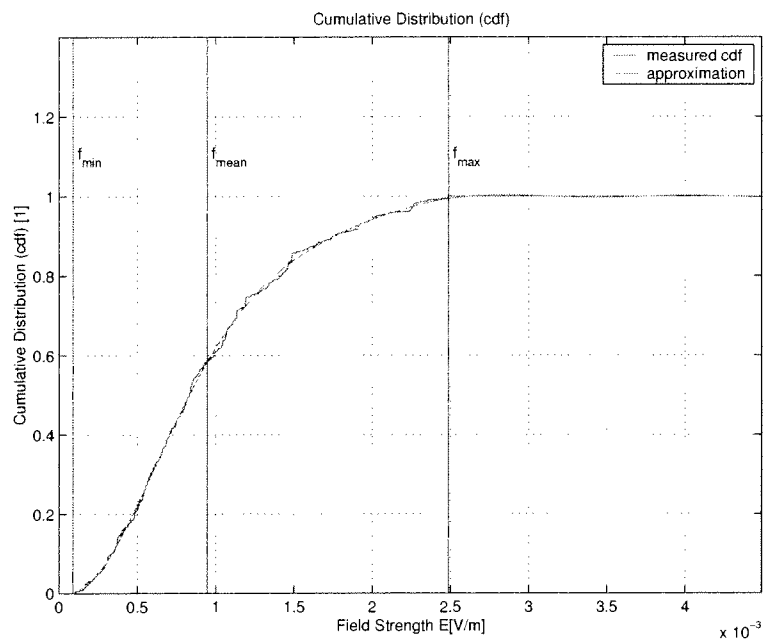


Figure 153: Cumulative distribution function (cdf) of the global field distribution of the third cube (SIM 3 - GSM 900 - Simulation of Room A07A011 Mobilkom Austria).

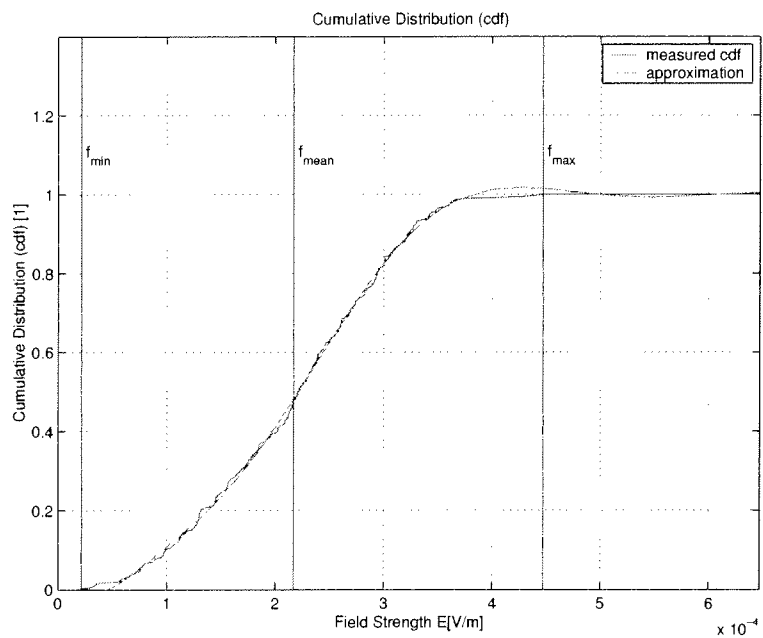


Figure 154: Cumulative distribution function (cdf) of the global field distribution of the fourth cube (SIM 4 - GSM 900 - Simulation of Room A07A011 Mobilkom Austria).

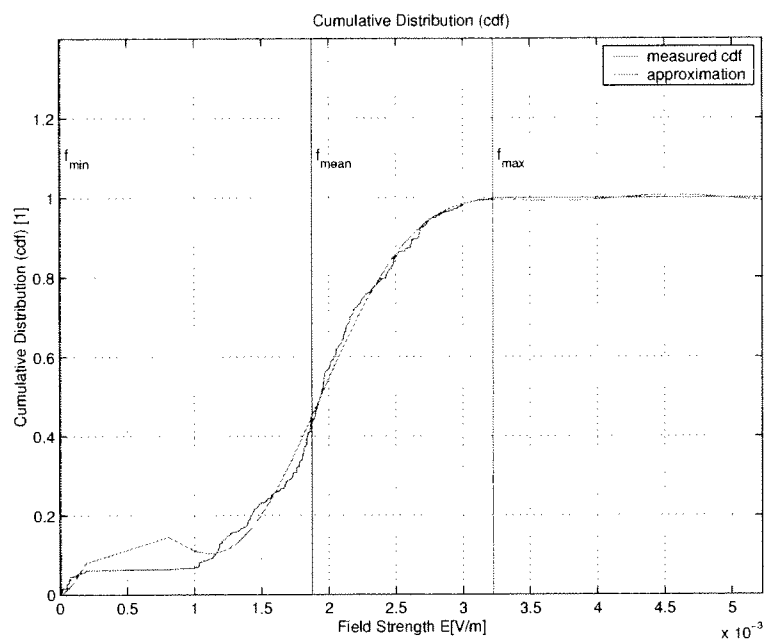


Figure 155: Cumulative distribution function (cdf) of the global field distribution of the fifth cube (SIM 5 - GSM 900 - Simulation of Room A07A011 Mobilkom Austria).

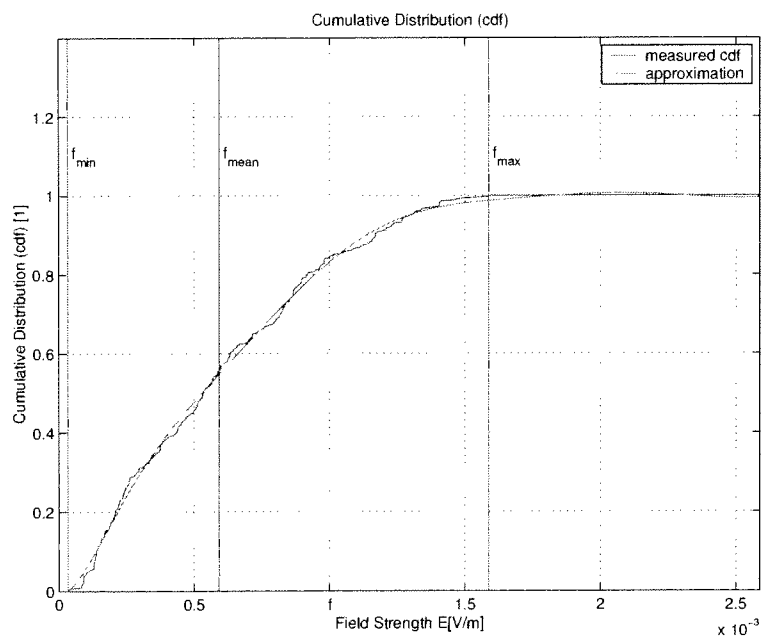


Figure 156: Cumulative distribution function (cdf) of the global field distribution of the sixth cube (SIM 6 - GSM 900 - Simulation of Room A07A011 Mobilkom Austria).

	$E_{10\%}$	$E_{25\%}$	$E_{50\%}$	$E_{75\%}$	$E_{90\%}$
	$\left[\frac{mV}{m}\right]$	$\left[\frac{mV}{m}\right]$	$\left[\frac{mV}{m}\right]$	$\left[\frac{mV}{m}\right]$	$\left[\frac{mV}{m}\right]$
Total	0.1	0.3	0.8	1.5	2.2
Sim 1	1.5	2.0	2.6	3.0	3.4
Sim 2	0.4	0.6	0.8	1.1	1.3
Sim 3	0.3	0.5	0.8	1.2	1.8
Sim 4	0.1	0.2	0.2	0.3	0.3
Sim 5	0.7	1.6	1.9	2.3	2.6
Sim 6	0.1	0.3	0.8	1.5	2.2

Table 49: Lower and higher quartile, lower and higher decile, quintile of the whole simulated area as well as for each of the six cubes (Simulation of the Mobilkom Austria Room A07A011 at GSM 900).

The percentiles of the cumulative distribution function of the whole simulated area as well as of each of the six cubes are shown in Table 49, while the percentiles normalized to the maximum electromagnetic field strength are shown in Table 50.

6.1.3 Identification of the Probability Density Function

The probability density function can be derived by differentiating the cumulative distribution function. For each of the six cubes, the probability function was derived and for all of them, a possible approximated distribution function (like LogNormal or Rayleigh) was found.

Figure 157 shows the probability density function of the first cube (SIM 1). A possible approximation for the function might be a Normal distribution. The Normal distribution can be derived by Equation 18. The probability density function of the second cube (SIM 2) is displayed in Figure 158, this pdf could be approximated by a LogNormal distribution. The LogNormal distribution, which can be derived by Equation 18, could also be a approximation for the probability density function of the third cube (SIM 3), which is displayed in Figure 159. Figure 160 shows the probability density function of the fourth cube (SIM 4) with a Normal distribution as approximation. The Normal distribution seems to be a good approximation for the fifth cube (SIM 5), which is shown in Figure 161. For the sixth cube (SIM 6), displayed in Figure 162 the Rayleigh distribution seems to fit best which can be derived by Equation 18. The validity of all polynomial approximations is in the range between minimum and maximum of the electromagnetic field strength values of each investigated area.

	E_{max}	$\frac{E_{10\%}}{E_{max}}$	$\frac{E_{25\%}}{E_{max}}$	$\frac{E_{50\%}}{E_{max}}$	$\frac{E_{75\%}}{E_{max}}$	$\frac{E_{90\%}}{E_{max}}$
	$[\frac{mV}{m}]$	%	%	%	%	%
Total	5.2	1.9	5.8	15.4	28.8	42.3
Sim 1	4.4	34.1	45.5	59.1	68.2	77.3
Sim 2	3.3	12.1	18.2	24.2	33.3	39.4
Sim 3	3.3	13.5	21.3	32.2	49.8	70.3
Sim 4	2.5	22.4	34.4	49.2	62.2	72.1
Sim 5	4.5	21.9	50.0	59.4	71.9	81.3
Sim 6	3.2	6.3	18.8	31.3	56.3	75.0

Table 50: Lower and higher quartile, lower and higher decile, quintile normalized to the maximum electromagnetic field strength of each investigated area. For the whole simulation data the maximum value and for each cube the maximum value is listed. (Simulation of the Mobilkom Austria Room A07A011 at GSM 900).

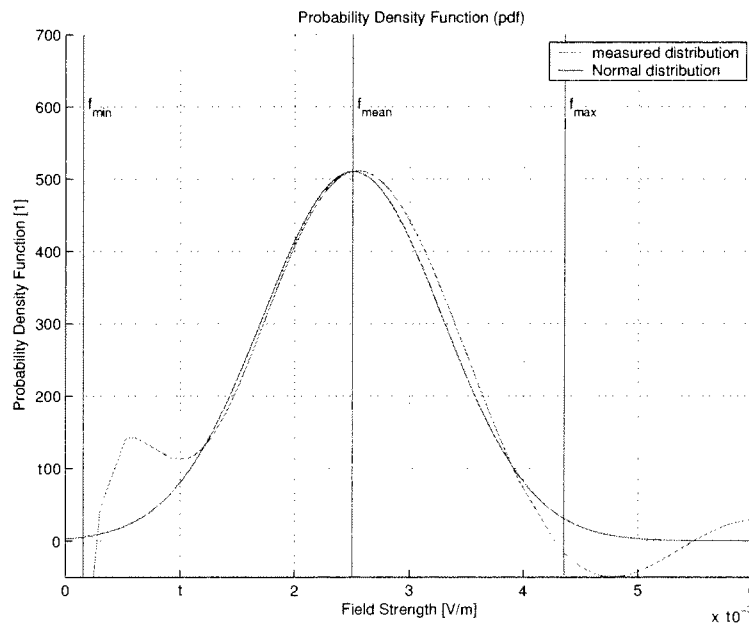


Figure 157: Probability Density function (pdf) of the first cube (SIM 1) and a possible approximation with a Normal distribution (GSM 900 - Simulation of Room A07A011 Mobilkom Austria).

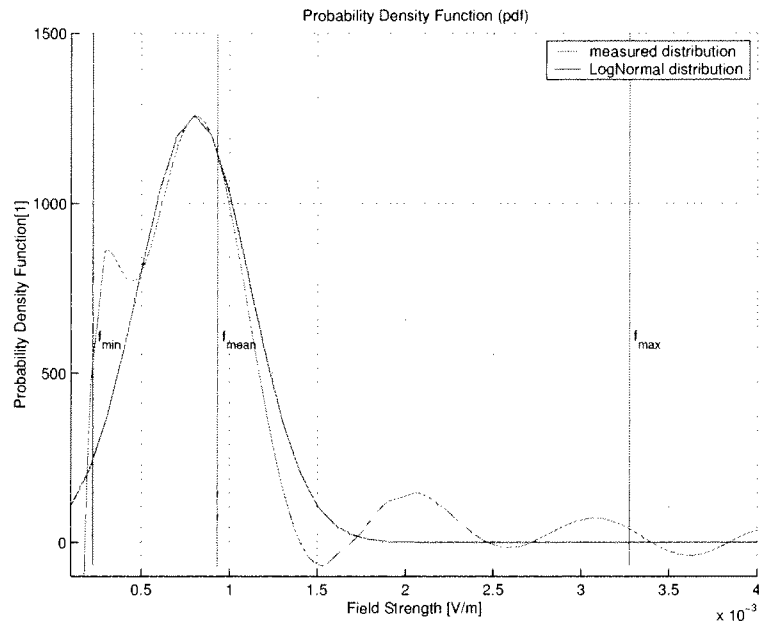


Figure 158: Probability Density function (pdf) of the second cube (SIM 2) and a possible approximation with a LogNormal distribution (GSM 900 - Simulation of Room A07A011 Mobilkom Austria).

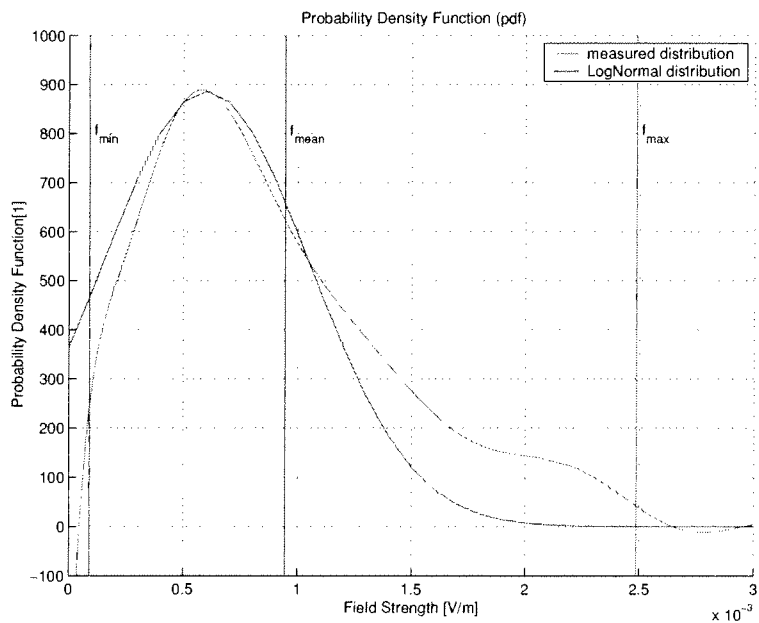


Figure 159: Probability Density function (pdf) of the third cube (SIM 3) and a possible approximation with a LogNormal distribution (GSM 900 - Simulation of Room A07A011 Mobilkom Austria).

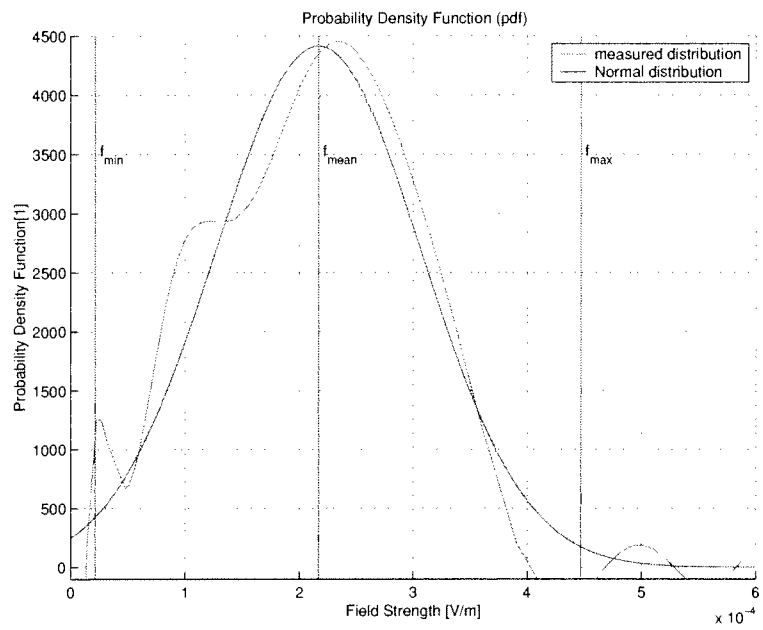


Figure 160: Probability Density function (pdf) of the fourth cube (SIM 4) and a possible approximation with a Normal distribution (GSM 900 - Simulation of Room A07A011 Mobilkom Austria).

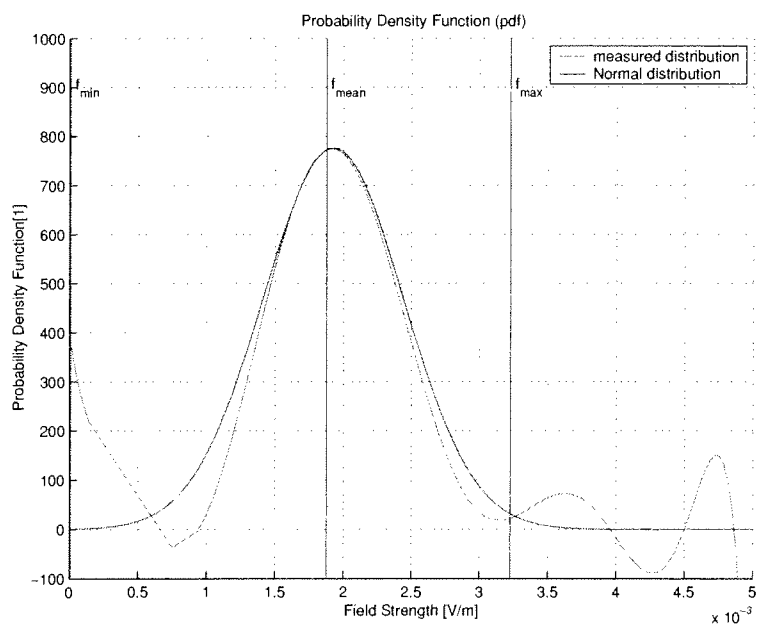


Figure 161: Probability Density function (pdf) of the fifth cube (SIM 5) and a possible approximation with a Normal distribution (GSM 900 - Simulation of Room A07A011 Mobilkom Austria).

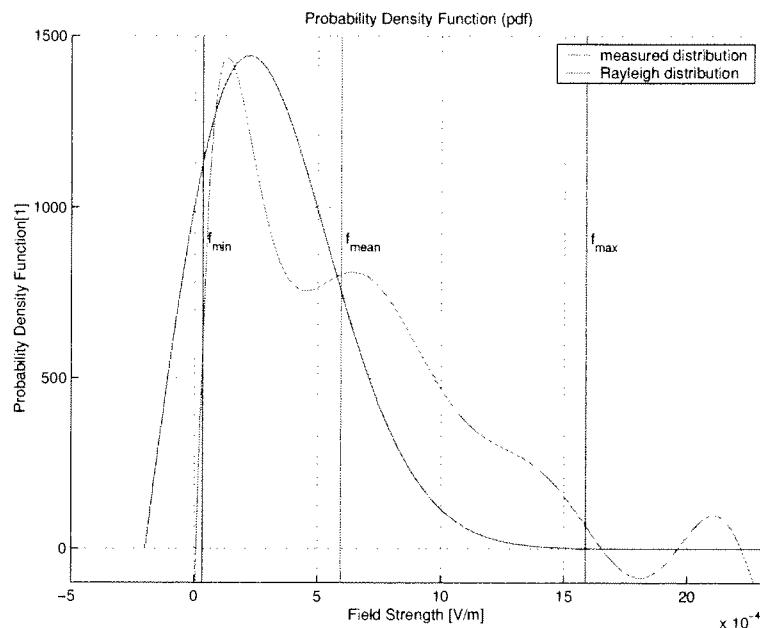


Figure 162: Probability Density function (pdf) of the sixth cube (SIM 6) and a possible approximation with a Rayleigh distribution (GSM 900 - Simulation of Room A07A011 Mobilkom Austria).

6.1.4 Local Distribution of the Measurement Data

After the global considerations of the field strength distributions the local demeanor was investigated. Therefore the electromagnetic field strength normalized to the global maximum for the seven levels is displayed for each cube.

Figure 163 shows the local distribution of the electromagnetic field strength for each of the seven levels of the cube SIM 1. It can be seen that in the middle of each level the field strength is higher than in the border of each level. Level 'z120' shows an area with lower field strength values.

Figure 164 shows the local distribution of the electromagnetic field strength for each of the seven levels of the cube SIM 2. This Figure shows very low field strength values in all seven levels with an exception in Level z105 and Level z120. In this two levels higher field strength values occur in the front left corner of the levels. Whereas Level z105 shows the widest area with higher field strength values.

Figure 165 shows the local distribution of the electromagnetic field strength for each of the seven levels of the cube SIM 3. Maximum field strength values can be observed in the front right corner of four levels (Level z90, z150, z165 and z180). The rest of the areas are showing lower field strength values with a minimum in Level z105.

Figure 166 shows the local distribution of the electromagnetic field strength for each of the seven levels of the cube SIM 4. This Figure shows higher field strength

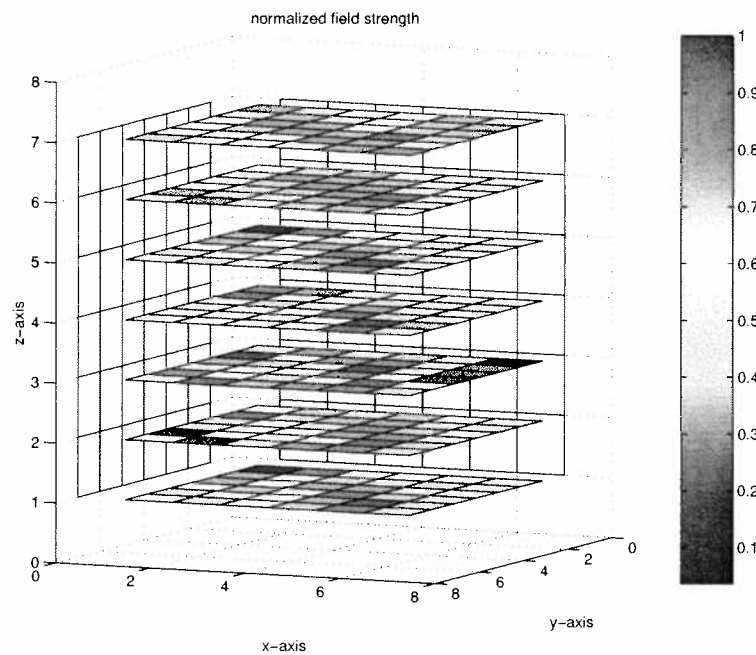


Figure 163: Distribution of the field strength values normalized to the maximum value of the investigated volume for SIM 1 (GSM 900 - Simulation of Room A07A011 Mobilkom Austria).

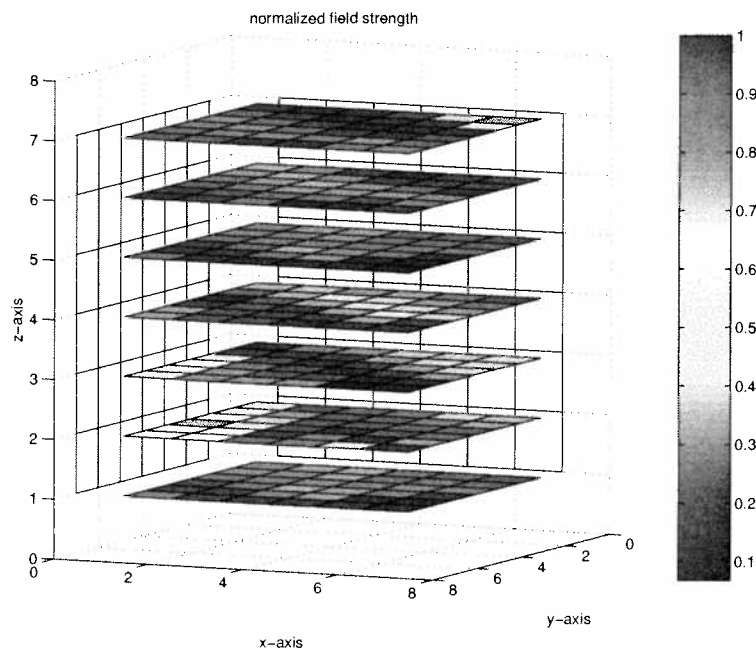


Figure 164: Distribution of the field strength values normalized to the maximum value of the investigated volume for SIM 2 (GSM 900 - Simulation of Room A07A011 Mobilkom Austria).

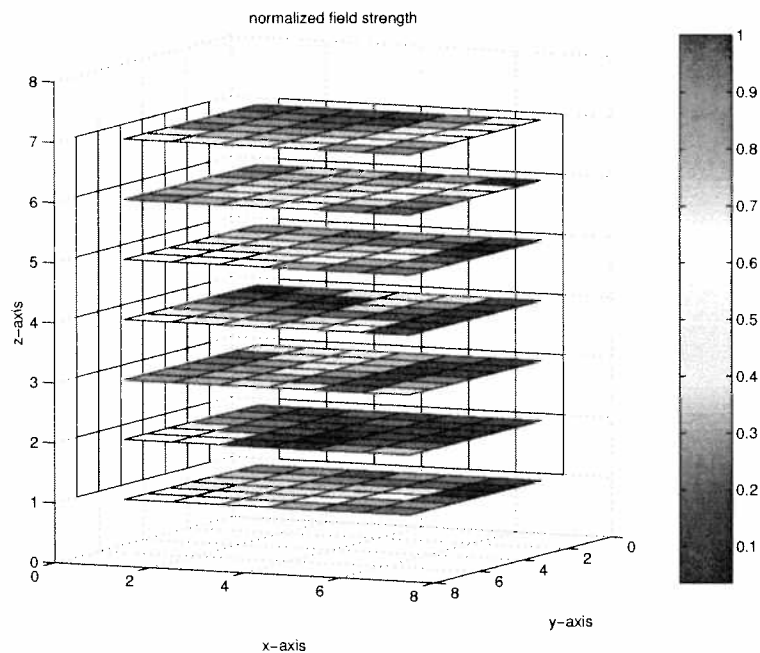


Figure 165: Distribution of the field strength values normalized to the maximum value of the investigated volume for SIM 3 (GSM 900 - Simulation of Room A07A011 Mobilkom Austria).

values in the middle of each level and lower field strength values on two opposite corners in each level

Figure 167 shows the local distribution of the electromagnetic field strength for each of the seven levels of the cube SIM 5 . Higher field strength values occur in every level with just a very small area in one corner of each level. In this corner the field strength is very low.

Figure 168 shows the local distribution of the electromagnetic field strength for each of the seven levels of the cube SIM 6. This Figure shows a distinctive low field strength value in each level on one side of the diagonal. On the opposite side, higher field strength values occur.

The results of the six cubes, evaluated from the simulation, might lead to the following preliminary conclusions. It seems that the approximated probability density functions doesn't show any significance for different locations within the simulated volumes, because different distribution functions were found. This may lead to one conclusion which would say that a specific scenario can't be characterized with a specific distribution function. Comparing the percentiles of each simulated cube might be more expressiveness. It might also be obvious that higher field strength values occur near the windows which are in direction of the transmitted field strength but the simulation and the results of those six cubes show a difference. Comparing the maximum field strengths values and also the global mean

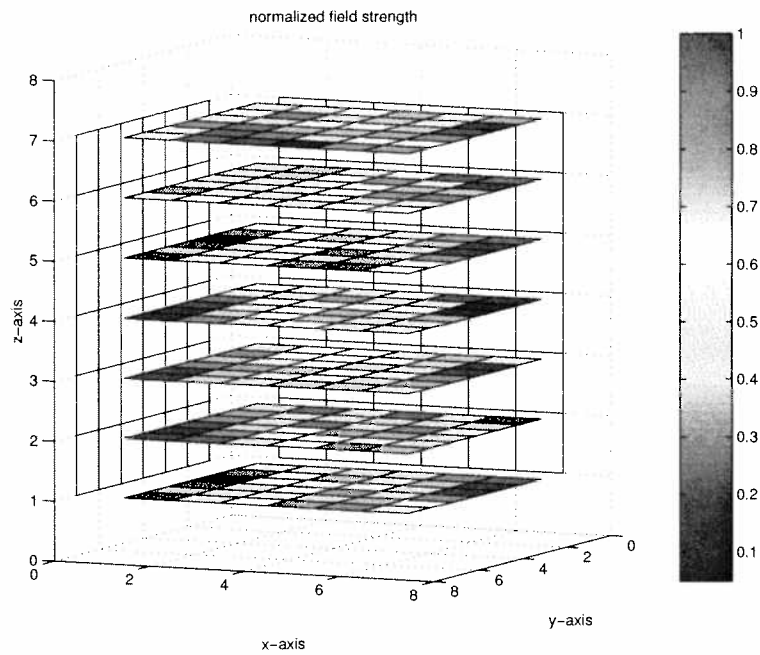


Figure 166: Distribution of the field strength values normalized to the maximum value of the investigated volume for SIM 4 (GSM 900 - Simulation of Room A07A011 Mobilkom Austria).

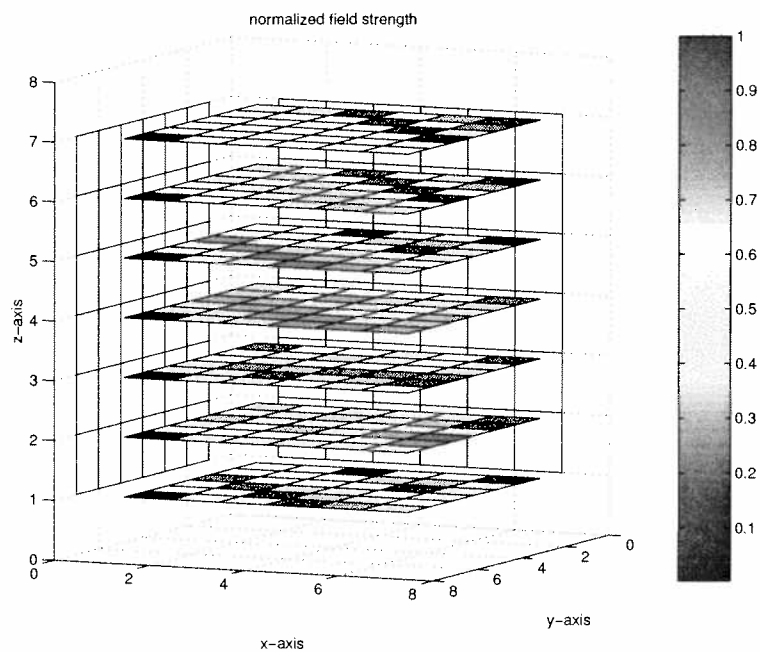


Figure 167: Distribution of the field strength values normalized to the maximum value of the investigated volume for SIM 5(GSM 900 - Simulation of Room A07A011 Mobilkom Austria).

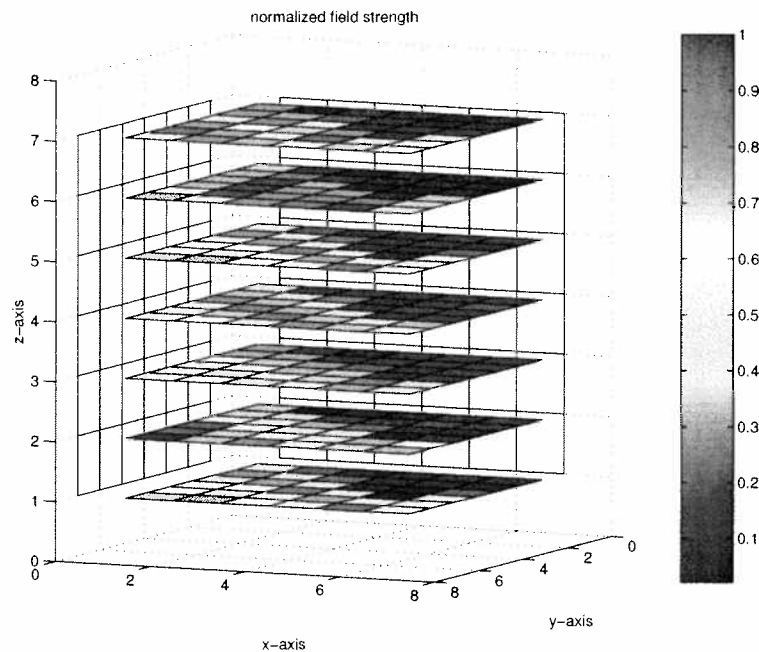


Figure 168: Distribution of the field strength values normalized to the maximum value of the investigated volume for SIM 6 (GSM 900 - Simulation of Room A07A011 Mobilkom Austria).

value of the field strengths (referring to Table 48) shows, that not SIM 1 and SIM 4 (which are in the main direction of the transmitted field strength) have the highest values, but SIM 2 and SIM 3 have the highest global mean values while SIM 1 and SIM 4 have lower global mean values compared to the results of the other cubes. Trying to understand the behavior of the field strength within a certain area was the next goal. Therefore three characteristic scenarios were investigated.

A first idea was, that the location of the investigated area (e.g. cube) plays a remarkable role. Therefore three characteristic scenarios were chosen and cubes were moved through the simulated area to find appropriate results. These characteristic scenarios were three cubes with specific field strength values: the first cube with field strength values in nearly the same range with only a little variance of the field strength values, called *Sim_{CONST}*, a second cube with a small region with higher field strength values ("Hot Spot") compared to the rest of the field strength values building the investigated area, called *Sim_{HS}* and a third cube with a mixture of the two mentioned cubes with an area of lower field strength values and an area with higher field strength values, called *Sim_{MIX}*.

Like in the sections before, the global and local aspects of the measurement were taken under consideration. A schematic of the location of those three examined cubes is shown in Figure 169, the location regarding the x-axis and y-axis of those three examined cubes is shown in Table 51. Table 52 shows the maximum value,

Cube	Location
<i>Sim_{CONST}</i>	(7/1)
<i>Sim_{HS}</i>	(1/40)
<i>Sim_{MIX}</i>	(15/15)

Table 51: Positions of the three cubes located at specific places with higher field strength values (*Sim_{CONST}*), with lower field strength values (*Sim_{HS}*) and with both, higher and lower field strength values (*Sim_{MIX}*) within the simulated area. The numbers in brackets show the coordinates in direction of the x-axis and y-axis. The first level in direction of the z-axis was z90, which is located 90cm above the floor.

	Exam. Pos.	Max.	Min.	Mean	Std. Dev.
		[mV/m]	[mV/m]	[mV/m]	[mV/m]
<i>Sim_{CONST}</i>	343	2.81	0.03	1.73	0.45
<i>Sim_{HS}</i>	343	1.00	0.04	0.22	0.16
<i>Sim_{MIX}</i>	343	2.75	0.01	0.87	0.92

Table 52: Mean value, minimum and maximum value and standard deviation - GSM 900, simulation of the Mobilkom Austria Room A07A011. Three different but significant scenarios were evaluated. The first cube was positioned in an area with higher electromagnetic field strength values (*Sim_{CONST}*), the second was placed in an area with lower field strength values and a small area with high field strength values ("Hot Spot" - *Sim_{HS}*) and the third was placed in an area where both, higher and lower field strength values occur (*Sim_{MIX}*).

the minimum value, the global mean value as well as the standard deviation of the three different cubes at three certain locations within the simulated volume which were evaluated to probably answer some questions and confirm some ideas.

Figure 170 shows the histogram of a cube (*Sim_{CONST}*) which was placed in an area with field strength values in nearly the same range. Figure 171 shows the histogram of a cube (*Sim_{HS}*) which was placed in an area with lower field strength values and a "Hot Spot" with higher field strength values and Figure 172 shows the histogram of a cube (*Sim_{MIX}*) which was placed in an area with both, higher and lower field strength values. Comparing the amplitude distribution of the three cubes, it can be seen that Figure 170 shows amplitude values focused on higher field strength values, while Figure 171 shows a amplitude distribution which is focused on low field strength values. Figure 172 is a combination of both which can easily be seen in the amplitude distribution which is focused in a region with lower field strength values and a region with higher field strength values.



Figure 169: Schematic of the three cubes on specific locations within the simulated volume. Cube Sim_{CONST} is located in a region with field strength values in nearly the same range, Cube Sim_{HS} is located in a region with lower field strength values and a small region with higher field strength values ("Hot Spot") and cube Sim_{MIX} is located in a region with both, higher and lower field strength values.

For those three cubes the cumulative distribution functions were evaluated, too. The cumulative distribution function (cdf) can be derived as described in Section 3.2.2. Figure 173 shows the cumulative distribution function of the cube (Sim_{CONST}) in an area of higher field strength values, Figure 174 shows the cumulative distribution function of the cube (Sim_{HS}) in an area of lower field strength values with a small region with higher field strength values and Figure 175 shows the cumulative distribution function of the cube (Sim_{MIX}) in an area with both, higher and lower field strength values.

The percentiles can be derived from the cumulative distribution functions of each cube. Table 53 shows the percentiles of all three cubes. Due to the approximation process, the approximated cdf can have values higher than 1 which can be seen in Figure 173, Figure 174 and Figure 175. By differentiating the cumulative distribution function the probability density function can be derived. The probability density functions of the three cubes are displayed in Figure 176 for the cube (Sim_{CONST}) placed in an area with field strength values in nearly the same range, Figure 177 for the cube (Sim_{HS}) placed in an area with lower field strength values and an area with higher field strength values and Figure 178 for the cube (Sim_{MIX}) placed in an area with both, higher and lower field strength values. A probable approximation for the first probability density function might be a Normal distribution, for the second probability density function the LogNormal distribution might

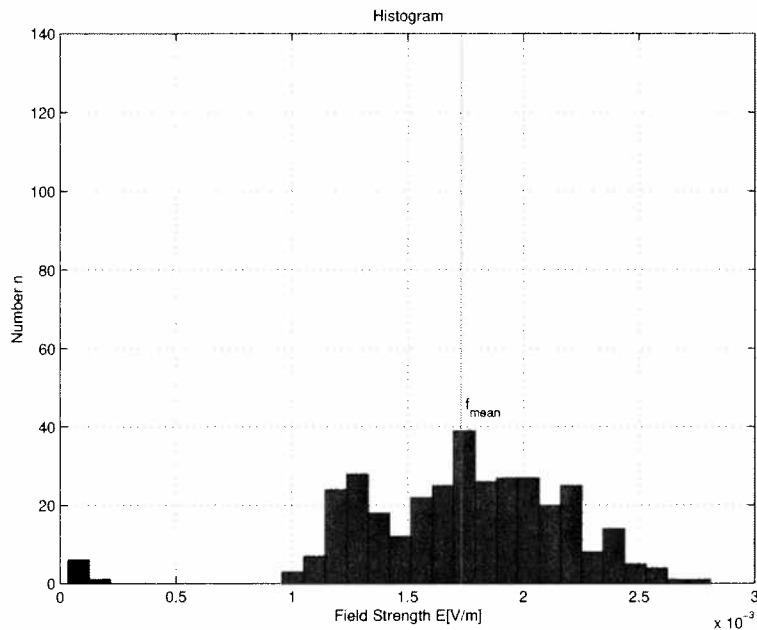


Figure 170: Global distribution of the electromagnetic field strength values of a cube located in an area with electromagnetic field strength values in nearly the same range disposed in 30 amplitude grades. Simulation of the Mobilkom Austria office building Room A07A011 at a frequency of 946MHz - *SimCONST*.

be a good approximation and for the last probability density function no distribution function could be found which would fit.

After the global consideration also the local behavior of the three cubes was investigated. Figure 179 shows the local distribution of the electromagnetic field strength for each of the seven levels of a cube placed in an area with field strength values in nearly the same range (*SimCONST*). It can be seen, that no specific areas with a minima of the field strength occurs.

Figure 180 shows the local distribution of the electromagnetic field strength for each of the seven levels of the cube placed in an area with lower field strength values and a region with higher field strength values. With only one exception in Level z180 ("Hot Spot"), the field strength values are very low in each level. It can be stated, that the field strength values in the whole cube are very low and therefore this cube seems to be a good model for a cube with low field strength values.

Figure 181 shows the local distribution of the electromagnetic field strength for each of the seven levels of the cube placed in an area with higher and lower field strength values. It can be seen, that the cube is placed in an area where a strong propagation path with high field strength values is on the border to an area where the propagation path is strongly attenuated. According to the diagonal, one side consists of higher field strength values and the other side consists of lower field strength values. This phenomena can be seen in each of the seven levels.

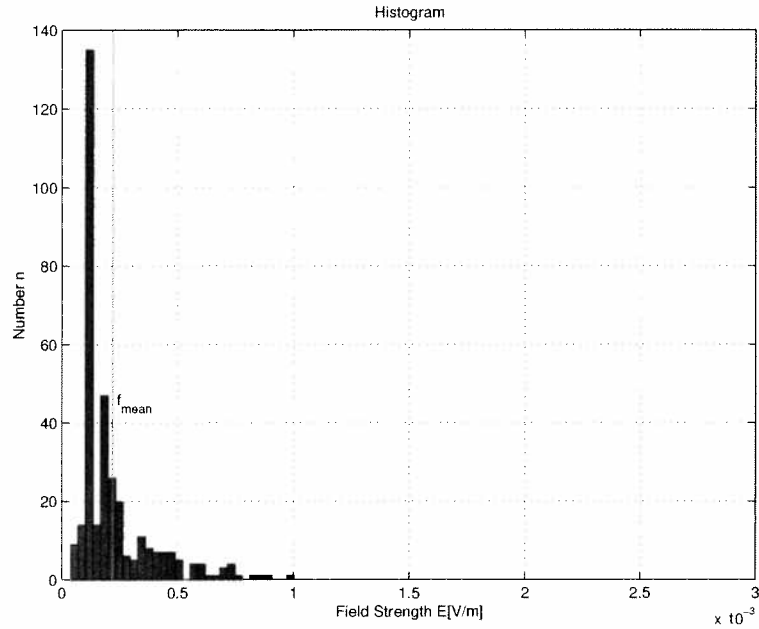


Figure 171: Global distribution of the electromagnetic field strength values of a cube located in an area with lower electromagnetic field strength values and an area with higher field strength values disposed in 30 amplitude grades. Simulation of the Mobilkom Austria office building Room A07A011 at a frequency of 946MHz - Sim_{HS} .

	E_{max}	$\frac{E_{10\%}}{E_{max}}$	$\frac{E_{25\%}}{E_{max}}$	$\frac{E_{50\%}}{E_{max}}$	$\frac{E_{75\%}}{E_{max}}$	$\frac{E_{90\%}}{E_{max}}$
	$[\frac{mV}{m}]$	%	%	%	%	%
Sim MB	2.8	42.9	53.6	60.7	71.4	82.1
Sim nMB	1.0	10	11.3	16.4	24.0	52.6
Sim MIX	2.8	1.3	3.3	8.0	63.7	79.3

Table 53: Lower and higher quartile, lower and higher decile, quintile normalized to the maximum electromagnetic field strength of each investigated cube. MB stands for main beam and this is the cube positioned in an area with high field strength values, nMB stands for not main beam and this is the cube positioned in an area with low field strength values and MIX means the cube positioned in an area with both, high and low field strength values. (Simulation of the Mobilkom Austria Room A07A011 at GSM 900).

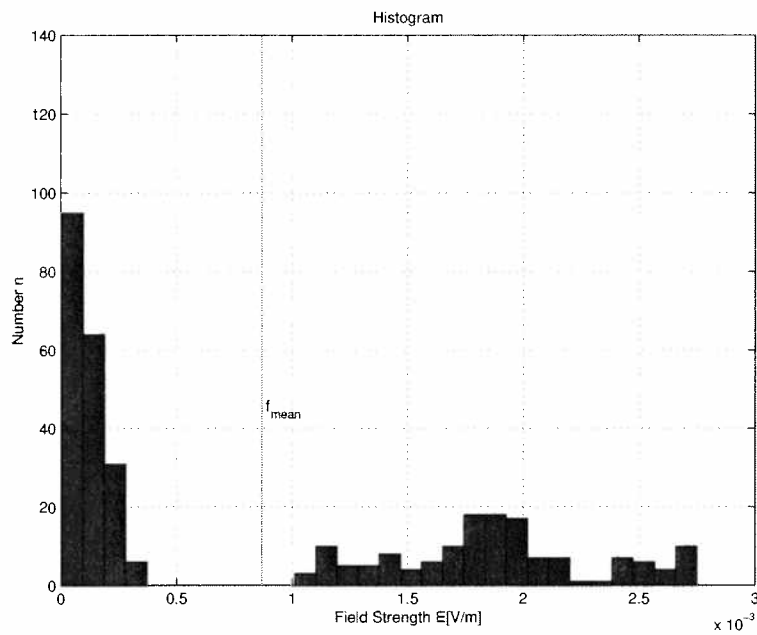


Figure 172: Global distribution of the electromagnetic field strength values of a cube located in an area with both, higher and lower electromagnetic field strength values disposed in 30 amplitude grades. Simulation of the Mobilkom Austria office building Room A07A011 at a frequency of 946MHz - Sim_{MIX} .

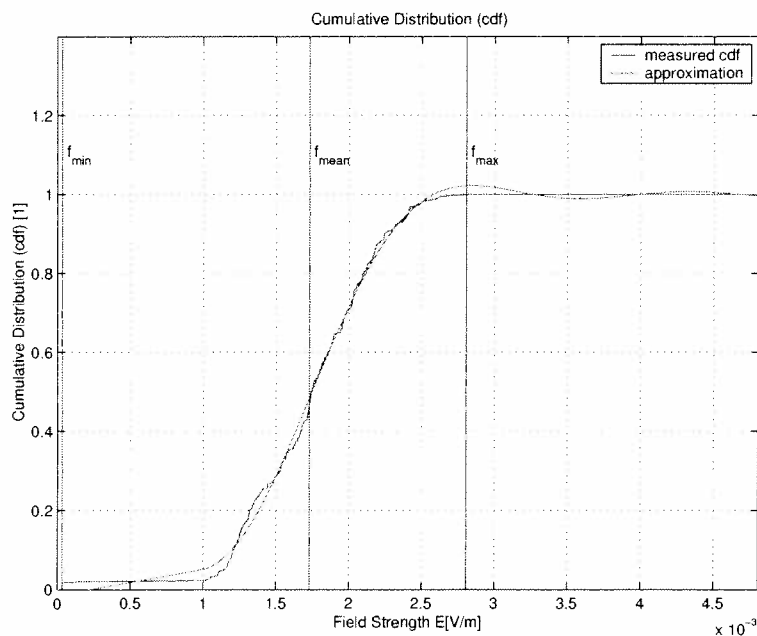


Figure 173: Cumulative distribution function (cdf) of the global field distribution of the cube (Sim_{CONST}) which was placed in an area with higher field strength values (GSM 900 - Simulation of Room A07A011 Mobilkom Austria).

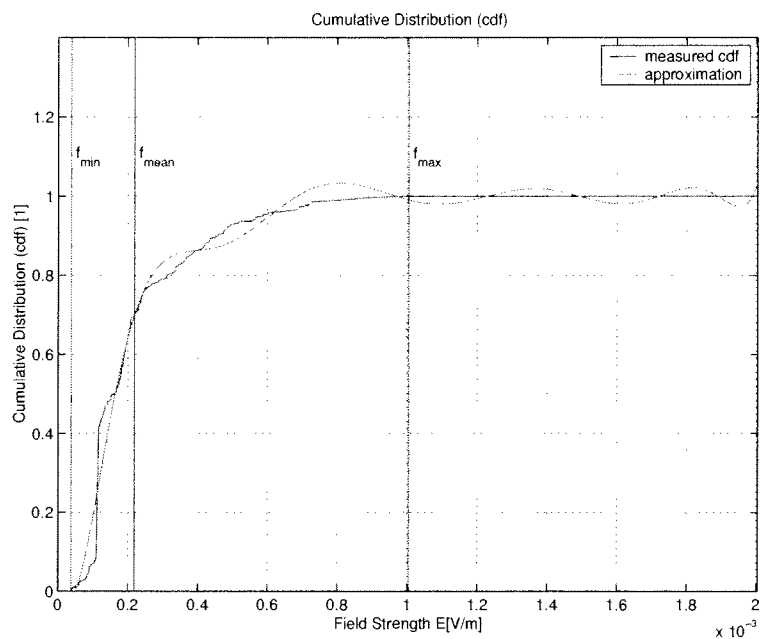


Figure 174: Cumulative distribution function (cdf) of the global field distribution of the cube (Sim_{HS}) which was placed in an area with lower field strength values (GSM 900 - Simulation of Room A07A011 Mobilkom Austria).

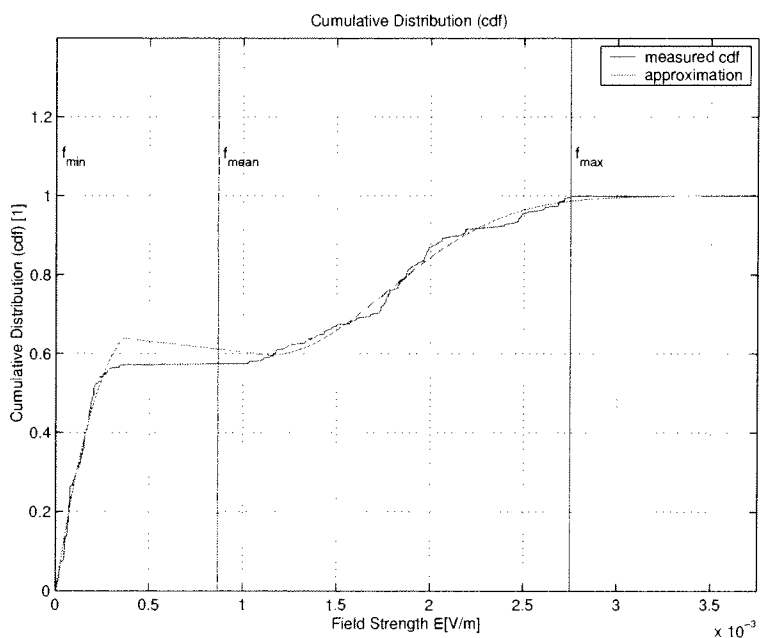


Figure 175: Cumulative distribution function (cdf) of the global field distribution of the cube (Sim_{MLX}) which was placed in an area with both, high and low field strength values (GSM 900 - Simulation of Room A07A011 Mobilkom Austria).

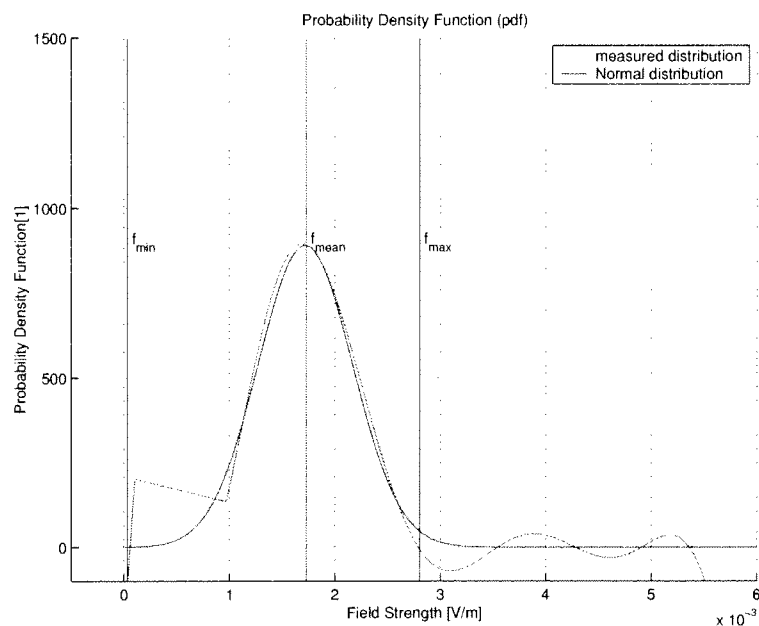


Figure 176: Probability density function (pdf) of the cube which was placed in an area with field strength values in nearly the same range (Sim_{CONST}) and a possible approximation with a Normal distribution (GSM 900 - Simulation of Room A07A011 Mobilkom Austria).

Comparing the evaluated data it might seem that scenarios like the cube which was located in an area with field strength values in nearly the same range (Sim_{CONST}) has a ratio between the maximum field strength and the global mean value of little less than 2.0 with a percentile $E_{10\%}$ normalized to the maximum field strength starting at an higher value (e.g. around 40%). The percentile $E_{90\%}$ normalized to the maximum has also higher values around 80%. An other behavior can be observed at the scenario with a cube located in an area with lower field strength values and a small region with higher field strength values - Sim_{HS} . The ratio between the maximum field strength and the global mean value is around 4.0 or more, whereas the lower percentile normalized to the maximum has an value of around 10%. The percentile $E_{90\%}$ normalized to the maximum has a lower value of around 50%. Comparing the behavior of Sim_{CONST} and Sim_{HS} shows therefore a significant difference.

The measured scenarios can now be compared to the simulation and it can be evaluated if those behavior can also be observed in different scenarios which were measured in the different measurement campaigns. Also the cubes on different locations in the simulated volume (SIM 1, SIM 2, SIM 3, SIM 4, SIM 5 and SIM 6) can be compared to this behavior which might confirm the observations.

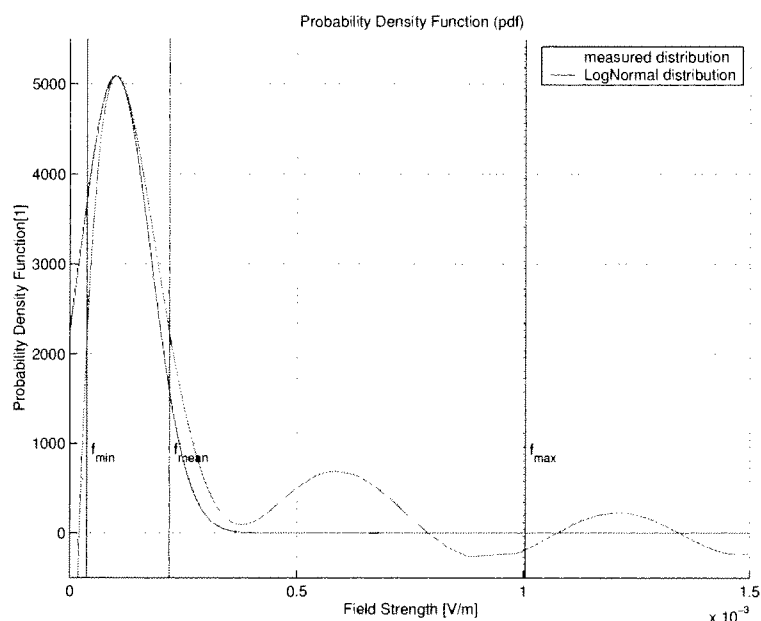


Figure 177: Probability density function (pdf) of the cube which was placed in an area with lower field strength values (Sim_{HS}) and a possible approximation with a LogNormal distribution (GSM 900 - Simulation of Room A07A011 Mobilkom Austria).

6.2 Comparison of Simulations and Measurements

The cube of SIM 1 (see Figure 163) and the cube of SIM 5 (see Figure 167) are showing field strength values in the same range in most levels, thus would be comparable to case 1: a cube located in an area with field strength values in nearly the same range. A measured cube with the same behavior could be the cube measured in UHF frequency band as well as the small cube measured in this frequency band. Therefore the ratio between the maximum field strength and the global mean value as well as the ratio between the percentiles and the maximum field strength value are compared to each other. Table 54 shows the results. It can be observed that the ratio between the maximum field strength value and the global mean value is in the range of 1.7 up to 1.8. The percentiles normalized to the maximum are in the range of 21.9% up to 82.1%

Comparing cubes located in areas with lower field strength values and a small region with higher field strength values is the next step. The cube of SIM 2 (see Figure 164) might fit this description. A measured cube with the same characteristics could be the cube measured in the GSM 900 frequency band (see Figure 25) but also the small cube, measured at GSM 900, would fit this model (see Figure 61. Both cubes, the cube and the small cube of the DCS 1800 frequency band could also be characterized in this context by comparing Figure 33 and Figure 68 with the evaluated cube Sim_{HS} . Therefore the ratio between the maximum field strength

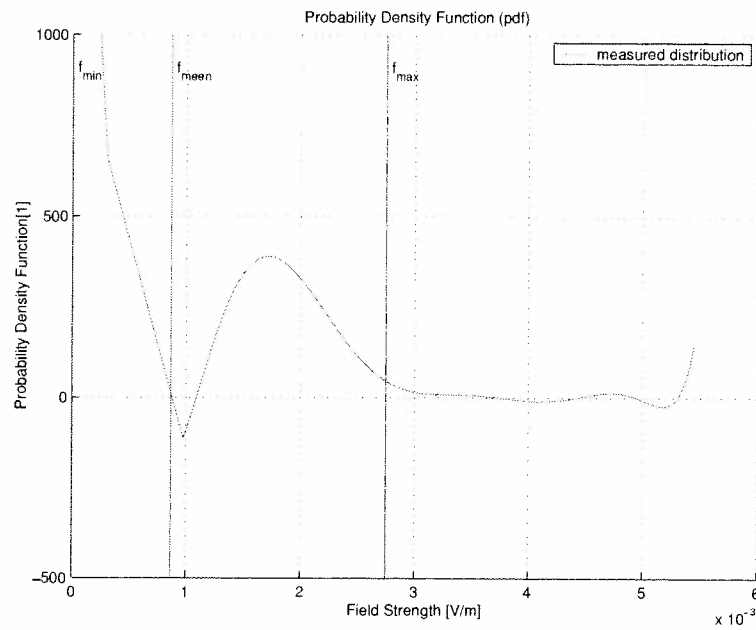


Figure 178: Probability density function (pdf) of the cube which was placed in an area with both, high and low field strength values (Sim_{MIX}). No function could be found to fit this probability density function (GSM 900 - Simulation of Room A07A011 Mobilkom Austria).

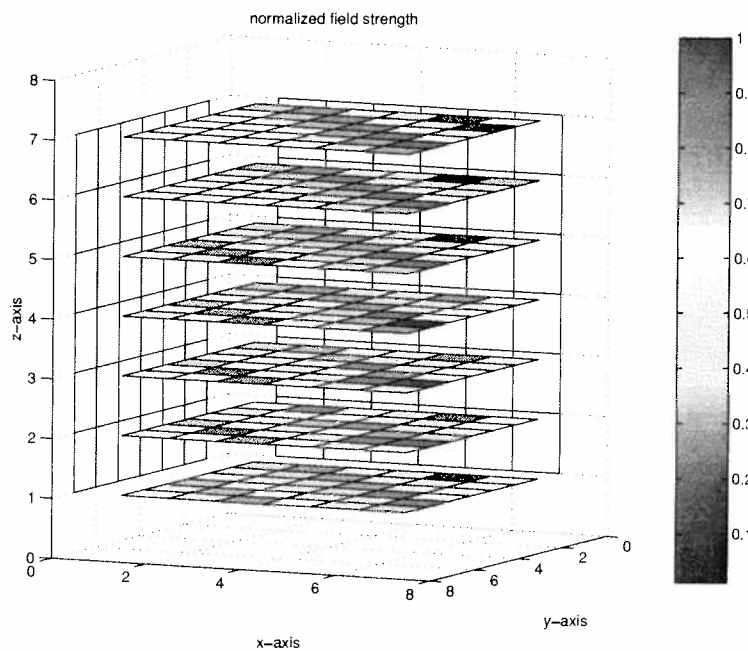


Figure 179: Distribution of the field strength values normalized to the maximum value for a cube placed in an area with field strength values in nearly the same range - Sim_{CONST} (GSM 900 - Simulation of Room A07A011 Mobilkom Austria).

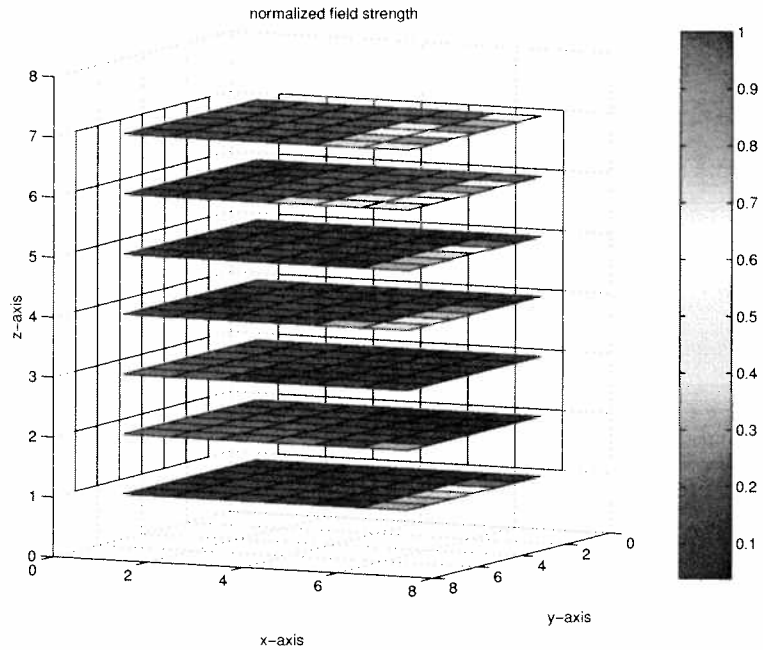


Figure 180: Distribution of the field strength values normalized to the maximum value for a cube placed in an area with lower field strength values and a region with higher field strength values - Sim_{HS} (GSM 900 - Simulation of Room A07A011 Mobilkom Austria).

	$\frac{E_{max}}{E_{mean}}$	$\frac{E_{10\%}}{E_{max}}$	$\frac{E_{25\%}}{E_{max}}$	$\frac{E_{50\%}}{E_{max}}$	$\frac{E_{75\%}}{E_{max}}$	$\frac{E_{90\%}}{E_{max}}$
	$\left[\frac{mV}{m}\right]$	%	%	%	%	%
Sim_{CONST}	1.7	42.9	53.6	60.7	71.4	82.1
Sim 1	1.8	34.1	45.5	59.1	68.2	77.3
Sim 5	1.7	21.9	50.0	59.4	71.9	81.3

Table 54: Comparison of the ratio between the maximum field strength and the mean field strength value and the percentiles normalized to the maximum field strength value of the simulation data and the measurement data. Only cubes with high field strength values in nearly every level were compared to each other. The table shows, that the values are approximately in the same range.

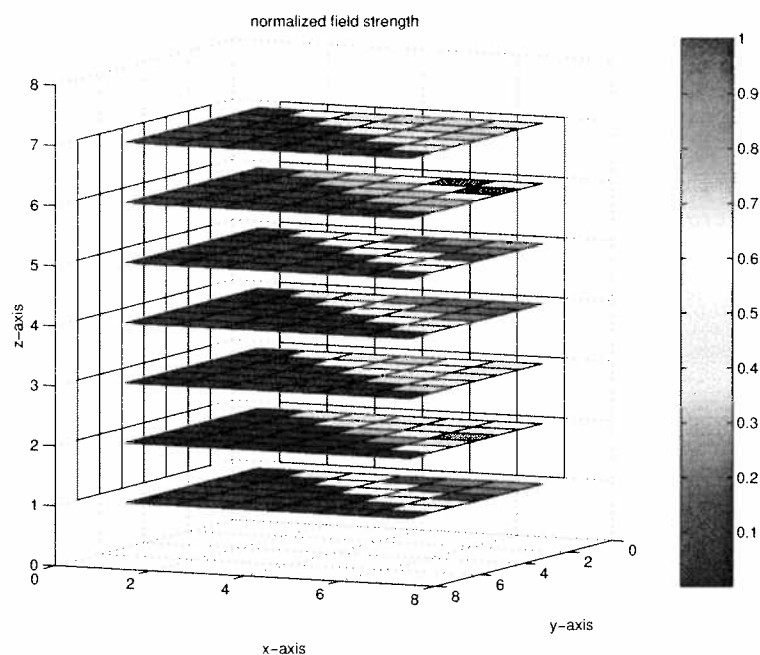


Figure 181: Distribution of the field strength values normalized to the maximum value for a cube placed in an area with both, higher and lower field strength values - *Sim_{MIX}* (GSM 900 - Simulation of Room A07A011 Mobilkom Austria).

and the global mean value as well as the ratio between the percentiles and the maximum field strength value are compared to each other. Table 55 shows the results. As Table 55 shows, the maximum field strength normalized to the global mean value is in the range of 2.3 up to 4.9. Compared to the values of cubes located in areas with nearly constant field strength values in the whole volume the values of the maximum field strength values normalized to the global mean value is concentrated at higher values between 3.0 and 4.0, with a few exceptions. The percentiles are in the range of 7.0% up to 64.0%. Compared to the values shown in the previous table, Table 55, the percentiles are located at lower ranges.

After all those comparisons it might seem, that cubes which are located in areas with field strength values in nearly the same range distributed over all levels, have less deviation between the maximum value and the global mean value and the percentiles are reaching higher values, whereas cubes which are located in areas with lower field strength values with a region of higher field strength values seem to have higher deviations between the maximum value and the global mean value of the field strength and the percentiles are in a lower range and do not reach higher values of the 90% percentiles.

The rest of the measurements could be characterized as cubes with mixed field strength values because regions with higher field strength values occur more or less as often as regions with lower field strength values. The range of the ratio between

	$\frac{E_{max}}{E_{mean}}$	$\frac{E_{10\%}}{E_{max}}$	$\frac{E_{25\%}}{E_{max}}$	$\frac{E_{50\%}}{E_{max}}$	$\frac{E_{75\%}}{E_{max}}$	$\frac{E_{90\%}}{E_{max}}$
	$[\frac{mV}{m}]$	%	%	%	%	%
<i>Sim_{HS}</i>	4.6	10.0	11.3	16.4	24.0	52.6
Sim 2	3.5	12.1	18.2	24.2	33.3	39.4
Mobilkom Austria						
GSM 900	3.2	17.5	22.3	28.5	37.2	49.4
GSM 900 small cube	2.3	27.8	34.0	42.1	50.3	57.2
DCS 1800	4.9	7.2	14.6	18.8	24.2	31.9
DCS 1800 small cube	2.3	26.6	32.8	41.9	53.6	64.4

Table 55: Comparison of the ratio between the maximum field strength and the mean field strength value and the percentiles normalized to the maximum field strength value of the simulation data and the measurement data. Only cubes with low field strength values in nearly every level were compared to each other. The table shows, that the values are approximately in the same range.

the maximum value and the global mean value of the field strength lies between the range of the cubes which are located in areas with field strength values in nearly the same range and cubes located in areas with lower field strength values and a small region with higher field strength values. But there is no sharp border between those three categories, rough values of each category also appear in the other category, this might only be an idea of categorizing different regions within the simulated area and therefore within a room but doesn't represent any kind of strict behavior.

Table 56 shows the rest of the evaluated data which could be characterized as cubes with higher and lower field strength values. It can easily be seen, that the ratios of the maximum field strength values and the global mean values as well as the percentiles normalized to the maximum field strength values vary in a wider range than the ratios in Table 54 and Table 55.

6.3 Additional Evaluations of Cubes within the Simulated Area

To proof some conclusions right or wrong, additional cubes with more specific locations within the simulated volume were examined. Therefore five more cubes were located around the cube of SIM 1 which is equal to the area which was under investigation at the Mobilkom Austria office building. Those cubes were chosen to investigate the variance of the evaluated data (ratio between maximum and global mean value of the field strength and the percentiles normalized to the maximum field strength value) when a cube was positioned in a different location but near to another one. The area of interest was of course the area where the measurements

	$\frac{E_{max}}{E_{mean}}$	$\frac{E_{10\%}}{E_{max}}$	$\frac{E_{25\%}}{E_{max}}$	$\frac{E_{50\%}}{E_{max}}$	$\frac{E_{75\%}}{E_{max}}$	$\frac{E_{90\%}}{E_{max}}$
	$[\frac{mV}{m}]$	%	%	%	%	%
<i>Sim_{MIX}</i>	3.2	1.3	3.3	8.0	63.7	79.3
Sim 3	2.64	12.0	20.1	32.1	48.0	72.0
Sim 4	2.1	22.2	44.4	44.5	66.7	66.8
Sim 6	2.7	6.3	18.8	31.3	56.3	75.0
Mobilkom Austria						
VHF	3.1	47.3	54.1	60.5	66.4	73.3
ARCS TOX 7						
GSM 900	2.0	32.6	39.1	47.8	58.7	67.4

Table 56: Comparison of the ratio between the maximum field strength and the mean field strength value and the percentiles normalized to the maximum field strength value of the simulation data and the measurement data. Cubes with high and low field strength values were compared to each other. The table shows, that the values are approximately in the same range but vary more then the ratios of cubes located in areas with higher field strength values and cubes located in area with lower field strength values.

were performed. Around the location of SIM 1 some additional cubes were evaluated where a specific behavior would be expected, as shown in Figure 182. In Table 57 the locations of these cubes can be found.

The global behavior was taken under consideration first, therefore the distribution of the field strength disposed in 30 amplitude grades of the five additional cubes were evaluated. Figure 183 and Figure 187 are showing a distribution similar to distributions of the measured cubes in the GSM 900 frequency band, whereas Figure 184, Figure 185 and Figure 186 are showing a different distribution with field strength values concentrated in a lower range and in a higher range. The maximum, minimum and global mean value of the electromagnetic field strength of each cube can be found in Table 58.

The cumulative function can be derived by arranging the field strength by increasing values, as described in Section 3.2.2. It can be seen in Figure 189, Figure 190 and Figure 191 that each diagram has a flat rise in the middle which is caused by the leak of field strength values in this particular range. The percentiles of each cube are shown in Table 59. The percentiles normalized to the global mean value of each cube are shown in Table 60. SIM 7 and SIM 10 are showing a very similar behavior as well as SIM 8 and SIM 9.

The probability density function (pdf) can be derived by differentiating the cu-

Cube	Location
Sim 7	(35/20)
Sim 8	(35/34)
Sim 9	(28/27)
Sim 10	(21/23)
Sim 11	(38/27)

Table 57: Positions within the simulated area of the additional cubes which were located near the position of the cube which was measured at the Mobilkom Austria office building. The numbers in brackets show the coordinates in direction of the x-axis and y-axis. The first level in direction of the z-axis was z90, which is 90cm above the floor.

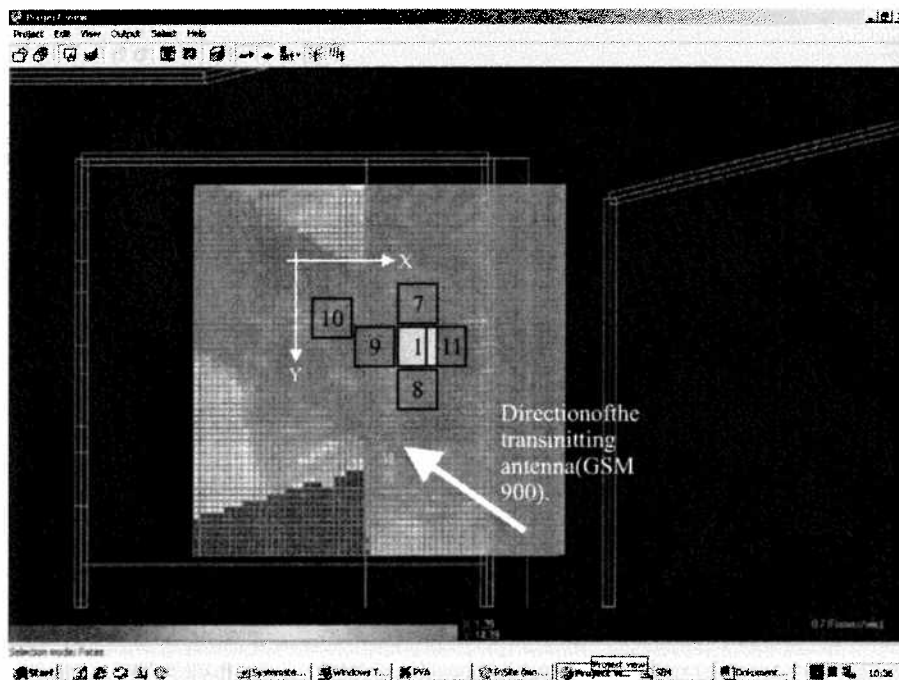


Figure 182: Schematic of the cubes located approximately at the same positions as the investigated area at the Mobilkom Austria office building.

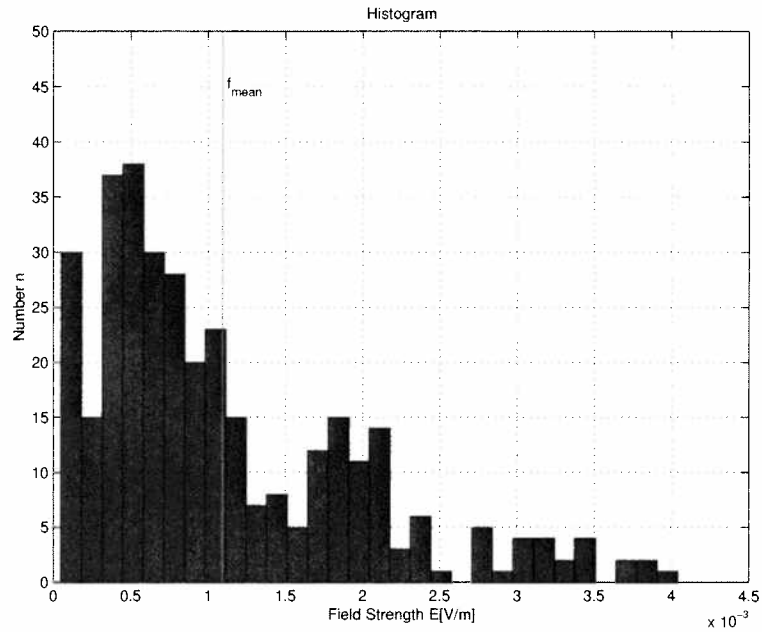


Figure 183: Global distribution of the electromagnetic field strength values disposed in 30 amplitude grades. Simulation of a cube (SIM 7) at a frequency of 946MHz.

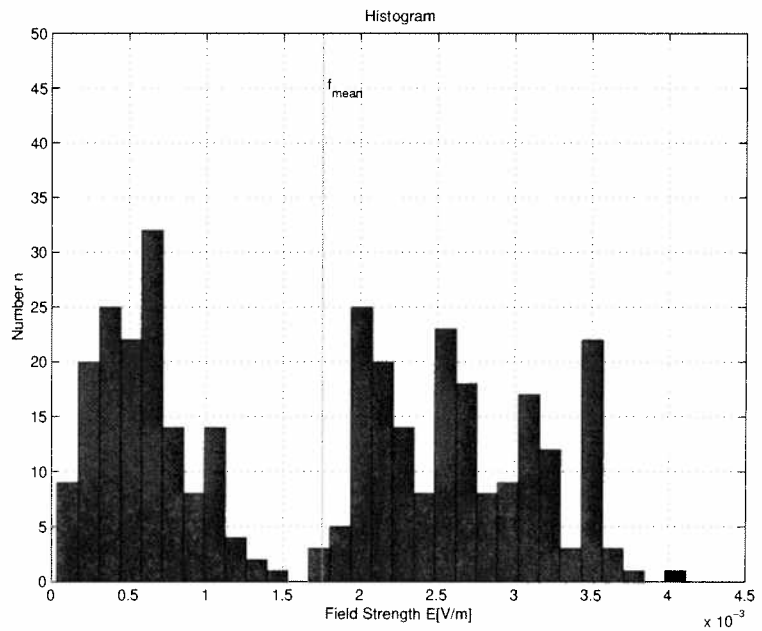


Figure 184: Global distribution of the electromagnetic field strength values disposed in 30 amplitude grades. Simulation of a cube (SIM 8) at a frequency of 946MHz.

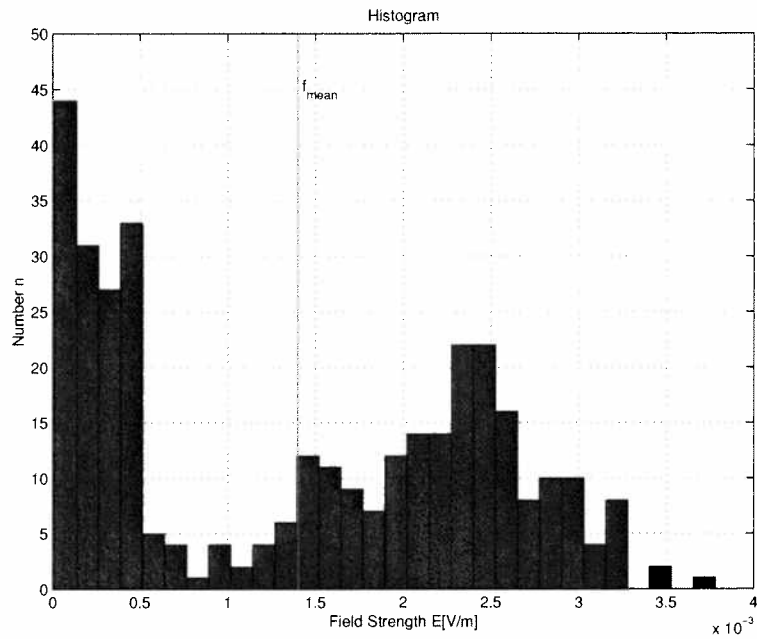


Figure 185: Global distribution of the electromagnetic field strength values disposed in 30 amplitude grades. Simulation of a cube (SIM 9) at a frequency of 946MHz.

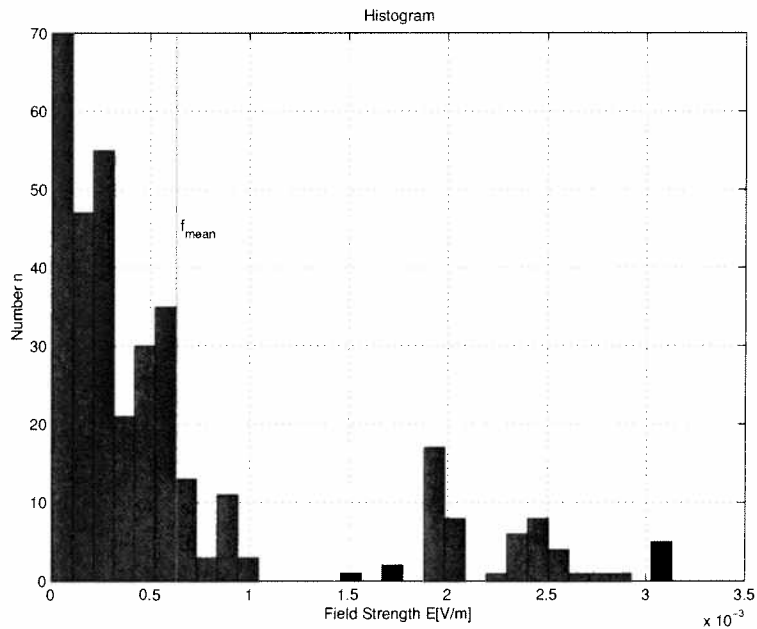


Figure 186: Global distribution of the electromagnetic field strength values disposed in 30 amplitude grades. Simulation of a cube (SIM 10) at a frequency of 946MHz.

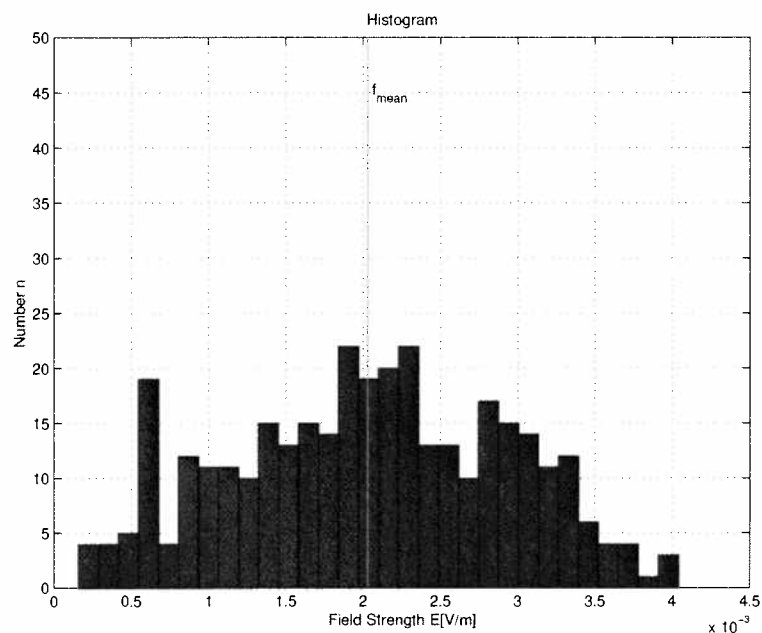


Figure 187: Global distribution of the electromagnetic field strength values disposed in 30 amplitude grades. Simulation of a cube (SIM 11) at a frequency of 946MHz.

	Exam. Pos.	Max.	Min.	Mean	Std. Dev.
		[mV/m]	[mV/m]	[mV/m]	[mV/m]
Sim 7	343	4.0	0.05	1.1	0.9
Sim 8	343	4.1	0.04	1.8	1.1
Sim 9	343	3.8	0.03	1.4	1.1
Sim 10	343	3.1	0.02	0.6	0.8
Sim 11	343	4.0	0.16	2.0	0.9

Table 58: Mean value, minimum and maximum value and standard deviation - GSM 900, simulation of the Mobilkom Austria Room A07A011. Additional 5 cubes were calculated from the simulated area.

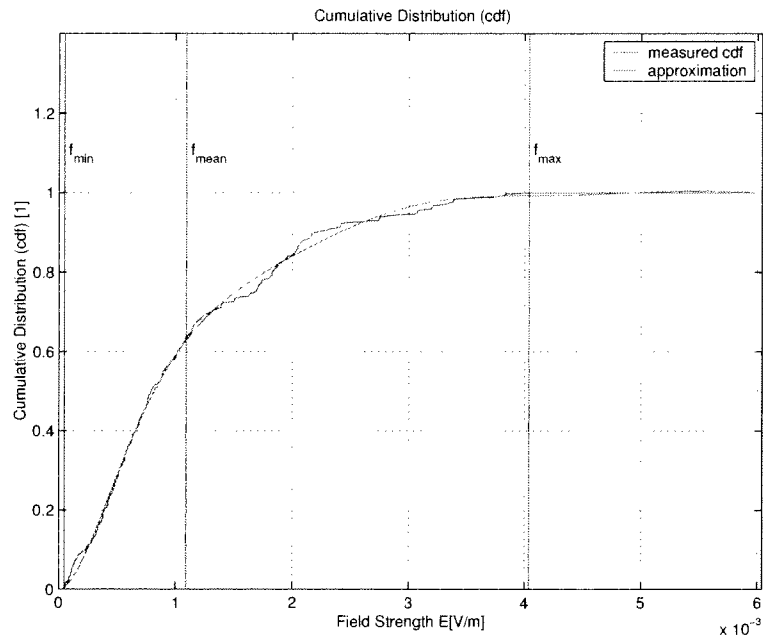


Figure 188: Cumulative distribution function (cdf) of the global field distribution of SIM 7 (GSM 900 - Simulation of Room A07A011 Mobilkom Austria).

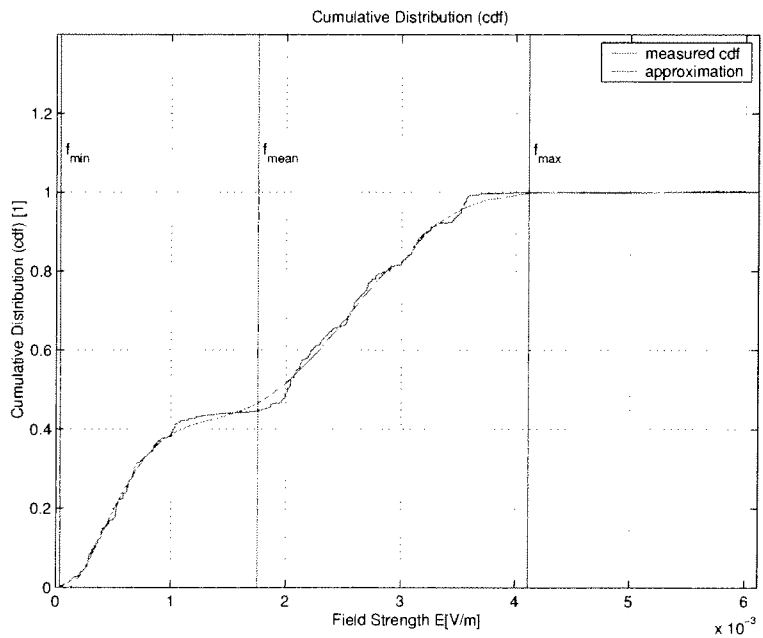


Figure 189: Cumulative distribution function (cdf) of the global field distribution of SIM 8 (GSM 900 - Simulation of Room A07A011 Mobilkom Austria).

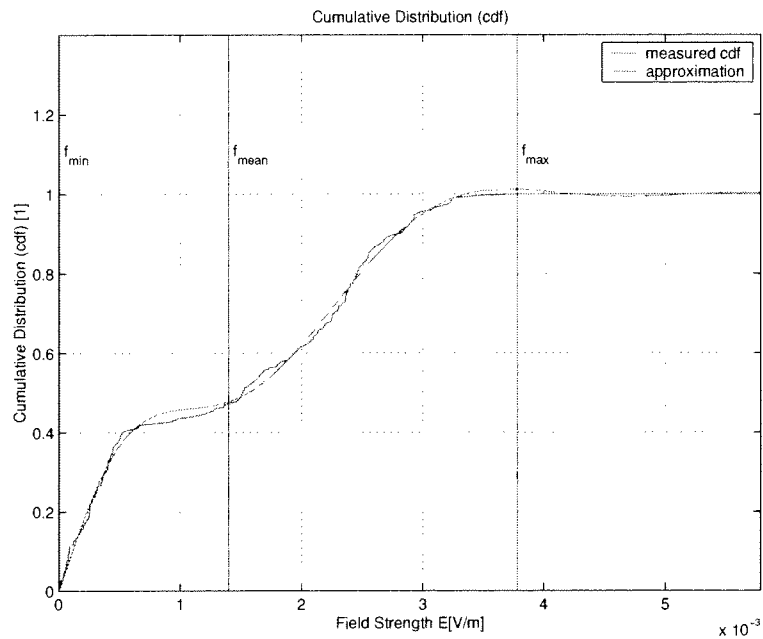


Figure 190: Cumulative distribution function (cdf) of the global field distribution of SIM 9 (GSM 900 - Simulation of Room A07A011 Mobilkom Austria).

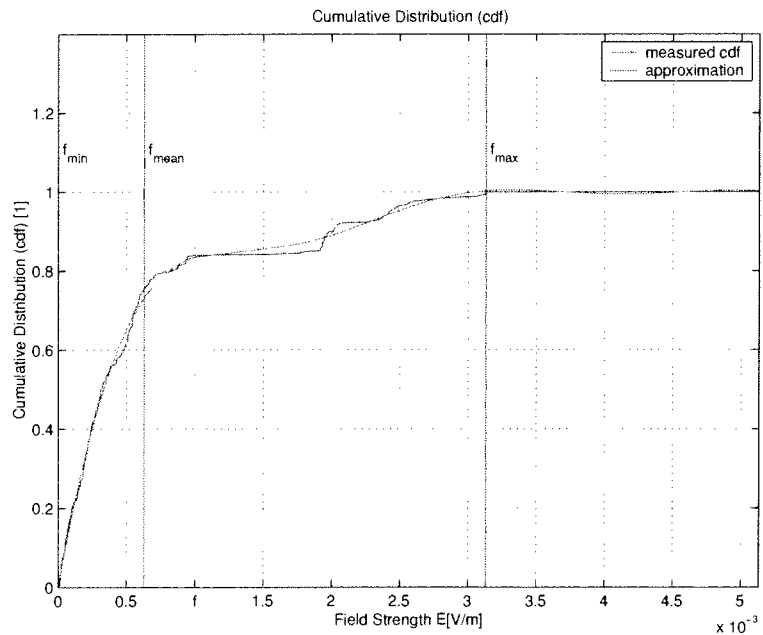


Figure 191: Cumulative distribution function (cdf) of the global field distribution of SIM 10 (GSM 900 - Simulation of Room A07A011 Mobilkom Austria).

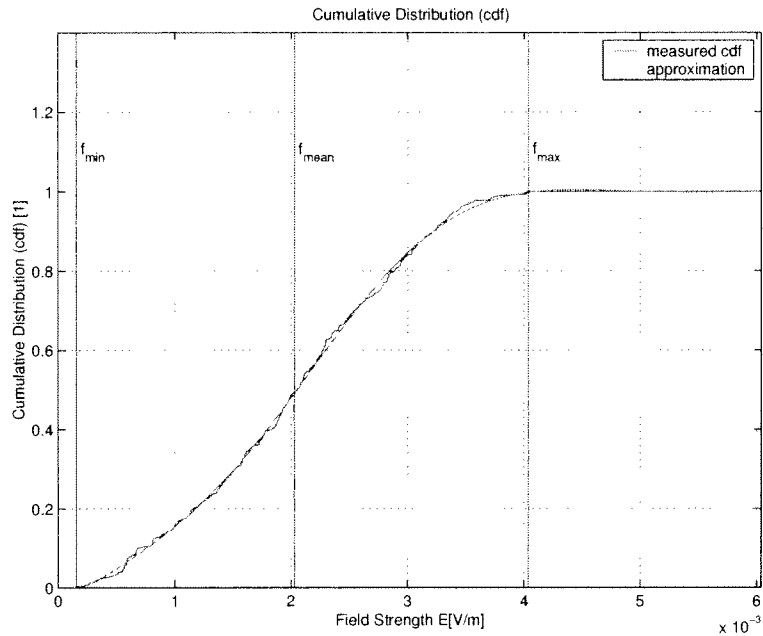


Figure 192: Cumulative distribution function (cdf) of the global field distribution of SIM 11 (GSM 900 - Simulation of Room A07A011 Mobilkom Austria).

	$E_{10\%}$	$E_{25\%}$	$E_{50\%}$	$E_{75\%}$	$E_{90\%}$
	$[\frac{mV}{m}]$	$[\frac{mV}{m}]$	$[\frac{mV}{m}]$	$[\frac{mV}{m}]$	$[\frac{mV}{m}]$
Sim 7	0.2	0.5	0.8	1.5	2.4
Sim 8	0.3	0.6	1.9	2.7	3.2
Sim 9	0.1	0.3	1.5	2.4	2.8
Sim 10	0.1	0.1	0.3	0.7	2.1
Sim 11	0.7	1.4	2.0	2.7	3.2

Table 59: Lower and higher quartile, lower and higher decile, quintile of each of the five cubes (Simulation of the Mobilkom Austria Room A07A011 at GSM 900).

	E_{max}	$\frac{E_{10\%}}{E_{max}}$	$\frac{E_{25\%}}{E_{max}}$	$\frac{E_{50\%}}{E_{max}}$	$\frac{E_{75\%}}{E_{max}}$	$\frac{E_{90\%}}{E_{max}}$
	$[\frac{mV}{m}]$	%	%	%	%	%
Sim 7	4.0	5.0	12.5	20.0	37.5	60.0
Sim 8	4.1	7.3	14.6	46.3	65.9	78.1
Sim 9	3.8	2.6	7.9	39.5	63.2	73.7
Sim 10	3.1	3.2	3.3	9.7	22.6	67.7
Sim 11	4.0	17.5	35.0	50.0	67.5	80.0

Table 60: Lower and higher quartile, lower and higher decile, quintile normalized to the maximum electromagnetic field strength of each investigated area. For each cube the maximum value is also listed. (Simulation of the Mobilkom Austria Room A07A011 at GSM 900).

mulative distribution function. Figure 193 shows the probability density function of SIM 7. A possible approximation for this function might be a Rayleigh distribution. The Rayleigh distribution can be derived by Equation 17. Figure 197 shows the probability density function of SIM 11. A possible approximation for this function might be a Normal distribution. The Normal distribution can be derived by Equation 18. For all other probability density functions no functions were found which could be fitted to the measured one.

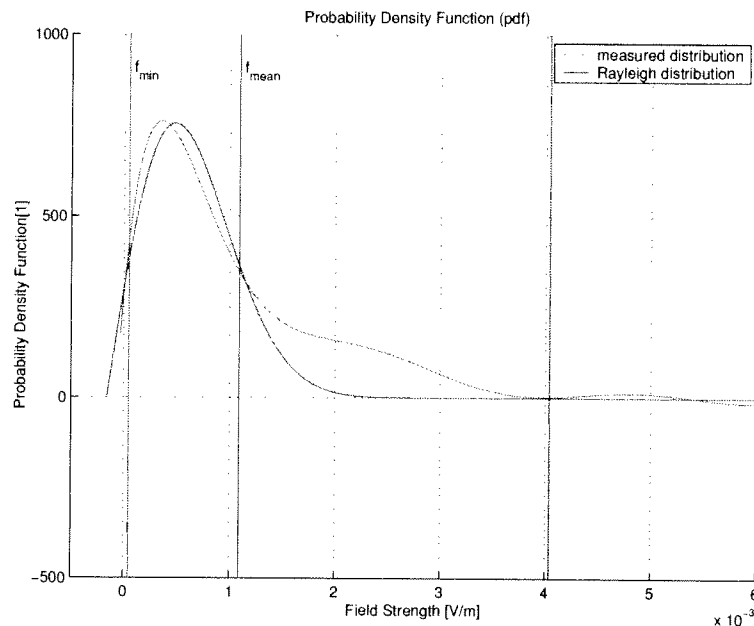


Figure 193: Probability Density function (pdf) of SIM 7 and a possible approximation with a Rayleigh distribution (GSM 900 - Simulation of Room A07A011 Mobilkom Austria).

After the global considerations, the local behavior of the electromagnetic field strength values was investigated. Therefore the local field strength values, normalized to the global mean value of the cube, were displayed for each level.

Figure 198 shows the local distribution of the electromagnetic field strength for each of the seven levels of the cube SIM 7. This figure shows higher field strength values concentrated in one corner of all seven levels. This cube was placed on the top side of the cube of SIM 1, which is approximately equal to the location of the measured cube. On the first sight it could be suggested that this cube should have an equal behavior than the cube of SIM 1 but it is completely different. This led to a very important conclusion: the location of such a cube within a room plays a very important role because the whole environment can change tremendously within a small region.

The cube placed on the bottom side of the cube of SIM 1 shows a similar behavior than the cube of SIM 7 (see Figure 199). As Figure 199 shows, higher field strength values occur on one half of the cube. Regarding the three local field distributions (Figure 163, Figure 198 and Figure 199) it can be seen that there is a path of higher field strength values in the anteroom of the conference room in the direction of the main beam of the transmitting antenna. The same behavior can be observed by viewing Figure 200 and Figure 201. All those cubes located around the cube of SIM 1, which is similar to the area which was under investigation at the Mobilkom Austria office building, are showing this behavior and it can be stated,

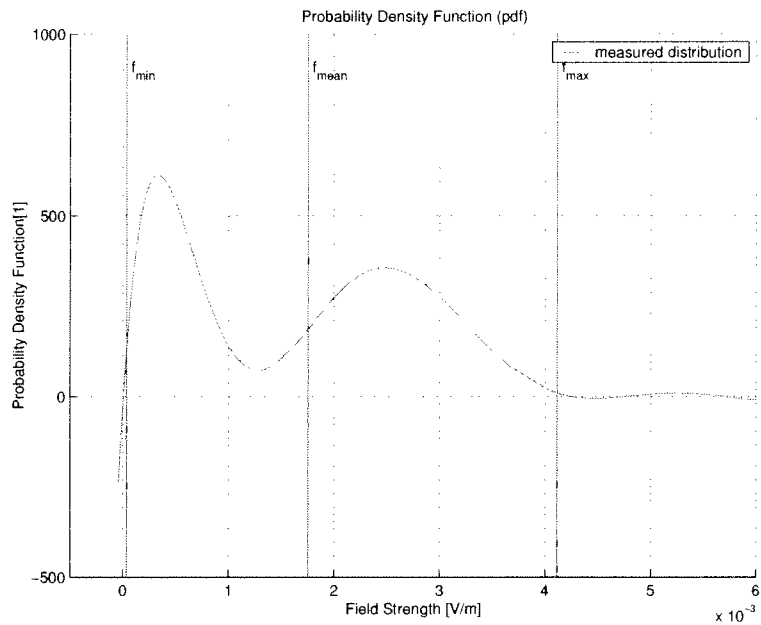


Figure 194: Probability Density function (pdf) of SIM 8. No approximated function was found fitting this one (GSM 900 - Simulation of Room A07A011 Mobilkom Austria).

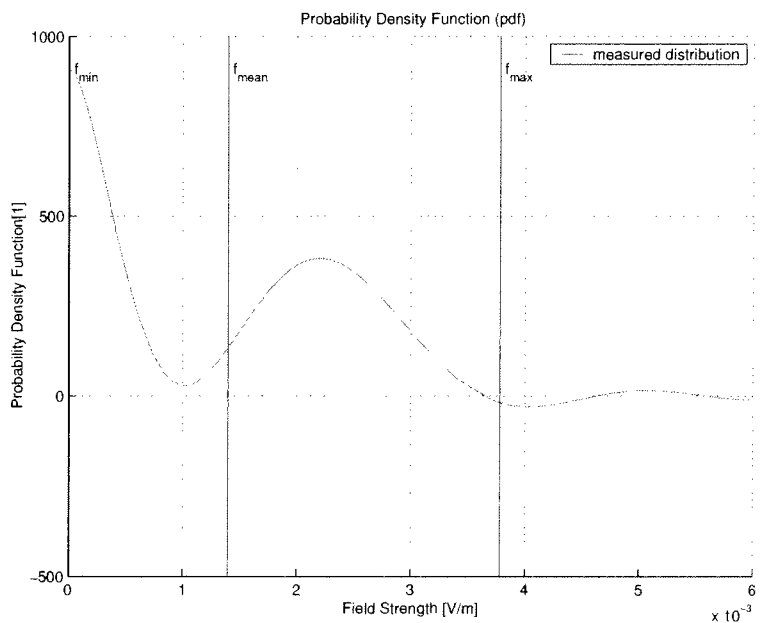


Figure 195: Probability Density function (pdf) of SIM 9. No approximated function was found fitting this one (GSM 900 - Simulation of Room A07A011 Mobilkom Austria).

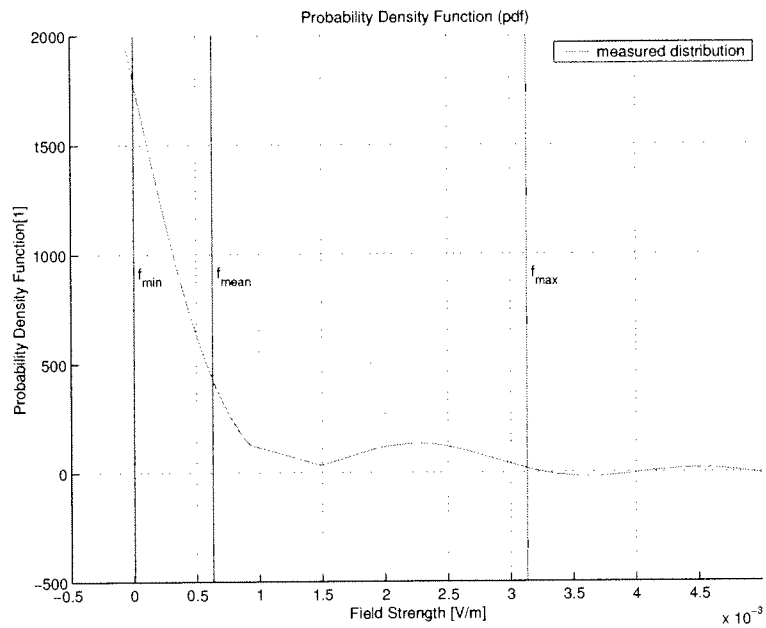


Figure 196: Probability Density function (pdf) of SIM 10. No approximated function was found fitting this one (GSM 900 - Simulation of Room A07A011 Mobilkom Austria).

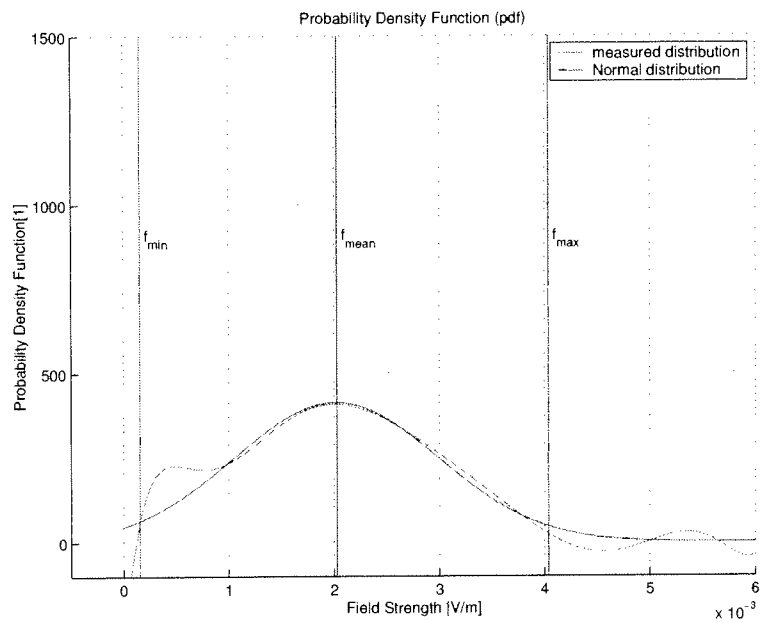


Figure 197: Probability Density function (pdf) of SIM 11 and a possible approximation with a Normal distribution (GSM 900 - Simulation of Room A07A011 Mobilkom Austria).

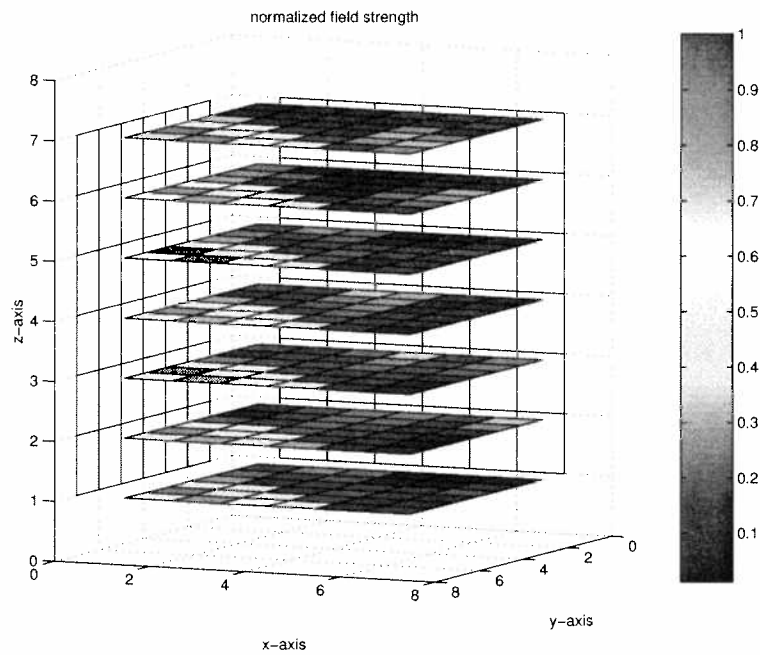


Figure 198: Distribution of the field strength values normalized to the maximum value for SIM 7 (GSM 900 - Simulation of Room A07A011 Mobilkom Austria).

that the location of the area which should be evaluated plays a very important role.

A good example for the former statement is the local distribution of the field strength values evaluated in SIM 11, where the location of the cube was only changed a bit in direction of the x-axis. Half of this cube covers the region of SIM 1 and the rest is located nearer to the windows. It can be observed that the distribution of the field strength isn't continuous, a region with lower field strength values can be seen in one corner of each level.

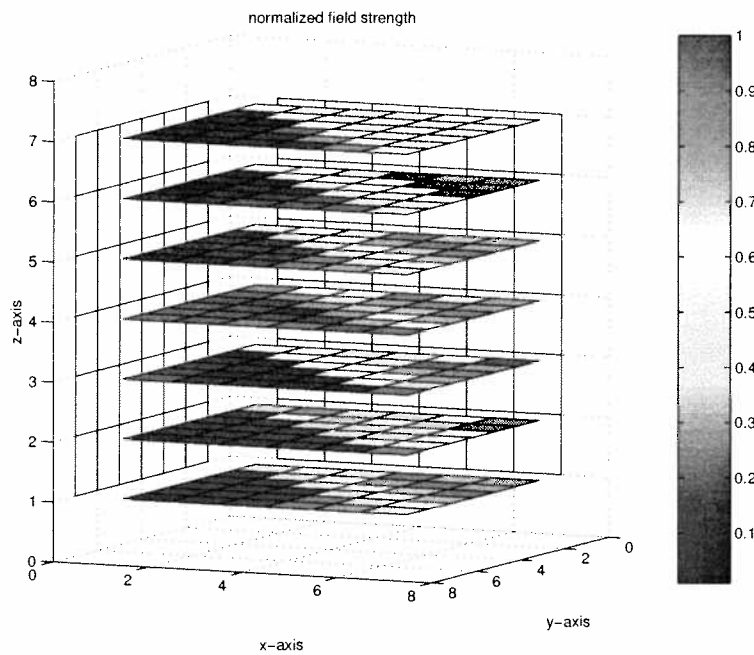


Figure 199: Distribution of the field strength values normalized to the maximum value for SIM 8 (GSM 900 - Simulation of Room A07A011 Mobilkom Austria).

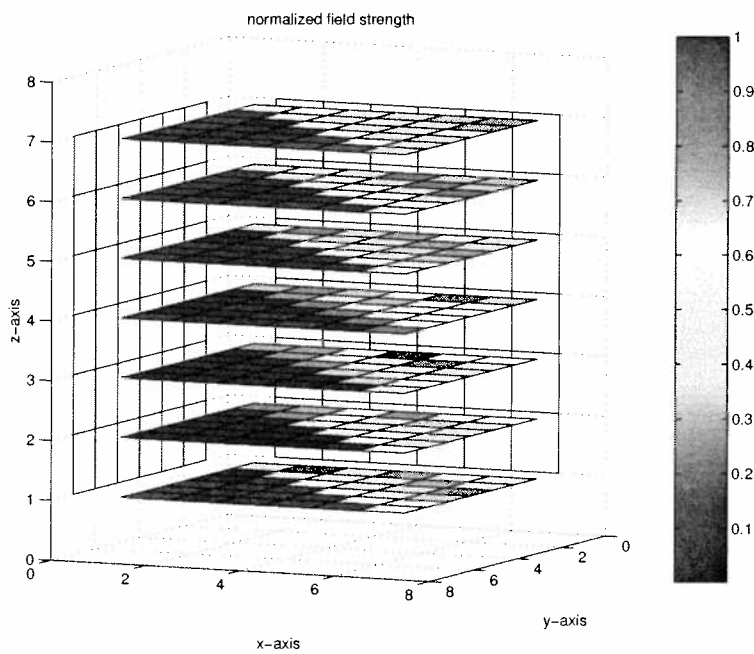


Figure 200: Distribution of the field strength values normalized to the maximum value for SIM 9 (GSM 900 - Simulation of Room A07A011 Mobilkom Austria).

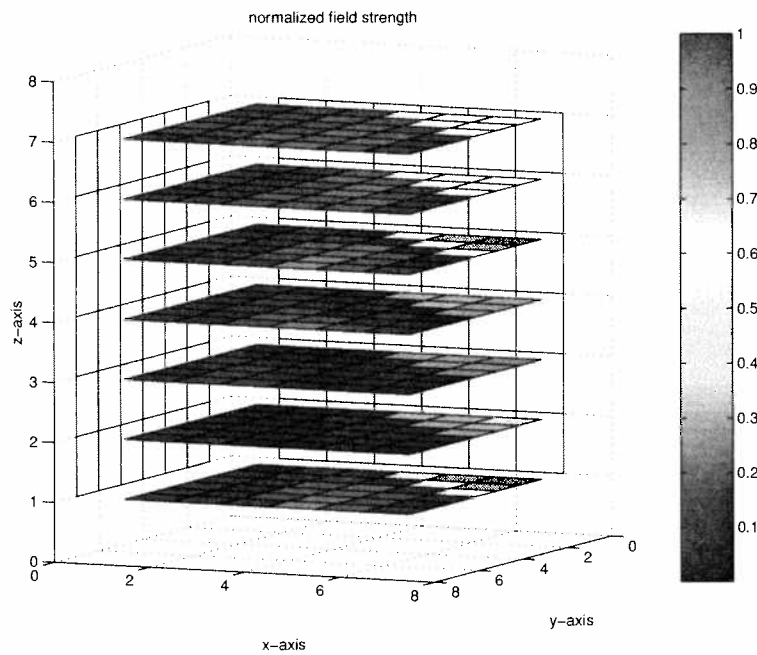


Figure 201: Distribution of the field strength values normalized to the maximum value for SIM 10 (GSM 900 - Simulation of Room A07A011 Mobilkom Austria).

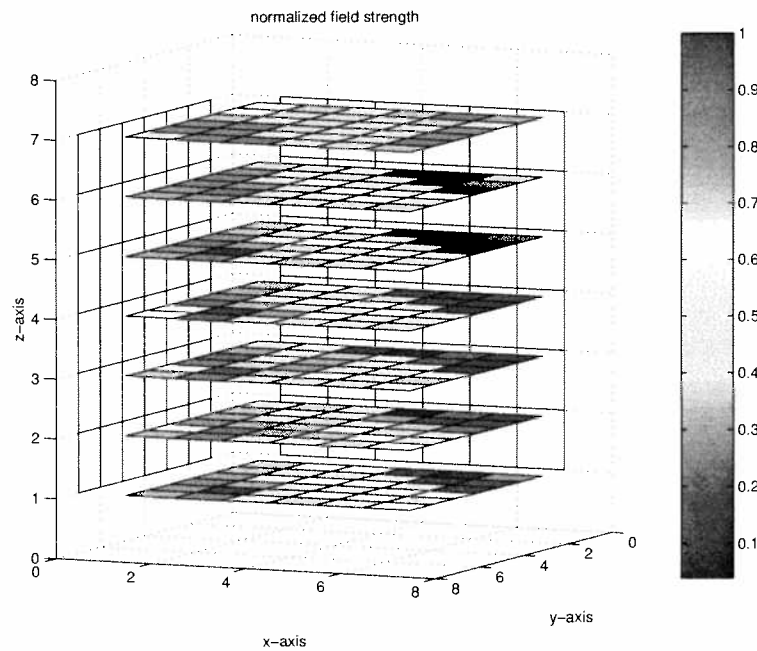


Figure 202: Distribution of the field strength values normalized to the maximum value for SIM 11 (GSM 900 - Simulation of Room A07A011 Mobilkom Austria).

7 Averaging Methods

Measurements like the measurement of a cube or an other geometrical Figure discussed in this thesis takes a very long time (approximately 14 hours for a cube with 343 measurement positions). To reduce the time of a measurement campaign the amount of examined positions must be reduced, but with every reduction the accuracy of statements according the electromagnetic field strength reduces, too.

This section discusses methods to reduce the amount of time by measuring only a few positions which should allow a representative statement about the global mean value of the electromagnetic field strength. Deriving the mean value of positions building a template and comparing them to the global mean value of a whole cube should deliver statements about the accuracy of different templates. With this knowledge measurements could be made more simpler and conclusions according the global mean value can be estimated. The investigation of the deviations between the mean value of the electromagnetic field strength of a template and the global mean value of a cube were subject of this section.

The amount of positions building a template were changed as well as the geometrical Figure which was built by arranging the positions in a one-dimensional, two-dimensional or three-dimensional array. However, the simplicity of templates was in the foreground because with their help measurement campaigns should be made more practical.

7.1 Different Templates

Ten different templates were created and moved through nearly all measured cubes. Some possible combinations of one-dimensional, two-dimensional or three-dimensional geometrical figures were defined. According to a simple measurement setup and faster measurement procedure very simple templates were generated which could be measured in a fraction of the amount of time compared to a measurement of a whole cube. Positions along a vertical line are much easier to measure because the measurement antenna must only be changed in its height. Vertical areas are easy to measure, too, because the measurement antenna must only be changed in its height and in one other direction (regarding to the coordinate system used in this thesis: in direction of the x-axis and y-axis). The templates were created according to fit the human body, which means, that measurements along a vertical area, for example, makes more sense than measuring a horizontal area. Much more templates could be created fitting the size of a human body but those ten templates should be a good approach for some important geometrical figures and should be representative for the deviations of the mean value of a template compared to the global mean value.

One-dimensional, two-dimensional and three dimensional templates are shown in Figure 203. Figure 204 shows for example only one-dimensional templates,

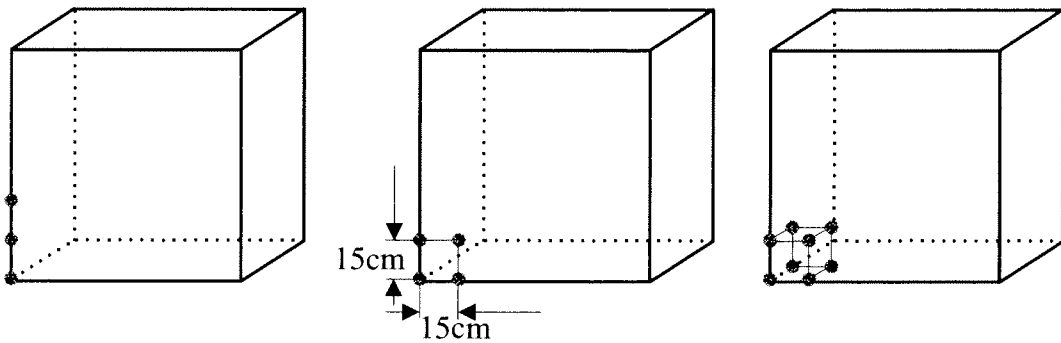


Figure 203: A one-dimensional, a two-dimensional and a three-dimensional template which were moved through some measured cubes. 15cm grid step.

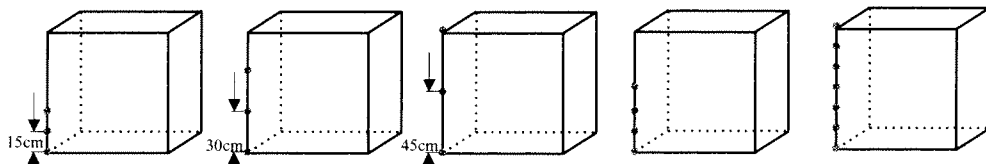


Figure 204: Line templates (One-dimensional) with a different number of positions and different grid steps (15cm, 30cm and 45cm).

which were called "*line templates*" with different grid steps (15cm, 30cm and 45cm) as well as a different number of positions. Two-dimensional templates, which were called "*area templates*" with a different number of positions as well as different grid steps (15cm and 45cm) can be seen in Figure 205. The former described templates have a grid step between two positions of 15cm but the impact of the variance of the grid step was also investigated by creating one-dimensional templates consisting of three positions with a grid step of 15cm, 30cm and 45cm displayed in Figure 204.

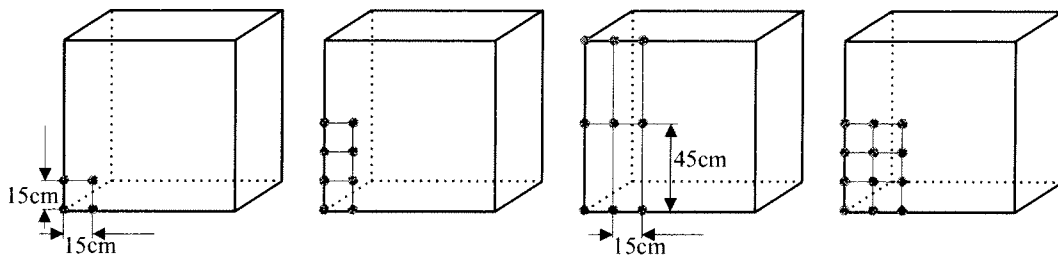


Figure 205: Area templates (two-dimensional) with a different number of positions and different grid steps (15cm and 45cm).

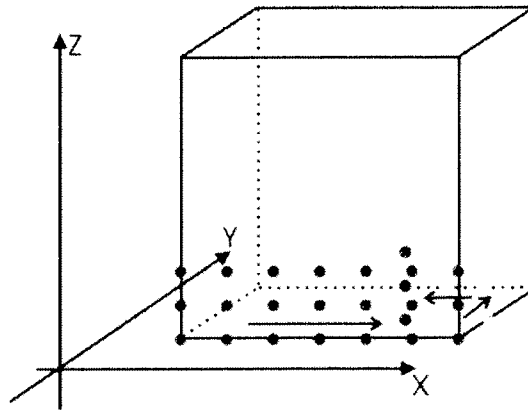


Figure 206: Moving a template (in this case a one-dimensional template consisting of three vertical positions building the template) through a cube means changing the position within the cube. The grey dots are showing positions already calculated. The position of the templates can be changed in all three directions (x-, y- and z-direction).

7.2 Deviations of the Mean Value: Templates - Measured Cubes

The templates described in the section before were moved through the measured cubes. This means that the mean value of the field strength of the positions building a template was calculated and was then compared to the global mean value of a whole cube. Moving a template through a cube means building the mean value of the positions representing the template and then changing the location of the template within the cube in direction of, for example the x-axis, the y-axis or the z-axis, as can be seen in Figure 206. In this way all templates were moved through the measurement data of an examined cube.

The deviations between each mean value of a template on a certain position and the global mean value were derived. Moving such a template through a whole cube delivers a large number of deviations, the maximum deviation and the minimum deviation for each template and for each investigated cube was written in tables. For the GSM 900 frequency band Table 61 displays the maximum and minimum deviations, for the DCS 1800 frequency band, Table 62 shows the derived deviations. For all other frequencies investigated in the measurement campaigns, the deviations between the global mean value and the mean values of a templates were derived, too and displayed in Table 63

The calculation procedure is described in detail now. The mean value of a template can be derived by Equation 24:

$$\overline{E}_{template} = \frac{\sum_{i=1}^{n_i} E_i}{n_i} \quad (24)$$

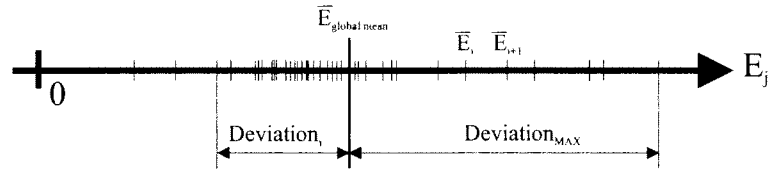


Figure 207: This figure should make the evaluation procedure visible. The global mean value $\overline{E}_{globalmean}$ and the mean values build by a template on certain positions within the cube \overline{E}_i are marked on the x-axis. In this case the maximum deviation is located on the right side of the global mean value.

With n_i as the number of the examined positions building the template and E_i as the electromagnetic field strength value for each position.

The global mean value is derived by following Equation 25:

$$\overline{E}_{global} = \frac{\sum_{j=1}^{n_j} E_j}{n_j} \quad (25)$$

With n_j as the number of examined positions in a cube ($n_j=343$) and E_j as the field strength value (measured with the Add3D method) for each position.

The deviation between the mean value of a template and the global mean can be derived by Equation 26:

$$Deviation = \frac{\overline{E}_{template} - \overline{E}_{globale}}{\overline{E}_{globale}} = \frac{\frac{\sum_{i=1}^{n_i} E_i}{n_i} - \frac{\sum_{j=1}^{n_j} E_j}{n_j}}{\frac{\sum_{j=1}^{n_j} E_j}{n_j}} \quad (26)$$

This evaluation procedure should be made visible by Figure 207, it shows the global mean value ($\overline{E}_{globalmean}$) as well as the mean values (\overline{E}_j) build by a template on certain positions within the cube. In this figure the maximum deviation occurs in the positive direction regarding the global mean value.

Table 61, Table 62 and Table 63 should show the maximum deviations in both directions (positive and negative direction). It might seem, that templates with a higher number of positions show less deviations from the global mean value and might deliver a more accurate statement regarding the global mean value of a cube (for example the area template consisting of eight positions are delivering smaller

GSM 900 Templates		A0A011 15cm	A0A011 7.5cm	Roof 15cm	TOX7 15cm	CC2-17 15cm
Area (12)	MAX [%]	27.0	52.6	49.7	28.0	59.2
	MIN [%]	-32.2	-34.6	-28.6	-22.9	-39.7
Area (9)	MAX [%]	59.4	39.0	38.1	28.3	55.9
	MIN [%]	-18.4	-26.9	-28.9	-23.7	-33.5
Cube (8)	MAX [%]	53.5	68.4	71.0	44.5	38.4
	MIN [%]	-48.3	-47.3	-60.5	-29.6	-36.5
Area (8)	MAX [%]	29.8	67.7	54.2	33.5	70.6
	MIN [%]	-37.6	-37.7	-32.7	-30.6	-41.1
Line (7)	MAX [%]	38.5	50.7	30.3	46.1	72.6
	MIN [%]	-26.3	-32.9	-28.6	-23.6	-39.5
Area (4)	MAX [%]	72.4	86.0	97.0	49.4	74.4
	MIN [%]	-52.2	-52.7	-64.6	-39.8	-46.4
Line (4)	MAX [%]	43.3	69.5	62.0	55.3	79.9
	MIN [%]	-40.9	-45.1	-47.1	-41.5	-43.8
Line (3)	MAX [%]	63.8	78.2	81.1	62.5	2.0
	MIN [%]	-48.7	-54.4	-57.4	-41.3	-49.5
<i>Line_{medium}</i> (3)	MAX [%]	77.0	60.3	56.1	55.5	91.7
	MIN [%]	-52.5	-40.0	-63.4	-36.3	-42.5
<i>Line_{big}</i> (3)	MAX [%]	91.3	61.2	68.0	55.5	79.2
	MIN [%]	-36.2	-32.6	-43.1	32.9	-40.5

Table 61: Comparison of the ten templates which were operated through measured cubes in the GSM 900 frequency band. The number in brackets is the amount of positions building the template.

DCS 1800 Templates		A0A011 15cm	A0A011 7.5cm	CC2-17 15cm
Area (12)	MAX [%]	47.6	51.7	36.8
	MIN [%]	-30.3	-35.0	-41.1
Area (9)	MAX [%]	80.9	25.0	19.9
	MIN [%]	-25.1	-35.0	-23.1
Cube (8)	MAX [%]	81.0	57.1	40.6
	MIN [%]	-46.5	-41.5	-44.5
Area (8)	MAX [%]	59.9	54.4	41.7
	MIN [%]	-34.3	-39.6	-42.5
Line (7)	MAX [%]	47.6	43.0	25.6
	MIN [%]	-38.5	-31.7	-24.8
Area (4)	MAX [%]	106.8	70.5	52.6
	MIN [%]	-53.0	-48.4	-51.4
Line (4)	MAX [%]	101.9	76.1	53.7
	MIN [%]	-45.3	-43.1	-44.5
Line (3)	MAX [%]	137.5	78.5	58.7
	MIN [%]	-47.5	-48.7	-48.7
<i>Line_{medium}</i> (3)	MAX [%]	122.5	76.2	55.7
	MIN [%]	-43.4	-42.8	-36.8
<i>Line_{big}</i> (3)	MAX [%]	107.9	47.2	40.2
	MIN [%]	-35.0	-36.9	-29.4

Table 62: Comparison of the ten templates which were operated through measured cubes in the DCS 1800 frequency band. The number in brackets is the amount of positions building the template.

Templates		UMTS	UHF	UHF
		(A0A011) 15cm	(A0A011) 15cm	(A0A011) 7.5cm
Area (12)	MAX [%]	23.5	28.6	20.7
	MIN [%]	-17.7	-34.6	-32.0
Area (9)	MAX [%]	24.6	9.4	23.0
	MIN [%]	-14.6	-23.7	-12.7
Cube (8)	MAX [%]	31.3	42.2	53.0
	MIN [%]	-26.1	-26.8	38.1
Area (8)	MAX [%]	32.0	35.7	28.6
	MIN [%]	-21.4	34.1	-40.3
Line (7)	MAX [%]	26.5	42.5	27.8
	MIN [%]	-22.6	-37.6	-30.5
Area (4)	MAX [%]	45.0	45.3	56.8
	MIN [%]	-31.3	-42.5	-41.1
Line (4)	MAX [%]	40.0	70.2	35.3
	MIN [%]	-34.5	-44.1	-47.9
Line (3)	MAX [%]	42.4	78.0	48.8
	MIN [%]	-36.2	-50.1	-50.1
<i>Line_{medium}</i> (3)	MAX [%]	39.3	60.7	44.6
	MIN [%]	-28.1	-50.2	-42.3
<i>Line_{big}</i> (3)	MAX [%]	42.8	31.7	45.5
	MIN [%]	-31.2	-29.7	-28.4

Table 63: Comparison of the ten templates which were operated through measured cubes in the UMTS frequency band and the UHF frequency band. The number in brackets is the amount of positions building the template.

deviations regarding the global mean than an area template with only 4 positions - referring to Table 61, Table 62 and Table 63). But this statement is only valid in combination with the size of the area (in case of two-dimensional and three-dimensional templates) covered by a template. For example the area template consisting of nine Positions covers a much bigger area than the template consisting of 12 positions (see Figure 205) and therefore delivers mean values with less deviation to the global mean value than the template with 12 positions. This means, that templates with a smaller number of positions which are covering a bigger area might deliver field strength values closer to the global mean value. It might be obvious when viewing the figures of the local distribution of the measurement data in Section 3, Section 4 and Section 6. If a template covers a bigger area the probability that spots with higher field strength values are included in the positions building the template is higher and delivers therefore mean values closer to the global mean.

Two-dimensional templates seems to deliver smaller deviations between the mean value of the template and global mean value compared to three-dimensional templates with an equal number of positions. This could also be manifested with the argument that the size of the area covered by a template is important for statements of the accuracy regarding the global mean value.

Now the behavior of the deviations of each template on certain positions should be tested more exactly. When applying a template in a measurement campaign it is very important to know what the measured field strength values are compared to the global mean. This means that there must be the knowledge of what the measured values are representing. The maximum and minimum deviations of the different templates are known but when a measurement procedure delivers a mean value of a template it doesn't say if this value is higher or lower regarding the global mean, therefore the deviations must be well investigated. In a next step the directions of the deviations (in positive and negative direction regarding the global mean value which means that the mean values build by templates on different positions within the cube are higher or lower regarding the global mean value) of the different templates were examined for the different frequency bands. The results are displayed in Table 64 and Table 65.

It can be seen, that in most cases the maximum deviation occurs in the positive direction which would be an overestimation of the global mean value. In the GSM 900 frequency band 94% of the mean values of different templates are higher than the global mean value, in the DCS 1800 frequency band 83% of the mean values of the templates are higher than the global mean. Only one cube was measured in the UMTS frequency band and therefore only one maximum and minimum deviation for each template could be derived. Table 65 shows that all mean values of the templates are higher than the global mean value of the UMTS cube which would be an overestimation. The TV channel (UHF) delivers values which differ from this trend because only 65% of the mean values from templates are higher than the global mean value.

Templates	GSM 900			DCS1800		
	above	below	[%]	above	below	[%]
Area (12pt)	4	1	80	2	1	67
Area (9pt)	5	0	100	1	2	33
Cube (8pt)	5	0	100	2	1	67
Area (8pt)	4	1	80	2	1	67
Line (7pt)	5	0	100	3	0	100
Area (4pt)	5	0	100	3	0	100
Line (4pt)	5	0	100	3	0	100
Line (3pt)	5	0	100	3	0	100
<i>Line_{medium}</i> (3pt)	4	1	80	3	0	100
<i>Line_{large}</i> (3pt)	5	0	100	3	0	100
TOTAL	47	3	94	25	5	83

Table 64: This table shows how many percent of the deviations are above the global mean value, which is important for measurement campaigns to estimate the probability if the measured value delivered from the template is above or below the global mean value. Most of the deviations to the global mean value are below the measured value of the template. The percentage shows how many measured values of the different templates are above the global mean value of a whole cube.

Templates	UMTS			UHF - FS ORF2		
	above	below	[%]	above	below	[%]
Area (12pt)	1	0	100	0	2	0
Area (9pt)	1	0	100	1	1	50
Cube (8pt)	1	0	100	2	0	100
Area (8pt)	1	0	100	1	1	50
Line (7pt)	1	0	100	1	1	50
Area (4pt)	1	0	100	2	0	100
Line (4pt)	1	0	100	1	1	50
Line (3pt)	1	0	100	1	1	50
<i>Line_{medium}</i> (3pt)	1	0	100	2	0	100
<i>Line_{large}</i> (3pt)	1	0	100	2	0	100
TOTAL	10	0	100	13	7	65

Table 65: This table shows how many percent of the deviations are above the global mean value, which is important for measurement campaigns to estimate the probability if the measured value delivered from the template is above or below the global mean value. Most of the deviations to the global mean value are below the measured value of the template. The percentage shows how many measured values of the different templates are above the global mean value of a whole cube.

But before we make any further conclusions those results should be investigated more detailed. Not only the maximum deviations of the mean value of a template compared to the global mean value of a cube should be evaluated but every mean value of a template should be tested regarding the global mean value.

Therefore the positive and negative deviations for the templates should deliver a better overview of the behavior of the mean value of templates compared to the global mean. For each template moved through a cube the positive deviation (which means that the mean value of a template on a certain positions within the cube is higher compared to the global mean value) or the negative deviation (which means that the mean value of a template is lower compared to the global mean value) was counted to estimate if there is a trend that mean values derived from templates tend to be lower or higher than the global mean value. This should give an idea of how the mean value of templates are compared to the global mean value. The results are displayed in tables. The deviations of templates moved through cubes which were evaluated in the GSM 900 frequency band are displayed in Table 66, for the deviations of templates moved through cubes examined in the DCS 1800 frequency band Table 67 shows the results, for UMTS Table 68 and for the TV channel (UHF) refer to Table 69.

Those four Tables (Table 66, Table 67, Table 68 and Table 69) are showing how many mean values of templates are lower or higher compared to the global mean value of a cube (second column and third column), the average deviation of all mean values of templates which are lower compared to the global mean value (fourth column) as well as the average deviation of all mean values of templates which are higher than the global mean value (fifth column) is derived as well. The last column shows how many percent of the templates deliver values higher than the global mean value. If those values are below the 50 % border, more mean values of a specific template are lower than the global mean value and the other way around. The bold values in column two and three should highlight the amount of values which are higher.

By visual inspection of those Tables (Table 66, Table 67, Table 68 and Table 69) it can be seen that templates with lower mean values compared to the global mean value are dominating in the GSM 900 frequency band and also at UMTS. Table 67 shows that the domination of lower values is not as high as in Table 66 and Table 68 but it still can be seen that more mean values of templates are lower than the global mean value for each cube. The evaluation of the UHF TV channel shows, that there is a balance of the amount of mean values which are lower or higher compared to the global mean value.

Scenario	lower	higher	neg. deviation	pos. deviation	% higher
			[%]	[%]	[%]
Line (3)					
TOX 7	144	101	-14.43	17.75	41.2

Scenario	lower	higher	neg. deviation	pos. deviation	% higher
			[%]	[%]	[%]
A07A011 (15cm)	167	78	-17.9	13.71	31.8
A07A011 (7,5cm)	130	115	-16.64	27.1	46.9
CC2-17	120	125	-17.8	20.83	51
Line (3 medium)					
TOX 7	75	72	-14.26	10.54	49
A07A011 (15cm)	92	55	-16.59	19.86	37.4
A07A011 (7,5cm)	83	64	-14.16	29.73	43.5
CC2-17	79	68	-16.05	20.65	46.2
Line (3 large)					
TOX 7	35	14	-13.33	17.75	28.6
A07A011 (15cm)	19	30	-15.3	22.67	61.2
A07A011 (7,5cm)	25	24	-12.63	16.43	49
CC2-17	29	20	-19.2	22.62	40.8
Line (4)					
TOX 7	116	80	-12.83	14.53	40.8
A07A011 (15cm)	145	51	-17.07	11.99	26
A07A011 (7,5cm)	106	90	-15.51	20.21	45.9
CC2-17	99	97	-16.29	20.65	49.5
Line (7)					
TOX 7	25	24	-10.96	11.42	49
A07A011 (15cm)	28	21	-10.68	14.24	42.9
A07A011 (7,5cm)	27	22	-13.68	16.78	44.9
CC2-17	27	22	-15.72	19.3	44.9
Area (4)					
TOX 7	134	118	-12.6	13.46	46.8
A07A011 (15cm)	159	93	-16.36	12.64	36.9
A07A011 (7,5cm)	151	101	-16.53	20.07	40.1
CC2-17	120	132	-17.77	17.86	52.4
Area (8)					
TOX 7	92	76	-10.99	9.16	45.2
A07A011 (15cm)	114	26	-12.1	4.27	15.5

Scenario	lower	higher	neg. deviation	pos. deviation	% higher
			[%]	[%]	[%]
A07A011 (7,5cm)	95	73	-14.25	17.89	43.5
CC2-17	78	90	-15.93	17.17	53.57
Area (9)					
TOX 7	23	12	-11.56	8.96	34.3
A07A011 (15cm)	14	21	-12.42	4.27	60
A07A011 (7,5cm)	21	14	-9.64	15.77	40
CC2-17	23	12	-15.93	21.56	34.3
Area (12)					
TOX 7	82	58	-7.7	7.7	41.4
A07A011 (15cm)	114	26	-14.2	7.7	18.6
A07A011 (7,5cm)	80	60	-13.6	16.1	42.9
CC2-17	65	75	-15.8	16.2	53.6
Cube (8)					
TOX 7	111	105	-11.23	11.47	48.6
A07A011 (15cm)	139	77	-13.05	9.78	35.7
A07A011 (7,5cm)	115	101	-14.6	18.68	46.8
CC2-17	106	110	-12.85	14.94	50.9

Table 66: GSM 900 - detailed overview of the deviations of different templates in different scenarios. This table shows how many mean values of a template are lower or higher than the global mean value

Scenario	lower	higher	neg. deviation	pos. deviation	% higher
			[%]	[%]	[%]
Line (3)					
A07A011 (15cm)	126	119	-16.7	22.8	48.6
A07A011 (7,5cm)	118	127	-16.4	19.8	51.8
CC2-17	137	108	-12.4	18.3	44
Line (3 medium)					
A07A011 (15cm)	95	52	-15.1	22.9	35.4
A07A011 (7,5cm)	71	76	-15.6	16.8	51.7

Scenario	lower	higher	neg. deviation	pos. deviation	% higher
			[%]	[%]	[%]
CC2-17	83	64	-11.8	9.8	43.5
Line (3 large)					
A07A011 (15cm)	14	35	-12.7	30.5	71.4
A07A011 (7,5cm)	31	18	-16.4	10.3	36.7
CC2-17	29	20	-11.6	11	40.8
Line (4)					
A07A011 (15cm)	91	105	-13.5	22.1	53.6
A07A011 (7,5cm)	84	112	-16.9	17.1	57.1
CC2-17	99	48	-15.1	13.3	32.7
Line (7)					
A07A011 (15cm)	30	19	-12.2	19.3	38.8
A07A011 (7,5cm)	22	27	-14.9	12.1	55.1
CC2-17	25	24	-9.3	10	49
Area (4)					
A07A011 (15cm)	136	116	-20.25	20.4	46
A07A011 (7,5cm)	129	123	-16.3	21.5	48.8
CC2-17	138	114	-14	16	45.2
Area (8)					
A07A011 (15cm)	75	93	-12.2	20	55.4
A07A011 (7,5cm)	68	100	-14.5	13.5	59.5
CC2-17	85	83	-12.9	10.9	49.4
Area (9)					
A07A011 (15cm)	10	25	-8	27.4	71.4
A07A011 (7,5cm)	22	13	-13.3	9.6	37.1
CC2-17	21	14	-9	8.1	40
Area (12)					
A07A011 (15cm)	62	78	-11.1	18.5	55.7
A07A011 (7,5cm)	56	84	-12	12.63	60
CC2-17	71	69	-11.5	9.5	49.3
Cube (8)					
A07A011 (15cm)	122	94	-14.7	19	43.5

Scenario	lower	higher	neg. deviation	pos. deviation	% higher
			[%]	[%]	[%]
A07A011 (7,5cm)	108	108	-14.2	16.4	50
CC2-17	113	103	-11.9	12.3	47.7

Table 67: DCS 1800 - detailed overview of the deviations of different templates in different scenarios. This table shows how many mean values of a template are lower or higher than the global mean value.

Scenario	lower	higher	neg. deviation	pos. deviation	% higher
			[%]	[%]	[%]
Line (3)					
A07A011 (15cm)	140	105	-10.9	11.11	42.9
Line (3 medium)					
A07A011 (15cm)	83	64	-10.34	11.44	43.5
Line (3 large)					
A07A011 (15cm)	20	29	-9.4	13.08	59.2
Line (4)					
A07A011 (15cm)	110	86	-10.48	10.19	43.9
Line (7)					
A07A011 (15cm)	22	27	-10.45	8.51	55.1
Area (4)					
A07A011 (15cm)	143	109	-9.64	10.2	43.3
Area (8)					
A07A011 (15cm)	90	78	-8.99	7.79	46.4
Area (9)					
A07A011 (15cm)	12	23	-5.94	8.69	65.7
Area (12)					
A07A011 (15cm)	77	63	-7.68	6.38	45
Cube (8)					
A07A011 (15cm)	117	99	-8.43	8.6	45.83

Scenario	lower	higher	neg. deviation	pos. deviation	% higher
			[%]	[%]	[%]

Table 68: UMTS - detailed overview of the deviations of different templates in different scenarios. This table shows how many mean values of a template are lower or higher than the global mean value.

Scenario	lower	higher	neg. deviation	pos. deviation	% higher
			[%]	[%]	[%]
Line (3)					
A07A011 (15cm)	117	128	-19.3	24.3	52.2
A07A011 (7,5cm)	148	97	-16.9	14.7	39.6
Line (3 medium)					
A07A011 (15cm)	74	73	-18.6	20.4	49.7
A07A011 (7,5cm)	82	65	-15.5	15.7	44.2
Line (3 large)					
A07A011 (15cm)	30	19	-13.9	10.2	38.8
A07A011 (7,5cm)	21	28	-13.4	17.9	57.1
Line (4)					
A07A011 (15cm)	93	103	-17.8	24.8	52.6
A07A011 (7,5cm)	116	80	-17.2	12.5	40.8
Line (7)					
A07A011 (15cm)	24	25	-17.2	16.5	51
A07A011 (7,5cm)	25	24	-14.3	14.8	49
Area (4)					
A07A011 (15cm)	106	146	-11.7	14.2	57.9
A07A011 (7,5cm)	147	105	-15.8	11.4	41.7
Area (8)					
A07A011 (15cm)	47	121	-10.6	11.3	72
A07A011 (7,5cm)	105	63	-13.6	7.7	37.5
Area (9)					
A07A011 (15cm)	25	10	-7.8	4.5	28.6
A07A011 (7,5cm)	9	26	-5.9	8.7	74.3

Scenario	lower	higher	neg. deviation	pos. deviation	% higher
			[%]	[%]	[%]
Area (12)					
A07A011 (15cm)	48	92	-9.1	10.6	65.7
A07A011 (7,5cm)	90	50	-9.7	5.7	35.7
Cube (8)					
A07A011 (15cm)	79	137	-8.4	11.9	63.4
A07A011 (7,5cm)	131	85	-13.3	10.5	39.4

Table 69: UHF - detailed overview of the deviations of different templates in different scenarios. This table shows how many mean values of a template are lower or higher than the global mean value.

7.3 Statements Regarding the Deviations of the Mean Value: Templates - Measured Cubes

Statements regarding the ten templates are made in this chapter. Those statements should lead to useful averaging procedures and estimations regarding the global mean value by only measuring a few positions.

Table 64 and Table 65 are displaying the behavior of the maximum and minimum deviations. Table 64 shows, that 94 % of the deviations are values higher than the global mean value of templates moved through the measured cubes in the GSM 900 frequency band. This means that the measured values are an over estimation. 83% of the deviations of templates operated through the measured cubes in the DCS 1800 frequency band are higher than the global mean value, again this would be an over estimation.

Due to the fact that only one cube was investigated in the UMTS frequency band, the result might be not so representable but are showing a similar trend than the maximum and minimum deviations of the templates moved through cubes measured in the GSM 900 and DCS 1800 frequency band. Again, all deviations are showing a maximum which is higher than the global mean (see Table 65), which results in an over estimation. A more balanced result can be found in Table 65 in the UHF - FS ORF2 frequency band. Only 63% of the deviations are higher than the global mean value. But not only the maximum and minimum deviations should be taken into account every single deviation of a mean value build by a template and compared to the global mean value should be observed. As the previous section showed, this might give a more detailed insight into the behavior of templates. Regarding Table 66, Table 67, Table 68 and Table 69 more deviations of the mean value of templates compared to the global mean value are lower which results in an under estimation.

The following Tables (Table 70, Table 71, Table 72 and Table 73) should give an overview of the deviations of the different templates for each frequency band. Those Tables show the probability of failures made by measuring only a few positions instead of a whole cube.

These Tables should provide a good overview of the probability of failure for each of the different templates. For example by using the line template consisting of 7 positions (Line (7)) for a measurement in the GSM 900 frequency band the probability that the mean value derived by the 7 measured positions is lower than the global mean value is 54.6%. The average deviation is -12.8% regarding the global mean. The probability that the derived mean value is higher than the global mean value is 45.4% with an average deviation of 15.4%. The knowledge of the probability as well as the average deviation in both directions (negative and positive) is very important because during a measurement procedure you do not have any information of the global mean value you only have a value derived by the positions building the template. The global mean value might be lower or higher than the measured value, therefore we need the information of the probability that a measured value is lower or higher compared to the global mean value.

With the help of those four Tables (Table 70, Table 71, Table 72 and Table 73) estimations about the uncertainty of measurements with only a few measurement positions can be made. It might seem that using such templates is a good approach for estimations of the global mean value because Table 70, Table 71, Table 72 and Table 73 are showing, that the average deviations of the templates regarding the global mean value are in a very small range. For example in the GSM 900 frequency band the deviations vary from -16.7% to 20.2%, in the DCS 1800 frequency band from -16.9% to 20.3%, in the UMTS frequency band from -10.9% to 13.1% and in the UHF frequency band from -18.1% to 19.5% regarding the global mean. This means that the maximum deviations are in the range of only approximately 20% regarding the global mean value.

GSM 900	lower	higher	neg. dev. [%]	% lower [%]	pos. dev. [%]	% higher [%]
Line (3)	561	419	-16.7	57.2	19.9	42.8
Line (3 medium)	329	259	-15.3	56.0	20.2	44.0
Line (3 large)	108	88	-15.1	55.1	19.9	44.9
Line (4)	466	318	-15.4	59.4	16.9	40.6
Line (7)	107	89	-12.8	54.6	15.4	45.4
Area (4)	564	444	-15.8	56.0	16.0	44.0
Area (8)	379	265	-13.3	58.9	12.1	41.1
Area (9)	81	59	-12.4	57.9	12.6	42.1
Area (12)	341	219	-12.8	60.9	11.9	39.1
Cube (8)	471	393	-12.9	54.5	13.7	45.5

Table 70: This tables shows the probability of failures made by measuring only a few positions instead of measuring a whole cube. For the GSM 900 Frequency band the probability of measuring a value lower or higher than the global mean with the average deviation regarding the global mean value is shown here.

DCS 1800	lower	higher	neg. dev. [%]	% lower [%]	pos. dev. [%]	% higher [%]
Line (3)	381	354	-15.2	51.8	20.3	48.2
Line (3 medium)	249	192	-14.2	56.5	16.5	43.5
Line (3 large)	74	73	-13.6	50.3	17.3	49.7
Line (4)	274	265	-15.2	50.8	17.5	49.2
Line (7)	77	70	-12.1	52.4	13.8	47.6
Area (4)	403	353	-16.9	53.3	19.3	46.7
Area (8)	228	276	-13.2	45.2	14.8	54.8
Area (9)	53	52	-10.1	50.5	15.0	49.5
Area (12)	189	231	-11.5	45.0	13.5	55.0
Cube (8)	343	305	-13.6	52.9	15.9	47.1

Table 71: This tables shows the probability of failures made by measuring only a few positions instead of measuring a whole cube. For the DCS 1800 Frequency band the probability of measuring a value lower or higher than the global mean with the average deviation regarding the global mean value is shown here.

UMTS	lower	higher	neg. dev. [%]	% lower [%]	pos. dev. [%]	% higher [%]
Line (3)	140	105	-10.9	57.1	11.1	42.9
Line (3 medium)	83	64	-10.3	56.5	11.4	43.5
Line (3 large)	20	29	-9.4	40.8	13.1	59.2
Line (4)	110	86	-10.5	56.1	10.2	43.9
Line (7)	22	27	-10.5	44.9	8.5	55.1
Area (4)	143	109	-9.6	56.7	10.2	43.3
Area (8)	90	78	-9.0	53.6	7.8	46.4
Area (9)	12	23	-5.9	34.3	8.7	65.7
Area (12)	77	63	-7.7	55.0	6.4	45.0
Cube (8)	117	99	-8.4	54.2	8.6	45.8

Table 72: This tables shows the probability of failures made by measuring only a few positions instead of measuring a whole cube. For the UMTS Frequency band the probability of measuring a value lower or higher than the global mean with the average deviation regarding the global mean value is shown here.

UHF (FS ORF2)	lower	higher	neg. dev. [%]	% lower [%]	pos. dev. [%]	% higher [%]
Line (3)	265	225	-18.1	54.1	19.5	45.9
Line (3 medium)	156	138	-17.1	53.1	18.1	46.9
Line (3 large)	51	47	-13.7	52.0	14.1	48.0
Line (4)	209	183	-17.5	53.3	18.7	46.7
Line (7)	49	49	-15.8	50.0	15.7	50.0
Area (4)	253	251	-13.8	50.2	12.8	49.8
Area (8)	152	184	-12.1	45.2	9.5	54.8
Area (9)	34	36	-6.9	48.6	6.6	51.4
Area (12)	138	142	-9.4	49.3	8.2	50.7
Cube (8)	210	222	-10.9	48.6	11.2	51.4

Table 73: This tables shows the probability of failures made by measuring only a few positions instead of measuring a whole cube. For the UHF Frequency band the probability of measuring a value lower or higher than the global mean with the average deviation regarding the global mean value is shown here.

8 Discussion and Conclusion

In the frame of this project 20 measurement campaigns and one simulation were performed. This means more than 3900 measured positions, as well as 3600 simulated positions. In addition, over 90000 measured samples were delivered from 10 continuous measurement campaigns. The measurements were performed in the frequency band of VHF, UHF, GSM 900, DCS 1800 and UMTS.

No reproducible relation between descriptors of scenarios and laws of field distribution could be found. The measurement campaigns showed, that the variation between the maximum value and the mean value varies between $887.0 \frac{mV}{m}$ (measured in Room CC2-17 at GSM 900 in an area measurement campaign) and $4.6 \frac{mV}{m}$ (measured in Room TOX 7 at GSM 900 in a cube measurement campaign).

Assignments of functions to the field distributions like Normal, LogNormal or Rayleigh were found only for some measurement campaigns. The simulation showed, that numerous distributions are possible within one single room which means, that a distribution function might not be representative for one specific scenario.

The averaging methods showed that different templates are delivering different results. Following conclusions about templates are referring to templates with approximately similar amount of measuring positions. It might seem that one-dimensional templates with a bigger distance between the measuring positions are more suitable for statements regarding the global mean value. The investigations showed, that line templates with a bigger distance between the three measuring positions are delivering mean values with smaller deviations regarding the global mean value. Two-dimensional templates might be better suited than three-dimensional templates because two-dimensional templates are comprising a bigger area than three-dimensional templates with an equal number of measuring positions and equal distances between the measuring positions. Geometrical figures with a smaller number of measuring positions which comprise a bigger area are better suited than templates with more measuring positions comprising a smaller area.

Templates used in this project delivered deviations between -16.9% (DCS 1800) and 20.3% (DCS 1800) regarding the global mean value. It might seem that such templates are a good approach for statements regarding the global mean value. The reduction in the amount of time needed for measuring only a few positions than measuring 343 positions is tremendous, while the results of the different templates showed only smaller (in the range of approximately 20%) deviations regarding the global mean value.

Appendix

A Far Field Calculation

For the Mobilkom Austria measurement campaign the far field was calculated for the GSM 900, DCS 1800 and the UMTS frequency bands. Following Equation 27 was used to calculate the power density S_{MAX} :

$$S_{MAX} = \frac{P \cdot (AG - CF)}{4 \cdot \pi \cdot d^2} \quad (27)$$

P is the input power in the unity of [W], AG is the antenna power gain in the unity of [1] and d is the distance in the unity of [m] to the antenna. S_{MAX} is in the unity of $[W/m^2]$. A correction factor (CF) must be evaluated from each antenna pattern and has to be subtracted from the antenna power gain. The antenna power gain must be in the unity of [1] instead of [dB] which is displayed in the antenna pattern. The value can be calculated by following Equation 28:

$$AG - CF = 10^{\frac{AG_{[dB]} - CF_{H[dB]} - CF_{V[dB]}}{10}} \quad (28)$$

$CF_{H[dB]}$ is the correction factor in the horizontal direction and $CF_{V[dB]}$ is the correction factor in the vertical direction. Those two factors can be read off the antenna pattern for each antenna.

Table 74 shows the values and the derived power S_{MAX} . The seventh column is derived by Equation 28 and the last column is derived by Equation 27. Column three and four shows the angle in the horizontal (α_H) direction and in (α_V) vertical direction.

Frequency	AG	α_H	α_V	CF_H	CF_V	AG - CF	P	d	S_{MAX}
	[dB]	[°]	[°]	[dB]	[dB]	[1]	[W]	[m]	$[\frac{W}{m^2}]$
A07A011									
GSM 900	18	30	22	-2.7	-21.5	0.24	5.01	33	8.78E-05
DCS 1800	18	30	22	-2.7	-19	0.43	15.85	35	4.39E-04
UMTS	17.5	30	22	-3	-20	0.28	10.3	37	1.69E-04
CC2-17									
GSM 900	10.5	-	6	0	-1	8.91	1	60	1.97E-04
TOX 7									
GSM 900	10.5	-	13	0	-2	7.08	1	200	1.41E-05

Table 74: Far field calculation for each frequency band. The last column shows the power density S_{MAX} .

B Antenna Factor and Cable Attenuation Factor

Table 75 shows the measured antenna factors for each frequency. The antenna factors are including the cable attenuations. After the measurement campaigns were finished, the attenuation factors of the measurement antenna with the cable used for all measurements as well as for the reference antenna with the cable used for all measurements were tested.

Frequency	Ref. Ant.	Measurement Ant.
	incl. Cable	incl. Cable
[MHz]	$[\frac{dB}{m}]$	$[\frac{dB}{m}]$
105.8	46.25	46.45
575.25	32.59	32.38
946.0	36.57	38.14
1812.4	45.75	44.88
2154.7	48.51	44.88

Table 75: Antenna Factors including the cable attenuation factors for all measurements at the Mobilkom Austria for both, the reference antenna set up and the measurement antenna set up.

C COST 259

The European COST (*Cooperation in Science and Technology*) action 259[13], named "Wireless Flexible Personalized Communications", has developed a new spatial channel model that describes the radio channel in both the delay and the angular dimensions (azimuth and elevation). Many measurements have established, that the multipath components show a clustered structure in delay and angular domain and references therein. The COST 259 directional channel model (DCM) is highly accurate, because - in contrast to earlier models - it takes into account both the inter- and the intra-cluster properties in delay and angular domains. Furthermore, it also includes microcellular environments, which are of increasing importance in today's interference-limited networks. The COST 259 - DCM distinguishes between different "radio environments" (e.g. typical urban macrocellular), each of which is characterized by a set of 10-15 parameters[21].

The COST 259 - DCM consists of several layers in order to facilitate the distinction between large-scale and small-scale effects. On the top of this structure, there is a subdivision into different radio environments, which describe a "canonical" geographical and morphological environment in which the base station and the mobile station can be. It covers a total of 13 environments in macrocells (general typical urban - GTU, general bad urban - GBU, general rural area - GRA and general hilly terrain - GHT), as well as microcells and picocells[21].

The classification by means of morphology of sites is driven by a more subjective view on the channel - the human's. Instead of the parameters observed by a system - the delay, Doppler shift, spatial correlation - the parameters observed by human beings - distance, building height, and room size - are taken as input to the classification[29].

For the measurements performed during this project the characterization of only

two environments were used to characterize the investigated scenarios - GRA and GTU.

References

- [1] Ayman F. Abouraddy and Said M. Elnoubi. Statistical modeling of the indoor radio channel at 10 ghz through propagation measurements - part i: Narrow-band measurements and modeling. *IEEE*, 49(5), September 2000.
- [2] Alejandro Aragon and Simon R. Saunders. Mobile robots for indoor radio wave propagation measurements. Technical report, Centre for Communication Systems Research University of Surrey, UK.
- [3] Richard Überbacher, Georg Neubauer, and Agnes Kaczmarczyk. Untersuchung zur entwicklung von normierungsfähigen meßmethoden für elektromagnetische felder im bereich von gsm basisstationen. Technical report, ARC Seibersdorf research GmbH, Geschäftsfeld Sichere Mobilkommunikation, 2002.
- [4] Ulf Bergqvist^a, Gerd Friedrich^b, Yngve Hamnerius^c, Luc Martens^d, Georg Neubauer^e, György Thuroczyf^f, Evi Vogel^g, and Joe Wiart^h. Mobile telecommunication base stations - exposure to electromagnetic fields. Technical report, ^a University of Linköping, Sweden; ^b Forschungsgemeinschaft Funk, Germany; ^c Chalmers University of Technology, Göteborg; ^d Universiteit Gent, Belgium; ^e ARC Seibersdorf research GmbH, Austria; ^f National Research Institute for Radiobiology and Radiohygiene, Hungary; ^g Bavarian Ministry for Regional Development and Environmental Affairs, Germany; ^h France Telecom, France.
- [5] Ernst Bonek. *Mobilkommunikation*. Institut für Nachrichtentechnik und Hochfrequenztechnik Technische Universität Wien, 7. edition, Februar 2001.
- [6] Ernst Bonek and Gottfried Magerl. *Wellenausbreitung 2*. Institut für Nachrichtentechnik und Hochfrequenztechnik Technische Universität Wien, März 2003.
- [7] Prof. Dr.-Ing. Ulrich Buchter, Dipl.-Ing. Roland Eidher, and Prof. Dr.-Ing. Matthias Wuschek. Großräumige ermittlung von funkwellen in baden-württemberg. Technical report, Juli 2003.
- [8] J.M. Cramer*, R.A. Scholtz*, and M.Z. Win**. Spatio-temporal diversity in ultra-wideband radio. Technical report, *Communication Sciencee Institute, EEB 500 Department of Electrical Engineering - Systems University of Southern California, Los Angeles, USA; ** Wireless Systems Research Department Newman Springs Laboratory, AT&T Labs-Research, NJ USA, 1998.
- [9] Business Unit EMC and RF-Engineering. *Precision Conical Dipole Antenna - PCD User's Guide*. ARC Seibersdorf research GmbH.

- [10] Ray A. Foran*, Thad B. Welch*, and Michael J. Walker**. Very near ground radio frequency propagation measurements and analysis for military applications. Technical report, *Department of Electrical Engineering United States Naval Academy, Annapolis; **Department of Electrical Engineering United States Air Force Academy.
- [11] Harald Haider, Wolfgang Müllner, and Georg Neubauer. Eine neue technik für präzise frequenzselektive feldstärkemessungen z.b. für gsm basisstationen. Technical report, ARC Seibersdorf research GmbH, 2002.
- [12] Mudhafar Hassan-Ali and Kaveh Pahlavan. A new statistical model for site-specific indoor radio propagation prediction based on geometric optics and geometric propability. *IEEE*, 1(1), January 2002.
- [13] Internet homepage of the European scientific COST action. <http://www.lx.it.pt/cost259/>.
- [14] Internet homepage of the Forum Mobilkommunikation. Fmk homepage: <http://www.lx.it.pt/cost259/>.
- [15] R. Hoppe, P. Wertz, G. Wölfle, and F.M. Landstorfer. Wideband propagation modelling for indoor environments and for radio transmission into buildings. Technical report, Institut für Hochfrequenztechnik, University of Stuttgart, Germany.
- [16] R. Hoppe*, G. Wölfle**, P. Wertz*, and F. M. Landstorfer*. Advanced ray-optical wave propagation modelling for indoor environments including wide-band properties. Technical report, *Institute of Radio Frequency Technology, University of Stuttgart; **AWE Communications GmbH, Germany.
- [17] j. D. Parson. *Mobile Radio Propagation Channel*. John Wiley and Sons Ltd, second edition, 2000.
- [18] F. M. Landstorfer and R. Hoppe. Advanced ray-optical wave propagation modelling for urban and indoor scenarios. Technical report, Institute of Radio Frequency Technology, University of Stuttgart, Germany.
- [19] H. Lehmann, B. Eicher, and P. Fritschi. Indoor measurements of the electrical field close to mobile phone base stations. Technical report, Coporate Technology, Environment and Electromagnetic Compatibility, Swisscom Ltd., Switzerland.
- [20] H. Luediger*, B. Kull*, S. Zeisberg**, and A. Finger**. An ultra-wideband indoor nlos radio channel amplitude probability density distribution. Technical report, *IMST GmbH, Germany; **Department of Electrical Engineering, Communications Laboratory, Dresden University of Technology, Germany.

- [21] Anfreas F. Molisch. *Spatial Characterization of Urban Radio Channels*. PhD thesis, Technische Universität Wien, 2002.
- [22] G. Neubauer*, H. Haider*, K. Lamedschwandner*, and M. Riederer** und R. Coray**. Measurement methods and legal requirements for exposure assessment next to gsm base stations. Technical report, *ARC Seibersdorf research GmbH, **OFCOM.
- [23] Homayoun Nikoolar and Homayoun Hashemi. Phase modeling of indoor radio propagation channels. *IEEE*, 49(2), March 2000.
- [24] Shuichi Obayashi and Jens Zander. A body-shadowing model for indoor radio communication environments. *IEEE*, 46(6), June 1998.
- [25] Martin Ollson. Impacts of meteorological conditions on field propagation in the frequency range 0.8-3 ghz. Technical report, Bioelectromagnetics Department of Electromagnetics Chalmers University of Technology and ARC Seibersdorf research GmbH, 2004.
- [26] Matthias Pätzold. *Mobilfunkkanäle - Modellierung, Analyse und Simulation*. Vieweg Verlag Braunschweig, Wiesbaden, 1999.
- [27] REMCOM. *Wireless Insite User's Manual version 1.5.1*, 2003.
- [28] Adel A. M. Saleh and Reinaldo A. Valenzuela. A statistical model for indoor multipath propagation. *IEEE*, SAC-5(2), February 1987.
- [29] Martin Steinbauer. *The Radio Propagation Channel - A Non-Directional, Directional, and Double-Directional Point-of-View*. PhD thesis, Technische Universität Wien, November 2001.
- [30] Stefan Suckrow, Martin Böttcher, Mohammad Bashir, and Bernd Edelmann. *Stationäre und mobile Antennen*. Verlag Technik Berlin, 1995.
- [31] L. Talbi and G. Y. Delisle. Finite difference time domain characterization of indoor radio propagation. Technical report, Progress In Electromagnetics Research.
- [32] Reinaldo A. Valenzuela, Dmitry Chizhik, and Jonathan Ling. Measured and predicted correlation between local average power and small scale fading in indoor wireless communication channels. Technical report, Lucent technologies, Bell Laboratories, USA.
- [33] Moe Z. Win, Robert A. Scholtz, and Mark A. Barnes. Ultra-wide bandwidth signal propagation for indoor wireless communications. *IEEE International Conference on Communications - Montreal, Canada*, June 1997.

- [34] Prof. Dr-Ing. Matthias Wuschek. Ergebnisbericht über die messung elektromagnetischer felder in der umgebung von mobilfunksendeanlagen. Technical report, Juli 2003.